

A SURFACE CRACK IN AN ORTHOTROPIC MEDIUM SUBJECTED TO
SLIDING CONTACT BY A RIGID STAMP

A THESIS SUBMITTED TO
THE GRADUATE SCHOOL OF NATURAL AND APPLIED SCIENCES
OF
MIDDLE EAST TECHNICAL UNIVERSITY

BY
DUYGU SARIKAYA

IN PARTIAL FULFILLMENT OF THE REQUIREMENTS
FOR
THE DEGREE OF DOCTOR OF PHILOSOPHY
IN
MECHANICAL ENGINEERING

JUNE 2014

Approval of the thesis:

**A SURFACE CRACK IN AN ORTHOTROPIC MEDIUM SUBJECTED TO
SLIDING CONTACT BY A RIGID STAMP**

submitted by **DUYGU SARIKAYA** in partial fulfillment of the requirements for the degree of **Doctor of Philosophy in Mechanical Engineering Department, Middle East Technical University** by,

Prof. Dr. Canan Özgen
Dean, Graduate School of **Natural and Applied Sciences**

Prof. Dr. Süha Oral
Head of Department, **Mechanical Engineering**

Prof. Dr. Serkan Dağ
Supervisor, **Mechanical Engineering Dept., METU**

Examining Committee Members:

Prof. Dr. Levend Parnas
Mechanical Engineering Dept., METU

Prof. Dr. Serkan Dağ
Mechanical Engineering Dept., METU

Prof. Dr. Müfit Gülgeç
Mechatronics Engineering Dept., Çankaya University

Prof. Dr. Suat Kadioğlu
Mechanical Engineering Dept., METU

Assoc. Prof. Dr. Demirkan Çöker
Mechanical Engineering Dept., METU

Date: 05/06/2014

I hereby declare that all information in this document has been obtained and presented in accordance with academic rules and ethical conduct. I also declare that, as required by these rules and conduct, I have fully cited and referenced all material and results that are not original to this work.

Name, Last name : Duygu SARIKAYA

Signature :

ABSTRACT

A SURFACE CRACK IN AN ORTHOTROPIC MEDIUM SUBJECTED TO SLIDING CONTACT BY A RIGID STAMP

Sarıkaya, Duygu

Ph.D., Department of Mechanical Engineering

Supervisor: Prof. Dr. Serkan Dağ

June 2014, 195 pages

This study is concerned with the surface crack problem in an elastic orthotropic half-plane subjected to sliding contact by a rigid stamp of an arbitrary profile. In this study the effect of sliding contact on the mixed-mode stress intensity factors and contact stresses is investigated. Within the scope of the research, surface crack problem for orthotropic materials is examined. The well-known equations of elasticity for an orthotropic semi-infinite medium are used to formulate the fracture and contact problems in coupled form. The coupled elasticity problem is solved by means of a direct approach. Integral transforms are utilized to satisfy the governing equations of the problem and boundary conditions exactly. The coupled problem is reduced to a system of three singular integral equations. By adopting a collocation approach, the equations are solved numerically to determine the stress intensity factors and contact stresses. The main results of the analyses are the effect of the material properties and friction coefficient on the mixed mode stress intensity factors at the crack tip, contact stresses and required contact force.

Keywords: Sliding contact/crack problems, Stress Intensity Factors, Singular Integral Equations.

ÖZ

RİJİT BİR ZIMBA İLE KAYMA TEMASINA MARUZ KALAN ORTOTROPİK ORTAMDAKİ BİR YÜZEY ÇATLAĞI

Sarıkaya, Duygu

Doktora, Makina Mühendisliği Bölümü

Tez Yöneticisi: Prof. Dr. Serkan Dağ

Haziran 2014, 195 sayfa

Bu çalışma, çeşitli profillerdeki rijit bir zimba ile kayma temasına maruz kalan ortotropik ortamdaki bir yüzey çatlak ile ilgilidir. Bu çalışmada kayma temasının, karışık mod gerilme şiddeti çarpanı ve temas gerilmeleri üzerindeki etkisi araştırılmıştır. Bu çalışma kapsamında yüzey çatlak problemleri ortotropik malzemeler için incelenmiştir. Kırılma ve temas problemlerinin bağlaşıklık formda elde edilebilmesi için, yarı sonsuz ortotropik bir ortam için elastisite denklemleri kullanılmıştır. Bu bağlaşıklık elastisite problemi direk yaklaşım ile çözülmüştür. Problemin ana denklemlerini ve sınır şartlarını sağlamak için integral dönüşümleri kullanılmıştır. Bağlaşıklık problem, üç adet tekil integral denkleme indirgenmiştir. Gerilme şiddeti çarpanı ve temas gerilmelerini saptamak için, düzenleme tekniği kullanılarak integral denklemleri nümerik olarak çözülmüştür. Analizlerin asıl sonuçları, malzeme özelliklerinin ve sürtünme katsayısının karışık mod gerilme şiddeti çarpanı, temas gerilmeleri ve gerekli temas kuvveti üzerindeki etkileridir.

Anahtar Kelimeler: Kayma Temas/Çatlak Problemleri, Gerilme Şiddeti Çarpanı, Tekil İntegral Denklemleri.

To my loving mother Nevres Solmaz SARIKAYA

ACKNOWLEDGMENTS

The author wishes to express her grateful appreciation and thanks to her advisor, Prof. Dr. Serkan Dađ for his continuous support and valuable guidance throughout the Ph.D. study. The guidance and cooperation of the Ph.D. committee members, Prof. Dr. Müfit Gülgeç and Prof. Dr. Suat Kadiođlu, are also appreciated. Thanks are also due to Prof. Dr. Levend Parnas for his useful ideas and discussions.

The author would like to thank to TÜBİTAK giving financial support during this study.

Finally, the author would also like to thank to her parents Mrs. Nevres Solmaz Sarıkaya and Mr. Veysel Sarıkaya to her brother Mr. Abdullah Sarıkaya, to her sister Mrs. Çiđdem Albayrak Sarıkaya, to her aunt Emine Ekinciođlu and to her friends Eryurt Barın, Yılmaz Koç, Serhat Akgün, Merve Bakıcı and Sevil Avciođlu for their support, encouragement, patience and understanding throughout the course of her studies.

TABLE OF CONTENTS

ABSTRACT.....	v
ÖZ	vi
ACKNOWLEDGMENTS	viii
TABLE OF CONTENTS.....	ix
LIST OF TABLES	xi
LIST OF FIGURES	xiv
CHAPTERS	
1. INTRODUCTION	1
1.1 Literature Survey.....	1
1.2 Scope of the Research	9
2. PROBLEM STATEMENT AND FORMULATION	11
2.1 Problem Definition.....	11
2.2 Formulation of the Problem	11
2.2.1 Problem 1: The Contact Problem	16
2.2.2 Problem 2: The Crack Problem	20
2.2.3 Derivation of the Singular Integral Equations	44
2.2.4 Singular Behavior of the Solution	74

2.2.5 On the Solution of the Integral Equations.....	80
3. NUMERICAL RESULTS.....	97
3.1 Flat Stamp.....	98
3.2 Triangular Stamp.....	101
3.3 Circular Stamp.....	102
3.4 Figures.....	105
3.5 Tables.....	136
4. CONCLUSIONS AND FUTURE WORK.....	151
4.1 Conclusions.....	151
4.2 Future Work.....	155
REFERENCES.....	157
APPENDICES	
A. ASYMPTOTIC EXPANSION COEFFICIENTS.....	165
B. CLOSED FORM EXPRESSIONS FOR CAUCHY PRINCIPAL VALUE INTEGRALS.....	183
C. FUNCTIONS USED IN THE NUMERICAL SOLUTION OF THE INTEGRAL EQUATIONS.....	185
D. CLOSED FORM CONTACT MECHANICS SOLUTIONS INVOLVING ISOTROPIC AND ANISOTROPIC HALF-PLANES.....	189
CURRICULUM VITAE.....	195

LIST OF TABLES

TABLES

Table 3.1: The material parameters of plasma-sprayed alumina	98
Table 3.2: Normalized force values computed for various values of a/d and coefficient of friction η for an isotropic half-plane loaded by a triangular stamp as shown in Figure 2.8, $(b-a)/d=1.0$, $\nu=0.25$, $d_{11}=2.9996$, $d_{12}=1.0008$, $d_{22}=3.0052$	136
Table 3.3: Normalized force values computed for various values of a/d and coefficient of friction η for an orthotropic half-plane loaded by a triangular stamp as shown in Figure 2.8, $(b-a)/d=0.1$	137
Table 3.4: Normalized force values computed for various values of a/d and coefficient of friction η for an orthotropic half-plane loaded by a triangular stamp as shown in Figure 2.8, $(b-a)/d=1.0$	138
Table 3.5: Normalized force values computed for various values of a/d and E_1/E_2 for an orthotropic half-plane loaded by a triangular stamp as shown in Figure 2.8, $(b-a)/d=1.0$, $\eta=0.4$	139
Table 3.6: Normalized force values computed for various values of E_1/E_2 and coefficient of friction η for an orthotropic half-plane loaded by a triangular stamp as shown in Figure 2.8, $(b-a)/d=1.0$, $a/d=0.1$	140

Table 3.7: Normalized force values computed for various values of a/d and E_1/E_3 for an orthotropic half-plane loaded by a triangular stamp as shown in Figure 2.8, $(b-a)/d=1.0$, $\eta=0.4$ 141

Table 3.8: Normalized force values computed for various values of E_1/E_3 and coefficient of friction η for an orthotropic half-plane loaded by a triangular stamp as shown in Figure 2.8, $(b-a)/d=1.0$, $a/d=0.1$ 142

Table 3.9: Normalized force values computed for various values of a/R and coefficient of friction η for an isotropic half-plane loaded by a circular stamp as shown in Figure 2.9, $(b-a)/R=1.0$, $d/R=1.0$, $\nu=0.25$, $d_{11}=2.9996$, $d_{12}=1.0008$, $d_{22}=3.0052$ 143

Table 3.10: Normalized force values computed for various values of a/R and coefficient of friction η for an orthotropic half-plane loaded by a circular stamp as shown in Figure 2.9, $(b-a)/R=0.1$, $d/R=1.0$ 144

Table 3.11: Normalized force values computed for various values of a/R and coefficient of friction η for an orthotropic half-plane loaded by a circular stamp as shown in Figure 2.9, $(b-a)/R=1.0$, $d/R=1.0$ 145

Table 3.12: Normalized force values computed for various values of a/R and E_1/E_2 for an orthotropic half-plane loaded by a circular stamp as shown in Figure 2.9, $(b-a)/R=1.0$, $d/R=1.0$, $\eta=0.4$ 146

Table 3.13: Normalized force values computed for various values of E_1/E_2 and coefficient of friction η for an orthotropic half-plane loaded by a circular stamp as shown in Figure 2.9, $(b-a)/R=1.0$, $d/R=1.0$, $a/R=0.1$ 147

Table 3.14: Normalized force values computed for various values of a/d and E_1/E_3 for an orthotropic half-plane loaded by a circular stamp as shown in Figure 2.9, $(b-a)/R=1.0$, $d/R=1.0$, $\eta=0.4$ 148

Table 3.15: Normalized force values computed for various values of E_1/E_3 and coefficient of friction η for an orthotropic half-plane loaded by a circular stamp as shown in Figure 2.9, $(b-a)/R=1.0$, $d/R=1.0$, $a/R=0.1$ 149

LIST OF FIGURES

FIGURES

Figure 2.1: Geometry of the problem.....	12
Figure 2.2: Solution Procedure.....	16
Figure 2.3: Geometry of the contact problem	17
Figure 2.4: Geometry of the crack problem	21
Figure 2.5: Superimposition for the crack problem	22
Figure 2.6: The contour for evaluation of the integral.	31
Figure 2.7: The geometry of the crack/contact problem for a flat stamp.....	81
Figure 2.8: The geometry of the crack/contact problem for a triangular stamp.....	85
Figure 2.9: The geometry of the crack/contact problem for a circular stamp	90
Figure 3.1: Direction of crack extension.....	99
Figure 3.2: Comparisons of contact stress distributions for an isotropic half-plane loaded by a flat stamp, $(b-a)/d=1.0$, $a/d=6$, $d_{11}=2.9996$, $d_{12}=1.0008$, $d_{22}=3.0052$ for plane strain.	105
Figure 3.4: Comparisons of contact stress distributions for an orthotropic half-plane loaded by a flat stamp, $(b-a)/d=1.0$, $a/d=6$, $d_{11}=2.9996$, $d_{12}=1.0008$, $d_{22}=3.0052$ for plane strain.	106

Figure 3.5: Comparison of contact stress distributions for an orthotropic half-plane loaded by a flat stamp, $(b-a)/d=1.0$, $a/d=6$, $d_{11}=2.9996$, $d_{12}=1.0008$, $d_{22}=3.0052$ for plane stress.	106
Figure 3.6: Mode I stress intensity factors for an edge crack in an isotropic half-plane loaded by a flat stamp as shown in Figure 2.7, $(b-a)/d=1.0$, $\nu=0.25$, $d_{11}=2.9996$, $d_{12}=1.0008$, $d_{22}=3.0052$	107
Figure 3.7: Mode II stress intensity factors for an edge crack in an isotropic half-plane loaded by a flat stamp as shown in Figure 2.7, $(b-a)/d=1.0$, $\nu=0.25$, $d_{11}=2.9996$, $d_{12}=1.0008$, $d_{22}=3.0052$	107
Figure 3.8: Contact stress distributions for an isotropic half-plane with an edge crack and loaded by a flat stamp as shown in Figure 2.7, $(b-a)/d=1.0$, $\nu=0.25$, $a/d=0.4$, $d_{11}=2.9996$, $d_{12}=1.0008$, $d_{22}=3.0052$	108
Figure 3.9: Mode I stress intensity factors for an edge crack in an orthotropic half-plane loaded by a flat stamp as shown in Figure 2.7, $(b-a)/d=0.1$	108
Figure 3.10: Mode II stress intensity factors for an edge crack in an orthotropic half-plane loaded by a flat stamp as shown in Figure 2.7, $(b-a)/d=0.1$	109
Figure 3.11: Contact stress distributions for an orthotropic half-plane with an edge crack and loaded by a flat stamp as shown in Figure 2.7, $(b-a)/d=0.1$, $a/d=0.4$	109
Figure 3.12: Mode I stress intensity factors for an edge crack in an orthotropic half-plane loaded by a flat stamp as shown in Figure 2.7, $(b-a)/d=1.0$	110
Figure 3.13: Mode II stress intensity factors for an edge crack in an orthotropic half-plane loaded by a flat stamp as shown in Figure 2.7, $(b-a)/d=1.0$	110
Figure 3.14: Contact stress distributions for an orthotropic half-plane with an edge crack and loaded by a flat stamp as shown in Figure 2.7, $(b-a)/d=1.0$, $a/d=0.4$	111

Figure 3.15: Effect of the elastic modulus ratio E_1/E_2 on mode I stress intensity factors for an edge crack in an orthotropic half-plane loaded by a flat stamp as shown in Figure 2.7, $(b-a)/d=1.0$, $\eta=0.4$ 111

Figure 3.16: Effect of the elastic modulus ratio E_1/E_2 on mode II stress intensity factors for an edge crack in an orthotropic half-plane loaded by a flat stamp as shown in Figure 2.7, $(b-a)/d=1.0$, $\eta=0.4$ 112

Figure 3.17: Effect of the elastic modulus ratio E_1/E_2 on the contact stress distribution for an edge crack in an orthotropic half-plane loaded by a flat stamp as shown in Figure 2.7, $(b-a)/d=1.0$, $a/d=0.1$, $\eta=0.4$ 112

Figure 3.18: Normalized k_1 versus E_1/E_2 and η for an edge crack in an orthotropic half-plane loaded by a flat stamp as shown in Figure 2.7, $(b-a)/d=1.0$, $a/d=0.1$.
..... 113

Figure 3.19: Normalized k_2 versus E_1/E_2 and η for an edge crack in an orthotropic half-plane loaded by a flat stamp as shown in Figure 2.7, $(b-a)/d=1.0$, $a/d=0.1$. 113

Figure 3.20: Effect of the elastic modulus ratio E_1/E_3 on mode I stress intensity factors for an edge crack in an orthotropic half-plane loaded by a flat stamp as shown in Figure 2.7, $(b-a)/d=1.0$, $\eta=0.4$ 114

Figure 3.21: Effect of the elastic modulus ratio E_1/E_3 on mode II stress intensity factors for an edge crack in an orthotropic half-plane loaded by a flat stamp as shown in Figure 2.7, $(b-a)/d=1.0$, $\eta=0.4$ 114

Figure 3.22: Effect of the elastic modulus ratio E_1/E_3 on contact stress distribution for an edge crack in an orthotropic half-plane loaded by a flat stamp as shown in Figure 2.7, $(b-a)/d=1.0$, $a/d=0.1$, $\eta=0.4$ 115

Figure 3.23: Normalized k_1 versus E_1/E_3 and η for an edge crack in an orthotropic half-plane loaded by a flat stamp as shown in Figure 2.7, $(b-a)/d=1.0$, $a/d=0.1$	115
Figure 3.24: Normalized k_2 versus E_1/E_3 and η for an edge crack in an orthotropic half-plane loaded by a flat stamp as shown in Figure 2.7, $(b-a)/d=1.0$, $a/d=0.1$	116
Figure 3.25: Mode I stress intensity factors for an edge crack in an isotropic half-plane loaded by a triangular stamp as shown in Figure 2.8, $(b-a)/d=1.0$, $\nu=0.25$, $d_{11}=2.9996$, $d_{12}=1.0008$, $d_{22}=3.0052$	116
Figure 3.26: Mode II stress intensity factors for an edge crack in an isotropic half-plane loaded by a triangular stamp as shown in Figure 2.8, $(b-a)/d=1.0$, $\nu=0.25$, $d_{11}=2.9996$, $d_{12}=1.0008$, $d_{22}=3.0052$	117
Figure 3.27: Contact stress distributions for an isotropic half-plane with an edge crack and loaded by a triangular stamp as shown in Figure 2.8, $\nu=0.25$, $a/d=0.1$, $b/d=1.1$, $d_{11}=2.9996$, $d_{12}=1.0008$, $d_{22}=3.0052$	117
Figure 3.28: Mode I stress intensity factors for an edge crack in an orthotropic half-plane loaded by a triangular stamp as shown in Figure 2.8, $(b-a)/d=0.1$	118
Figure 3.29: Mode II stress intensity factors for an edge crack in an orthotropic half-plane loaded by a triangular stamp as shown in Figure 2.8, $(b-a)/d=0.1$	118
Figure 3.30: Contact stress distributions for an orthotropic half-plane with an edge crack and loaded by a triangular stamp as shown in Figure 2.8, $a/d=0.1$, $b/d=0.2$	119
Figure 3.31: Mode I stress intensity factors for an edge crack in an orthotropic half-plane loaded by a triangular stamp as shown in Figure 2.8, $(b-a)/d=1.0$	119

Figure 3.32: Mode II stress intensity factors for an edge crack in an orthotropic half-plane loaded by a triangular stamp as shown in Figure 2.8, $(b - a)/d = 1.0$ 120

Figure 3.33: Contact stress distribution for an orthotropic half-plane with an edge crack and loaded by a triangular stamp as shown in Figure 2.8, $a/d = 0.1$, $b/d = 1.1$.
..... 120

Figure 3.34: Effect of the elastic modulus ratio E_1/E_2 on mode I stress intensity factors for an edge crack in an orthotropic half-plane loaded by a triangular stamp as shown in Figure 2.8, $(b - a)/d = 1.0$, $\eta = 0.4$ 121

Figure 3.35: Effect of the elastic modulus ratio E_1/E_2 on mode II stress intensity factors for an edge crack in an orthotropic half-plane loaded by a triangular stamp as shown in Figure 2.8, $(b - a)/d = 1.0$, $\eta = 0.4$ 121

Figure 3.36: Effect of the elastic modulus ratio E_1/E_2 on the contact stress distribution for an edge crack in an orthotropic half-plane loaded by a triangular stamp as shown in Figure 2.8, $a/d = 0.1$, $b/d = 1.1$, $\eta = 0.4$ 122

Figure 3.37: Normalized k_1 versus E_1/E_2 and η for an edge crack in an orthotropic half-plane loaded by a triangular stamp as shown in Figure 2.8, $(b - a)/d = 1.0$, $a/d = 0.1$ 122

Figure 3.38: Normalized k_2 versus E_1/E_2 and η for an edge crack in an orthotropic half-plane loaded by a triangular stamp as shown in Figure 2.8, $(b - a)/d = 1.0$, $a/d = 0.1$ 123

Figure 3.39: Effect of the elastic modulus ratio E_1/E_3 on mode I stress intensity factors for an edge crack in an orthotropic half-plane loaded by a triangular stamp as shown in Figure 2.8, $(b - a)/d = 1.0$, $\eta = 0.4$ 123

Figure 3.40: Effect of the elastic modulus ratio E_1/E_3 on mode II stress intensity factors for an edge crack in an orthotropic half-plane loaded by a triangular stamp as shown in Figure 2.8, $(b-a)/d=1.0$, $\eta=0.4$	124
Figure 3.41: Effect of the elastic modulus ratio E_1/E_3 on the contact stress distribution for an edge crack in an orthotropic half-plane loaded by a triangular stamp as shown in Figure 2.8, $a/d=0.1$, $b/d=1.1$, $\eta=0.4$	124
Figure 3.42: Normalized k_1 versus E_1/E_3 and η for an edge crack in an orthotropic half-plane loaded by a triangular stamp as shown in Figure 2.8, $(b-a)/d=1.0$, $a/d=0.1$	125
Figure 3.43: Normalized k_2 versus E_1/E_3 and η for an edge crack in an orthotropic half-plane loaded by a triangular stamp as shown in Figure 2.8, $(b-a)/d=1.0$, $a/d=0.1$	125
Figure 3.44: Mode I stress intensity factors for an edge crack in an isotropic half-plane loaded by a circular stamp as shown in Figure 2.9, $(b-a)/R=1.0$, $d/R=1.0$, $\nu=0.25$, $d_{11}=2.9996$, $d_{12}=1.0008$, $d_{22}=3.0052$	126
Figure 3.45: Mode II stress intensity factors for an edge crack in an isotropic half-plane loaded by a circular stamp as shown in Figure 2.9, $(b-a)/R=1.0$, $d/R=1.0$, $\nu=0.25$, $d_{11}=2.9996$, $d_{12}=1.0008$, $d_{22}=3.0052$	126
Figure 3.46: Contact stress distribution for an isotropic half-plane with an edge crack and loaded by a circular stamp as shown in Figure 2.9, $a/R=0.1$, $b/R=1.1$, $d/R=1.0$, $\nu=0.25$, $d_{11}=2.9996$, $d_{12}=1.0008$, $d_{22}=3.0052$	127
Figure 3.47: Mode I stress intensity factors for an edge crack in an orthotropic half-plane loaded by a circular stamp as shown in Figure 2.9, $(b-a)/R=0.1$, $d/R=1.0$	127

Figure 3.48: Mode II stress intensity factors for an edge crack in an orthotropic half-plane loaded by a circular stamp as shown in Figure 2.9, $(b - a)/R=0.1$, $d/R=1.0$.
..... 128

Figure 3.49: Contact stress distributions for an orthotropic half-plane with an edge crack and loaded by a circular stamp as shown in Figure 2.9, $a/R=0.1$, $b/R=0.2$, $d/R=1.0$.
..... 128

Figure 3.50: Mode I stress intensity factors for an edge crack in an orthotropic half-plane loaded by a circular stamp as shown in Figure 2.9, $(b - a)/R=1.0$, $d/R=1.0$.
..... 129

Figure 3.51: Mode II stress intensity factors for an edge crack in an orthotropic half-plane loaded by a circular stamp as shown in Figure 2.9, $(b - a)/R=1.0$, $d/R=1.0$.
..... 129

Figure 3.52: Contact stress distributions for an orthotropic half-plane with an edge crack and loaded by a circular stamp as shown in Figure 2.9, $a/R=0.1$, $b/R=1.1$, $d/R=1.0$.
..... 130

Figure 3.53: Effect of the elastic modulus ratio E_1/E_2 on mode I stress intensity factors for an edge crack in an orthotropic half-plane loaded by a circular stamp as shown in Figure 2.9, $(b - a)/R=1.0$, $d/R=1.0$, $\eta=0.4$.
..... 130

Figure 3.54: Effect of the elastic modulus ratio E_1/E_2 on mode II stress intensity factors for an edge crack in an orthotropic half-plane loaded by a circular stamp as shown in Figure 2.9, $(b - a)/R=1.0$, $d/R=1.0$, $\eta=0.4$.
..... 131

Figure 3.55: Effect of the elastic modulus ratio E_1/E_2 on the contact stress distribution for an edge crack in an orthotropic half-plane loaded by a circular stamp as shown in Figure 2.9, $a/R=0.1$, $b/R=1.1$, $d/R=1.0$, $\eta=0.4$.
..... 131

Figure 3.56: Normalized k_1 versus E_1/E_2 and η for an edge crack in an orthotropic half-plane loaded by a circular stamp as shown in Figure 2.9, $(b-a)/R=1.0$, $d/R=1.0, a/R=0.1$	132
Figure 3.57: Normalized k_2 versus E_1/E_2 and η for an edge crack in an orthotropic half-plane loaded by a circular stamp as shown in Figure 2.9, $(b-a)/R=1.0$, $d/R=1.0, a/R=0.1$	132
Figure 3.58: Effect of the elastic modulus ratio E_1/E_3 on mode I stress intensity factors for an edge crack in an orthotropic half-plane loaded by a circular stamp as shown in Figure 2.9, $(b-a)/R=1.0, d/R=1.0, \eta=0.4$	133
Figure 3.59: Effect of the elastic modulus ratio E_1/E_3 on mode II stress intensity factors for an edge crack in an orthotropic half-plane loaded by a circular stamp as shown in Figure 2.9, $(b-a)/R=1.0, d/R=1.0, \eta=0.4$	133
Figure 3.60: Effect of elastic modulus ratio E_1/E_3 on the contact stress distribution for an edge crack in an orthotropic half-plane loaded by a circular stamp as shown in Figure 2.9, $a/R=0.1, b/R=1.1, d/R=1.0, \eta=0.4$	134
Figure 3.61: Normalized k_1 versus E_1/E_3 and η for an edge crack in an orthotropic half-plane loaded by a circular stamp as shown in Figure 2.9, $(b-a)/R=1.0$, $d/R=1.0, a/R=0.1$	134
Figure 3.62: Normalized k_2 versus E_1/E_3 and η for an edge crack in an orthotropic half-plane loaded by a circular stamp as shown in Figure 2.9, $(b-a)/R=1.0$, $d/R=1.0, a/R=0.1$	135
Figure D. 1: Geometry of the contact problem	189
Figure D. 2: Geometry of the contact problem and principal axes x_1, x_2	192

CHAPTER 1

INTRODUCTION

The aim of this study is to develop a method to examine the surface crack problem in an elastic orthotropic half-plane subjected to sliding contact by a rigid stamp. Main interest of the study is on the effect of sliding contact on the mixed-mode stress intensity factors and contact stresses. In this chapter, literature review of related fracture and contact mechanics problems are given. Then, the scope of this study is described.

1.1 Literature Survey

Fracture and contact mechanics are foundational to the field of engineering. Many studies are conducted regarding the behavior of solids subjected to contact, and those of that contain cracks and defects. Here, recent researches in this field are summarized.

Dag and Erdogan [1] consider the coupled problem of crack/contact mechanics in a nonhomogeneous medium and investigate the behavior of a surface crack in a functionally graded medium loaded by a sliding rigid stamp in the presence of friction. In this study, the dimensions of the graded medium are assumed to be very large in comparison with the local length parameters of the crack/contact region. Thus, in formulating the problem the graded medium is assumed to be semi-infinite. Contact stresses, the in-plane component of the surface stress and stress intensity factors at the crack tip are determined. The results are presented for various

combinations of friction coefficient, material nonhomogeneity constant and crack/contact length parameters.

A surface crack in a semi-infinite elastic graded medium under general loading conditions is studied by Dag and Erdogan [2]. In this study it is assumed that first by solving the problem in the absence of a crack it is reduced to a local perturbation problem with arbitrary self-equilibrating crack surface tractions. The local problem is then solved by approximating the normal and shear tractions on the crack surfaces by polynomials and the normalized modes I and II stress intensity factors are given. As an example the results for a graded half-plane loaded by a sliding rigid circular stamp are presented.

The problem of internal and edge cracks in an orthotropic strip is considered by Delale and Erdogan [3]. This problem is formulated in terms of singular integral equations. For the symmetric case the stress intensity factors are calculated and are compared with the isotropic results. The results show that the stress intensity factors are dependent on the elastic constants and are generally different from the corresponding isotropic results.

Mode I crack problem for a functionally graded orthotropic strip is considered by Guo et al. [4]. In this study, internal and edge cracks perpendicular to the boundaries are examined. The elastic property of the material is assumed to vary continuously along the thickness direction. The principal directions of orthotropy are parallel and perpendicular to the boundaries of the strip. The singular integral equation for solving the problem and the corresponding asymptotic expression of the singular kernel are obtained. Three different loading conditions, namely crack surface pressure, fixed-grip loading and bending, are considered during the analysis. The influences of parameters such as the material constants and the geometry parameters on the stress intensity factors (SIFs) are studied.

Ozturk and Erdogan [5] consider Mode I crack problem in an inhomogeneous orthotropic medium. In this study, the symmetric crack problem is considered and the material is both oriented and graded. The mode I crack problem for the inhomogeneous orthotropic plane is formulated and the solution is obtained for various loading conditions and material parameters.

The mixed mode crack problem in plane elasticity for a graded and oriented material is considered by Ozturk and Erdogan [6]. It is assumed that the crack is located in a plane perpendicular to the direction of property grading and the principal axes of orthotropy are parallel and perpendicular to the crack plane. The problem is formulated in terms of the averaged constants of plane orthotropic elasticity and reduced to a system of singular integral equations which is solved for various loading conditions and material parameters. The presented results consist of the strain energy release rate, the stress intensity factors and the crack opening displacements. It is found that generally the stress intensity factors increase with increasing material inhomogeneity parameter, shear parameter and decreasing stiffness ratio.

Gupta and Erdogan [6] consider the problem of edge cracks in an infinite strip. In this study, the elastostatic plane problem of an infinite strip containing two symmetrically located internal cracks perpendicular to the boundary is formulated in terms of a singular integral equation with the derivative of the crack surface displacement as the density function. The solution of the problem is obtained for various crack geometries and for uniaxial tension applied to the strip away from the crack region. The limiting case of the edge crack is considered in some detail. The results presented consist of stress intensity factors. The results also include the solution of the edge crack problem in an elastic half-plane.

The crack problem for an orthotropic half-plane stiffened by elastic films problem is considered by Mahajan et al.[8]. In this study, various contact and crack problems for an orthotropic substrate, stiffened by elastic films, are considered. The film is

modeled as a membrane and the substrate as an orthotropic half-plane with the principal axes of orthotropy parallel and perpendicular to the boundary. The problem is formulated in terms of a system of singular integral equations. The influence of the relative crack/stiffener dimensions, the film/substrate stiffness ratios and the material orthotropy on the stress intensity factors is studied.

The elasticity solution of cracking due to sliding contact in a homogeneous half-plane for different stamp profiles is considered by Hasebe et al. ([9]-[12]). In these problems, the homogeneous half-plane is in sliding contact with a rigid stamp. The coupled crack and contact problems are solved using complex stress functions and the conformal mapping technique. This technique is limited to the crack and contact problems in homogeneous half-plane and also since the homogeneous half-plane is mapped into a unit circle, the solution procedure does not account for singularities at some irregular points.

De and Patra [13] consider edge crack in orthotropic elastic half-plane problem. In this study, two edge crack problems, (1) having prescribed crack shape and (2) having been opened by prescribed normal pressure, are examined. Numerical results, for various loading functions of stress intensity factor and crack energy are determined.

The plane elasticity problem for an infinite medium containing a line crack is considered by Konda and Erdogan [14]. The main results of this study are the calculated modes I and II stress intensity factors. The effects of the material nonhomogeneity constant, the crack orientation, the loading conditions and the Poisson's ratio on the stress intensity factors are studied.

Cinar and Erdogan [15] consider the crack and wedging problem for an orthotropic strip. In this study, first the plane elasticity problem for an orthotropic strip containing a crack parallel to its boundaries is considered. The problem is formulated

under general mixed mode loading conditions. It is shown that the stress intensity factors depend on two dimensionless orthotropic constants only. The problem of loading the strip by a rigid rectangular wedge is then considered. It is found that for relatively small wedge lengths continuous contact is maintained along the wedge-strip interface, at a certain critical wedge length the separation starts at the midsection of the wedge and the length of the separation zone increases rapidly with increasing wedge length.

The problem of orthotropic semi-infinite strip with a crack along the fixed end is considered by Loboda [16]. In the study, the model of a crack with frictionless contact zones near its tips is used. The stress intensity factors at the crack tips and the corners of the strip, which are the main parameters of fracture, are evaluated.

Kim and Paulino [17] consider the interaction integral for fracture analysis of orthotropic FGMs. In this study, stress intensity factors for mode I and mixed-mode two-dimensional problems are evaluated by means of the interaction integral and the finite element method. Extensive computational experiments have been performed to validate the proposed formulation. The accuracy of numerical results is discussed by comparisons to available analytical, semi-analytical, or numerical solutions.

Interface crack problems in graded orthotropic media are considered by Dag et al. [18]. In this study, the authors examine the problem using analytical and computational techniques. In the analytical formulation an interface crack between a graded orthotropic coating and a homogeneous orthotropic substrate is considered. The problem is formulated in terms of the averaged constants of plane orthotropic elasticity and reduced to a pair of singular integral equations which are solved numerically to compute the mixed mode stress intensity factors and the energy release rate. In the second part of the study, enriched finite elements are formulated and implemented for graded orthotropic materials. Comparisons of the finite element

and analytical results show that enriched finite element technique is capable of producing highly accurate results for crack problems in graded orthotropic media.

In the study by Kim and Paulino [19], a finite element methodology is developed for fracture analysis of orthotropic functionally graded materials (FGMs) where cracks are arbitrarily oriented with respect to the principal axes of material orthotropy. The effects of boundary conditions, crack tip mesh discretization and material properties on fracture behavior are investigated in detail. To validate the methodology many numerical examples are submitted. The accuracy of the results is discussed by comparison to available (semi-) solutions.

Contact mechanics of graded coatings under isothermal conditions is considered by Guler and Erdogan [20]. The objective of this study was to obtain a series of analytical benchmark solutions for examining the influence of such factors as material inhomogeneity constants, the coefficient of friction and various length parameters on the contact stresses. Extensive results are given for the influence of material nonhomogeneity and friction on the contact stress at the contacting surface.

Shah and Wang [21] considered two homogeneous spheres in contact and determined the contact stress in the bodies under full-slip and partial-slip conditions. These stresses are then used to solve the Hertzian fracture problem. The critical fracture load required for the development of Hertzian crack system is also calculated.

Giannakopoulos and Pallot [22] consider two-dimensional isothermal contact of a rigid cylinder on an elastic graded substrate. In this study, the normal, sliding, and rolling types of contacts are addressed. Flat ended and cylindrical punches are examined in detail. The effect of adhesion in frictionless contact is also studied.

Barber [23] examines contact problems for a thin elastic layer. In this study, indentation by a rigid frictionless punch of a thin elastic layer on a rigid foundation is

considered in a three-dimensional setting. Results are given for the case where an incompressible layer is indented by an ellipsoidal punch. Also an approximate solution for the contact area and the load-penetration relation by considering frictionless indentation of an elastic half space by a punch of an arbitrary profile is developed by Barber and Billings [24].

Prasad et al. [25] develops a systematic methodology to quantify the mechanics of steady-state frictional sliding response for a plastically graded material. Specifically, the effect of linear gradient in yield stress on the frictional sliding response is examined through parametric FEM computation of the instrumented scratch test.

A multi-layered model for isothermal sliding frictional contact analysis of functionally graded materials (FGMs) with arbitrarily varying shear modulus under plane strain state is developed by Ke and Wang [26]. Ke and Wang [27] also considered a multi-layered model for frictionless contact analysis of functionally graded materials (FGMs) with arbitrarily varying elastic modulus under plane strain-state deformation.

Fracture initiation and propagation in a homogeneous coating due to sliding indentation is studied both experimentally and theoretically by Malzbender and With [28]. Using simplified closed form expressions for the stress intensity factors the authors try to estimate the critical crack length that would cause fracture.

Fracture of thin homogeneous elastic coatings due to sliding contact by a cylindrical indenter is investigated by Oliveira and Bower [29]. After calculating the contact stresses in the coating substrate system, several fracture problems in the coating and at the interface of the coating and substrate are studied.

Contact loading of orthotropic materials is investigated by Stephen ([30], [31]). These works show that a general procedure for calculating stress due to contact

loading can be obtained by combining two solution techniques. The first is the procedure outlined by Willis, in which the numerical contour integration is used to determine the size and aspect ratio of the elliptical contact area, and the contact pressure distribution. Detailed stress fields are then obtained by using these parameters in the general solution for transverse pressure loading of laminated orthotropic materials due to Pagano and Srinivas and Rao.

Mahajan [32] considers contact behavior of an orthotropic laminated beam indented by a rigid cylinder. In this research, the influence of various parameters such as beam thickness, indenter size, presence of compliant layer and delamination on the contact behavior of a symmetric orthotropic laminate is studied.

A plane contact problem for an orthotropic strip is considered by Erbas et al. [33]. In this study, a singular integral equation is derived for the contact pressure. The analytic expression of the associated kernel is unique for all types of orthotropy. An iterative solution method is developed to investigate a thick strip.

De and Patra [34] consider dynamic punch problems in an orthotropic elastic half-plane. In this study, complex variable technique is employed to obtain closed form solution of the elastodynamic problems of a single moving punch and a row of equally spaced identical moving punches, situated along the boundary of a semi-infinite orthotropic elastic medium.

In the contact problem of a rigid flat-ended punch on an elastic half-plane, the contact stress under punch is studied by Chen et al. [35]. In the research, a fundamental solution for the multiple flat punch problems on the elastic half-plane is investigated where the punches are disconnected and the forces applied on the punches are arbitrary. The singular integral equation method is suggested to obtain the fundamental solution. Also the contact problem for rigidly connected punches on an elastic half-plane is considered.

Lin [36] considers punch problem for planar anisotropic elastic half-plane. Four different conditions of contact problem for the rigid punch are analyzed in this study. From the surface traction and Green's function of anisotropic half-plane, the full-field solutions of stresses are constructed. Numerical calculations of surface traction under the rigid punch are presented base on the analysis and are discussed.

Sliding punches with or without friction along the surface of an anisotropic elastic half-plane is considered by Hwu and Fan [37]. In this research, a general unified solution for the full field stresses and displacements is derived by the complex-variable formulation. With this general full field solution, a simple unified solution for the contact pressure and surface deformation is derived.

1.2 Scope of the Research

The main objective of this study is to examine the problem of surface cracking in orthotropic materials due to sliding contact. As mentioned Section 1.1 solutions of certain contact and crack problems of plane elasticity are available in the technical literature. Some basic crack geometries in orthotropic materials have been considered until now. Also, several contact mechanics problems for orthotropic materials have been solved. Coupled crack and contact problems for isotropic materials have also been examined. But, there are no previous studies examining the behavior of a surface crack located in a homogeneous orthotropic medium subjected to sliding contact.

It is known that in mechanical structures, many failures occur due to the fracture. Under the applications involving high stress, friction or wear, crack initiation and propagation may take place. The surface cracking which is caused by friction forces and leading to fretting fatigue is within the scope of this problem (see [38] for details). To estimate the subcritical growth of a surface crack under contact stress, the mixed mode stress intensity factors at the tip of the crack are needed.

In Chapter 2, a solution method to examine the fracture problem due to sliding contact in an orthotropic medium is developed. To solve the surface crack, contact and coupled crack/contact problems in an orthotropic medium, a formulation is developed by using Fourier transformation technique. In the crack problem, surface crack in the orthotropic medium under mixed mode loading conditions is considered. For homogeneous materials, mode I and mode II problems can be solved in uncoupled form. Then the coupled crack and contact problem in an orthotropic half-plane is considered. The coupled problem is reduced to three singular integral equations, and singular behavior of the solution at the end points is examined. In order to solve the integral equations, methods are developed for stamps of flat, triangular and circular profiles. Numerical results of the problem are given in Chapter 3. Numerical results are given for mixed mode stress intensity factors at the crack tip, contact stresses and required normal contact force. The results obtained for an isotropic medium are compared with those of given by Dag [40] and accuracy of the solution is verified. Contact stress calculation is verified by making comparisons to the results given by Galin [46]. The effect of the material properties and friction coefficient on the mixed mode stress intensity factors at the crack tip, contact stresses and required contact force are examined for the mentioned profiles. In Chapter 4, conclusions obtained in this study are summarized.

CHAPTER 2

PROBLEM STATEMENT AND FORMULATION

2.1 Problem Definition

In this study, orthotropic materials are considered. The configuration of the problem to be examined is depicted in Figure 2.1. An orthotropic elastic half - plane is in sliding frictional contact with a rigid stamp of an arbitrary profile. The contact area extends from $x_2 = a$ to $x_2 = b$ at the surface and the half-plane contains an edge crack of length d . The crack is perpendicular to the boundary of the half-plane. The normal and tangential forces transferred by the contact are P and $Q = \eta P$, respectively, where η is the coefficient of friction. E_1 , E_2 and μ represent the Young's moduli and shear modulus of the half-plane respectively and ν is the Poissons's ratio .

2.2 Formulation of the Problem

First, the boundary conditions that must be satisfied in the solution of the problem are expressed. There are mixed boundary conditions at the surface $x_1 = 0$ and at the crack plane $x_2 = 0$. At the surface of the half-plane $x_1 = 0$, shear and normal stresses are zero outside the contact area. In the contact area, normal displacement component $u_1(0, x_2)$ is known. Normal displacement derivative with respect to x_2 is related to the stamp profile and this derivative can be represented as a function of x_2 . At the crack plane $x_2 = 0$, shear and normal stresses are zero at the crack faces. The faces displace relative to each other in normal and tangential directions, but outside

the crack i.e. for $x_1 > d$, there is no relative tangential or normal displacement at $x_2 = 0$ plane. Integration of the normal stresses in the contact area gives the total force P applied to the stamp and stresses must vanish as $(x_1^2 + x_2^2) \rightarrow \infty$. Shear stress in the contact area is represented by Coulomb's Law.

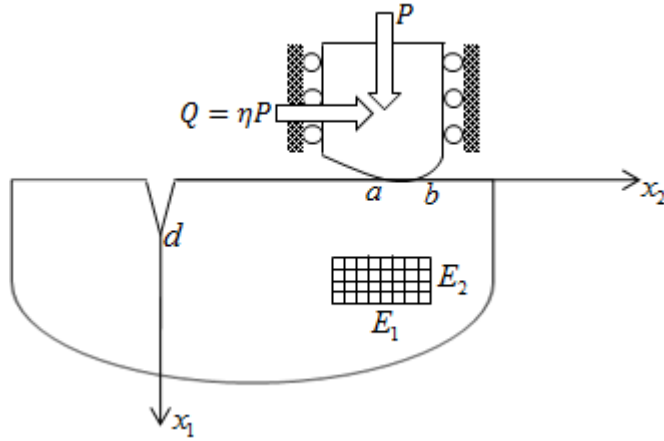


Figure 2.1: Geometry of the problem

The boundary conditions can be expressed in the following form:

$$\sigma_{11}(0, x_2) = 0, \quad x_2 < a \text{ and } x_2 > b, \quad (2.1a)$$

$$\sigma_{12}(0, x_2) = 0, \quad x_2 < a \text{ and } x_2 > b, \quad (2.1b)$$

$$\frac{C_{66}}{2} \frac{\partial}{\partial x_2} u_1(0, x_2) = f(x_2), \quad a < x_2 < b, \quad (2.1c)$$

$$\sigma_{12}(0, x_2) = \eta \sigma_{11}(0, x_2), \quad a < x_2 < b, \quad (2.1d)$$

$$\sigma_{22}(x_1, 0) = 0, \quad 0 < x_1 < d, \quad (2.1e)$$

$$\sigma_{12}(x_1, 0) = 0, \quad 0 < x_1 < d, \quad (2.1f)$$

$$\int_a^b \sigma_{11}(0, x_2) dx_2 = -P, \quad (2.1g)$$

$$(\sigma_{22}, \sigma_{12}, \sigma_{11}) \rightarrow 0 \text{ as } (x_1^2 + x_2^2) \rightarrow \infty, \quad (2.1h)$$

where $u_1(x_1, x_2)$ is the normal displacement component, $f(x_2)$ is a known function and C_{66} is a material property, related to shear modulus, given by (2.4a). The problem is formulated using three unknown functions. Following unknown functions can be defined:

$$\frac{C_{66}}{2} \frac{\partial}{\partial x_1} (u_2(x_1, 0^+) - u_2(x_1, 0^-)) = f_1(x_1), \quad 0 < x_1 < d, \quad (2.2a)$$

$$\frac{C_{66}}{2} \frac{\partial}{\partial x_1} (u_1(x_1, 0^+) - u_1(x_1, 0^-)) = f_2(x_1), \quad 0 < x_1 < d, \quad (2.2b)$$

$$\sigma_{11}(0, x_2) = f_3(x_2), \quad a < x_2 < b, \quad (2.2c)$$

where u_1 and u_2 are the displacement components in x_1 and x_2 directions, respectively.

In the absence of body forces equations of equilibrium are expressed as follows:

$$\frac{\partial \sigma_{11}}{\partial x_1} + \frac{\partial \sigma_{12}}{\partial x_2} = 0, \quad (2.3a)$$

$$\frac{\partial \sigma_{12}}{\partial x_1} + \frac{\partial \sigma_{22}}{\partial x_2} = 0. \quad (2.3b)$$

The constitutive relations of orthotropic materials can be represented in the following form (see [39] for details):

$$\begin{bmatrix} \sigma_{11} \\ \sigma_{22} \\ \sigma_{12} \end{bmatrix} = \begin{bmatrix} C_{11} & C_{12} & 0 \\ C_{12} & C_{22} & 0 \\ 0 & 0 & C_{66} \end{bmatrix} \begin{bmatrix} \varepsilon_{11} \\ \varepsilon_{22} \\ \varepsilon_{12} \end{bmatrix}, \quad (2.4a)$$

where,

$$C_{11} = \begin{cases} \frac{E_1^2}{E_1 - \nu_{12}^2 E_2}, & \text{plane stress} \\ \frac{(1 - \nu_{23} \nu_{32}) E_1^2}{\Delta}, & \text{plane strain} \end{cases} \quad (2.4b)$$

$$C_{12} = \begin{cases} \frac{\nu_{12} E_1 E_2}{E_1 - \nu_{12}^2 E_2}, & \text{plane stress} \\ \frac{(\nu_{12} + \nu_{13} \nu_{32}) E_1 E_2}{\Delta}, & \text{plane strain} \end{cases} \quad (2.4c)$$

$$C_{22} = \begin{cases} \frac{E_1 E_2}{E_1 - \nu_{12}^2 E_2}, & \text{plane stress} \\ \frac{(1 - \nu_{31} \nu_{13}) E_1 E_2}{\Delta}, & \text{plane strain} \end{cases} \quad (2.4d)$$

$$C_{66} = 2 \mu_{12} \quad \text{for both plane stress and plane strain} \quad (2.4e)$$

and

$$\Delta = E_1 (1 - \nu_{23} \nu_{32} - \nu_{31} \nu_{13} + \nu_{31} \nu_{13} \nu_{23} \nu_{32}) - E_2 (\nu_{12}^2 + 2 \nu_{12} \nu_{13} \nu_{32} + \nu_{13}^2 \nu_{32}^2), \quad (2.4f)$$

In the case of an orthotropic material (which has three mutually perpendicular planes of material symmetry), the number of elastic constants is nine for a 3D stress state. For plane stress case, constitutive relations of orthotropic materials can be represented in terms of four independent elastic parameters. For plane strain case, there are seven independent elastic parameters in constitutive relations (see [39] for details). Substituting equations (2.4) into equations (2.3), governing equations are obtained as:

$$d_{11} \frac{\partial^2 u_1}{\partial x_1^2} + \frac{\partial^2 u_1}{\partial x_2^2} + (1+d_{12}) \frac{\partial^2 u_2}{\partial x_1 x_2} = 0, \quad (2.5a)$$

$$\frac{\partial^2 u_2}{\partial x_1^2} + d_{22} \frac{\partial^2 u_2}{\partial x_2^2} + (1+d_{12}) \frac{\partial^2 u_1}{\partial x_1 x_2} = 0, \quad (2.5b)$$

where,

$$d_{11} = \frac{2C_{11}}{C_{66}}, \quad (2.5c)$$

$$d_{12} = \frac{2C_{12}}{C_{66}}, \quad (2.5d)$$

$$d_{22} = \frac{2C_{22}}{C_{66}}. \quad (2.5e)$$

Adopted solution procedure is shown in Figure 2.2. In this figure, the contact problem without crack is represented as Problem 1 and in this case the stresses and displacements will be determined in terms of f_3 which is given by (2.2c). In Problem 2, stress and displacement fields will be determined in terms of the f_1 and f_2 given by (2.2a) and (2.2b). For contact problem (problem 1), f_1 and f_2 are zero and f_3 is zero for crack problem (problem 2). By summing the solutions of problems 1 and 2, the total stress and displacement fields for the original problem can be obtained and the boundary conditions of the original coupled problem can be satisfied.

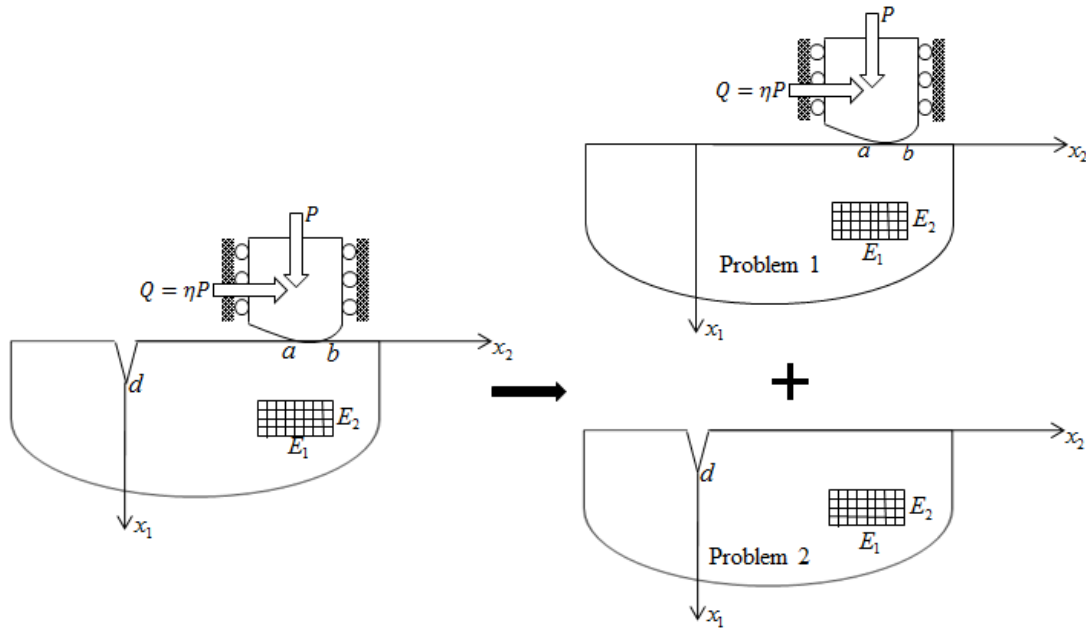


Figure 2.2: Solution Procedure

2.2.1 Problem 1: The Contact Problem

Geometry of the contact problem is shown in Figure 2.3. The primary unknown function is,

$$\sigma_{11}(0, x_2) = \begin{cases} f_3(x_2), & a < x_2 < b \\ 0, & -\infty < x_2 < a \text{ and } b < x_2 < \infty. \end{cases} \quad (2.6)$$

Shear stress at the surface can be written as follows:

$$\sigma_{12}(0, x_2) = \begin{cases} \eta f_3(x_2), & a < x_2 < b \\ 0, & -\infty < x_2 < a \text{ and } b < x_2 < \infty, \end{cases} \quad (2.7)$$

where η is the friction coefficient. The stress and displacement fields are derived in terms of $f_3(x_2)$.

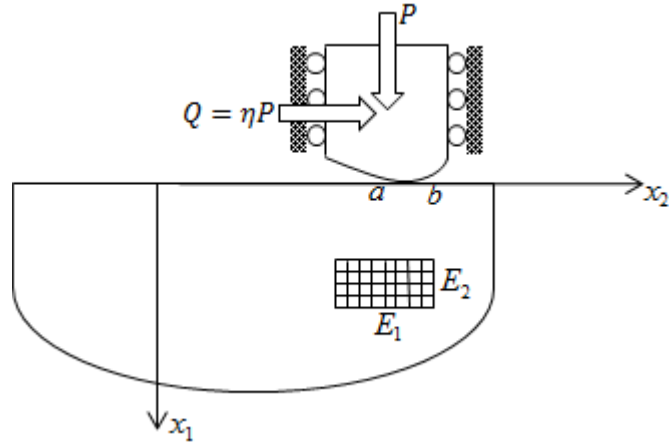


Figure 2.3: Geometry of the contact problem

Considering Fourier Transformation in x_2 direction, the displacement components can be expressed as follows:

$$u_{13}(x_1, x_2) = \frac{1}{2\pi} \int_{-\infty}^{\infty} U_{13}(x_1, \rho) \exp(i \rho x_2) d\rho, \quad (2.8a)$$

$$u_{23}(x_1, x_2) = \frac{1}{2\pi} \int_{-\infty}^{\infty} U_{23}(x_1, \rho) \exp(i \rho x_2) d\rho. \quad (2.8b)$$

In equations (2.8), subscript 3 represents the displacements due to stamp loading. Substituting (2.8) in (2.5), following ordinary differential equations are obtained.

$$d_{11} \frac{d^2 U_{13}}{d x_1^2} - \rho^2 U_{13} + (1 + d_{12}) i \rho \frac{d U_{23}}{d x_1} = 0, \quad (2.9a)$$

$$\frac{d^2 U_{23}}{d x_1^2} - \rho^2 d_{22} U_{23} + (1 + d_{12}) i \rho \frac{d U_{13}}{d x_1} = 0. \quad (2.9b)$$

One can assume a solution of the form $\exp(s x_1)$ for U_{13} and U_{23} . Then, following characteristic equation is determined,

$$s^4 - \frac{\rho^2 (d_{11} d_{22} - 2d_{12} - d_{12}^2)}{d_{11}} s^2 + \frac{\rho^4 d_{22}}{d_{11}} = 0. \quad (2.10)$$

For $-\frac{\rho^2 (d_{11} d_{22} - 2d_{12} - d_{12}^2)}{d_{11}} < 0$, $\left(-\frac{\rho^2 (d_{11} d_{22} - 2d_{12} - d_{12}^2)}{d_{11}}\right)^2 - 4 \frac{\rho^4 d_{22}}{d_{11}} > 0$ there are four real roots, $s_1, s_2, s_3 = -s_1, s_4 = -s_2$ in this case the corresponding material is classified as type I [3].

If the roots are complex, the related material is classified as type II. The problem of interest here is that of type I. Assuming type I, roots are written as,

$$s_1 = -A|\rho|, \quad \Re(s_1) < 0, \quad (2.11a)$$

$$s_2 = -B|\rho|, \quad \Re(s_2) < 0, \quad (2.11b)$$

$$s_3 = A|\rho|, \quad \Re(s_3) > 0, \quad (2.11c)$$

$$s_4 = B|\rho|, \quad \Re(s_4) > 0, \quad (2.11d)$$

where,

$$A = \frac{\sqrt{2}}{2d_{11}} \sqrt{d_{11} \left(\frac{d_{11} d_{22} - 2d_{12} - d_{12}^2}{+\sqrt{d_{11}^2 d_{22}^2 - 4d_{11} d_{22} d_{12} - 2d_{11} d_{22} d_{12}^2 + 4d_{12}^2 + 4d_{12}^3 + d_{12}^4 - 4d_{11} d_{22}}} \right)}, \quad (2.12a)$$

$$B = \frac{1}{2d_{11}} \sqrt{-2d_{11} \left(\frac{-d_{11} d_{22} + 2d_{12} + d_{12}^2}{+\sqrt{d_{11}^2 d_{22}^2 - 4d_{11} d_{22} d_{12} - 2d_{11} d_{22} d_{12}^2 + 4d_{12}^2 + 4d_{12}^3 + d_{12}^4 - 4d_{11} d_{22}}} \right)}. \quad (2.12b)$$

The displacement components u_{13} and u_{23} can then be written as

$$u_{13}(x_1, x_2) = \frac{1}{2\pi} \int_{-\infty}^{\infty} \sum_{j=1}^2 M_j \exp(s_j x_1 + i \rho x_2) d\rho, \quad (2.13a)$$

$$u_{23}(x_1, x_2) = \frac{1}{2\pi} \int_{-\infty}^{\infty} \sum_{j=1}^2 M_j N_j \exp(s_j x_1 + i \rho x_2) d\rho, \quad (2.13b)$$

where $M_j(\rho)$ are unknown functions and

$$N_j(\rho) = \frac{\rho^2 - d_{11}s_j^2}{(1 + d_{12})i\rho s_j}, \quad (j=1, 2). \quad (2.14)$$

By using equation (2.4a), stresses and displacement derivative can be obtained as follows:

$$\sigma_{113}(x_1, x_2) = \frac{C_{66}}{2} \frac{1}{2\pi} \int_{-\infty}^{\infty} \sum_{j=1}^2 (d_{11}s_j + d_{12}N_j i\rho) M_j \exp(s_j x_1 + i\rho x_2) d\rho, \quad (2.15a)$$

$$\sigma_{223}(x_1, x_2) = \frac{C_{66}}{2} \frac{1}{2\pi} \int_{-\infty}^{\infty} \sum_{j=1}^2 (d_{12}s_j + d_{22}N_j i\rho) M_j \exp(s_j x_1 + i\rho x_2) d\rho, \quad (2.15b)$$

$$\sigma_{123}(x_1, x_2) = \frac{C_{66}}{2} \frac{1}{2\pi} \int_{-\infty}^{\infty} \sum_{j=1}^2 (i\rho + N_j s_j) M_j \exp(s_j x_1 + i\rho x_2) d\rho, \quad (2.15c)$$

$$\frac{\partial}{\partial x_2} u_{13}(x_1, x_2) = \frac{1}{2\pi} \int_{-\infty}^{\infty} i\rho \sum_{j=1}^2 M_j \exp(s_j x_1 + i\rho x_2) d\rho. \quad (2.15d)$$

Using the boundary conditions (2.6) and (2.7), following equations can be written,

$$\begin{aligned} & \frac{1}{2\pi} \int_{-\infty}^{\infty} \sum_{j=1}^2 (C_{11}s_j + C_{12}N_j i\rho) M_j \exp(i\rho x_2) d\rho \\ & = \begin{cases} f_3(x_2), & a < x_2 < b \\ 0, & -\infty < x_2 < a \text{ and } b < x_2 < \infty \end{cases}, \end{aligned} \quad (2.16a)$$

$$\frac{C_{66}}{2} \frac{1}{2\pi} \int_{-\infty}^{\infty} \sum_{j=1}^2 (i\rho + N_j s_j) M_j \exp(i\rho x_2) d\rho$$

$$= \begin{cases} \eta f_3(x_2), & a < x_2 < b \\ 0, & -\infty < x_2 < a \text{ and } b < x_2 < \infty, \end{cases} \quad (2.16b)$$

and $M_j(\rho)$ can be expressed as follows:

$$M_j(\rho) = \frac{2}{C_{66}} \psi_j(\rho) \int_a^b f_3(t) \exp(-i\rho t) dt. \quad (2.17)$$

To determine $\psi_j(\rho)$, Fourier transform is applied to (2.16) and using (2.17), following equations are obtained,

$$\sum_{j=1}^2 (d_{11} s_j + d_{12} N_j i\rho) \psi_j(\rho) = 1, \quad (2.18a)$$

$$\sum_{j=1}^2 (i\rho + N_j s_j) \psi_j(\rho) = \eta. \quad (2.18b)$$

At this point, the formulation of the contact problem for an orthotropic half-plane is completed. Stress and displacement field are expressed in terms of the unknown function $f_3(x_2)$ by equations (2.13), (2.15), (2.17) and (2.18).

2.2.2 Problem 2: The Crack Problem

Figure 2.4 presents the geometry of the surface crack problem in an orthotropic half-plane. In this case stresses and displacements are derived in terms of f_1 and f_2 given by (2.2a) and (2.2b). In order to formulate the crack problem, a superposition method is used as shown in Figure 2.5. In this method, a crack in an infinite plane and the half-plane solution for $x_1 > 0$ are considered and these solutions are

superimposed so as to satisfy the boundary conditions at the free surface. Then, the stresses and displacements are derived.

The half-plane contains a surface crack at $x_2 = 0$ and mixed mode loading conditions appear on the crack plane. For this crack, the mode I (or the opening mode) and mode II (or the sliding mode) problems can be considered as uncoupled. This is due to the fact that, normal loading on crack faces does not induce mode II stress intensity factor and shear loading does not induce mode I stress intensity factor. Also mode I and mode II problems can be formulated separately.

In each problem first the infinite plane containing a crack is considered and stress and displacement fields are derived in terms of f_1 and f_2 which are given by (2.2a) and (2.2b), respectively. In this case, Fourier transforms of the equations (2.5) can be taken in x_1 direction, and solving the resulting system of ordinary differential equations stress and displacement expressions for both half-planes $x_2 > 0$ and $x_2 < 0$ can be obtained. Then, the general solution of a half-plane without a crack and the infinite plane solution will be superimposed to satisfy the boundary conditions at the free surface.

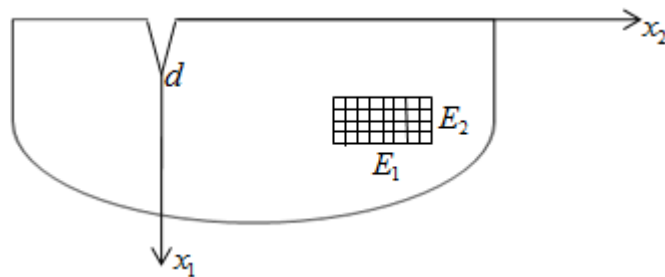


Figure 2.4: Geometry of the crack problem

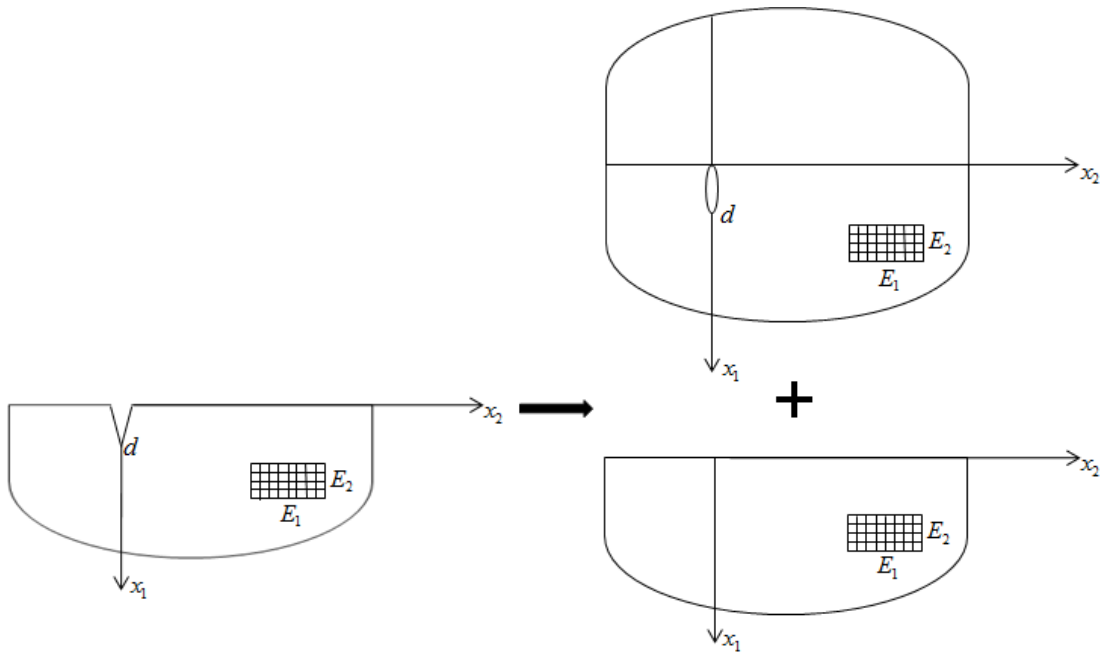


Figure 2.5: Superimposition for the crack problem

2.2.2.1 The Opening Mode Problem ($f_2 = 0$)

In order to solve the opening mode problem, a crack in an infinite plane located at $0 < x_1 < d$ is considered. In this case, $f_2(x_1)$ given by (2.2b) is equal to zero. The stress and displacement fields are derived in terms of $f_1(x_1)$ given by (2.2a). By using Fourier integrals, displacement components for the infinite plane are expressed as follows:

$$u_{11}^{(i)}(x_1, x_2) = \frac{1}{2\pi} \int_{-\infty}^{\infty} U_{11}^{(i)}(\omega, x_2) \exp(i\omega x_1) d\omega, \quad (2.19a)$$

$$u_{21}^{(i)}(x_1, x_2) = \frac{1}{2\pi} \int_{-\infty}^{\infty} U_{21}^{(i)}(\omega, x_2) \exp(i\omega x_1) d\omega, \quad (2.19b)$$

where subscript 1 and superscript (i) stand for opening mode problem and an infinite medium, respectively. Substituting (2.19) in (2.5) following differential equations are determined:

$$-d_{11} \omega^2 U_{11}^{(i)} + \frac{d^2 U_{11}^{(i)}}{d x_2^2} - \rho^2 U_{13} + (1 + d_{12}) i \omega \frac{d U_{21}^{(i)}}{d x_2} = 0, \quad (2.20a)$$

$$-\omega^2 U_{21}^{(i)} + d_{22} \frac{d^2 U_{21}^{(i)}}{d x_2^2} - \rho^2 U_{13} + (1 + d_{12}) i \omega \frac{d U_{11}^{(i)}}{d x_2} = 0. \quad (2.20b)$$

One can assume a solution of the form $\exp(n x_2)$. By using this form, the characteristic equation of the problem is determined as,

$$n^4 - \frac{\omega^2 (d_{11} d_{22} - 2 d_{12} - d_{12}^2)}{d_{22}} n^2 + \frac{\omega^4 d_{11}}{d_{22}} = 0. \quad (2.21)$$

Roots of the characteristic equation for a type I material are found to be

$$n_1 = E|\omega|, \quad \Re(n_1) > 0, \quad (2.22a)$$

$$n_2 = F|\omega|, \quad \Re(n_2) > 0, \quad (2.22b)$$

$$n_3 = -E|\omega|, \quad \Re(n_3) < 0, \quad (2.22c)$$

$$n_4 = -F|\omega|, \quad \Re(n_4) < 0, \quad (2.22d)$$

where

$$E = \frac{\sqrt{2}}{2d_{22}} \sqrt{d_{22} \left(\frac{d_{11} d_{22} - 2d_{12} - d_{12}^2}{\sqrt{d_{11}^2 d_{22}^2 - 4d_{11} d_{22} d_{12} - 2d_{11} d_{22} d_{12}^2 + 4d_{12}^2 + 4d_{12}^3 + d_{12}^4 - 4d_{11} d_{22}}} \right)}, \quad (2.23a)$$

$$F = \frac{1}{2d_{22}} \sqrt{-2d_{22} \left(\frac{-d_{11} d_{22} + 2d_{12} + d_{12}^2}{\sqrt{d_{11}^2 d_{22}^2 - 4d_{11} d_{22} d_{12} - 2d_{11} d_{22} d_{12}^2 + 4d_{12}^2 + 4d_{12}^3 + d_{12}^4 - 4d_{11} d_{22}}} \right)}. \quad (2.23b)$$

Following stresses and displacements equations are obtained for $x_2 < 0$ and $x_2 > 0$,

$x_2 < 0$:

$$u_{11}^{(i^-)}(x_1, x_2) = \frac{1}{2\pi} \int_{-\infty}^{\infty} \sum_{j=1}^2 C_j \exp(n_j x_2 + i \omega x_1) d\omega, \quad (2.24a)$$

$$u_{21}^{(i^-)}(x_1, x_2) = \frac{1}{2\pi} \int_{-\infty}^{\infty} \sum_{j=1}^2 C_j A_j \exp(n_j x_2 + i \omega x_1) d\omega, \quad (2.24b)$$

$$\sigma_{111}^{(i^-)}(x_1, x_2) = \frac{C_{66}}{2} \frac{1}{2\pi} \int_{-\infty}^{\infty} \sum_{j=1}^2 S_{111j}^{(i^-)}(\omega) \exp(n_j x_2 + i \omega x_1) d\omega, \quad (2.24c)$$

$$\sigma_{221}^{(i^-)}(x_1, x_2) = \frac{C_{66}}{2} \frac{1}{2\pi} \int_{-\infty}^{\infty} \sum_{j=1}^2 S_{221j}^{(i^-)}(\omega) \exp(n_j x_2 + i \omega x_1) d\omega, \quad (2.24d)$$

$$\sigma_{121}^{(i^-)}(x_1, x_2) = \frac{C_{66}}{2} \frac{1}{2\pi} \int_{-\infty}^{\infty} \sum_{j=1}^2 (n_j + i \omega A_j) C_j \exp(n_j x_2 + i \omega x_1) d\omega, \quad (2.24e)$$

$$\frac{\partial}{\partial x_2} u_{11}^{(i^-)}(x_1, x_2) = \frac{1}{2\pi} \int_{-\infty}^{\infty} \sum_{j=1}^2 C_j n_j \exp(n_j x_2 + i \omega x_1) d\omega, \quad (2.24f)$$

$$S_{111j}^{(i^-)}(x_1, x_2) = \sum_{j=1}^2 (d_{11} i \omega + d_{12} A_j n_j) C_j, \quad (2.24g)$$

$$S_{221j}^{(i^-)}(x_1, x_2) = \sum_{j=1}^2 (d_{12} i \omega + d_{22} A_j n_j) C_j, \quad (2.24h)$$

where superscript (i^-) refers to $x_2 < 0$.

$x_2 > 0$:

$$u_{11}^{(i^+)}(x_1, x_2) = \frac{1}{2\pi} \int_{-\infty}^{\infty} \sum_{j=3}^4 C_j \exp(n_j x_2 + i \omega x_1) d\omega, \quad (2.25a)$$

$$u_{21}^{(i^+)}(x_1, x_2) = \frac{1}{2\pi} \int_{-\infty}^{\infty} \sum_{j=3}^4 C_j A_j \exp(n_j x_2 + i \omega x_1) d\omega, \quad (2.25b)$$

$$\sigma_{111}^{(i^+)}(x_1, x_2) = \frac{C_{66}}{2} \frac{1}{2\pi} \int_{-\infty}^{\infty} \sum_{j=3}^4 S_{111j}^{(i^+)}(\omega) \exp(n_j x_2 + i \omega x_1) d\omega, \quad (2.25c)$$

$$\sigma_{221}^{(i^+)}(x_1, x_2) = \frac{C_{66}}{2} \frac{1}{2\pi} \int_{-\infty}^{\infty} \sum_{j=3}^4 S_{221j}^{(i^+)}(\omega) \exp(n_j x_2 + i \omega x_1) d\omega, \quad (2.25d)$$

$$\sigma_{121}^{(i^+)}(x_1, x_2) = \frac{C_{66}}{2} \frac{1}{2\pi} \int_{-\infty}^{\infty} \sum_{j=3}^4 (n_j + i \omega A_j) C_j \exp(n_j x_2 + i \omega x_1) d\omega, \quad (2.25e)$$

$$\frac{\partial}{\partial x_2} u_{11}^{(i^+)}(x_1, x_2) = \frac{1}{2\pi} \int_{-\infty}^{\infty} \sum_{j=3}^4 C_j n_j \exp(n_j x_2 + i \omega x_1) d\omega, \quad (2.25f)$$

$$S_{111j}^{(i^+)}(x_1, x_2) = \sum_{j=3}^4 (d_{11} i \omega + d_{12} A_j n_j) C_j, \quad (2.25g)$$

$$S_{221j}^{(i^+)}(x_1, x_2) = \sum_{j=3}^4 (d_{12} i \omega + d_{22} A_j n_j) C_j, \quad (2.25h)$$

where superscript (i^+) refers to $x_2 > 0$. $C_j(\omega)$ ($j=1,2,3,4$) are unknown functions given in (2.24) and (2.25) and $A_j(\omega)$ is obtained as

$$A_j(\omega) = \frac{d_{11} \omega^2 - n_j^2}{(1 + d_{12}) i \omega n_j}, \quad (j=1,2,3,4). \quad (2.26)$$

Now, the half-plane ($x_1 > 0$) problem without a crack is considered. For the opening mode problem, $u_{11}(x_1, x_2)$ is an even function of x_2 and $u_{21}(x_1, x_2)$ is an odd function of x_2 ; therefore, for the half-plane ($x_1 > 0$) problem without a crack, the displacement components can be expressed by using Fourier cosine and sine integrals as follows:

$$u_{11}^{(h)}(x_1, x_2) = \int_0^{\infty} U_{11}^{(h)}(x_1, \alpha) \cos(\alpha x_2) d\alpha, \quad (2.27a)$$

$$u_{21}^{(h)}(x_1, x_2) = \int_0^{\infty} U_{21}^{(h)}(x_1, \alpha) \sin(\alpha x_2) d\alpha, \quad (2.27b)$$

where subscript 1 and superscript h stand for opening mode and half-plane problems, respectively. Equation (2.27) implies that $u_{11}^{(h)}(x_1, x_2) = u_{11}^{(h)}(x_1, -x_2)$, $u_{21}^{(h)}(x_1, x_2) = -u_{21}^{(h)}(x_1, -x_2)$. Substituting (2.27) in (2.5), differential equations are obtained as:

$$d_{11} \frac{d^2 U_{11}^{(h)}}{d x_1^2} - \alpha^2 U_{11}^{(h)} + (1 + d_{12}) \alpha \frac{d U_{21}^{(h)}}{d x_1} = 0, \quad (2.28a)$$

$$\frac{d^2 U_{21}^{(h)}}{d x_1^2} - \alpha^2 d_{22} U_{21}^{(h)} - (1 + d_{12}) \alpha \frac{d U_{11}^{(h)}}{d x_1} = 0. \quad (2.28b)$$

One can assume a solution of the form $\exp(p x_1)$. By using this form, the characteristic equation of the problem is determined in the form:

$$p^4 - \frac{\alpha^2 (d_{11} d_{22} - 2 d_{12} - d_{12}^2)}{d_{11}} p^2 + \frac{\alpha^4 d_{22}}{d_{11}} = 0. \quad (2.29)$$

Roots of the characteristic equation for a type I material are found to be

$$p_1 = A|\alpha|, \quad \Re(p_1) > 0, \quad (2.30a)$$

$$p_2 = B|\alpha|, \quad \Re(p_2) > 0, \quad (2.30b)$$

$$p_3 = -A|\alpha|, \quad \Re(p_3) < 0, \quad (2.30c)$$

$$p_4 = -B|\alpha|, \quad \Re(p_4) < 0. \quad (2.30d)$$

where, A and B are given by (2.12).

For the half-plane problem ($x_1 > 0$), the stresses and displacements are determined as follows:

$$u_{11}^{(h)}(x_1, x_2) = \int_0^{\infty} (B_3 \exp(p_3 x_1) + B_4 \exp(p_4 x_1)) \cos(\alpha x_2) d\alpha, \quad (2.31a)$$

$$u_{21}^{(h)}(x_1, x_2) = \int_0^{\infty} (B_3 D_3 \exp(p_3 x_1) + B_4 D_4 \exp(p_4 x_1)) \sin(\alpha x_2) d\alpha, \quad (2.31b)$$

$$\sigma_{111}^{(h)}(x_1, x_2) = \frac{C_{66}}{2} \int_0^{\infty} \sum_{j=3}^4 (d_{11} p_j + d_{12} D_j \alpha) B_j \exp(p_j x_1) \cos(\alpha x_2) d\alpha, \quad (2.31c)$$

$$\sigma_{221}^{(h)}(x_1, x_2) = \frac{C_{66}}{2} \int_0^{\infty} \sum_{j=3}^4 (d_{12} p_j + d_{22} D_j \alpha) B_j \exp(p_j x_1) \cos(\alpha x_2) d\alpha, \quad (2.31d)$$

$$\sigma_{121}^{(h)}(x_1, x_2) = \frac{C_{66}}{2} \int_0^{\infty} \sum_{j=3}^4 (D_j p_j - \alpha) B_j \exp(p_j x_1) \sin(\alpha x_2) d\alpha, \quad (2.31e)$$

$$\frac{\partial}{\partial x_2} u_{11}^{(h)}(x_1, x_2) = - \int_0^{\infty} \alpha (B_3 \exp(p_3 x_1) + B_4 \exp(p_4 x_1)) \sin(\alpha x_2) d\alpha, \quad (2.31f)$$

where $B_j(\omega)$ ($j=3,4$) are unknown functions and $D_j(\alpha)$ is expressed as follows:

$$D_j(\alpha) = \frac{\alpha^2 - d_{11} p_j^2}{(1 + d_{12}) \alpha p_j}. \quad (2.32)$$

The solution of mode I problem for $x_1 > 0$ and $x_2 > 0$ can be expressed as follows:

$$u_{11}(x_1, x_2) = u_{11}^{(i^+)}(x_1, x_2) + u_{11}^{(h)}(x_1, x_2), \quad x_1 > 0, x_2 > 0, \quad (2.33a)$$

$$u_{21}(x_1, x_2) = u_{21}^{(i^+)}(x_1, x_2) + u_{21}^{(h)}(x_1, x_2), \quad x_1 > 0, x_2 > 0, \quad (2.33b)$$

$$\sigma_{kj1}(x_1, x_2) = \sigma_{kj1}^{(i^+)}(x_1, x_2) + \sigma_{kj1}^{(h)}(x_1, x_2), \quad k, j=1, 2, \quad x_1 > 0, x_2 > 0. \quad (2.33c)$$

In the formulation, there are six unknown functions $C_1(\omega), \dots, C_4(\omega), B_3(\alpha), B_4(\alpha)$. These functions can be expressed in terms of unknown function $f_1(x_1)$.

Boundary conditions of the opening mode problem are determined as,

$$\sigma_{221}(x_1, +0) = \sigma_{221}(x_1, -0), \quad 0 < x_1 < \infty, \quad (2.34a)$$

$$\sigma_{121}(x_1, +0) = \sigma_{121}(x_1, -0), \quad 0 < x_1 < \infty, \quad (2.34b)$$

$$u_{11}(x_1, +0) = u_{11}(x_1, -0), \quad 0 < x_1 < \infty, \quad (2.34c)$$

$$\frac{C_{66}}{2} \frac{\partial}{\partial x_1} (u_{21}(x_1, +0) - u_{21}(x_1, -0)) = f_1(x_1), \quad 0 < x_1 < d, \quad (2.34d)$$

$$u_{21}(x_1, +0) = u_{21}(x_1, -0), \quad d < x_1 < \infty, \quad (2.34e)$$

$$\sigma_{111}(0, x_2) = 0, \quad -\infty < x_2 < \infty, \quad (2.34f)$$

$$\sigma_{121}(0, x_2) = 0, \quad -\infty < x_2 < \infty. \quad (2.34g)$$

In order to obtain $C_1(\omega), \dots, C_4(\omega)$ in terms of $f_1(x_1)$, equations (2.34a-e) and equations (2.24) and (2.25) are utilized and following equations are obtained,

$$C_j(\omega) = \frac{2}{C_{66}} P_j(\omega) \int_0^d f_1(t) \exp(-i\omega t) dt, \quad (j=1, 2, 3, 4), \quad (2.35a)$$

$$\sum_{j=3}^4 (i\omega d_{12} + A_j n_j d_{22}) P_j(\omega) - \sum_{j=1}^2 (i\omega d_{12} + A_j n_j d_{22}) P_j(\omega) = 0, \quad (2.35b)$$

$$\sum_{j=3}^4 (n_j + i\omega A_j) P_j(\omega) - \sum_{j=1}^2 (n_j + i\omega A_j) P_j(\omega) = 0, \quad (2.35c)$$

$$i\omega \left\{ \sum_{j=3}^4 A_j P_j(\omega) - \sum_{j=1}^2 A_j P_j(\omega) \right\} = 1, \quad (2.35d)$$

$$P_4(\omega) + P_3(\omega) - P_2(\omega) - P_1(\omega) = 0. \quad (2.35e)$$

Since the half-plane solution ($x_1 > 0$) does not include a crack, the half-plane solution ($x_1 > 0$) given by (2.31) and the unknown functions $B_3(\alpha)$ and $B_4(\alpha)$ do not contribute to equations (2.35). Boundary conditions (2.34a-e) are satisfied by the half-plane ($x_1 > 0$) solution. $B_3(\alpha)$ and $B_4(\alpha)$, which are the unknown functions of the half-plane ($x_1 > 0$) problem, are expressed in terms of $f_1(x_1)$ by using the free surface boundary conditions. So in the determination of $B_3(\alpha)$ and $B_4(\alpha)$, (2.34f), (2.34g), (2.31c), (2.31e), (2.25c) and (2.25e) are used and the following equations are obtained,

$$\int_0^{\infty} \sum_{j=3}^4 (d_{11} p_j + d_{12} D_j \alpha) B_j \cos(\alpha x_2) d\alpha + \frac{1}{2\pi} \int_{-\infty}^{\infty} \sum_{j=3}^4 (d_{11} i\omega + d_{12} A_j n_j) C_j \exp(n_j x_2) d\omega = 0, \quad 0 < x_2 < \infty, \quad (2.36a)$$

$$\int_0^{\infty} \sum_{j=3}^4 (D_j p_j - \alpha) B_j \sin(\alpha x_2) d\alpha + \frac{1}{2\pi} \int_{-\infty}^{\infty} \sum_{j=3}^4 (n_j + i\omega A_j) C_j \exp(n_j x_2) d\omega = 0, \quad 0 < x_2 < \infty. \quad (2.36b)$$

Because of the symmetry, only $x_2 > 0$ case is considered. $C_j(\omega)$ ($j=1, \dots, 4$) can be determined using (2.35a-e) in terms of f_1 . After lengthy manipulations using MAPLE (2.36) following equations are obtained,

$$\sum_{j=3}^4 (d_{11} p_j + d_{12} D_j \alpha) B_j(\alpha) = \frac{1}{\pi^2} \frac{2}{C_{66}} \int_0^d f_1(t) dt \int_{-\infty}^{\infty} F_{111}(\omega, \alpha) \exp(-i\omega t) d\omega, \quad (2.37a)$$

$$\sum_{j=3}^4 (D_j p_j - \alpha) B_j(\alpha) = -\frac{1}{\pi^2} \frac{2}{C_{66}} \int_0^d f_1(t) dt \int_{-\infty}^{\infty} F_{121}(\omega, \alpha) \exp(-i\omega t) d\omega, \quad (2.37b)$$

where,

$$F_{111}(\omega, \alpha) = \frac{N_{111}(\omega, \alpha)}{d_{11} D(\omega, \alpha)}, \quad (2.38a)$$

$$F_{121}(\omega, \alpha) = \frac{N_{121}(\omega, \alpha)}{d_{11} D(\omega, \alpha)}, \quad (2.38b)$$

$$\begin{aligned} N_{111}(\omega, \alpha) = & \frac{1}{2} i \omega (-d_{12} F^2 \omega^2 d_{11} E^2 d_{12} - d_{12} E^2 d_{12} F^2 \alpha^2 \\ & - d_{12} E^2 d_{11} \alpha^2 - d_{12} F^2 \omega^2 d_{11} E^2 + d_{12} d_{11}^2 \alpha^2 \\ & - d_{12} F^2 d_{11} \alpha^2 + E^2 F^2 d_{11} \omega^2 d_{12}^2 + E^2 F^2 d_{11} \omega^2 d_{12} \\ & - d_{11} d_{11} \alpha^2 d_{12} - d_{11} d_{11} \alpha^2), \end{aligned} \quad (2.39a)$$

$$N_{121}(\omega, \alpha) = \frac{1}{2} i \omega^2 (E^2 F^2 d_{12}^2 + E^2 d_{11} d_{12} + d_{11} F^2 d_{12} + d_{11}^2) \alpha, \quad (2.39b)$$

$$D(\omega, \alpha) = (F^2 \omega^2 + \alpha^2)(E^2 \omega^2 + \alpha^2)(1 + d_{12}), \quad (2.39c)$$

and, E and F are given by (2.23).

Residue theorem can be used to evaluate the inner integrals in (2.37) (for detailed explanation of the theorem see [41] and [42]). In order to apply this theorem, first a positively oriented simple contour in the complex plane is considered as shown in Figure 2.6.

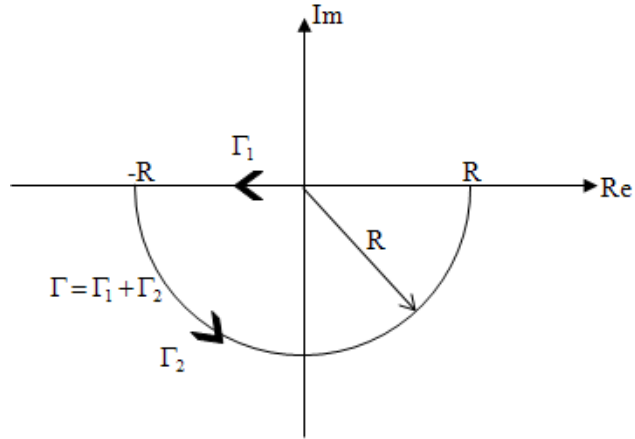


Figure 2.6: The contour for evaluation of the integral.

By considering the integration on the contour $\Gamma = \Gamma_1 + \Gamma_2$ is considered, following equation can be written.

$$\int_{\Gamma} F_{111}(\omega, \alpha) \exp(-i \omega t) d\omega = \int_{\Gamma_1} F_{111}(\omega, \alpha) \exp(-i \omega t) d\omega + \int_{\Gamma_2} F_{111}(\omega, \alpha) \exp(-i \omega t) d\omega. \quad (2.40)$$

If the integrand in (2.40) is analytic on the positively oriented simple closed contour Γ , except possibly for a finite number of singular points interior to Γ , using the residue theorem following equation can be written,

$$\int_{\Gamma} F_{111}(\omega, \alpha) \exp(-i \omega t) d\omega = 2\pi i \sum_{k=1}^n (\text{Residues of the integrand in } \Gamma). \quad (2.41)$$

Taking the limit as $R \rightarrow \infty$ in (2.40),

$$\begin{aligned}
& \int_{\infty}^{-\infty} F_{111}(\omega, \alpha) \exp(-i \omega t) d\omega + \lim_{R \rightarrow \infty} \int_{\Gamma_2} F_{111}(\omega, \alpha) \exp(-i \omega t) d\omega = \\
& = 2\pi i \sum_{k=1}^n (\text{Residues of the integrand in lower half complex plane}).
\end{aligned} \tag{2.42}$$

By using MAPLE, it can be shown that second term on the left hand side of (2.42) vanishes, then (2.40) can be rewritten as follows:

$$\begin{aligned}
& \int_{-\infty}^{\infty} F_{111}(\omega, \alpha) \exp(-i \omega t) d\omega = \\
& = -2\pi i \sum_{k=1}^n (\text{Residues of the integrand in lower half complex plane}).
\end{aligned} \tag{2.43}$$

The integral can be evaluated by determining the residues in the lower complex plane. The poles of the integrand in (2.43) are obtained as,

$$\omega_1 = \frac{i\alpha}{F}, \quad \Im(\omega_1) > 0, \tag{2.44a}$$

$$\omega_2 = -\frac{i\alpha}{F}, \quad \Im(\omega_2) < 0, \tag{2.44b}$$

$$\omega_3 = \frac{i\alpha}{E}, \quad \Im(\omega_3) > 0, \tag{2.44c}$$

$$\omega_4 = -\frac{i\alpha}{E}, \quad \Im(\omega_4) < 0. \tag{2.44d}$$

Imaginary parts of ω_2 and ω_4 are less than zero which means ω_2 and ω_4 are in lower half plane. Therefore, the poles of ω_2 and ω_4 are used to evaluate the integral. The integral can be written as follows:

$$\int_{-\infty}^{\infty} F_{111}(\omega, \alpha) \exp(-i \omega t) d\omega = -2\pi i \left[\lim_{\omega \rightarrow \omega_2} (\omega - \omega_2) F_{111}(\omega, \alpha) \exp(-i \omega t) + \lim_{\omega \rightarrow \omega_4} (\omega - \omega_4) F_{111}(\omega, \alpha) \exp(-i \omega t) \right]. \quad (2.45)$$

After lengthy calculations, the integral is evaluated as,

$$\int_{-\infty}^{\infty} F_{111}(\omega, \alpha) \exp(-i \omega t) d\omega = \frac{\pi}{2 d_{11} (E^2 - F^2) (1 + d_{12})} \times \left[R_1 \exp\left(-\frac{\alpha t}{F}\right) + R_2 \exp\left(-\frac{\alpha t}{E}\right) \right], \quad (2.46)$$

where,

$$R_1 = (E^2 d_{12} + d_{11}) (d_{11} (1 + d_{12}) + d_{12} (F^2 - d_{11})), \quad (2.47a)$$

$$R_2 = -(F^2 d_{12} + d_{11}) (d_{11} (1 + d_{12}) + d_{12} (E^2 - d_{11})). \quad (2.47b)$$

By using a similar method, the inner integral in (2.37b) is evaluated. After simplifications (2.37) are reduced to following form,

$$\sum_{j=3}^4 (d_{11} p_j + d_{12} D_j \alpha) B_j(\alpha) = \frac{2}{C_{66}} \frac{1}{2\pi d_{11} (E^2 - F^2) (1 + d_{12})} \int_0^d \left[R_1 \exp\left(-\frac{\alpha t}{F}\right) + R_2 \exp\left(-\frac{\alpha t}{E}\right) \right] f_1(t) dt, \quad (2.48a)$$

$$\sum_{j=3}^4 (D_j p_j - \alpha) B_j(\alpha) = \frac{2}{C_{66}} \frac{E^2 F^2 d_{11}^2 + d_{11} d_{12} (E^2 + F^2) + d_{11}^2}{2\pi d_{11} E F (E^2 - F^2) (1 + d_{12})} \times \int_0^d \left[-E \exp\left(-\frac{\alpha t}{F}\right) + F \exp\left(-\frac{\alpha t}{E}\right) \right] f_1(t) dt, \quad (2.48b)$$

where,

$$B_j(\alpha) = \frac{2}{C_{66}} \int_0^d \left[B_j^*(\alpha, t) \exp\left(-\frac{\alpha t}{F}\right) + B_j^{**}(\alpha, t) \exp\left(-\frac{\alpha t}{E}\right) \right] f_1(t) dt. \quad (2.49)$$

Equations (2.48) can be rewritten as follows:

$$\sum_{j=3}^4 (d_{11} p_j + d_{12} D_j \alpha) B_j^*(\alpha, t) = R_{1111}(\alpha, t), \quad (2.50a)$$

$$\sum_{j=3}^4 (D_j p_j - \alpha) B_j^*(\alpha, t) = R_{1211}(\alpha, t), \quad (2.50b)$$

$$\sum_{j=3}^4 (d_{11} p_j + d_{12} D_j \alpha) B_j^{**}(\alpha, t) = R_{1112}(\alpha, t), \quad (2.50c)$$

$$\sum_{j=3}^4 (D_j p_j - \alpha) B_j^{**}(\alpha, t) = R_{1212}(\alpha, t), \quad (2.50d)$$

where,

$$R_{1111}(\alpha, t) = \frac{R_1}{2\pi d_{11} (E^2 - F^2)(1 + d_{12})}, \quad (2.51a)$$

$$R_{1211}(\alpha, t) = -\frac{(E^2 F^2 d_{11}^2 + d_{11} d_{12} (E^2 + F^2) + d_{11}^2)}{2\pi d_{11} F (E^2 - F^2)(1 + d_{12})}, \quad (2.51b)$$

$$R_{1112}(\alpha, t) = \frac{R_2}{2\pi d_{11} (E^2 - F^2)(1 + d_{12})}, \quad (2.51c)$$

$$R_{1212}(\alpha, t) = \frac{(E^2 F^2 d_{11}^2 + d_{11} d_{12} (E^2 + F^2) + d_{11}^2)}{2\pi d_{11} E (E^2 - F^2)(1 + d_{12})}. \quad (2.51d)$$

At this point, the formulation of the opening mode problem is completed. The stresses and displacement fields are derived in terms of f_1 . The unknown functions used in the formulation of the opening mode problem are given by equations (2.35) and (2.50).

2.2.2.2 The Sliding Mode Problem ($f_1 = 0$)

In order to solve the sliding mode problem, it is assumed that a crack in an infinite plane is located at $0 < x_1 < d$. In this case, $f_1(x_1)$ given by (2.2a) is equal to zero. The stress and displacement fields are derived in terms of $f_2(x_1)$ given by (2.2b). Displacement and stress components for the infinite plane can be obtained by following a similar procedure as given in Section 2.2.2.1. These components for the infinite plane are determined as follows:

$x_2 < 0$:

$$u_{12}^{(i-)}(x_1, x_2) = \frac{1}{2\pi} \int_{-\infty}^{\infty} \sum_{j=1}^2 F_j \exp(n_j x_2 + i\omega x_1) d\omega, \quad (2.52a)$$

$$u_{22}^{(i-)}(x_1, x_2) = \frac{1}{2\pi} \int_{-\infty}^{\infty} \sum_{j=1}^2 F_j A_j \exp(n_j x_2 + i\omega x_1) d\omega, \quad (2.52b)$$

$$\sigma_{112}^{(i-)}(x_1, x_2) = \frac{C_{66}}{2} \frac{1}{2\pi} \int_{-\infty}^{\infty} \sum_{j=1}^2 S_{112j}^{(i-)}(\omega) \exp(n_j x_2 + i\omega x_1) d\omega, \quad (2.52c)$$

$$\sigma_{222}^{(i-)}(x_1, x_2) = \frac{C_{66}}{2} \frac{1}{2\pi} \int_{-\infty}^{\infty} \sum_{j=1}^2 S_{222j}^{(i-)}(\omega) \exp(n_j x_2 + i\omega x_1) d\omega, \quad (2.52d)$$

$$\sigma_{122}^{(i-)}(x_1, x_2) = \frac{C_{66}}{2} \frac{1}{2\pi} \int_{-\infty}^{\infty} \sum_{j=1}^2 (n_j + i\omega A_j) F_j \exp(n_j x_2 + i\omega x_1) d\omega, \quad (2.52e)$$

$$\frac{\partial}{\partial x_2} u_{12}^{(i-)}(x_1, x_2) = \frac{1}{2\pi} \int_{-\infty}^{\infty} \sum_{j=1}^2 F_j n_j \exp(n_j x_2 + i\omega x_1) d\omega, \quad (2.52f)$$

$$S_{112j}^{(i-)}(x_1, x_2) = \sum_{j=1}^2 (d_{11} i\omega + d_{12} A_j n_j) F_j, \quad (2.52g)$$

$$S_{222j}^{(i^-)}(x_1, x_2) = \sum_{j=1}^2 (d_{12} i \omega + d_{22} A_j n_j) F_j, \quad (2.52h)$$

where subscript 2 refers to the sliding mode or mode II problem and superscript (i^-) refers to $x_2 < 0$. $F_j(\omega)$ ($j=1, \dots, 4$) are unknown functions and n_j and $A_j(\omega)$ are given by (2.22) and (2.26), respectively.

$x_2 > 0$:

$$u_{12}^{(i^+)}(x_1, x_2) = \frac{1}{2\pi} \int_{-\infty}^{\infty} \sum_{j=3}^4 F_j \exp(n_j x_2 + i \omega x_1) d\omega, \quad (2.53a)$$

$$u_{22}^{(i^+)}(x_1, x_2) = \frac{1}{2\pi} \int_{-\infty}^{\infty} \sum_{j=3}^4 F_j A_j \exp(n_j x_2 + i \omega x_1) d\omega, \quad (2.53b)$$

$$\sigma_{112}^{(i^+)}(x_1, x_2) = \frac{C_{66}}{2} \frac{1}{2\pi} \int_{-\infty}^{\infty} \sum_{j=3}^4 S_{112j}^{(i^+)}(\omega) \exp(n_j x_2 + i \omega x_1) d\omega, \quad (2.53c)$$

$$\sigma_{222}^{(i^+)}(x_1, x_2) = \frac{C_{66}}{2} \frac{1}{2\pi} \int_{-\infty}^{\infty} \sum_{j=3}^4 S_{222j}^{(i^+)}(\omega) \exp(n_j x_2 + i \omega x_1) d\omega, \quad (2.53d)$$

$$\sigma_{122}^{(i^+)}(x_1, x_2) = \frac{C_{66}}{2} \frac{1}{2\pi} \int_{-\infty}^{\infty} \sum_{j=3}^4 (n_j + i \omega A_j) F_j \exp(n_j x_2 + i \omega x_1) d\omega, \quad (2.53e)$$

$$\frac{\partial}{\partial x_2} u_{12}^{(i^+)}(x_1, x_2) = \frac{1}{2\pi} \int_{-\infty}^{\infty} \sum_{j=3}^4 F_j n_j \exp(n_j x_2 + i \omega x_1) d\omega, \quad (2.53f)$$

$$S_{112j}^{(i^+)}(x_1, x_2) = \sum_{j=3}^4 (d_{11} i \omega + d_{12} A_j n_j) F_j, \quad (2.53g)$$

$$S_{222j}^{(i^+)}(x_1, x_2) = \sum_{j=3}^4 (d_{12} i \omega + d_{22} A_j n_j) F_j, \quad (2.53h)$$

where superscript (i^+) stands for $x_2 > 0$.

For the sliding mode problem, $u_{22}(x_1, x_2)$ is an even function of x_2 and $u_{12}(x_1, x_2)$ is an odd function of x_2 , therefore for the half-plane ($x_1 > 0$) problem without a crack, displacement components can be expressed by using Fourier sine and cosine integrals as follows:

$$u_{12}^{(h)}(x_1, x_2) = \int_0^{\infty} U_{12}^{(h)}(x_1, \alpha) \sin(\alpha x_2) d\alpha, \quad (2.54a)$$

$$u_{22}^{(h)}(x_1, x_2) = \int_0^{\infty} U_{22}^{(h)}(x_1, \alpha) \cos(\alpha x_2) d\alpha, \quad (2.54b)$$

where subscript 2 and superscript h stand for sliding mode and half-plane problems, respectively. Equation (2.54) implies that $u_{12}^{(h)}(x_1, x_2) = -u_{12}^{(h)}(x_1, -x_2)$, $u_{22}^{(h)}(x_1, x_2) = u_{22}^{(h)}(x_1, -x_2)$. Substituting (2.54) in (2.5) following differential equations are obtained,

$$d_{11} \frac{d^2 U_{12}^{(h)}}{d x_1^2} - \alpha^2 U_{12}^{(h)} - (1 + d_{12}) \alpha \frac{d U_{22}^{(h)}}{d x_1} = 0, \quad (2.55a)$$

$$\frac{d^2 U_{22}^{(h)}}{d x_1^2} - \alpha^2 d_{22} U_{22}^{(h)} + (1 + d_{12}) \alpha \frac{d U_{12}^{(h)}}{d x_1} = 0. \quad (2.55b)$$

One can assume a solution of the form $\exp(\alpha x_1)$. By using this form the characteristic equation of the problem is determined as,

$$t^4 - \frac{\alpha^2 (d_{11} d_{22} - 2d_{12} - d_{12}^2)}{d_{11}} t^2 + \frac{\alpha^4 d_{22}}{d_{11}} = 0. \quad (2.56)$$

Roots of the characteristic equation for a type I material are found to be

$$t_1 = A|\alpha|, \quad \Re(t_1) > 0, \quad (2.57a)$$

$$t_2 = B|\alpha|, \quad \Re(t_2) > 0, \quad (2.57b)$$

$$t_3 = -A|\alpha|, \quad \Re(t_3) < 0, \quad (2.57c)$$

$$t_4 = -B|\alpha|, \quad \Re(t_4) < 0, \quad (2.57d)$$

where, A and B are given by (2.12).

For the half-plane problem ($x_1 > 0$), the stresses and displacements are obtained as follows:

$$u_{12}^{(h)}(x_1, x_2) = \int_0^{\infty} (G_3 \exp(t_3 x_1) + G_4 \exp(t_4 x_1)) \sin(\alpha x_2) d\alpha, \quad (2.58a)$$

$$u_{22}^{(h)}(x_1, x_2) = \int_0^{\infty} (G_3 H_3 \exp(t_3 x_1) + G_4 H_4 \exp(t_4 x_1)) \cos(\alpha x_2) d\alpha, \quad (2.58b)$$

$$\sigma_{112}^{(h)}(x_1, x_2) = \frac{C_{66}}{2} \int_0^{\infty} \sum_{j=3}^4 (C_{11} t_j - C_{12} H_j \alpha) G_j \exp(t_j x_1) \sin(\alpha x_2) d\alpha, \quad (2.58c)$$

$$\sigma_{222}^{(h)}(x_1, x_2) = \frac{C_{66}}{2} \int_0^{\infty} \sum_{j=3}^4 (C_{12} t_j - C_{22} H_j \alpha) G_j \exp(t_j x_1) \sin(\alpha x_2) d\alpha, \quad (2.58d)$$

$$\sigma_{122}^{(h)}(x_1, x_2) = \frac{C_{66}}{2} \int_0^{\infty} \sum_{j=3}^4 (H_j t_j + \alpha) G_j \exp(t_j x_1) \cos(\alpha x_2) d\alpha, \quad (2.58e)$$

$$\frac{\partial}{\partial x_2} u_{12}^{(h)}(x_1, x_2) = \int_0^{\infty} \alpha (G_3 \exp(t_3 x_1) + G_4 \exp(t_4 x_1)) \cos(\alpha x_2) d\alpha, \quad (2.58f)$$

where $G_j(\omega)$ ($j=3,4$) are unknown functions and $H_j(\alpha)$ is expressed as,

$$H_j(\alpha) = \frac{d_{11} t_j^2 - \alpha^2}{(1 + d_{12}) \alpha t_j}. \quad (2.59)$$

For $x_1 > 0$ and $x_2 > 0$ the solution of mode II problem is given as follows:

$$u_{12}(x_1, x_2) = u_{12}^{(i+)}(x_1, x_2) + u_{12}^{(h)}(x_1, x_2), \quad x_1 > 0, x_2 > 0, \quad (2.60a)$$

$$u_{22}(x_1, x_2) = u_{22}^{(i+)}(x_1, x_2) + u_{22}^{(h)}(x_1, x_2), \quad x_1 > 0, x_2 > 0, \quad (2.60b)$$

$$\sigma_{k j 2}(x_1, x_2) = \sigma_{k j 2}^{(i+)}(x_1, x_2) + \sigma_{k j 2}^{(h)}(x_1, x_2), \quad k, j=1,2, \quad x_1 > 0, x_2 > 0. \quad (2.60c)$$

In the formulation, there are six unknown functions $F_1(\omega), \dots, F_4(\omega), G_3(\alpha), G_4(\alpha)$. These functions can be expressed in terms of unknown function $f_2(x_1)$. Boundary conditions of the sliding mode problem are determined as,

$$\sigma_{222}(x_1, +0) = \sigma_{222}(x_1, -0), \quad 0 < x_1 < \infty, \quad (2.61a)$$

$$\sigma_{122}(x_1, +0) = \sigma_{122}(x_1, -0), \quad 0 < x_1 < \infty, \quad (2.61b)$$

$$, u_{22}(x_1, +0) = u_{22}(x_1, -0), \quad 0 < x_1 < \infty \quad (2.61c)$$

$$\frac{C_{66}}{2} \frac{\partial}{\partial x_1} (u_{12}(x_1, +0) - u_{12}(x_1, -0)) = f_2(x_1), \quad 0 < x_1 < d, \quad (2.61d)$$

$$u_{12}(x_1, +0) = u_{12}(x_1, -0), \quad d < x_1 < \infty, \quad (2.61e)$$

$$\sigma_{112}(0, x_2) = 0, \quad -\infty < x_2 < \infty, \quad (2.61f)$$

$$\sigma_{122}(0, x_2) = 0, \quad -\infty < x_2 < \infty. \quad (2.61g)$$

In order to obtain unknown functions $F_1(\omega)$, \dots , $F_4(\omega)$ in terms of $f_2(x_1)$, equations (2.61a-e) and equations (2.52) and (2.53) are used and following equations are found,

$$F_j(\omega) = \frac{2}{C_{66}} Z_j(\omega) \int_0^d f_2(t) \exp(-i\omega t) dt, \quad (j=1,2,3,4), \quad (2.62a)$$

$$\sum_{j=3}^4 (i\omega d_{12} + A_j n_j d_{22}) Z_j(\omega) - \sum_{j=1}^2 (i\omega d_{12} + A_j n_j d_{22}) Z_j(\omega) = 0, \quad (2.62b)$$

$$\sum_{j=3}^4 (n_j + i\omega A_j) Z_j(\omega) - \sum_{j=1}^2 (n_j + i\omega A_j) Z_j(\omega) = 0, \quad (2.62c)$$

$$A_4 Z_4 + A_3 Z_3 - A_2 Z_2 - A_1 Z_1 = 0, \quad (2.62d)$$

$$i\omega \{Z_4(\omega) + Z_3(\omega) - Z_2(\omega) - Z_1(\omega)\} = 1. \quad (2.62e)$$

Since the half-plane solution ($x_1 > 0$) does not include a crack, the half-plane solution ($x_1 > 0$) given by (2.58) and the unknown functions $G_3(\alpha)$, $G_4(\alpha)$ do not contribute to equations (2.62). Boundary conditions (2.61a-e) are satisfied by the half-plane ($x_1 > 0$) solution. $G_3(\alpha)$ and $G_4(\alpha)$, which are the unknown functions of the half-plane ($x_1 > 0$) problem, are expressed in terms of $f_2(x_1)$ by using the free surface boundary conditions. So, in the determination of the $G_3(\alpha)$ and $G_4(\alpha)$, (2.61f), (2.61g), (2.58c), (2.58e), (2.53c) and (2.53e) are used and the following equations are obtained,

$$\int_0^{\infty} \sum_{j=3}^4 (d_{11} t_j - d_{12} H_j \alpha) G_j \sin(\alpha x_2) d\alpha + \frac{1}{2\pi} \int_{-\infty}^{\infty} \sum_{j=3}^4 (d_{11} i \omega + d_{12} A_j n_j) F_j \exp(n_j x_2) d\omega = 0, \quad 0 < x_2 < \infty, \quad (2.63a)$$

$$\int_0^{\infty} \sum_{j=3}^4 (H_j t_j + \alpha) G_j \cos(\alpha x_2) d\alpha + \frac{1}{2\pi} \int_{-\infty}^{\infty} \sum_{j=3}^4 (n_j + i\omega A_j) F_j \exp(n_j x_2) d\omega = 0, \quad 0 < x_2 < \infty. \quad (2.63b)$$

Because of symmetry, only $x_2 > 0$ case is considered. $F_j(\omega)$ ($j=1, \dots, 4$) can be determined using (2.62a-e) in terms of f_2 . After lengthy manipulations using MAPLE, (2.63) equations are obtained as follows:

$$\sum_{j=3}^4 (d_{11} t_j - d_{12} H_j \alpha) G_j(\alpha) = -\frac{2}{C_{66}} \frac{1}{\pi^2} \int_0^d f_2(t) dt \int_{-\infty}^{\infty} F_{112}(\omega, \alpha) \exp(-i\omega t) d\omega, \quad (2.64a)$$

$$\sum_{j=3}^4 (H_j t_j + \alpha) G_j(\alpha) = \frac{2}{C_{66}} \frac{1}{\pi^2} \int_0^d f_2(t) dt \int_{-\infty}^{\infty} F_{122}(\omega, \alpha) \exp(-i\omega t) d\omega, \quad (2.64b)$$

where,

$$F_{112}(\omega, \alpha) = \frac{N_{112}(\omega, \alpha)}{d_{22} D(\omega, \alpha)}, \quad (2.65a)$$

$$F_{122}(\omega, \alpha) = \frac{N_{122}(\omega, \alpha)}{d_{22} D(\omega, \alpha)}, \quad (2.65b)$$

$N_{112}(\omega, \alpha)$ and $N_{122}(\omega, \alpha)$ are equal to:

$$\begin{aligned}
N_{112}(\omega, \alpha) = & \frac{1}{2} \alpha (-d_{12}^2 d_{11} \omega^2 d_{12} - d_{12}^2 d_{12} \alpha^2 - d_{12}^2 d_{11} \omega^2 - d_{12}^2 \alpha^2 \\
& - d_{12} E^2 d_{22} \omega^2 d_{11} + \omega^2 d_{22} F^2 d_{12} E^2 + d_{12} d_{11} \omega^2 d_{12}^2 \\
& + 2d_{12} d_{11} \omega^2 d_{12} + d_{12} \omega^2 d_{22} d_{11}^2 + d_{12} d_{11} \omega^2 \\
& - d_{22} F^2 d_{12} \omega^2 d_{11} + E^2 d_{11} d_{22} \omega^2 d_{12} + E^2 d_{11} d_{22} \omega^2 \\
& - d_{12} d_{11} d_{22} d_{11} \omega^2 + d_{12} \omega^2 d_{11} d_{22} F^2 + d_{11} d_{22} d_{12} \alpha^2 \\
& - d_{11} d_{22} d_{11} \omega^2 + \omega^2 d_{11} d_{22} F^2 + d_{11} d_{22} \alpha^2),
\end{aligned} \tag{2.66a}$$

$$\begin{aligned}
N_{122}(\omega, \alpha) = & -\frac{1}{2} i \omega (-d_{12} \alpha^2 d_{12}^2 + d_{12} d_{11} \omega^2 d_{12} - d_{12} d_{12} \alpha^2 + d_{12} d_{11} \omega^2 \\
& + E^2 \omega^2 d_{22} F^2 d_{12} + E^2 d_{22} d_{11} \omega^2 + d_{11} d_{22} d_{12} \alpha^2 \\
& - \omega^2 d_{22} d_{11}^2 + \omega^2 d_{22} F^2 d_{11} + d_{22} d_{11} \alpha^2).
\end{aligned} \tag{2.66b}$$

E and F are given by (2.23) and $D(\omega, \alpha)$ is given by (2.39c).

By using the residue theorem, the inner integrals in (2.64) are evaluated as described in Section 2.2.2.1 and $G_j(\alpha)$ can be defined in the following form,

$$G_j(\alpha) = \frac{2}{C_{66}} \int_0^d \left[G_j^*(\alpha, t) \exp\left(-\frac{\alpha t}{F}\right) + G_j^{**}(\alpha, t) \exp\left(-\frac{\alpha t}{E}\right) \right] f_2(t) dt. \tag{2.67}$$

Then equations (2.64) can be written as:

$$\sum_{j=3}^4 (d_{11} t_j - d_{12} H_j \alpha) G_j^*(\alpha, t) = R_{1121}(\alpha, t), \tag{2.68a}$$

$$\sum_{j=3}^4 (H_j t_j + \alpha) G_j^*(\alpha, t) = R_{1221}(\alpha, t), \tag{2.68b}$$

$$\sum_{j=3}^4 (d_{11} t_j - d_{12} H_j \alpha) G_j^{**}(\alpha, t) = R_{1122}(\alpha, t), \tag{2.68c}$$

$$\sum_{j=3}^4 (H_j t_j + \alpha) G_j^{**}(\alpha, t) = R_{1222}(\alpha, t), \tag{2.68d}$$

where,

$$R_{1121}(\alpha, t) = -\frac{R_3}{2\pi C_{22} EF (E^2 - F^2)(1 + d_{12})}, \quad (2.69a)$$

$$R_{1221}(\alpha, t) = \frac{R_5}{2\pi C_{22} E^2 F^2 (E^2 - F^2)(1 + d_{12})}, \quad (2.69b)$$

$$R_{1122}(\alpha, t) = -\frac{R_4}{2\pi C_{22} EF (E^2 - F^2)(1 + d_{12})}, \quad (2.69c)$$

$$R_{1222}(\alpha, t) = \frac{R_6}{2\pi C_{22} E^2 F^2 (E^2 - F^2)(1 + d_{12})}, \quad (2.69d)$$

and

$$R_3 = E(d_{12}(1 + d_{12}) + d_{22}(E^2 - d_{11}))(d_{11}(1 + d_{12}) + d_{12}(F^2 - d_{11})), \quad (2.70a)$$

$$R_4 = -F(d_{12}(1 + d_{12}) + d_{22}(F^2 - d_{11}))(d_{11}(1 + d_{12}) + d_{12}(E^2 - d_{11})), \quad (2.70b)$$

$$R_5 = -E^2(d_{11} + d_{12}F^2)(d_{12}(1 + d_{12}) + d_{22}(E^2 - d_{11})), \quad (2.70c)$$

$$R_6 = F^2(d_{11} + d_{12}E^2)(d_{12}(1 + d_{12}) + d_{22}(F^2 - d_{11})). \quad (2.70d)$$

At this point, the formulation of the sliding mode problem is completed. The stresses and displacement fields are derived in terms of f_2 . The unknown functions used in the formulation of the sliding mode problem are given by equations (2.62) and (2.68). For a surface crack subjected to mixed-mode loading, the stress and displacement fields can be expressed as,

$$u_1(x_1, x_2) = u_{11}(x_1, x_2) + u_{12}(x_1, x_2), \quad x_1 > 0, x_2 > 0, \quad (2.71a)$$

$$u_2(x_1, x_2) = u_{21}(x_1, x_2) + u_{22}(x_1, x_2), \quad x_1 > 0, x_2 > 0, \quad (2.71b)$$

$$\sigma_{kj}(x_1, x_2) = \sigma_{kj1}(x_1, x_2) + \sigma_{kj2}(x_1, x_2), \quad k, j = 1, 2, \quad x_1 > 0, x_2 > 0. \quad (2.71c)$$

For the coupled crack and contact problem, stress and displacement fields can be expressed as follows:

$$u_1(x_1, x_2) = u_{11}(x_1, x_2) + u_{12}(x_1, x_2) + u_{13}(x_1, x_2), \quad x_1 > 0, x_2 > 0, \quad (2.72a)$$

$$u_2(x_1, x_2) = u_{21}(x_1, x_2) + u_{22}(x_1, x_2) + u_{23}(x_1, x_2), \quad x_1 > 0, x_2 > 0, \quad (2.72b)$$

$$\sigma_{kj}(x_1, x_2) = \sigma_{kj1}(x_1, x_2) + \sigma_{kj2}(x_1, x_2) + \sigma_{kj3}(x_1, x_2), \quad (2.72c)$$

$$k, j = 1, 2, \quad x_1 > 0, x_2 > 0,$$

where displacement and stresses are given by (2.13), (2.15) and (2.18).

2.2.3 Derivation of the Singular Integral Equations

In equation (2.72), the stress and displacement fields for the coupled crack and contact problem are provided. For the coupled problem, stresses and displacement derivative are written as follows:

$$\sigma_{22}(x_1, x_2) = \int_0^d \sum_{j=1}^2 k_{1j}(x_1, x_2, t) f_j(t) dt + \int_a^b k_{13}(x_1, x_2, t) f_3(t) dt, \quad (2.73a)$$

$$\sigma_{12}(x_1, x_2) = \int_0^d \sum_{j=1}^2 k_{2j}(x_1, x_2, t) f_j(t) dt + \int_a^b k_{23}(x_1, x_2, t) f_3(t) dt, \quad (2.73b)$$

$$\frac{C_{66}}{2} \frac{\partial}{\partial x_2} u_1(x_1, x_2) = \int_0^d \sum_{j=1}^2 k_{3j}(x_1, x_2, t) f_j(t) dt + \int_a^b k_{33}(x_1, x_2, t) f_3(t) dt. \quad (2.73c)$$

In order to determine unknown functions f_1 , f_2 and f_3 , boundary conditions (2.1e), (2.1f) and (2.1c) are applied, the following integral equations are obtained,

$$\sigma_{22}(x_1, 0) = \lim_{x_2 \rightarrow 0} \int_0^d \sum_{j=1}^2 k_{1j}(x_1, x_2, t) f_j(t) dt + \lim_{x_2 \rightarrow 0} \int_a^b k_{13}(x_1, x_2, t) f_3(t) dt = 0, \quad (2.74a)$$

$$0 < x_1 < d,$$

$$\sigma_{12}(x_1, 0) = \lim_{x_2 \rightarrow 0} \int_0^d \sum_{j=1}^2 k_{2j}(x_1, x_2, t) f_j(t) dt + \lim_{x_2 \rightarrow 0} \int_a^b k_{23}(x_1, x_2, t) f_3(t) dt = 0, \quad (2.74b)$$

$$0 < x_1 < d,$$

$$\frac{C_{66}}{2} \frac{\partial}{\partial x_2} u_1(0, x_2) = \lim_{x_1 \rightarrow 0} \int_0^d \sum_{j=1}^2 k_{3j}(x_1, x_2, t) f_j(t) dt \quad (2.74c)$$

$$+ \lim_{x_1 \rightarrow 0} \int_a^b k_{33}(x_1, x_2, t) f_3(t) dt = f(x_2), \quad a < x_2 < b.$$

Due to symmetry, $\sigma_{222}(x_1, 0) = 0$ for $f_1(t) = 0$, $f_2(t) \neq 0$, $f_3(t) = 0$ and $\sigma_{121}(x_1, 0) = 0$ for $f_1(t) \neq 0$, $f_2(t) = 0$, $f_3(t) = 0$, hence

$$k_{12}(x_1, 0, t) = 0, \quad (2.75a)$$

$$k_{21}(x_1, 0, t) = 0. \quad (2.75b)$$

The kernels are expressed as follows:

$$k_{ij}(x_1, 0, t) = \int_0^\infty K_{ij}(x_1, t, \rho) d\rho, \quad (i=1, 2, \quad j=1, 2, 3), \quad (2.76a)$$

$$k_{ij}(0, x_2, t) = \int_0^\infty K_{ij}(x_2, t, \rho) d\rho, \quad (i=3, \quad j=1, 2, 3). \quad (2.76b)$$

Equations (2.73) can be rewritten as

$$\sigma_{22}(x_1, 0) = \int_0^d k_{11}(x_1, 0, t) f_1(t) dt + \int_a^b k_{13}(x_1, 0, t) f_3(t) dt = 0, \quad 0 < x_1 < d, \quad (2.77a)$$

$$\sigma_{12}(x_1, 0) = \int_0^d k_{22}(x_1, 0, t) f_2(t) dt + \int_a^b k_{23}(x_1, 0, t) f_3(t) dt = 0, \quad 0 < x_1 < d, \quad (2.77b)$$

$$\begin{aligned} \frac{C_{66}}{2} \frac{\partial}{\partial x_2} u_1(0, x_2) = & \int_0^d k_{31}(0, x_2, t) f_1(t) dt + \int_0^d k_{32}(0, x_2, t) f_2(t) dt \\ & + \int_a^b k_{33}(0, x_2, t) f_3(t) dt = f(x_2), \quad a < x_2 < b. \end{aligned} \quad (2.77c)$$

Asymptotic analyses have to be performed in order to extract the singularities in the kernels as ρ approaches to infinity. The asymptotic analyses for the kernels are given in the following section.

2.2.3.1 Asymptotic Analysis of $k_{11}(x_1, x_2, t)$

$k_{11}(x_1, x_2, t)$ is expressed as follows:

$$k_{11}(x_1, x_2, t) = k_{11}^{(i)}(x_1, x_2, t) + k_{11}^{(h)}(x_1, x_2, t). \quad (2.78)$$

By using the infinite plane solution and the half-plane ($x_1 > 0$) solution $k_{11}^{(i)}$ and $k_{11}^{(h)}$ are obtained. Referring to (2.25d) and (2.35), $k_{11}^{(i)}(x_1, x_2, t)$ is written as

$$k_{11}^{(i)}(x_1, x_2, t) = \frac{1}{2\pi} \int_{-\infty}^{\infty} \phi_{11}^{(i)}(\omega, x_2) \exp(i\omega(x_1 - t)) d\omega, \quad (2.79a)$$

$$\phi_{11}^{(i)}(\omega, x_2) = \sum_{j=3}^4 (d_{12} i \omega + d_{22} A_j n_j) P_j(\omega) \exp(n_j x_2), \quad (2.79b)$$

where n_j ($j=1,2,3,4$), A_j and P_j are given by (2.22), (2.26) and (2.35), respectively. Changing the limits of integration (2.79a) becomes,

$$k_{11}^{(i)}(x_1, x_2, t) = \frac{1}{2\pi} \int_0^{\infty} \left[K_{111}^{(i)}(\omega, x_2) \cos(\omega(x_1 - t)) + K_{112}^{(i)}(\omega, x_2) \sin(\omega(x_1 - t)) \right] d\omega, \quad (2.80)$$

where,

$$K_{111}^{(i)}(\omega, x_2) = \phi_{11}^{(i)}(\omega, x_2) + \phi_{11}^{(i)}(-\omega, x_2), \quad (2.81a)$$

$$K_{112}^{(i)}(\omega, x_2) = i(\phi_{11}^{(i)}(\omega, x_2) - \phi_{11}^{(i)}(-\omega, x_2)). \quad (2.81b)$$

$K_{111}^{(i)}$ and $K_{112}^{(i)}$ can be expressed as,

$$K_{111}^{(i)}(\omega, x_2) = K_{1111}^{(i)}(\omega) \exp(n_3 x_2) + K_{1112}^{(i)}(\omega) \exp(n_4 x_2), \quad (2.82a)$$

$$K_{112}^{(i)}(\omega, x_2) = K_{1121}^{(i)}(\omega) \exp(n_3 x_2) + K_{1122}^{(i)}(\omega) \exp(n_4 x_2), \quad (2.82b)$$

and,

$$K_{1111}^{(i)}(\omega) = [d_{12} i \omega + d_{22} A_3(\omega) n_3] P_3(\omega) + [-d_{12} i \omega + d_{22} A_3(-\omega) n_3] P_3(-\omega), \quad (2.83a)$$

$$K_{1112}^{(i)}(\omega) = [d_{12} i \omega + d_{22} A_4(\omega) n_4] P_4(\omega) + [-d_{12} i \omega + d_{22} A_4(-\omega) n_4] P_4(-\omega), \quad (2.83b)$$

$$K_{1121}^{(i)}(\omega) = i \{ [d_{12} i \omega + d_{22} A_3(\omega) n_3] P_3(\omega) - [-d_{12} i \omega + d_{22} A_3(-\omega) n_3] P_3(-\omega) \}, \quad (2.83c)$$

$$K_{1122}^{(i)}(\omega) = i \{ [d_{12} i \omega + d_{22} A_4(\omega) n_4] P_4(\omega) - [-d_{12} i \omega + d_{22} A_4(-\omega) n_4] P_4(-\omega) \}. \quad (2.83d)$$

In order to extract the singular terms, asymptotic analyses of $K_{111}^{(i)}$ and $K_{112}^{(i)}$ are required as $\omega \rightarrow \infty$. Asymptotic expansions of $K_{111}^{(i)}$ and $K_{112}^{(i)}$ are given by,

$$K_{111}^{(i)\infty}(\omega, x_2) = K_{1111}^{(i)\infty}(\omega) \exp(n_3 x_2) + K_{1112}^{(i)\infty}(\omega) \exp(n_4 x_2), \quad (2.84a)$$

$$K_{112}^{(i)\infty}(\omega, x_2) = K_{1121}^{(i)\infty}(\omega) \exp(n_3 x_2) + K_{1122}^{(i)\infty}(\omega) \exp(n_4 x_2). \quad (2.84b)$$

By using MAPLE, asymptotic expansions are obtained as follows:

$$K_{1111}^{(i)\infty}(\omega)=0, \quad (2.85a)$$

$$K_{1112}^{(i)\infty}(\omega)=0, \quad (2.85b)$$

$$K_{1121}^{(i)\infty}(\omega)=a_{210}, \quad (2.85c)$$

$$K_{1122}^{(i)\infty}(\omega)=a_{220}. \quad (2.85d)$$

The coefficients of the expansion a_{210} and a_{220} are given in Appendix A by equations (A.1a) and (A.1b), respectively. Subtracting the asymptotic expansions from the integrands in (2.80), using integration cutoff points, evaluating some of the integrals in closed form, taking the limit as $x_2 \rightarrow 0$, and after some manipulations

$k_{11}^{(i)}(x_1, x_2, t)$ is expressed as:

$$k_{11}^{(i)}(x_1, 0, t) = \frac{1}{2\pi} \frac{a_{20}}{x_1 - t} + J_{112}^{(i)}(x_1, t), \quad (2.86)$$

where a_{20} is given in Appendix A by (A.1c) and,

$$J_{112}^{(i)}(x_1, t) = \frac{1}{2\pi} \int_0^{A_{112}^{(i)}} [K_{112}^{(i)}(\omega, 0) - a_{20}] \sin(\omega(x_1 - t)) d\omega \\ + \frac{1}{2\pi} \int_{A_{112}^{(i)}}^{\infty} [K_{112}^{(i)}(\omega, 0) - a_{20}] \sin(\omega(x_1 - t)) d\omega, \quad (2.87)$$

in which, $A_{112}^{(i)}$ is an integration cutoff point.

Referring to (2.31d) and (2.49), $k_{11}^{(h)}(x_1, x_2, t)$ is written in the following form,

$$k_{11}^{(h)}(x_1, x_2, t) = \int_0^{\infty} K_{11}^{(h)}(\alpha, t, x_1) \cos(\alpha x_2) d\alpha, \quad (2.88)$$

where,

$$K_{11}^{(h)}(\alpha, t, x_1) = \sum_{j=3}^4 \phi_{11j}^{(h)}(\alpha) \left[B_j^*(\alpha, t) \exp\left(-\frac{\alpha t}{F}\right) + B_j^{**}(\alpha, t) \exp\left(-\frac{\alpha t}{E}\right) \right] \times \exp(p_j x_1), \quad (2.89a)$$

$$\phi_{11j}^{(h)}(\alpha) = (d_{12} p_j + d_{22} D_j \alpha), \quad (j=3,4), \quad (2.89b)$$

and p_j ($j=1,2,3,4$), D_j , and B_j^*/B_j^{**} are given by (2.30), (2.32) and (2.50), respectively. $K_{11}^{(h)}$ can be expressed as

$$K_{11}^{(h)}(\alpha, t, x_1) = \left[K_{1111}^{(h)}(\alpha) \exp\left(-\frac{\alpha t}{F}\right) + K_{1112}^{(h)}(\alpha) \exp\left(-\frac{\alpha t}{E}\right) \right] \exp(p_3 x_1) + \left[K_{1121}^{(h)}(\alpha) \exp\left(-\frac{\alpha t}{F}\right) + K_{1122}^{(h)}(\alpha) \exp\left(-\frac{\alpha t}{E}\right) \right] \exp(p_4 x_1), \quad (2.90)$$

where,

$$K_{1111}^{(h)}(\alpha) = (d_{12} p_3 + d_{22} D_3 \alpha) B_3^*, \quad (2.91a)$$

$$K_{1112}^{(h)}(\alpha) = (d_{12} p_3 + d_{22} D_3 \alpha) B_3^{**}, \quad (2.91b)$$

$$K_{1121}^{(h)}(\alpha) = (d_{12} p_4 + d_{22} D_4 \alpha) B_4^*, \quad (2.91c)$$

$$K_{1122}^{(h)}(\alpha) = (d_{12} p_4 + d_{22} D_4 \alpha) B_4^{**}. \quad (2.91d)$$

In order to extract the singular terms, $K_{11}^{(h)}$ is expanded into a series as $\alpha \rightarrow \infty$.

Asymptotic expansion of $K_{11}^{(h)}$ is given by

$$K_{11}^{(h)\infty}(\alpha, t, x_1) = K_{1111}^{(h)\infty}(\alpha) \exp\left(-\frac{\alpha t}{F} + p_3 x_1\right) + K_{1112}^{(h)\infty}(\alpha) \exp\left(-\frac{\alpha t}{E} + p_3 x_1\right) + K_{1121}^{(h)\infty}(\alpha) \exp\left(-\frac{\alpha t}{F} + p_4 x_1\right) + K_{1122}^{(h)\infty}(\alpha) \exp\left(-\frac{\alpha t}{E} + p_4 x_1\right). \quad (2.92)$$

By using MAPLE, asymptotic expansions are obtained as follows:

$$K_{1111}^{(h)\infty}(\alpha) = b_{110}, \quad (2.93a)$$

$$K_{1112}^{(h)\infty}(\alpha) = b_{120}, \quad (2.93b)$$

$$K_{1121}^{(h)\infty}(\alpha) = b_{210}, \quad (2.93c)$$

$$K_{1122}^{(h)\infty}(\alpha) = b_{220}. \quad (2.93d)$$

The coefficients of the expansion b_{110} , b_{120} , b_{210} and b_{220} are given in Appendix A by (A.2). Subtracting the asymptotic expansions from the integrands in (2.88), using integration cutoff points, evaluating some of the integrals in closed form, taking the limit as $x_2 \rightarrow 0$, and after some manipulations $k_{11}^{(h)}(x_1, x_2, t)$ is expressed as:

$$k_{11}^{(h)}(x_1, 0, t) = \frac{b_{110} F}{t + A x_1 F} + \frac{b_{120} E}{t + A x_1 E} + \frac{b_{210} F}{t + B x_1 F} + \frac{b_{220} E}{t + B x_1 E} + J_{11}^{(h)}(x_1, t), \quad (2.94)$$

where A and B are expressed by (2.12), E and F are expressed by (2.23) and,

$$J_{11}^{(h)}(x_1, t) = \int_0^{A_{11}^{(h)}} \left(K_{11}^{(h)}(\alpha, t, x_1) - K_{11}^{(h)\infty}(\alpha, t, x_1) \right) d\alpha + \int_{A_{11}^{(h)}}^{\infty} \left[K_{11}^{(h)}(\alpha, t, x_1) - K_{11}^{(h)\infty}(\alpha, t, x_1) \right] d\alpha, \quad (2.95)$$

in which, $A_{11}^{(h)}$ is an integration cutoff point.

$K_{11}^{(h)\infty}$ can be rewritten as follows,

$$K_{11}^{(h)\infty}(\alpha, t, x_1) = b_{110} \exp\left(-\frac{\alpha t}{F} - A \alpha x_1\right) + b_{120} \exp\left(-\frac{\alpha t}{E} - A \alpha x_1\right) + b_{210} \exp\left(-\frac{\alpha t}{F} - B \alpha x_1\right) + b_{220} \exp\left(-\frac{\alpha t}{E} - B \alpha x_1\right). \quad (2.96)$$

$k_{11}^{(i)}(x_1, 0, t)$ and $k_{11}^{(h)}(x_1, 0, t)$ are given by equations (2.86) and (2.94), respectively.

Adding these two equations $k_{11}(x_1, 0, t)$ is written as,

$$k_{11}(x_1, 0, t) = \frac{1}{2\pi} \frac{a_{20}}{x_1 - t} + h_{11s}(x_1, t) + h_{11f}(x_1, t), \quad (2.97)$$

where,

$$h_{11s}(x_1, t) = \frac{b_{110} F}{t + A x_1 F} + \frac{b_{120} E}{t + A x_1 E} + \frac{b_{210} F}{t + B x_1 F} + \frac{b_{220} E}{t + B x_1 E}, \quad (2.98a)$$

$$h_{11f}(x_1, t) = J_{112}^{(i)}(x_1, t) + J_{11}^{(h)}(x_1, t). \quad (2.98b)$$

$J_{112}^{(i)}(x_1, t)$ and $J_{11}^{(h)}(x_1, t)$ are provided by equations (2.87) and (2.95), respectively.

2.2.3.2 Asymptotic Analysis of $k_{13}(x_1, x_2, t)$

Referring to (2.15b), $k_{13}(x_1, x_2, t)$ is written as

$$k_{13}(x_1, x_2, t) = \frac{1}{2\pi} \int_{-\infty}^{\infty} \phi_{13}(\rho, x_1) \exp(i\rho(x_2 - t)) d\rho, \quad (2.99a)$$

$$\phi_{13}(\rho, x_1) = \sum_{j=1}^2 (d_{12} s_j + d_{22} N_j i \rho) \psi_j(\rho) \exp(s_j x_1), \quad (2.99b)$$

where, s_j , ($j=1, 2, 3, 4$) and $\psi_j(\rho)$ are given by (2.11) and (2.18), respectively.

Changing the limits of integration in (2.99a), k_{13} becomes,

$$k_{13}(x_1, x_2, t) = \frac{1}{2\pi} \int_0^{\infty} [K_{131}(\rho, x_1) \cos(\rho(x_2 - t)) + K_{132}(\rho, x_1) \sin(\rho(x_2 - t))] d\rho, \quad (2.100)$$

where,

$$K_{131}(\rho, x_1) = \phi_{13}(\rho, x_1) + \phi_{13}(-\rho, x_1), \quad (2.101a)$$

$$K_{132}(\rho, x_1) = i(\phi_{13}(\rho, x_1) - \phi_{13}(-\rho, x_1)), \quad (2.101b)$$

K_{131} and K_{132} is expressed as,

$$K_{131}(\rho, x_1) = K_{1311}(\rho) \exp(s_1 x_1) + K_{1312}(\rho) \exp(s_2 x_1), \quad (2.102a)$$

$$K_{132}(\rho, x_1) = K_{1321}(\rho) \exp(s_1 x_1) + K_{1322}(\rho) \exp(s_2 x_1), \quad (2.102b)$$

in which

$$K_{1311}(\rho) = (d_{12} s_1 + d_{22} N_1(\rho) i \rho) \psi_1(\rho) + (d_{12} s_1 - d_{22} N_1(-\rho) i \rho) \psi_1(-\rho), \quad (2.103a)$$

$$K_{1312}(\rho) = (d_{12} s_2 + d_{22} N_2(\rho) i \rho) \psi_2(\rho) + (d_{12} s_2 - d_{22} N_2(-\rho) i \rho) \psi_2(-\rho), \quad (2.103b)$$

$$K_{1321}(\rho) = i \{ (d_{12} s_1 + d_{22} N_1(\rho) i \rho) \psi_1(\rho) - (d_{12} s_1 - d_{22} N_1(-\rho) i \rho) \psi_1(-\rho) \}, \quad (2.103c)$$

$$K_{1322}(\rho) = i \left\{ \begin{array}{l} (d_{12} s_2 + d_{22} N_2(\rho) i \rho) \psi_2(\rho) \\ - (d_{12} s_2 - d_{22} N_2(-\rho) i \rho) \psi_2(-\rho) \end{array} \right\}. \quad (2.103d)$$

In order to extract the singular terms, asymptotic analyses of K_{131} and K_{132} are required as $\rho \rightarrow \infty$. Asymptotic expansions of K_{131} and K_{132} are given by

$$K_{131}^{\infty}(\rho, x_1) = K_{1311}^{\infty}(\rho) \exp(s_1 x_1) + K_{1312}^{\infty}(\rho) \exp(s_2 x_1), \quad (2.104a)$$

$$K_{132}^{\infty}(\rho, x_1) = K_{1321}^{\infty}(\rho) \exp(s_1 x_1) + K_{1322}^{\infty}(\rho) \exp(s_2 x_1). \quad (2.104b)$$

By using MAPLE, asymptotic expansions are obtained as follows:

$$K_{1311}^{\infty}(\rho, x_1) = g_{110}, \quad (2.105a)$$

$$K_{1312}^{\infty}(\rho, x_1) = g_{120}, \quad (2.105b)$$

$$K_{1321}^{\infty}(\rho, x_1) = g_{210}, \quad (2.105c)$$

$$K_{1322}^{\infty}(\rho, x_1) = g_{220} . \quad (2.105d)$$

The coefficients of the expansion g_{110} , g_{120} , g_{210} and g_{220} are given in Appendix A by equation (A.3). Subtracting the asymptotic expansions from the integrands in (2.100), using integration cutoff points, evaluating some of the integrals in closed form, taking the limit as $x_2 \rightarrow 0$, and after some manipulations $k_{13}(x_1, x_2, t)$ is expressed as

$$k_{13}(x_1, 0, t) = h_{13s}(x_1, t) + h_{13f}(x_1, t), \quad (2.106)$$

where,

$$h_{13s}(x_1, t) = \frac{1}{2\pi} \left\{ \begin{aligned} & \frac{x_1 t^2 (A g_{110} + B g_{120})}{(A^2 x_1^2 + t^2)(B^2 x_1^2 + t^2)} - \frac{t^3 g_{20}}{(A^2 x_1^2 + t^2)(B^2 x_1^2 + t^2)} \\ & + \frac{x_1^3 AB(B g_{110} + A g_{120})}{(A^2 x_1^2 + t^2)(B^2 x_1^2 + t^2)} - \frac{x_1 t^2 (B^2 g_{210} + A^2 g_{220})}{(A^2 x_1^2 + t^2)(B^2 x_1^2 + t^2)} \end{aligned} \right\}, \quad (2.107a)$$

$$h_{13f}(x_1, t) = J_{131}(x_1, t) + J_{132}(x_1, t). \quad (2.107b)$$

g_{20} is given in Appendix A by equation (A.3e) and,

$$\begin{aligned} J_{131}(x_1, t) = & \frac{1}{2\pi} \int_0^{A_{131}} [K_{131}(\rho, x_1) - (g_{110} \exp(-A|\rho|x_1) + g_{120} \exp(-B|\rho|x_1))] \cos(\rho t) d\rho \\ & + \frac{1}{2\pi} \int_{A_{131}}^{\infty} [K_{131}(\rho, x_1) - (g_{110} \exp(-A|\rho|x_1) + g_{120} \exp(-B|\rho|x_1))] \cos(\rho t) d\rho, \end{aligned} \quad (2.108a)$$

$$\begin{aligned}
J_{132}(x_2, t) = & \\
& -\frac{1}{2\pi} \int_0^{A_{132}} [K_{132}(\rho, x_1) - (g_{210} \exp(-A|\rho|x_1) + g_{220} \exp(-B|\rho|x_1))] \sin(\rho t) d\rho \\
& -\frac{1}{2\pi} \int_{A_{132}}^{\infty} [K_{132}(\rho, x_1) - (g_{210} \exp(-A|\rho|x_1) + g_{220} \exp(-B|\rho|x_1))] \sin(\rho t) d\rho,
\end{aligned} \tag{2.108b}$$

in which, A_{131} and A_{132} are integration cutoff points.

2.2.3.3 Asymptotic Analysis of $k_{22}(x_1, x_2, t)$

$k_{22}(x_1, x_2, t)$ is expressed as follows:

$$k_{22}(x_1, x_2, t) = k_{22}^{(i)}(x_1, x_2, t) + k_{22}^{(h)}(x_1, x_2, t), \tag{2.109}$$

By using the infinite plane solution and the half-plane ($x_1 > 0$) solution $k_{22}^{(i)}$ and $k_{22}^{(h)}$ are obtained. Referring to (2.53e) and (2.62), $k_{22}^{(i)}(x_1, x_2, t)$ is expressed as,

$$k_{22}^{(i)}(x_1, x_2, t) = \frac{1}{2\pi} \int_{-\infty}^{\infty} \phi_{22}^{(i)}(\omega, x_2) \exp(i\omega(x_1 - t)) d\omega, \tag{2.110a}$$

$$\phi_{22}^{(i)}(\omega, x_2) = \sum_{j=3}^4 (n_j + i\omega A_j) Z_j(\omega) \exp(n_j x_2), \tag{2.110b}$$

where n_j ($j=1,2,3,4$), A_j and Z_j are given by (2.22), (2.26) and (2.62), respectively. Changing the limits of integration (2.110a) becomes,

$$k_{22}^{(i)}(x_1, x_2, t) = \frac{1}{2\pi} \int_0^{\infty} [K_{221}^{(i)}(\omega, x_2) \cos(\omega(x_1 - t)) + K_{222}^{(i)}(\omega, x_2) \sin(\omega(x_1 - t))] d\omega, \tag{2.111}$$

where,

$$K_{221}^{(i)}(\omega, x_2) = \phi_{22}^{(i)}(\omega, x_2) + \phi_{22}^{(i)}(-\omega, x_2), \quad (2.112a)$$

$$K_{222}^{(i)}(\omega, x_2) = i(\phi_{22}^{(i)}(\omega, x_2) - \phi_{22}^{(i)}(-\omega, x_2)). \quad (2.112b)$$

$K_{221}^{(i)}$ and $K_{222}^{(i)}$ are expressed as,

$$K_{221}^{(i)}(\omega, x_2) = K_{2211}^{(i)}(\omega) \exp(n_3 x_2) + K_{2212}^{(i)}(\omega) \exp(n_4 x_2), \quad (2.113a)$$

$$K_{222}^{(i)}(\omega, x_2) = K_{2221}^{(i)}(\omega) \exp(n_3 x_2) + K_{2222}^{(i)}(\omega) \exp(n_4 x_2), \quad (2.113b)$$

in which

$$K_{2211}^{(i)}(\omega) = [n_3 + i\omega A_3(\omega)] Z_3(\omega) + [n_3 - i\omega A_3(-\omega)] Z_3(-\omega), \quad (2.114a)$$

$$K_{2212}^{(i)}(\omega) = [n_4 + i\omega A_4(\omega)] Z_4(\omega) + [n_4 - i\omega A_4(-\omega)] Z_4(-\omega), \quad (2.114b)$$

$$K_{2221}^{(i)}(\omega) = i\{[n_3 + i\omega A_3(\omega)] Z_3(\omega) - [n_3 - i\omega A_3(-\omega)] Z_3(-\omega)\}, \quad (2.114c)$$

$$K_{2222}^{(i)}(\omega) = i\{[n_4 + i\omega A_4(\omega)] Z_4(\omega) - [n_4 - i\omega A_4(-\omega)] Z_4(-\omega)\}. \quad (2.114d)$$

In order to extract the singular terms, asymptotic analyses of $K_{221}^{(i)}$ and $K_{222}^{(i)}$ are required as $\omega \rightarrow \infty$. Asymptotic expansions of $K_{221}^{(i)}$ and $K_{222}^{(i)}$ are given by

$$K_{221}^{(i)\infty}(\omega, x_2) = K_{2211}^{(i)\infty}(\omega) \exp(n_3 x_2) + K_{2212}^{(i)\infty}(\omega) \exp(n_4 x_2), \quad (2.115a)$$

$$K_{222}^{(i)\infty}(\omega, x_2) = K_{2221}^{(i)\infty}(\omega) \exp(n_3 x_2) + K_{2222}^{(i)\infty}(\omega) \exp(n_4 x_2). \quad (2.115b)$$

By using MAPLE, asymptotic expansions are obtained as follows:

$$K_{2211}^{(i)\infty}(\omega) = 0, \quad (2.116a)$$

$$K_{2212}^{(i)\infty}(\omega) = 0, \quad (2.116b)$$

$$K_{2221}^{(i)\infty}(\omega) = m_{210}, \quad (2.116c)$$

$$K_{2222}^{(i)\infty}(\omega) = m_{220}. \quad (2.116d)$$

The coefficients of the expansion m_{210} and m_{220} are given in Appendix A by equations (A.4a) and (A.4b), respectively. Subtracting the asymptotic expansions from the integrands in (2.111), using integration cutoff points, evaluating some of the integrals in closed form, taking the limit as $x_2 \rightarrow 0$, and after some manipulations $k_{22}^{(i)}(x_1, x_2, t)$ is expressed as

$$k_{22}^{(i)}(x_1, 0, t) = \frac{1}{2\pi} \frac{m_{20}}{x_1 - t} + J_{222}^{(i)}(x_1, t), \quad (2.117)$$

where m_{20} is given in Appendix A by equation (A.4c) and,

$$J_{222}^{(i)}(x_1, t) = \frac{1}{2\pi} \int_0^{A_{222}^{(i)}} [K_{222}^{(i)}(\omega, 0) - m_{20}] \sin(\omega(x_1 - t)) d\omega \\ + \frac{1}{2\pi} \int_{A_{222}^{(i)}}^{\infty} [K_{222}^{(i)}(\omega, 0) - m_{20}] \sin(\omega(x_1 - t)) d\omega, \quad (2.118)$$

in which, $A_{222}^{(i)}$ is an integration cutoff point.

Referring to (2.58e) and (2.67) $k_{22}^{(h)}(x_1, x_2, t)$ is written in the following form,

$$k_{22}^{(h)}(x_1, x_2, t) = \int_0^{\infty} K_{22}^{(h)}(\alpha, t, x_1) \cos(\alpha x_2) d\alpha, \quad (2.119)$$

where,

$$K_{22}^{(h)}(\alpha, t, x_1) = \sum_{j=3}^4 (H_j t_j + \alpha) \left[G_j^*(\alpha, t) \exp\left(-\frac{\alpha t}{F}\right) + G_j^{**}(\alpha, t) \exp\left(-\frac{\alpha t}{E}\right) \right] \\ \times \exp(t_j x_1), \quad (2.120)$$

t_j , ($j=1,2,3,4$), H_j , and G_j^*/G_j^{**} are given by (2.57), (2.59) and (2.68), respectively.

$K_{22}^{(h)}$ can be expressed as,

$$K_{22}^{(h)}(\alpha, t, x_1) = \left[K_{2211}^{(h)}(\alpha) \exp\left(-\frac{\alpha t}{F}\right) + K_{2212}^{(h)}(\alpha) \exp\left(-\frac{\alpha t}{E}\right) \right] \exp(t_3 x_1) + \left[K_{2221}^{(h)}(\alpha) \exp\left(-\frac{\alpha t}{F}\right) + K_{2222}^{(h)}(\alpha) \exp\left(-\frac{\alpha t}{E}\right) \right] \exp(t_4 x_1), \quad (2.121)$$

where,

$$K_{2211}^{(h)}(\alpha) = (H_3 t_3 + \alpha) G_3^*, \quad (2.122a)$$

$$K_{2212}^{(h)}(\alpha) = (H_3 t_3 + \alpha) G_3^{**}, \quad (2.122b)$$

$$K_{2221}^{(h)}(\alpha) = (H_4 t_4 + \alpha) G_4^*, \quad (2.122c)$$

$$K_{2222}^{(h)}(\alpha) = (H_4 t_4 + \alpha) G_4^{**}. \quad (2.122d)$$

In order to extract the singular terms, $K_{22}^{(h)}$ is expanded into a series as $\alpha \rightarrow \infty$.

Asymptotic expansion of $K_{22}^{(h)}$ is given by,

$$K_{22}^{(h)\infty}(\alpha, t, x_1) = K_{2211}^{(h)\infty}(\alpha) \exp\left(-\frac{\alpha t}{F} + t_3 x_1\right) + K_{2212}^{(h)\infty}(\alpha) \exp\left(-\frac{\alpha t}{E} + t_3 x_1\right) + K_{2221}^{(h)\infty}(\alpha) \exp\left(-\frac{\alpha t}{F} + t_4 x_1\right) + K_{2222}^{(h)\infty}(\alpha) \exp\left(-\frac{\alpha t}{E} + t_4 x_1\right), \quad (2.123)$$

By using MAPLE, asymptotic expansions are obtained as follows:

$$K_{2211}^{(h)\infty}(\alpha) = n_{110}, \quad (2.124a)$$

$$K_{2212}^{(h)\infty}(\alpha) = n_{120}, \quad (2.124b)$$

$$K_{2221}^{(h)\infty}(\alpha) = n_{210}, \quad (2.124c)$$

$$K_{2222}^{(h)\infty}(\alpha) = n_{220}. \quad (2.124d)$$

The coefficients of the expansion n_{110} , n_{120} , n_{210} and n_{220} are given in Appendix A by equation (A.5). Subtracting the asymptotic expansions from the integrands in (2.119), using integration cutoff points, evaluating some of the integrals in closed form, taking the limit as $x_2 \rightarrow 0$, and after some manipulations $k_{22}^{(h)}(x_1, x_2, t)$ is expressed as:

$$k_{22}^{(h)}(x_1, 0, t) = \left\{ \frac{n_{110} F}{t + A x_1 F} + \frac{n_{120} E}{t + A x_1 E} + \frac{n_{210} F}{t + B x_1 F} + \frac{n_{220} E}{t + B x_1 E} \right\} + J_{22}^{(h)}(x_1, t), \quad (2.125)$$

where A and B are given by (2.12), E and F are given by (2.23) and,

$$J_{22}^{(h)}(x_1, t) = \int_0^{A_{22}^{(h)}} \left(K_{22}^{(h)}(\alpha, t, x_1) - K_{22}^{(h)\infty}(\alpha, t, x_1) \right) d\alpha + \int_{A_{22}^{(h)}}^{\infty} \left[K_{22}^{(h)}(\alpha, t, x_1) - K_{22}^{(h)\infty}(\alpha, t, x_1) \right] d\alpha, \quad (2.126)$$

in which $A_{22}^{(h)}$ is an integration cutoff point. $K_{22}^{(h)\infty}$ can be rewritten as follows:

$$K_{22}^{(h)\infty}(\alpha, t, x_1) = n_{110} \exp\left(-\frac{\alpha t}{F} - A \alpha x_1\right) + n_{120} \exp\left(-\frac{\alpha t}{E} - A \alpha x_1\right) + n_{210} \exp\left(-\frac{\alpha t}{F} - B \alpha x_1\right) + n_{220} \exp\left(-\frac{\alpha t}{E} - B \alpha x_1\right). \quad (2.127)$$

$k_{22}^{(i)}(x_1, 0, t)$ and $k_{22}^{(h)}(x_1, 0, t)$ are provided by equations (2.117) and (2.125), respectively. Adding these two equations $k_{22}(x_1, 0, t)$ is written as,

$$k_{22}(x_1, 0, t) = \frac{1}{2\pi} \frac{m_{20}}{x_1 - t} + h_{22s}(x_1, t) + h_{22f}(x_1, t), \quad (2.128)$$

where,

$$h_{22s}(x_1, t) = \left[\frac{n_{110} F}{t + A x_1 F} + \frac{n_{120} E}{t + A x_1 E} + \frac{n_{210} F}{t + B x_1 F} + \frac{n_{220} E}{t + B x_1 E} \right], \quad (2.129a)$$

$$h_{22f}(x_1, t) = J_{222}^{(i)}(x_1, t) + J_{22}^{(h)}(x_1, t). \quad (2.129b)$$

$J_{222}^{(i)}(x_1, t)$ and $J_{22}^{(h)}(x_1, t)$ are given by equations (2.118) and (2.126), respectively.

2.2.3.4 Asymptotic Analysis of $k_{23}(x_1, x_2, t)$

Referring to (2.15c) $k_{23}(x_1, x_2, t)$ is written as

$$k_{23}(x_1, x_2, t) = \frac{1}{2\pi} \int_{-\infty}^{\infty} \phi_{23}(\rho, x_1) \exp(i\rho(x_2 - t)) d\rho, \quad (2.130a)$$

$$\phi_{23}(\rho, x_1) = \sum_{j=1}^2 (i\rho + N_j s_j) \psi_j(\rho) \exp(s_j x_1), \quad (2.130b)$$

where, s_j ($j=1,2,3,4$) and $\psi_j(\rho)$ are given by (2.11) and (2.18), respectively.

Changing the limits of integration in (2.130a), k_{23} becomes

$$k_{23}(x_1, x_2, t) = \frac{1}{2\pi} \int_0^{\infty} [K_{231}(\rho, x_1) \cos(\rho(x_2 - t)) + K_{232}(\rho, x_1) \sin(\rho(x_2 - t))] d\rho, \quad (2.131)$$

where,

$$K_{231}(\rho, x_1) = \phi_{23}(\rho, x_1) + \phi_{23}(-\rho, x_1), \quad (2.132a)$$

$$K_{232}(\rho, x_1) = i(\phi_{23}(\rho, x_1) - \phi_{23}(-\rho, x_1)). \quad (2.132b)$$

K_{231} and K_{232} are expressed as,

$$K_{231}(\rho, x_1) = K_{2311}(\rho) \exp(s_1 x_1) + K_{2312}(\rho) \exp(s_2 x_1), \quad (2.133a)$$

$$K_{232}(\rho, x_1) = K_{2321}(\rho) \exp(s_1 x_1) + K_{2322}(\rho) \exp(s_2 x_1), \quad (2.133b)$$

where,

$$K_{2311}(\rho) = (i\rho + N_1(\rho)s_1)\psi_1(\rho) + (-i\rho + N_1(-\rho)s_1)\psi_1(-\rho), \quad (2.134a)$$

$$K_{2312}(\rho) = (i\rho + N_2(\rho)s_2)\psi_2(\rho) + (-i\rho + N_2(-\rho)s_2)\psi_2(-\rho), \quad (2.134b)$$

$$K_{2321}(\rho) = i\{(i\rho + N_1(\rho)s_1)\psi_1(\rho) - (-i\rho + N_1(-\rho)s_1)\psi_1(-\rho)\}, \quad (2.134c)$$

$$K_{2322}(\rho) = i\{(i\rho + N_2(\rho)s_2)\psi_2(\rho) - (-i\rho + N_2(-\rho)s_2)\psi_2(-\rho)\}. \quad (2.134d)$$

In order to extract the singular terms, asymptotic analyses of K_{231} and K_{232} are required as $\rho \rightarrow \infty$. Asymptotic expansions of K_{231} and K_{232} are given by,

$$K_{231}^\infty(\rho, x_1) = K_{2311}^\infty(\rho) \exp(s_1 x_1) + K_{2312}^\infty(\rho) \exp(s_2 x_1), \quad (2.135a)$$

$$K_{232}^\infty(\rho, x_1) = K_{2321}^\infty(\rho) \exp(s_1 x_1) + K_{2322}^\infty(\rho) \exp(s_2 x_1). \quad (2.135b)$$

By using MAPLE, asymptotic expansions are obtained as follows:

$$K_{2311}^\infty(\rho, x_1) = f_{110}, \quad (2.136a)$$

$$K_{2312}^\infty(\rho, x_1) = f_{120}, \quad (2.136b)$$

$$K_{2321}^\infty(\rho, x_1) = f_{210}, \quad (2.136c)$$

$$K_{2322}^\infty(\rho, x_1) = f_{220}. \quad (2.136d)$$

The coefficients of the expansion f_{110} , f_{120} , f_{210} and f_{220} are given in Appendix A by equation (A.6). Subtracting the asymptotic expansions from the integrands in (2.131), using integration cutoff points, evaluating some of the integrals in closed form, taking the limit as $x_2 \rightarrow 0$, and after some manipulations $k_{23}(x_1, x_2, t)$ is expressed as:

$$k_{23}(x_1, 0, t) = h_{23s}(x_1, t) + h_{23f}(x_1, t), \quad (2.137)$$

where,

$$h_{23s}(x_1, t) = \frac{1}{2\pi} \left\{ \begin{array}{l} \frac{x_1 t^2 (A f_{110} + B f_{120})}{(A^2 x_1^2 + t^2)(B^2 x_1^2 + t^2)} - \frac{x_1^2 t (B^2 f_{210} + A^2 f_{220})}{(A^2 x_1^2 + t^2)(B^2 x_1^2 + t^2)} \\ - \frac{t^3 f_{20}}{(A^2 x_1^2 + t^2)(B^2 x_1^2 + t^2)} + \frac{x_1^3 AB (B f_{110} + A f_{120})}{(A^2 x_1^2 + t^2)(B^2 x_1^2 + t^2)} \end{array} \right\}, \quad (2.138a)$$

$$h_{23f}(x_1, t) = J_{231}(x_1, t) + J_{232}(x_1, t). \quad (2.138b)$$

f_{20} is given in Appendix A by equation (A.6e); A and B are provided by (2.12); and,

$$\begin{aligned} J_{231}(x_1, t) = & \\ & \frac{1}{2\pi} \int_0^{A_{231}} [K_{231}(\rho, x_1) - (f_{110} \exp(-A|\rho|x_1) + f_{120} \exp(-B|\rho|x_1))] \cos(\rho t) d\rho \\ & + \frac{1}{2\pi} \int_{A_{231}}^{\infty} [K_{231}(\rho, x_1) - (f_{110} \exp(-A|\rho|x_1) + f_{120} \exp(-B|\rho|x_1))] \cos(\rho t) d\rho, \end{aligned} \quad (2.139a)$$

$$\begin{aligned} J_{232}(x_2, t) = & \\ & - \frac{1}{2\pi} \int_0^{A_{232}} [K_{232}(\rho, x_1) - (f_{210} \exp(-A|\rho|x_1) + f_{220} \exp(-B|\rho|x_1))] \sin(\rho t) d\rho \\ & - \frac{1}{2\pi} \int_{A_{232}}^{\infty} [K_{232}(\rho, x_1) - (f_{210} \exp(-A|\rho|x_1) + f_{220} \exp(-B|\rho|x_1))] \sin(\rho t) d\rho, \end{aligned} \quad (2.139b)$$

in which A_{231} and A_{232} are integration cutoff points.

2.2.3.5 Asymptotic Analysis of $k_{31}(x_1, x_2, t)$

$k_{31}(x_1, x_2, t)$ is expressed as follows:

$$k_{31}(x_1, x_2, t) = k_{31}^{(i)}(x_1, x_2, t) + k_{31}^{(h)}(x_1, x_2, t), \quad (2.140a)$$

By using the infinite plane solution and the half-plane ($x_1 > 0$) solution, $k_{31}^{(i)}$ and $k_{31}^{(h)}$ are obtained.. Referring to (2.25f) and (2.35), $k_{31}^{(i)}(x_1, x_2, t)$ is written as

$$k_{31}^{(i)}(x_1, x_2, t) = \frac{1}{2\pi} \int_{-\infty}^{\infty} \phi_{31}^{(i)}(\omega, x_2) \exp(i\omega(x_1 - t)) d\omega, \quad (2.141a)$$

$$\phi_{31}^{(i)}(\omega, x_2) = \sum_{j=3}^4 n_j P_j(\omega) \exp(n_j x_2), \quad (2.141b)$$

where n_j ($j=1,2,3,4$) and P_j are given by (2.22) and (2.35), respectively. Changing the limits of integration (2.141a) becomes

$$k_{31}^{(i)}(x_1, x_2, t) = \frac{1}{2\pi} \int_0^{\infty} \left[K_{3111}^{(i)}(\omega, x_2) \cos(\omega(x_1 - t)) + K_{312}^{(i)}(\omega, x_2) \sin(\omega(x_1 - t)) \right] d\omega, \quad (2.142)$$

where,

$$K_{311}^{(i)}(\omega, x_2) = \phi_{31}^{(i)}(\omega, x_2) + \phi_{31}^{(i)}(-\omega, x_2), \quad (2.143a)$$

$$K_{312}^{(i)}(\omega, x_2) = i(\phi_{31}^{(i)}(\omega, x_2) - \phi_{31}^{(i)}(-\omega, x_2)), \quad (2.143b)$$

$K_{311}^{(i)}$ and $K_{312}^{(i)}$ can be expressed as

$$K_{311}^{(i)}(\omega, x_2) = K_{3111}^{(i)}(\omega) \exp(n_3 x_2) + K_{3112}^{(i)}(\omega) \exp(n_4 x_2), \quad (2.144a)$$

$$K_{312}^{(i)}(\omega, x_2) = K_{3121}^{(i)}(\omega) \exp(n_3 x_2) + K_{3122}^{(i)}(\omega) \exp(n_4 x_2), \quad (2.144b)$$

and,

$$K_{3111}^{(i)}(\omega) = n_3 [P_3(\omega) + P_3(-\omega)], \quad (2.145a)$$

$$K_{3112}^{(i)}(\omega) = n_4 [P_4(\omega) + P_4(-\omega)], \quad (2.145b)$$

$$K_{3121}^{(i)}(\omega) = i n_3 [P_3(\omega) - P_3(-\omega)], \quad (2.145c)$$

$$K_{3122}^{(i)}(\omega) = i n_4 [P_4(\omega) - P_4(-\omega)]. \quad (2.145d)$$

In order to extract the singular terms, asymptotic analyses of $K_{311}^{(i)}$ and $K_{312}^{(i)}$ are required as $\omega \rightarrow \infty$. Asymptotic expansion of $K_{311}^{(i)}$ and $K_{312}^{(i)}$ are given by

$$K_{311}^{(i)\infty}(\omega, x_2) = K_{3111}^{(i)\infty}(\omega) \exp(n_3 x_2) + K_{3112}^{(i)\infty}(\omega) \exp(n_4 x_2), \quad (2.146a)$$

$$K_{312}^{(i)\infty}(\omega, x_2) = K_{3121}^{(i)\infty}(\omega) \exp(n_3 x_2) + K_{3122}^{(i)\infty}(\omega) \exp(n_4 x_2). \quad (2.146b)$$

By using MAPLE, asymptotic expansions are obtained as follows:

$$K_{3111}^{(i)\infty}(\omega) = h_{110}, \quad (2.147a)$$

$$K_{3112}^{(i)\infty}(\omega) = h_{120}, \quad (2.147b)$$

$$K_{3121}^{(i)\infty}(\omega) = 0, \quad (2.147c)$$

$$K_{3122}^{(i)\infty}(\omega) = 0. \quad (2.147d)$$

The coefficients of the expansions h_{110} and h_{120} are given in Appendix A by equation (A.7). Subtracting the asymptotic expansions from the integrands in (2.142), using integration cutoff points, evaluating some of the integrals in closed form, taking the limit as $x_1 \rightarrow 0$, and after some manipulations $k_{31}^{(i)}(x_1, x_2, t)$ is expressed as:

$$k_{31}^{(i)}(0, x_2, t) = \frac{1}{2\pi} \left[\frac{x_2^3 EF (F h_{110} + E h_{120})}{(E^2 x_2^2 + t^2)(F^2 x_2^2 + t^2)} + \frac{x_2 t^2 (E h_{110} + F h_{120})}{(E^2 x_2^2 + t^2)(F^2 x_2^2 + t^2)} \right] + J_{311}^{(i)}(x_2, t), \quad (2.148)$$

where E and F are given by (2.23) and

$$\begin{aligned}
J_{311}^{(i)}(x_2, t) = & \frac{1}{2\pi} \int_0^{A_{311}^{(i)}} \left[K_{311}^{(i)}(\omega, x_2) - (h_{110} \exp(n_3 x_2) + h_{120} \exp(n_4 x_2)) \right] \cos(\omega t) d\omega \\
& + \frac{1}{2\pi} \int_{A_{311}^{(i)}}^{\infty} \left[K_{311}^{(i)}(\omega, x_2) - (h_{110} \exp(n_3 x_2) + h_{120} \exp(n_4 x_2)) \right] \cos(\omega t) d\omega,
\end{aligned} \tag{2.149}$$

in which $A_{311}^{(i)}$ is an integration cutoff point.

Referring to (2.31f) and (2.49) and (2.50), $k_{31}^{(h)}(x_1, x_2, t)$ is written in the following form,

$$k_{31}^{(h)}(x_1, x_2, t) = \int_0^{\infty} K_{31}^{(h)}(\alpha, t, x_1) \sin(\alpha x_2) d\alpha, \tag{2.150}$$

where,

$$K_{31}^{(h)}(\alpha, t, x_1) = -\alpha \sum_{j=3}^4 \left[B_j^*(\alpha, t) \exp\left(-\frac{\alpha t}{F}\right) + B_j^{**}(\alpha, t) \exp\left(-\frac{\alpha t}{E}\right) \right] \exp(p_j x_1). \tag{2.151}$$

p_j ($j=1,2,3,4$) and B_j^*/B_j^{**} are given by (2.30) and (2.50), respectively. $K_{31}^{(h)}$ can be expressed as,

$$\begin{aligned}
K_{31}^{(h)}(\alpha, t, x_1) = & \left[K_{3111}^{(h)}(\alpha) \exp\left(-\frac{\alpha t}{F}\right) + K_{3112}^{(h)}(\alpha) \exp\left(-\frac{\alpha t}{E}\right) \right] \exp(p_3 x_1) \\
& + \left[K_{3121}^{(h)}(\alpha) \exp\left(-\frac{\alpha t}{F}\right) + K_{3122}^{(h)}(\alpha) \exp\left(-\frac{\alpha t}{E}\right) \right] \exp(p_4 x_1),
\end{aligned} \tag{2.152}$$

where,

$$K_{3111}^{(h)}(\alpha) = -\alpha B_3^*, \tag{2.153a}$$

$$K_{3112}^{(h)}(\alpha) = -\alpha B_3^{**}, \tag{2.153b}$$

$$K_{3121}^{(h)}(\alpha) = -\alpha B_4^*, \quad (2.153c)$$

$$K_{3122}^{(h)}(\alpha) = -\alpha B_4^{**}. \quad (2.153d)$$

In order to extract the singular terms, $K_{31}^{(h)}$ is expanded into series as $\alpha \rightarrow \infty$.

Asymptotic expansion of $K_{31}^{(h)}$ is given by

$$\begin{aligned} K_{31}^{(h)\infty}(\alpha, t, x_1) = & K_{3111}^{(h)\infty}(\alpha) \exp\left(-\frac{\alpha t}{F} + p_3 x_1\right) + K_{3112}^{(h)\infty}(\alpha) \exp\left(-\frac{\alpha t}{E} + p_3 x_1\right) \\ & + K_{3121}^{(h)\infty}(\alpha) \exp\left(-\frac{\alpha t}{F} + p_4 x_1\right) + K_{3122}^{(h)\infty}(\alpha) \exp\left(-\frac{\alpha t}{E} + p_4 x_1\right). \end{aligned} \quad (2.154)$$

By using MAPLE, asymptotic expansions are obtained as follows:

$$K_{3111}^{(h)\infty}(\alpha) = l_{110}, \quad (2.155a)$$

$$K_{3112}^{(h)\infty}(\alpha) = l_{120}, \quad (2.155b)$$

$$K_{3121}^{(h)\infty}(\alpha) = l_{210}, \quad (2.155c)$$

$$K_{3122}^{(h)\infty}(\alpha) = l_{220}. \quad (2.155d)$$

The coefficients of the expansion l_{110} , l_{120} , l_{210} and l_{220} are given in Appendix A by equations (A.8a), (A.8b), (A.8c) and (A.8d), respectively. Subtracting the asymptotic expansions from the integrands in (2.150), using integration cutoff points, evaluating some of the integrals in closed form, taking the limit as $x_1 \rightarrow 0$, and after some manipulations $k_{31}^{(h)}(x_1, x_2, t)$ is expressed as

$$k_{31}^{(h)}(0, x_2, t) = \frac{x_2^3 F^2 E^2 l_0}{(E^2 x_2^2 + t^2)(F^2 x_2^2 + t^2)} + \frac{x_2 t^2 (F^2 l_{10} + E^2 l_{20})}{(E^2 x_2^2 + t^2)(F^2 x_2^2 + t^2)} + J_{31}^{(h)}(x_2, t), \quad (2.156)$$

where E and F are given by (2.23), l_{10} , l_{20} and l_0 are given in Appendix A by equations (A.8e), (A.8f) and (A.8g), respectively and

$$\begin{aligned}
J_{31}^{(h)}(x_2, t) &= \int_0^{A_{31}^{(h)}} \left[K_{31}^{(h)}(\alpha, t, 0) - \left(l_{10} \exp\left(-\frac{\alpha t}{F}\right) + l_{20} \exp\left(-\frac{\alpha t}{E}\right) \right) \right] \sin(\alpha x_2) d\alpha \\
&+ \int_{A_{31}^{(h)}}^{\infty} \left[K_{31}^{(h)}(\alpha, t, 0) - \left(l_{10} \exp\left(-\frac{\alpha t}{F}\right) + l_{20} \exp\left(-\frac{\alpha t}{E}\right) \right) \right] \sin(\alpha x_2) d\alpha.
\end{aligned} \tag{2.157}$$

in which $A_{31}^{(h)}$ is an integration cutoff point.

$k_{31}^{(i)}(0, x_2, t)$ and $k_{31}^{(h)}(0, x_2, t)$ are given by equations (2.148) and (2.156), respectively. Adding these two equations $k_{31}(0, x_2, t)$ is written as,

$$k_{31}(0, x_2, t) = h_{31s}(x_2, t) + h_{31f}(x_2, t), \tag{2.158}$$

where,

$$\begin{aligned}
h_{31s}(x_2, t) &= \frac{1}{2\pi} \left[\frac{x_2^3 EF (F h_{110} + E h_{120} + 2\pi E F l_0)}{(E^2 x_2^2 + t^2)(F^2 x_2^2 + t^2)} \right] \\
&+ \frac{1}{2\pi} \left[\frac{x_2 t^2 (E h_{110} + F h_{120} + 2\pi(F^2 l_{10} + E^2 l_{20}))}{(E^2 x_2^2 + t^2)(F^2 x_2^2 + t^2)} \right],
\end{aligned} \tag{2.159a}$$

$$h_{31f}(x_2, t) = J_{311}^{(i)}(x_2, t) + J_{31}^{(h)}(x_2, t). \tag{2.159b}$$

$J_{311}^{(i)}(x_2, t)$ and $J_{31}^{(h)}(x_2, t)$ are provided by equations (2.149) and (2.157), respectively.

2.2.3.6 Asymptotic Analysis of $k_{32}(x_1, x_2, t)$

$k_{32}(x_1, x_2, t)$ is expressed as follows:

$$k_{32}(x_1, x_2, t) = k_{32}^{(i)}(x_1, x_2, t) + k_{32}^{(h)}(x_1, x_2, t), \tag{2.160}$$

By using the infinite plane solution and the half-plane ($x_1 > 0$) solution, $k_{32}^{(i)}$ and $k_{32}^{(h)}$ are obtained. Referring to (2.53f) and (2.62), $k_{32}^{(i)}(x_1, x_2, t)$ is written as

$$k_{32}^{(i)}(x_1, x_2, t) = \frac{1}{2\pi} \int_{-\infty}^{\infty} \phi_{32}^{(i)}(\omega, x_2) \exp(i\omega(x_1 - t)) d\omega, \quad (2.161a)$$

$$\phi_{32}^{(i)}(\omega, x_2) = \sum_{j=3}^4 n_j Z_j(\omega) \exp(n_j x_2), \quad (2.161b)$$

where n_j ($j=1,2,3,4$) and Z_j are given by (2.22), and (2.62), respectively.

Changing the limits of integration (2.161a) becomes

$$k_{32}^{(i)}(x_1, x_2, t) = \frac{1}{2\pi} \int_0^{\infty} \left[K_{321}^{(i)}(\omega, x_2) \cos(\omega(x_1 - t)) + K_{322}^{(i)}(\omega, x_2) \sin(\omega(x_1 - t)) \right] d\omega, \quad (2.162)$$

where,

$$K_{321}^{(i)}(\omega, x_2) = \phi_{32}^{(i)}(\omega, x_2) + \phi_{32}^{(i)}(-\omega, x_2), \quad (2.163a)$$

$$K_{322}^{(i)}(\omega, x_2) = i(\phi_{32}^{(i)}(\omega, x_2) - \phi_{32}^{(i)}(-\omega, x_2)). \quad (2.163b)$$

$K_{321}^{(i)}$ and $K_{322}^{(i)}$ can be expressed as,

$$K_{321}^{(i)}(\omega, x_2) = K_{3211}^{(i)}(\omega) \exp(n_3 x_2) + K_{3212}^{(i)}(\omega) \exp(n_4 x_2), \quad (2.164a)$$

$$K_{322}^{(i)}(\omega, x_2) = K_{3221}^{(i)}(\omega) \exp(n_3 x_2) + K_{3222}^{(i)}(\omega) \exp(n_4 x_2), \quad (2.164b)$$

and,

$$K_{3211}^{(i)}(\omega) = n_3 [Z_3(\omega) + Z_3(-\omega)], \quad (2.165a)$$

$$K_{3212}^{(i)}(\omega) = n_4 [Z_4(\omega) + Z_4(-\omega)], \quad (2.165b)$$

$$K_{3221}^{(i)}(\omega) = i n_3 [Z_3(\omega) - Z_3(-\omega)], \quad (2.165c)$$

$$K_{3222}^{(i)}(\omega) = i n_4 [Z_4(\omega) - Z_4(-\omega)]. \quad (2.165d)$$

In order to extract the singular terms, asymptotic analyses of $K_{321}^{(i)}$ and $K_{322}^{(i)}$ are required as $\omega \rightarrow \infty$. Asymptotic expansion of $K_{321}^{(i)}$ and $K_{322}^{(i)}$ are given by

$$K_{321}^{(i)\infty}(\omega, x_2) = K_{3211}^{(i)\infty}(\omega) \exp(n_3 x_2) + K_{3212}^{(i)\infty}(\omega) \exp(n_4 x_2), \quad (2.166a)$$

$$K_{322}^{(i)\infty}(\omega, x_2) = K_{3221}^{(i)\infty}(\omega) \exp(n_3 x_2) + K_{3222}^{(i)\infty}(\omega) \exp(n_4 x_2). \quad (2.166b)$$

By using MAPLE, asymptotic expansions are obtained as follows:

$$K_{3211}^{(i)\infty}(\omega) = 0, \quad (2.167a)$$

$$K_{3212}^{(i)\infty}(\omega) = 0, \quad (2.167b)$$

$$K_{3221}^{(i)\infty}(\omega) = r_{210}, \quad (2.167c)$$

$$K_{3222}^{(i)\infty}(\omega) = r_{220}. \quad (2.167d)$$

The coefficients of the expansion r_{210} and r_{220} are given in Appendix A by equations (A.9a) and (A.9b), respectively. Subtracting the asymptotic expansions from the integrands in (2.162), using integration cutoff points, evaluating some of the integrals in closed form, taking the limit as $x_1 \rightarrow 0$, and after some manipulations

$k_{32}^{(i)}(x_1, x_2, t)$ is expressed as:

$$k_{32}^{(i)}(0, x_2, t) = -\frac{1}{2\pi} \left[\frac{x_2^2 t (F^2 r_{120} + E^2 r_{220})}{(E^2 x_2^2 + t^2)(F^2 x_2^2 + t^2)} + \frac{t^3 r_{20}}{(E^2 x_2^2 + t^2)(F^2 x_2^2 + t^2)} \right] + J_{322}^{(i)}(x_2, t), \quad (2.168)$$

where r_{20} is given in Appendix A by (A.9c) and

$$\begin{aligned}
J_{322}^{(i)}(x_2, t) = & -\frac{1}{2\pi} \int_0^{A_{322}^{(i)}} \left[K_{322}^{(i)}(\omega, x_2) - (r_{210} \exp(n_3 x_2) + r_{220} \exp(n_4 x_2)) \right] \sin(\omega t) d\omega \\
& - \frac{1}{2\pi} \int_{A_{322}^{(i)}}^{\infty} \left[K_{322}^{(i)}(\omega, x_2) - (r_{210} \exp(n_3 x_2) + r_{220} \exp(n_4 x_2)) \right] \sin(\omega t) d\omega,
\end{aligned} \tag{2.169}$$

in which $A_{322}^{(i)}$ is an integration cutoff point.

Referring to (2.58f) and (2.67) $k_{22}^{(h)}(x_1, x_2, t)$ is written in the following form,

$$k_{32}^{(h)}(x_1, x_2, t) = \int_0^{\infty} K_{32}^{(h)}(\alpha, t, x_1) \cos(\alpha x_2) d\alpha, \tag{2.170}$$

where,

$$K_{32}^{(h)}(\alpha, t, x_1) = \alpha \sum_{j=3}^4 \left[G_j^*(\alpha, t) \exp\left(-\frac{\alpha t}{F}\right) + G_j^{**}(\alpha, t) \exp\left(-\frac{\alpha t}{E}\right) \right] \exp(t_j x_1). \tag{2.171}$$

t_j ($j=1, 2, 3, 4$), and G_j^*/G_j^{**} are given by (2.57) and (2.68), respectively. $K_{32}^{(h)}$ can be expressed as,

$$\begin{aligned}
K_{32}^{(h)}(\alpha, t, x_1) = & \left[K_{3211}^{(h)}(\alpha) \exp\left(-\frac{\alpha t}{F}\right) + K_{3212}^{(h)}(\alpha) \exp\left(-\frac{\alpha t}{E}\right) \right] \exp(t_3 x_1) \\
& + \left[K_{3221}^{(h)}(\alpha) \exp\left(-\frac{\alpha t}{F}\right) + K_{3222}^{(h)}(\alpha) \exp\left(-\frac{\alpha t}{E}\right) \right] \exp(t_4 x_1),
\end{aligned} \tag{2.172}$$

where,

$$K_{3211}^{(h)}(\alpha) = \alpha G_3^*, \tag{2.173a}$$

$$K_{3212}^{(h)}(\alpha) = \alpha G_3^{**}, \tag{2.173b}$$

$$K_{3221}^{(h)}(\alpha) = \alpha G_4^*, \tag{2.173c}$$

$$K_{3222}^{(h)}(\alpha) = \alpha G_4^{**}. \quad (2.173d)$$

In order to extract the singular terms, $K_{32}^{(h)}$ is expanded into series as $\alpha \rightarrow \infty$.

Asymptotic expansion of $K_{32}^{(h)}$ is given by

$$\begin{aligned} K_{32}^{(h)\infty}(\alpha, t, x_1) = & K_{3211}^{(h)\infty}(\alpha) \exp\left(-\frac{\alpha t}{F} + t_3 x_1\right) + K_{3212}^{(h)\infty}(\alpha) \exp\left(-\frac{\alpha t}{E} + t_3 x_1\right) \\ & + K_{3221}^{(h)\infty}(\alpha) \exp\left(-\frac{\alpha t}{F} + t_4 x_1\right) + K_{3222}^{(h)\infty}(\alpha) \exp\left(-\frac{\alpha t}{E} + t_4 x_1\right), \end{aligned} \quad (2.174)$$

By using MAPLE, asymptotic expansions are obtained as follows:

$$K_{3211}^{(h)\infty}(\alpha) = s_{110}, \quad (2.175a)$$

$$K_{3212}^{(h)\infty}(\alpha) = s_{120}, \quad (2.175b)$$

$$K_{3221}^{(h)\infty}(\alpha) = s_{210}, \quad (2.175c)$$

$$K_{3222}^{(h)\infty}(\alpha) = s_{220}. \quad (2.175d)$$

The coefficients of the expansion s_{110} , s_{120} , s_{210} and s_{220} are given in Appendix A by equations (A.10a), (A.10b), (A.10c) and (A.10d), respectively. Subtracting the asymptotic expansions from the integrands in (2.170), using integration cutoff points, evaluating some of the integrals in closed form, taking the limit as $x_1 \rightarrow 0$, and after some manipulations $k_{32}^{(h)}(x_1, x_2, t)$ is expressed as

$$k_{32}^{(h)}(0, x_2, t) = \frac{x_2^2 t EF(E s_{10} + F s_{20})}{(E^2 x_2^2 + t^2)(F^2 x_2^2 + t^2)} + \frac{t^3 (F s_{10} + E s_{20})}{(E^2 x_2^2 + t^2)(F^2 x_2^2 + t^2)} + J_{32}^{(h)}(x_2, t), \quad (2.176)$$

where E and F are given by (2.23); s_{10} and s_{20} are given in Appendix A by equations (A.10e) and (A.10f), respectively; and

$$\begin{aligned}
J_{32}^{(h)}(x_2, t) = & \int_0^{A_{32}^{(h)}} \left[K_{32}^{(h)}(\alpha, t, 0) - \left(s_{10} \exp\left(-\frac{\alpha t}{F}\right) + s_{20} \exp\left(-\frac{\alpha t}{E}\right) \right) \right] \cos(\alpha x_2) d\alpha \\
& + \int_{A_{32}^{(h)}}^{\infty} \left[K_{32}^{(h)}(\alpha, t, 0) - \left(s_{10} \exp\left(-\frac{\alpha t}{F}\right) + s_{20} \exp\left(-\frac{\alpha t}{E}\right) \right) \right] \cos(\alpha x_2) d\alpha,
\end{aligned} \tag{2.177}$$

in which $A_{32}^{(h)}$ is an integration cutoff point.

$k_{32}^{(i)}(0, x_2, t)$ and $k_{32}^{(h)}(0, x_2, t)$ are given by equations (2.168) and (2.176), respectively. Adding these two equations $k_{32}(0, x_2, t)$ is written as

$$k_{32}(0, x_2, t) = h_{32s}(x_2, t) + h_{31f}(x_2, t), \tag{2.178}$$

where,

$$\begin{aligned}
h_{32s}(x_2, t) = & \frac{1}{2\pi} \left[\frac{x_2^2 t (-F^2 r_{210} - E^2 r_{220} + 2\pi EF(Es_{10} + Fs_{20}))}{(E^2 x_2^2 + t^2)(F^2 x_2^2 + t^2)} \right] \\
& + \frac{1}{2\pi} \left[\frac{-r_{20} + 2\pi(Fs_{10} + Es_{20})}{(E^2 x_2^2 + t^2)(F^2 x_2^2 + t^2)} \right],
\end{aligned} \tag{2.179a}$$

$$h_{32f}(x_2, t) = J_{322}^{(i)}(x_2, t) + J_{32}^{(h)}(x_2, t). \tag{2.179b}$$

$J_{322}^{(i)}(x_2, t)$ and $J_{32}^{(h)}(x_2, t)$ are provided by equations (2.169) and (2.177), respectively.

2.2.3.7 Asymptotic Analysis of $k_{33}(x_1, x_2, t)$

Referring to (2.15d) $k_{33}(x_1, x_2, t)$ is written as

$$k_{33}(x_1, x_2, t) = \frac{1}{2\pi} \int_{-\infty}^{\infty} \phi_{33}(\rho, x_1) \exp(i\rho(x_2 - t)) d\rho, \tag{2.180a}$$

$$\phi_{33}(\rho, x_1) = i\rho \sum_{j=1}^2 \psi_j(\rho) \exp(s_j x_1), \quad (2.180b)$$

where, s_j ($j=1,2,3,4$) and $\psi_j(\rho)$ are given by (2.11) and (2.18), respectively.

Changing the limits of integration in (2.180a), k_{33} becomes

$$k_{33}(x_1, x_2, t) = \frac{1}{2\pi} \int_0^{\infty} [K_{331}(\rho, x_1) \cos(\rho(x_2 - t)) + K_{332}(\rho, x_1) \sin(\rho(x_2 - t))] d\rho, \quad (2.181)$$

where,

$$K_{331}(\rho, x_1) = \phi_{33}(\rho, x_1) + \phi_{33}(-\rho, x_1), \quad (2.182a)$$

$$K_{332}(\rho, x_1) = i(\phi_{33}(\rho, x_1) - \phi_{33}(-\rho, x_1)). \quad (2.182b)$$

K_{331} and K_{332} can be expressed as,

$$K_{331}(\rho, x_1) = K_{3311}(\rho) \exp(s_1 x_1) + K_{3312}(\rho) \exp(s_2 x_1), \quad (2.183a)$$

$$K_{332}(\rho, x_1) = K_{3321}(\rho) \exp(s_1 x_1) + K_{3322}(\rho) \exp(s_2 x_1), \quad (2.183b)$$

and,

$$K_{3311}(\rho) = i\rho [\psi_1(\rho) - \psi_1(-\rho)], \quad (2.184a)$$

$$K_{3312}(\rho) = i\rho [\psi_2(\rho) - \psi_2(-\rho)], \quad (2.184b)$$

$$K_{3321}(\rho) = -\rho [\psi_1(\rho) + \psi_1(-\rho)], \quad (2.184c)$$

$$K_{3322}(\rho) = -\rho [\psi_2(\rho) + \psi_2(-\rho)]. \quad (2.184d)$$

In order to extract the singular terms, asymptotic analyses of K_{331} and K_{332} are required as $\rho \rightarrow \infty$. Asymptotic expansion of K_{331} and K_{332} are given by

$$K_{331}^{\infty}(\rho, x_1) = K_{3311}^{\infty}(\rho) \exp(s_1 x_1) + K_{3312}^{\infty}(\rho) \exp(s_2 x_1), \quad (2.185a)$$

$$K_{332}^{\infty}(\rho, x_1) = K_{3321}^{\infty}(\rho) \exp(s_1 x_1) + K_{3322}^{\infty}(\rho) \exp(s_2 x_1). \quad (2.185b)$$

By using MAPLE, asymptotic expansions are obtained as follows:

$$K_{3311}^{\infty}(\rho, x_1) = e_{110}, \quad (2.186a)$$

$$K_{3312}^{\infty}(\rho, x_1) = e_{120}, \quad (2.186b)$$

$$K_{3321}^{\infty}(\rho, x_1) = e_{210}, \quad (2.186c)$$

$$K_{3322}^{\infty}(\rho, x_1) = e_{220}. \quad (2.186d)$$

The coefficients of the expansion e_{110} , e_{120} , e_{210} and e_{220} are given in Appendix A by equations (A.11a), (A.11b), (A.11c) and (A.11d), respectively. Subtracting the asymptotic expansions from the integrands in (2.181), using integration cutoff points, evaluating some of the integrals in closed form, taking the limit as $x_1 \rightarrow 0$, and after some manipulations $k_{33}(x_1, x_2, t)$ is expressed as

$$k_{33}(0, x_2, t) = \frac{1}{2\pi} \left(\frac{e_{20}}{x_2 - t} \right) + \left(\frac{e_{10}}{2} \right) \delta(x_2 - t) + h_{33f}(x_2, t), \quad (2.187)$$

where e_{10} and e_{20} are given in Appendix A by equations (A.11e) and (A.11f), respectively and

$$h_{33f}(x_2, t) = J_{331}(x_2, t) + J_{332}(x_2, t), \quad (2.188)$$

where

$$J_{331}(x_2, t) = \frac{1}{2\pi} \int_0^{A_{331}} [K_{331}(\rho, 0) - e_{10}] \cos(\rho(x_2 - t)) d\rho \\ + \frac{1}{2\pi} \int_{A_{331}}^{\infty} [K_{331}(\rho, 0) - e_{10}] \cos(\rho(x_2 - t)) d\rho, \quad (2.189a)$$

$$\begin{aligned}
J_{332}(x_2, t) = & \frac{1}{2\pi} \int_0^{A_{332}} [K_{332}(\rho, 0) - e_{20}] \sin(\rho(x_2 - t)) d\rho \\
& + \frac{1}{2\pi} \int_{A_{332}}^{\infty} [K_{332}(\rho, 0) - e_{20}] \sin(\rho(x_2 - t)) d\rho,
\end{aligned} \tag{2.189b}$$

in which A_{331} and A_{332} are integration cutoff points.

2.2.4 Singular Behavior of the Solution

By using the expressions given in Section 2.2.3 for the kernels, integral equations provided by (2.77) are written as follows:

$$\begin{aligned}
\sigma_{22}(x_1, 0) = & \int_0^d \left[\frac{1}{2\pi} \frac{a_{20}}{x_1 - t} + h_{11s}(x_1, t) + h_{11f}(x_1, t) \right] f_1(t) dt \\
& + \int_a^b [h_{13s}(x_1, t) + h_{13f}(x_1, t)] f_3(t) dt = 0, \quad 0 < x_1 < d,
\end{aligned} \tag{2.190a}$$

$$\begin{aligned}
\sigma_{12}(x_1, 0) = & \int_0^d \left[\frac{1}{2\pi} \frac{m_{20}}{x_1 - t} + h_{22s}(x_1, t) + h_{22f}(x_1, t) \right] f_2(t) dt \\
& + \int_a^b [h_{23s}(x_1, t) + h_{23f}(x_1, t)] f_3(t) dt = 0, \quad 0 < x_1 < d,
\end{aligned} \tag{2.190b}$$

$$\begin{aligned}
\frac{C_{66}}{2} \frac{\partial}{\partial x_2} u_1(0, x_2) = & \int_0^d [h_{31s}(x_2, t) + h_{31f}(x_2, t)] f_1(t) dt \\
& + \int_0^d [h_{32s}(x_2, t) + h_{31f}(x_2, t)] f_2(t) dt \\
& + \int_a^b \left[\frac{1}{2\pi} \left(\frac{e_{20}}{x_2 - t} \right) + \left(\frac{e_{10}}{2} \right) \delta(x_2 - t) + h_{33f}(x_2, t) \right] f_3(t) dt = f(x_2), \\
& a < x_2 < b.
\end{aligned} \tag{2.190c}$$

In these integral equations, there are Cauchy kernels and Fredholm kernels. $h_{ijs}(x^*, t)$ and $h_{ijf}(x^*, t)$ ($x^* = x_1$ for $i=1,2$ and $x^* = x_2$ for $i=3$) are given in Section 2.2.3. $h_{ijs}(x^*, t)$ are the Cauchy kernels that become unbounded as x^* and t go to the end point simultaneously. $h_{ijf}(x^*, t)$ are bounded Fredholm kernels. The solution of the singular integral equations is obtained through the function-theoretic method as described by Dag [40] and Erdogan [43]. In this analysis, $a > 0$ case is considered. For $a > 0$, unknown functions f_i can be expressed as

$$f_1(x_1) = x_1^{\theta_1} (d - x_1)^{\lambda_1} F_1(x_1), \quad 0 < x_1 < d, \quad (2.191a)$$

$$f_2(x_1) = x_1^{\theta_2} (d - x_1)^{\lambda_2} F_2(x_1), \quad 0 < x_1 < d, \quad (2.191b)$$

$$f_3(x_2) = (x_2 - a)^\omega (b - x_2)^\beta F_3(x_2), \quad a < x_2 < b, \quad (2.191c)$$

where F_j ($j=1,2,3$) is Hölder-continuous in its respective interval and it is assumed that $-1 < \Re(\theta_1, \theta_2, \lambda_1, \lambda_2, \omega, \beta) < 0$. The following sectionally holomorphic functions are considered:

$$\psi_1(z) = \frac{1}{\pi} \int_0^d \frac{f_1(t)}{t - z} dt, \quad (2.192a)$$

$$\psi_2(z) = \frac{1}{\pi} \int_0^d \frac{f_2(t)}{t - z} dt, \quad (2.192b)$$

$$\psi_3(z) = \frac{1}{\pi} \int_0^d \frac{f_3(t)}{t - z} dt. \quad (2.192c)$$

The singular behavior of $\psi_j(z)$, ($j=1,2,3$) around the end points is given as follows (see, for example Dag [40] and Erdogan [43]):

$$\psi_1(z) = -F_1(0)(d)^{\lambda_1} \frac{\exp(-\pi i \theta_1)}{\sin(\pi \theta_1)} z^{\theta_1} + F_1(d)(d)^{\theta_1} \frac{1}{\sin(\pi \lambda_1)} (z-d)^{\lambda_1} + F_1^*(z), \quad (2.193a)$$

$$\psi_2(z) = -F_2(0)(d)^{\lambda_2} \frac{\exp(-\pi i \theta_2)}{\sin(\pi \theta_2)} z^{\theta_2} + F_2(d)(d)^{\theta_2} \frac{1}{\sin(\pi \lambda_2)} (z-d)^{\lambda_2} + F_2^*(z), \quad (2.193b)$$

$$\psi_3(z) = -F_3(a)(b-a)^{\beta} \frac{\exp(-\pi i \omega)}{\sin(\pi \omega)} (z-a)^{\omega} + F_3(b)(b-a)^{\omega} \frac{1}{\sin(\pi \beta)} (z-b)^{\beta} + F_3^*(z). \quad (2.193c)$$

The function F_n^* , ($n=1,2,3$) is bounded everywhere except possibly at the end points where it may have a weaker singularity. Using Plemelj formulas, equations (2.193) can be expressed as follows:

$$\frac{1}{\pi} \int_0^d \frac{f_1(t)}{t-x_1} dt = -F_1(0)(d)^{\lambda_1} \cot(\pi \theta_1) x_1^{\theta_1} + F_1(d)(d)^{\theta_1} \cot(\pi \lambda_1)(d-x_1)^{\lambda_1} + H_1(x_1), \quad 0 < x_1 < d, \quad (2.194a)$$

$$\frac{1}{\pi} \int_0^d \frac{f_2(t)}{t-x_1} dt = -F_2(0)(d)^{\lambda_2} \cot(\pi \theta_2) x_1^{\theta_2} + F_2(d)(d)^{\theta_2} \cot(\pi \lambda_2)(d-x_1)^{\lambda_2} + H_2(x_1), \quad 0 < x_1 < d, \quad (2.194b)$$

$$\frac{1}{\pi} \int_0^d \frac{f_3(t)}{t-x_2} dt = -F_3(a)(b-a)^{\beta} \cot(\pi \omega)(x_2-a)^{\omega} + F_3(b)(b-a)^{\omega} \cot(\pi \beta)(b-x_2)^{\beta} + H_3(x_2), \quad a < x_2 < b. \quad (2.194c)$$

In their respective intervals, $H_1(x_1)$, $H_2(x_1)$ and $H_3(x_2)$ are bounded and at the end points they have weaker singularities similar to $F^*(z)$ in equation (2.193). It is assumed that complex variables z_1 , z_2 and z_3 satisfy the following conditions:

$$z_1 \notin (0 < x_1 < d), \quad (2.195a)$$

$$z_2 \notin (0 < x_1 < d), \quad (2.195b)$$

$$z_3 \notin (a < x_2 < b). \quad (2.195c)$$

If these conditions are satisfied, $\psi_1(z_1)$, $\psi_2(z_2)$ and $\psi_3(z_3)$ are holomorphic. Thus, following equations are written,

$$\psi_1(z_1) = \frac{1}{\pi} \int_0^d \frac{f_1(t)}{t - z_1} dt, \quad (2.196a)$$

$$\psi_2(z_2) = \frac{1}{\pi} \int_0^d \frac{f_2(t)}{t - z_2} dt, \quad (2.196b)$$

$$\psi_3(z_3) = \frac{1}{\pi} \int_0^d \frac{f_3(t)}{t - z_3} dt. \quad (2.196c)$$

Apart from the Cauchy integrals, all kernels of the integral equations except k_{11} and k_{22} are bounded. The singular behavior of the terms h_{11s} and h_{22s} in kernels k_{11} and k_{22} , respectively can also be expressed by using (2.98a), (2.129a) and (2.196) in the following form:

$$\int_0^d h_{11s}(x_1, t) f_1(t) dt = \pi [b_{110} F\psi_1(-Ax_1F) + b_{120} E\psi_1(-Ax_1E) + b_{210} F\psi_1(-Bx_1F) + b_{220} E\psi_1(-Bx_1E)], \quad (2.197a)$$

$$\int_0^d h_{22s}(x_1, t) f_2(t) dt = \pi [n_{110} F\psi_2(-Ax_1F) + n_{120} E\psi_2(-Ax_1E) + n_{210} F\psi_2(-Bx_1F) + n_{220} E\psi_2(-Bx_1E)]. \quad (2.197b)$$

By using (2.193a) and (2.193b), singular behavior of h_{11s} and h_{22s} near $x_1 = 0$ are obtained as follows:

$$\int_0^d h_{11s}(x_1, t) f_1(t) dt \cong -\frac{\pi}{\sin(\pi\theta_1)} \left[b_{110} F(AF)^{\theta_1} + b_{120} E(AE)^{\theta_1} \right. \\ \left. + b_{210} F(BF)^{\theta_1} + b_{220} E(BE)^{\theta_1} \right] (d)^{\lambda_1} (x_1)^{\theta_1} F_1(0), \quad (2.198a)$$

$$\int_0^d h_{22s}(x_1, t) f_2(t) dt \cong -\frac{\pi}{\sin(\pi\theta_2)} \left[n_{110} F(AF)^{\theta_2} + n_{120} E(AE)^{\theta_2} \right. \\ \left. + n_{210} F(BF)^{\theta_2} + n_{220} E(BE)^{\theta_2} \right] (d)^{\lambda_2} (x_1)^{\theta_2} F_2(0). \quad (2.198b)$$

In equation (2.198), \cong sign implies that the bounded terms are not included. By using (2.194) and (2.198), the singular terms of the integral equations are written as follows:

$$\sigma_{22}(x_1, 0) \cong F_1(0)(d)^{\lambda_1} \left\{ \frac{a_{20}}{2} \cot(\pi\theta_1) - \frac{\pi}{\sin(\pi\theta_1)} \left[b_{110} F(AF)^{\theta_1} + b_{120} E(AE)^{\theta_1} \right. \right. \\ \left. \left. + b_{210} F(BF)^{\theta_1} + b_{220} E(BE)^{\theta_1} \right] \right\} (x_1)^{\theta_1} \quad (2.199a) \\ - F_1(d)(d)^{\theta_1} \cot(\pi\lambda_1)(d - x_1)^{\lambda_1},$$

$$\sigma_{12}(x_1, 0) \cong F_2(0)(d)^{\lambda_2} \left\{ \frac{m_{20}}{2} \cot(\pi\theta_2) - \frac{\pi}{\sin(\pi\theta_2)} \left[n_{110} F(AF)^{\theta_2} + n_{120} E(AE)^{\theta_2} \right. \right. \\ \left. \left. + n_{210} F(BF)^{\theta_2} + n_{220} E(BE)^{\theta_2} \right] \right\} (x_1)^{\theta_2} \quad (2.199b) \\ - F_2(d)(d)^{\theta_2} \cot(\pi\lambda_2)(d - x_1)^{\lambda_2},$$

$$\frac{C_{66}}{2} \frac{\partial}{\partial x_2} u_1(0, x_2) \cong \frac{e_{20}}{2} \left[F_3(a)(b-a)^\beta \cot(\pi\omega)(x_2 - a)^\omega \right. \\ \left. - F_3(b)(b-a)^\omega \cot(\pi\beta)(b - x_2)^\beta \right] + \frac{e_{10}}{2} F_3(x_2)(x_2 - a)^\omega (b - x_2)^\beta. \quad (2.199c)$$

In order to obtain the unknown exponents, the characteristic equations are derived by using (2.199). Multiplying (2.199a) by $(x_1)^{-\theta_1}$ and letting $x_1 \rightarrow 0$ following equation is obtained,

$$\frac{a_{20}}{2} \cot(\pi\theta_1) - \frac{\pi}{\sin(\pi\theta_1)} \left[b_{110} F(AF)^{\theta_1} + b_{120} E(AE)^{\theta_1} + b_{210} F(BF)^{\theta_1} + b_{220} E(BE)^{\theta_1} \right] = 0, \quad (2.200)$$

and multiplying (2.199a) by $(d - x_1)^{-\lambda_1}$ and letting $x_1 \rightarrow d$ following equation is found,

$$\cot(\pi\lambda_1) = 0. \quad (2.201)$$

$F_1(0)$ and $F_1(d)$ are assumed to be nonzero. Applying a similar procedure used for equation (2.199a), following equations are obtained by using equation (2.199b),

$$\frac{m_{20}}{2} \cot(\pi\theta_2) - \frac{\pi}{\sin(\pi\theta_2)} \left[n_{110} F(AF)^{\theta_2} + n_{120} E(AE)^{\theta_2} + n_{210} F(BF)^{\theta_2} + n_{220} E(BE)^{\theta_2} \right] = 0, \quad (2.202a)$$

$$\cot(\pi\lambda_2) = 0. \quad (2.202b)$$

Again it is assumed that $F_2(0)$ and $F_2(d)$ are nonzero, Multiplying (2.199c) by $(x_2 - a)^{-\omega}$ and letting $x_2 \rightarrow a$ following equation is obtained

$$\cot(\pi\omega) = -\frac{e_{10}}{e_{20}}, \quad (2.203)$$

and multiplying (2.199c) by $(b - x_2)^{-\beta}$ and letting $x_2 \rightarrow b$ another characteristic equation to determine β is obtained as follows:

$$\cot(\pi\beta) = \frac{e_{10}}{e_{20}}. \quad (2.204)$$

Also, $F_3(a)$ and $F_3(b)$ are assumed to be nonzero. From equations (2.201) and (2.202b), it follows that $\lambda_1 = \lambda_2 = -0.5$. The strengths of singularity at the ends of the contact area are given by equations (2.203) and (2.204) and e_{10} and e_{20} are given in Appendix A by equations (A.11e) and (A.11f), respectively. Due to the fact that for

f_1 and f_2 there is no singularity at $x_1 = 0$, they can be expressed in the following form (see Delale and Erdogan [3]):

$$f_1(t) = \frac{F_1(t)}{\sqrt{d-t}}, \quad 0 < t < d, \quad (2.205a)$$

$$f_2(t) = \frac{F_2(t)}{\sqrt{d-t}}, \quad 0 < t < d. \quad (2.205b)$$

2.2.5 On the Solution of the Integral Equations

The singular integral equations do not have closed form solutions. Therefore a numerical method has to be developed. Flat, triangular and circular stamps are considered in the solution. In this study, Jacobi polynomials are used to reduce the singular integral equations to systems of linear algebraic equations. The unknown functions f_1 , f_2 and f_3 are expanded into series of Jacobi polynomials. The unknown constants of expansions are determined by using the point collocation method. Then, main numerical results, which are the mixed mode stress intensity factors, contact stresses and required contact force, are generated.

2.2.5.1 Flat Stamp

The geometry of the flat stamp problem is shown in Figure 2.7. The length of the contact area ($b-a$) is independent of the applied force P . It is known that, the stresses are singular at both ends of the contact region.

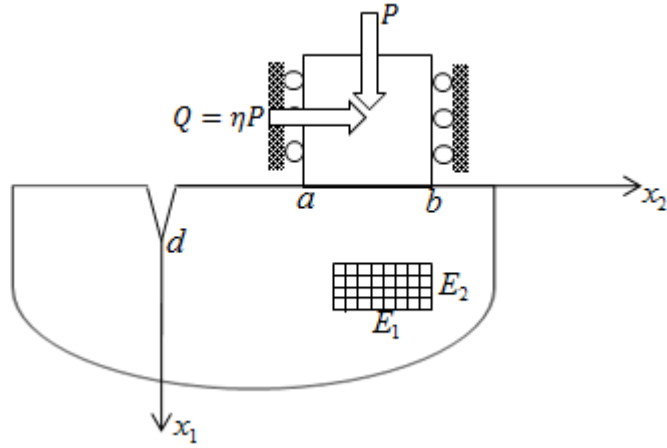


Figure 2.7: The geometry of the crack/contact problem for a flat stamp

At this point, the intervals and the unknowns of the problem are normalized. Then normalized forms of the integral equations are obtained. First, the intervals in (2.190) are normalized by defining

$$t = \frac{d}{2}r + \frac{d}{2}, \quad t = \frac{d}{2}r + \frac{d}{2} \quad \text{and} \quad t = \frac{b-a}{2}r + \frac{b+a}{2}, \quad (2.206a,b,c)$$

in integrals involving $f_1(t)$, $f_2(t)$ and $f_3(t)$, respectively. Then the normalized unknowns of the problem are defined as follows:

$$\phi_1(r) = \frac{f_1\left(\frac{d}{2}r + \frac{d}{2}\right)}{P/(b-a)}, \quad -1 < r < 1, \quad (2.207a)$$

$$\phi_2(r) = \frac{f_2\left(\frac{d}{2}r + \frac{d}{2}\right)}{P/(b-a)}, \quad -1 < r < 1, \quad (2.207b)$$

$$\phi_3(r) = \frac{f_3\left(\frac{b-a}{2}r + \frac{b+a}{2}\right)}{P/(b-a)}, \quad -1 < r < 1. \quad (2.207c)$$

The intervals $(0, d)$ and (a, b) are also normalized by defining,

$$x_1 = \frac{d}{2}s_1 + \frac{d}{2}, \quad \text{for eqn. (2.190a),} \quad (2.208a)$$

$$x_1 = \frac{d}{2}s_2 + \frac{d}{2}, \quad \text{for eqn. (2.190b),} \quad (2.208b)$$

$$x_2 = \frac{b-a}{2}s_3 + \frac{b+a}{2}, \quad \text{for eqn. (2.190c).} \quad (2.208c)$$

Using (2.207) and (2.208), normalized form of the integral equations (2.190) and equilibrium conditions (2.1g) are written as

$$\frac{a_{20}}{2\pi} \int_{-1}^1 \frac{\phi_1(r)}{s_1 - r} dr + \int_{-1}^1 H_{11}(s_1, r)\phi_1(r)dr + \int_{-1}^1 H_{13}(s_1, r)\phi_3(r)dr = 0, \quad (2.209a)$$

$$-1 < s_1 < 1,$$

$$\frac{m_{20}}{2\pi} \int_{-1}^1 \frac{\phi_2(r)}{s_2 - r} dr + \int_{-1}^1 H_{12}(s_2, r)\phi_2(r)dr + \int_{-1}^1 H_{23}(s_2, r)\phi_3(r)dr = 0, \quad (2.209b)$$

$$-1 < s_2 < 1,$$

$$\int_{-1}^1 H_{31}(s_3, r)\phi_1(r)dr + \int_{-1}^1 H_{32}(s_3, r)\phi_2(r)dr + \frac{e_{10}}{2}\phi_3(s_3) + \frac{e_{20}}{2\pi} \int_{-1}^1 \frac{\phi_3(r)}{s_3 - r} dr \quad (2.209c)$$

$$+ \int_{-1}^1 H_{33}(s_3, r)\phi_3(r)dr = 0, \quad -1 < s_3 < 1,$$

$$\int_{-1}^1 \phi_3(s_3)ds_3 = -2. \quad (2.209d)$$

Since, for a flat stamp normal displacement beneath the stamp is constant, right-hand side of equation (2.209c) is zero. The kernels $H_{ij}(s_i, r)$ are given in Appendix C. The unknown functions are expanded into series of Jacobi polynomials in the following form,

$$\phi_1(r) = \omega_1(r) \sum_{n=0}^{\infty} A_{1n} P_n^{(-1/2, \alpha_1)}(r), \quad \omega_1(r) = (1-r)^{-1/2} (1+r)^{\alpha_1}, \quad (2.210a)$$

$$\phi_2(r) = \omega_2(r) \sum_{n=0}^{\infty} A_{2n} P_n^{(-1/2, \alpha_1)}(r), \quad \omega_2(r) = (1-r)^{-1/2} (1+r)^{\alpha_1}, \quad (2.210b)$$

$$\phi_3(r) = \omega_3(r) \sum_{n=0}^{\infty} A_{3n} P_n^{(\beta, \alpha_2)}(r), \quad \omega_3(r) = (1-r)^\beta (1+r)^{\alpha_2}, \quad (2.210c)$$

where $P_n(r)$ are the Jacobi polynomials and A_{in} ($i=1,2,3$) are the unknown constants of the expansions. Also, for $a > 0$ $\alpha_1 = 0$, $\alpha_2 = \omega$, $\beta < 0$, $\omega < 0$ and $\beta + \omega = -1$. Substituting (2.210c) in equilibrium equation (2.209d) and by using the Jacobi polynomials, and orthogonality relations given by Erdogan [44], A_{30} is obtained as follows:

$$A_{30} = -\frac{2}{\theta_0}, \quad (2.211a)$$

$$\theta_0 = \frac{2^{\beta+\alpha_2+1} \Gamma(\beta+1) \Gamma(\alpha_2+1)}{\Gamma(\beta+\alpha_2+2)}, \quad (2.211b)$$

where Γ is the Gamma function. Substituting (2.210) into (2.209a-c), regularizing the singular parts of the equations using the expressions given in Appendix B and truncating the infinite series at N , following system of linear algebraic equations is obtained:

$$\sum_{n=0}^N m_{11n}(s_1) A_{1n} + \sum_{n=1}^N m_{13n}(s_1) A_{3n} = -m_{130}(s_1) A_{30}, \quad -1 < s_1 < 1, \quad (2.212a)$$

$$\sum_{n=0}^N m_{22n}(s_2) A_{2n} + \sum_{n=1}^N m_{23n}(s_2) A_{3n} = -m_{230}(s_2) A_{30}, \quad -1 < s_2 < 1, \quad (2.212b)$$

$$\sum_{n=0}^N m_{31n}(s_3) A_{1n} + \sum_{n=0}^N m_{32n}(s_3) A_{2n} + \sum_{n=1}^N m_{33n}(s_3) A_{3n} = -m_{330}(s_3) A_{30}, \quad (2.212c)$$

$$-1 < s_3 < 1.$$

The expressions for $m_{ijn}(s_i)$, ($i, j=1,2,3$) are given in Appendix C. By using the collocation technique, equations (2.212) can be solved. The number of unknowns is $(3N + 2)$. Roots of the Chebyshev polynomials of the first kind are used as the collocation points as follows:

$$s_{1i} = \cos\left(\frac{\pi(2i-1)}{2(N+1)}\right), \quad i = 1, \dots, N+1, \quad (2.213a)$$

$$s_{2i} = \cos\left(\frac{\pi(2i-1)}{2(N+1)}\right), \quad i = 1, \dots, N+1, \quad (2.213b)$$

$$s_{3i} = \cos\left(\frac{\pi(2i-1)}{2N}\right), \quad i = 1, \dots, N. \quad (2.213c)$$

Equations (2.212) can be solved for A_m , ($i=1,2,3$). The contact stresses $\sigma_{11}(0, x_2)$, $\sigma_{12}(0, x_2)$ and stress intensity factors at the crack tip $(d, 0)$ are evaluated by using the results. The stress intensity factors are obtained as

$$k_1 = \lim_{x_1 \rightarrow d+0} \sqrt{2(x_1 - d)} \sigma_{22}(x_1, 0) =$$

$$- \lim_{x_1 \rightarrow d-0} \frac{C_{66}}{2} \sqrt{2(d - x_1)} \frac{\partial}{\partial x_1} (u_2(x_1, 0^+) - u_2(x_1, 0^-)), \quad (2.214a)$$

$$k_2 = \lim_{x_1 \rightarrow d+0} \sqrt{2(x_1 - d)} \sigma_{12}(x_1, 0) =$$

$$- \lim_{x_1 \rightarrow d-0} \frac{C_{66}}{2} \sqrt{2(d - x_1)} \frac{\partial}{\partial x_1} (u_1(x_1, 0^+) - u_1(x_1, 0^-)). \quad (2.214b)$$

Using (2.210), the normalized stress intensity factors and the normal component of the contact stress are expressed as

$$\frac{k_1 \sqrt{d}}{P} = -2^{\alpha_1} \frac{d}{b-a} \sum_{n=0}^N A_{1n} P_n^{(-1/2, \alpha_1)}(1), \quad (2.215a)$$

$$\frac{k_2 \sqrt{d}}{P} = -2^{\alpha_1} \frac{d}{b-a} \sum_{n=0}^N A_{2n} P_n^{(-1/2, \alpha_1)}(1), \quad (2.215b)$$

$$\frac{\sigma_{11}\left(0, \frac{b-a}{2}s_3 + \frac{b+a}{2}\right)}{P/(b-a)} = (1-s_3)^\beta (1+s_3)^{\alpha_2} \sum_{n=0}^N A_{3n} P_n^{(\beta, \alpha_2)}(s_3). \quad (2.215c)$$

2.2.5.2 Triangular Stamp

The geometry of the triangular stamp problem is shown in Figure 2.8. The contact is smooth at $x_2 = b$ and there is a sharp corner at $x_2 = a$. The contact stress $\sigma_{11}(0, x_2)$ is singular at $x_2 = a$. In this case, the stamp has a constant slope of $\tan(\theta)$ in the contact region. Here, displacement derivative can be written as:

$$\frac{\partial}{\partial x_2} u(0, x_2) = -\tan(\theta) = -m, \quad a < x_2 < b. \quad (2.216)$$

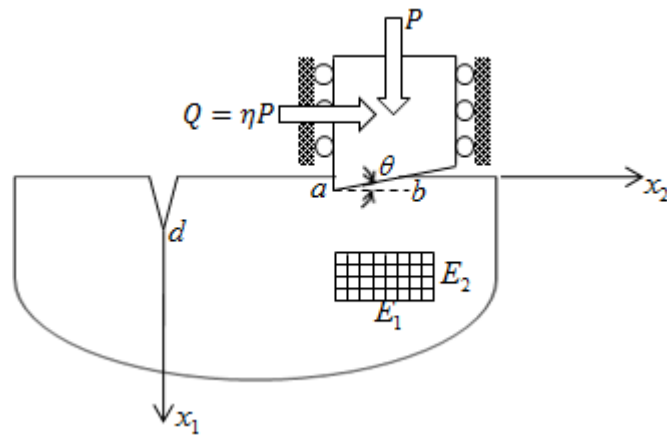


Figure 2.8: The geometry of the crack/contact problem for a triangular stamp

At this point, the intervals and the unknowns of the problem are normalized. Then, normalized form of the integral equations is obtained. First the intervals in (2.190) are normalized by defining

$$t = \frac{d}{2}r + \frac{d}{2}, \quad t = \frac{d}{2}r + \frac{d}{2} \quad \text{and} \quad t = \frac{b-a}{2}r + \frac{b+a}{2}, \quad (2.217\text{a,b,c})$$

in integrals involving $f_1(t)$, $f_2(t)$ and $f_3(t)$, respectively. Then, the normalized unknowns of the problem are defined as follows:

$$\phi_1(r) = \frac{f_1\left(\frac{d}{2}r + \frac{d}{2}\right)}{\mu_{12}m}, \quad -1 < r < 1, \quad (2.218\text{a})$$

$$\phi_2(r) = \frac{f_2\left(\frac{d}{2}r + \frac{d}{2}\right)}{\mu_{12}m}, \quad -1 < r < 1, \quad (2.218\text{b})$$

$$\phi_3(r) = \frac{f_3\left(\frac{b-a}{2}r + \frac{b+a}{2}\right)}{\mu_{12}m}, \quad -1 < r < 1. \quad (2.218\text{c})$$

The intervals $(0, d)$ and (a, b) are also normalized by defining,

$$x_1 = \frac{d}{2}s_1 + \frac{d}{2}, \quad \text{for eqn. (2.190a)}, \quad (2.219\text{a})$$

$$x_1 = \frac{d}{2}s_2 + \frac{d}{2}, \quad \text{for eqn. (2.190b)}, \quad (2.219\text{b})$$

$$x_2 = \frac{b-a}{2}s_3 + \frac{b+a}{2}, \quad \text{for eqn. (2.190c)}. \quad (2.219\text{c})$$

Using (2.218) and (2.219), normalized form of the integral equations (2.190) and equilibrium conditions (2.1g) are written as

$$\frac{a_{20}}{2\pi} \int_{-1}^1 \frac{\phi_1(r)}{s_1 - r} dr + \int_{-1}^1 H_{11}(s_1, r) \phi_1(r) dr + \int_{-1}^1 H_{13}(s_1, r) \phi_3(r) dr = 0, \quad (2.220a)$$

$$-1 < s_1 < 1,$$

$$\frac{m_{20}}{2\pi} \int_{-1}^1 \frac{\phi_2(r)}{s_2 - r} dr + \int_{-1}^1 H_{12}(s_2, r) \phi_2(r) dr + \int_{-1}^1 H_{23}(s_2, r) \phi_3(r) dr = 0, \quad (2.220b)$$

$$1 < s_2 < 1,$$

$$\int_{-1}^1 H_{31}(s_3, r) \phi_1(r) dr + \int_{-1}^1 H_{32}(s_3, r) \phi_2(r) dr + \frac{e_{10}}{2} \phi_3(s_3) + \frac{e_{20}}{2\pi} \int_{-1}^1 \frac{\phi_3(r)}{s_3 - r} dr$$

$$+ \int_{-1}^1 H_{33}(s_3, r) \phi_3(r) dr = -1, \quad -1 < s_3 < 1, \quad (2.220c)$$

$$\frac{b-a}{2} \int_{-1}^1 \phi_3(s_3) ds_3 = -\frac{P}{\mu_{12}m}. \quad (2.220d)$$

where $H_{ij}(s_i, r)$ are given in Appendix C. Unknown functions $\phi_i(r)$, ($i=1,2,3$) are expressed as follows:

$$\phi_1(r) = \omega_1(r) \sum_{n=0}^{\infty} A_{1n} P_n^{(-1/2, \alpha_1)}(r), \quad \omega_1(r) = (1-r)^{-1/2} (1+r)^{\alpha_1}, \quad (2.221a)$$

$$\phi_2(r) = \omega_2(r) \sum_{n=0}^{\infty} A_{2n} P_n^{(-1/2, \alpha_1)}(r), \quad \omega_2(r) = (1-r)^{-1/2} (1+r)^{\alpha_1}, \quad (2.221b)$$

$$\phi_3(r) = \omega_3(r) \sum_{n=0}^{\infty} A_{3n} P_n^{(\beta, \alpha_2)}(r), \quad \omega_3(r) = (1-r)^\beta (1+r)^{\alpha_2}, \quad (2.221c)$$

where $P_n(r)$ are the Jacobi polynomials and A_{in} ($i=1,2,3$) are the unknown constants of the expansions. Also, for $a > 0$ $\alpha_1 = 0$, $\alpha_2 = \omega$, $\beta > 0$, $\omega < 0$ and $\beta + \omega = 0$. Substituting (2.221c) in equilibrium equation (2.220d), normalized contact force is obtained as follows:

$$\frac{P}{\mu_{12}md} = -\frac{b-a}{2d} A_{30} \theta_0, \quad (2.222a)$$

$$\theta_0 = \frac{2^{\beta+\alpha_2+1} \Gamma(\beta+1) \Gamma(\alpha_2+1)}{\Gamma(\beta+\alpha_2+2)}. \quad (2.222b)$$

For the triangular stamp problem, solution approach is slightly different. It is known that the triangular stamp problem is defined as an incomplete contact mechanics problem where the size of the contact region is a function of the applied force. This problem is solved for a given contact area (i.e., for a known value of $(b-a)/d$) and corresponding force is calculated using equation (2.222a). Substituting equations (2.221) into (2.220a-c), regularizing the singular terms of the equations using the expressions given in Appendix B and truncating the infinite series at N , following system of linear algebraic equations is obtained:

$$\sum_{n=0}^N m_{11n}(s_1) A_{1n} + \sum_{n=0}^N m_{13n}(s_1) A_{3n} = 0, \quad -1 < s_1 < 1, \quad (2.223a)$$

$$\sum_{n=0}^N m_{22n}(s_2) A_{2n} + \sum_{n=0}^N m_{23n}(s_2) A_{3n} = 0, \quad -1 < s_2 < 1, \quad (2.223b)$$

$$\sum_{n=0}^N m_{31n}(s_3) A_{1n} + \sum_{n=0}^N m_{32n}(s_3) A_{2n} + \sum_{n=0}^N m_{33n}(s_3) A_{3n} = -1, \quad -1 < s_3 < 1. \quad (2.223c)$$

The expressions for $m_{ijn}(s_i)$ ($i, j=1,2,3$) are given in Appendix C. By using the collocation technique, equations (2.223) can be solved. The number of unknowns is $(3N+3)$. Roots of the Chebyshev polynomials of the first kind are used as the collocation points as follows:

$$s_{ji} = \cos\left(\frac{\pi(2i-1)}{2(N+1)}\right), \quad j = (1,2,3), \quad i = 1, \dots, N+1. \quad (2.224)$$

Equations (2.223) are solved for A_m , ($i=1,2,3$). The contact stress $\sigma_{11}(0, x_2)$, stress intensity factors at the crack tip $(d,0)$ and required contact force $P/\mu_{12}md$ are evaluated by using the results. The stress intensity factors are defined by (2.214). Using equations (2.221), the normalized stress intensity factors and the normal component of the contact stress are expressed as follows:

$$\frac{k_1 \sqrt{d}}{P} = 2^{\alpha_1} \frac{2}{A_{30} \theta_0} \frac{d}{b-a} \sum_{n=0}^N A_{1n} P_n^{(-1/2, \alpha_1)}(1), \quad (2.225a)$$

$$\frac{k_2 \sqrt{d}}{P} = 2^{\alpha_1} \frac{2}{A_{30} \theta_0} \frac{d}{b-a} \sum_{n=0}^N A_{2n} P_n^{(-1/2, \alpha_1)}(1), \quad (2.225b)$$

$$\frac{\sigma_{11}\left(0, \frac{b-a}{2} s_3 + \frac{b+a}{2}\right)}{\mu_{12} m} = (1-s_3)^\beta (1+s_3)^{\alpha_2} \sum_{n=0}^N A_{3n} P_n^{(\beta, \alpha_2)}(s_3). \quad (2.225c)$$

2.2.5.3 Circular Stamp

The geometry of the circular stamp problem is shown in Figure 2.9. The radius of the stamp is assumed to be equal to R and the centerline of the stamp passes through point $x_2 = c$. At the end points $x_2 = a$ and $x_2 = b$ the contact is smooth and contact stress $\sigma_{11}(0, x_2)$ is equal to zero. The length of the contact area depends on the applied force P . In the numerical solution, the problem is solved for known values of a and b corresponding values of P and c are calculated.

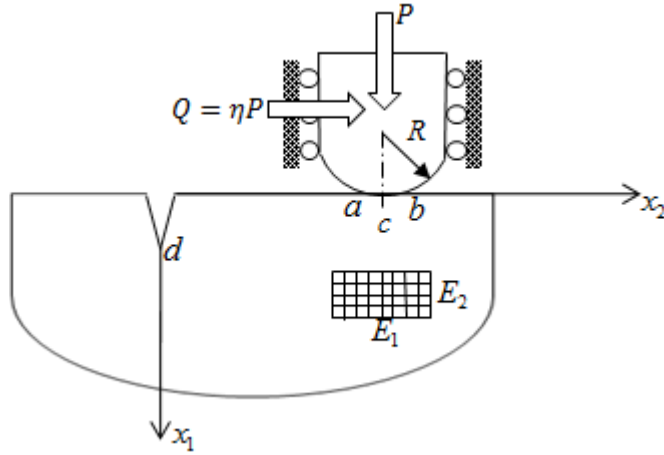


Figure 2.9: The geometry of the crack/contact problem for a circular stamp

In this problem, it is assumed that the contact area $(b - a)$ is much smaller than the radius R . The derivative of the normal displacement in the contact area is given as follows:

$$\frac{\partial}{\partial x_2} u(0, x_2) = \frac{c - x_2}{R}, \quad a < x_2 < b. \quad (2.226)$$

The intervals and the unknowns of this problem are also normalized. Then normalized forms of the integral equations are obtained. First, the intervals in (2.190) are normalized by defining

$$t = \frac{d}{2} r + \frac{d}{2}, \quad t = \frac{d}{2} r + \frac{d}{2} \quad \text{and} \quad t = \frac{b-a}{2} r + \frac{b+a}{2}, \quad (2.227a,b,c)$$

in integrals involving $f_1(t)$, $f_2(t)$ and $f_3(t)$, respectively. Then the normalized unknowns of the problem are defined as follows:

$$\phi_1(r) = \frac{f_1\left(\frac{d}{2} r + \frac{d}{2}\right)}{\mu_{12}}, \quad -1 < r < 1, \quad (2.228a)$$

$$\phi_2(r) = \frac{f_2\left(\frac{d}{2}r + \frac{d}{2}\right)}{\mu_{12}}, \quad -1 < r < 1, \quad (2.228b)$$

$$\phi_3(r) = \frac{f_3\left(\frac{b-a}{2}r + \frac{b+a}{2}\right)}{\mu_{12}}, \quad -1 < r < 1. \quad (2.228c)$$

The intervals $(0, d)$ and (a, b) are also normalized by defining,

$$x_1 = \frac{d}{2}s_1 + \frac{d}{2}, \quad \text{for eqn. (2.190a),} \quad (2.229a)$$

$$x_1 = \frac{d}{2}s_2 + \frac{d}{2}, \quad \text{for eqn. (2.190b),} \quad (2.229b)$$

$$x_2 = \frac{b-a}{2}s_3 + \frac{b+a}{2}, \quad \text{for eqn. (2.190c).} \quad (2.229c)$$

Using (2.228) and (2.229), normalized form of the integral equations (2.190) and equilibrium conditions (2.1g) are written as

$$\frac{a_{20}}{2\pi} \int_{-1}^1 \frac{\phi_1(r)}{s_1 - r} dr + \int_{-1}^1 H_{11}(s_1, r)\phi_1(r)dr + \int_{-1}^1 H_{13}(s_1, r)\phi_3(r)dr = 0, \quad (2.230a)$$

$$-1 < s_1 < 1,$$

$$\frac{m_{20}}{2\pi} \int_{-1}^1 \frac{\phi_2(r)}{s_2 - r} dr + \int_{-1}^1 H_{12}(s_2, r)\phi_2(r)dr + \int_{-1}^1 H_{23}(s_2, r)\phi_3(r)dr = 0, \quad (2.230b)$$

$$-1 < s_2 < 1,$$

$$\int_{-1}^1 H_{31}(s_3, r)\phi_1(r)dr + \int_{-1}^1 H_{32}(s_3, r)\phi_2(r)dr + \frac{e_{10}}{2}\phi_3(s_3) + \frac{e_{20}}{2\pi} \int_{-1}^1 \frac{\phi_3(r)}{s_3 - r} dr \quad (2.230c)$$

$$+ \int_{-1}^1 H_{33}(s_3, r)\phi_3(r)dr = \frac{2c - (b-a)s_3 - (b+a)}{2R}, \quad -1 < s_3 < 1,$$

$$\frac{b-a}{2} \int_{-1}^1 \phi_3(s_3) ds_3 = -\frac{P}{\mu_{12}}, \quad (2.230d)$$

where $H_{ij}(s_i, r)$ are given in Appendix C. Unknown functions $\phi_i(r)$, ($i=1,2,3$) are expressed in the following form,

$$\phi_1(r) = \omega_1(r) \sum_{n=0}^{\infty} A_{1n} P_n^{(-1/2,0)}(r), \quad \omega_1(r) = (1-r)^{-1/2}, \quad (2.231a)$$

$$\phi_2(r) = \omega_2(r) \sum_{n=0}^{\infty} A_{2n} P_n^{(-1/2,0)}(r), \quad \omega_2(r) = (1-r)^{-1/2}, \quad (2.231b)$$

$$\phi_3(r) = \omega_3(r) \sum_{n=0}^{\infty} A_{3n} P_n^{(\beta,\omega)}(r), \quad \omega_3(r) = (1-r)^\beta (1+r)^\omega, \quad (2.231c)$$

where $P_n(r)$ are the Jacobi polynomials and A_{in} ($i=1,2,3$) are the unknown constants of the expansions. Also note that $\beta > 0$, $\omega > 0$ and $\beta + \omega = 1$. Substituting (2.231c) into (2.230d), normalized contact force is obtained as follows:

$$\frac{P}{\mu_{12}R} = -\frac{b-a}{2R} A_{30} \theta_0, \quad (2.232a)$$

$$\theta_0 = \frac{2\beta(1-\beta)\pi}{\sin(\pi\beta)}. \quad (2.232b)$$

It is also known that the circular stamp problem is defined as an incomplete contact mechanics problem. This problem is solved for a given contact area (i.e., for a known value of $(b-a)/R$) and corresponding force is calculated using equation (2.232a). Substituting equations (2.231) into (2.230a-c), regularizing the singular terms of the equations using the expressions given in Appendix B and truncating the infinite series at N , following system of linear algebraic equations is obtained:

$$\sum_{n=0}^N g_{11n}(s_1) A_{1n} + \sum_{n=0}^N g_{13n}(s_1) A_{3n} = 0, \quad -1 < s_1 < 1, \quad (2.233a)$$

$$\sum_{n=0}^N g_{22n}(s_2) A_{2n} + \sum_{n=0}^N g_{23n}(s_2) A_{3n} = 0, \quad -1 < s_2 < 1, \quad (2.233b)$$

$$\sum_{n=0}^N g_{31n}(s_3) A_{1n} + \sum_{n=0}^N g_{32n}(s_3) A_{2n} + \sum_{n=0}^N g_{33n}(s_3) A_{3n} = \frac{2c - (b-a)s_3 - (b+a)}{2R}, \quad (2.233c)$$

$-1 < s_3 < 1,$

where $g_{ijn}(s_i)$ ($i, j=1, 2, 3$) are given in Appendix C. In the circular stamp problem, the variables a/R , b/R and c/R are not independent. In order to determine c/R for given values of a/R and b/R the consistency condition for the circular stamp is used. Consider the singular terms in (2.230c)

$$F(s_3) = \frac{e_{10}}{2} \phi_3(s_3) + \frac{e_{20}}{2\pi} \int_{-1}^1 \frac{\phi_3(r)}{s_3 - r} dr, \quad -1 < s_3 < 1. \quad (2.234)$$

If this term is divided by the weight function $\omega_3(s_3)$ and integrated from -1 to 1 following equation is obtained,

$$\int_{-1}^1 F(s_3) (1-s_3)^{-\beta} (1+s_3)^{-\omega} ds_3 = 0. \quad (2.235)$$

Integrating other terms similarly, rearranging and after manipulations, the relationship between a/R , b/R and c/R is expressed as:

$$\left\{ \frac{c}{R} - \frac{b-a}{2R} (2\beta - 1) - \frac{b+a}{2R} \right\} \frac{\pi}{\sin(\pi\beta)} = \sum_{n=0}^N A_{1n} \psi_{1n} + \sum_{n=0}^N A_{2n} \psi_{2n} + \sum_{n=0}^N A_{3n} \psi_{3n}, \quad (2.236)$$

where,

$$\psi_{1n} = \int_{-1}^1 \left\{ \int_{-1}^1 (1-r)^{-1/2} P_n^{(-1/2,0)}(r) H_{31}(s_3, r) dr \right\} (1-s_3)^{-\beta} (1+s_3)^{-\omega} ds_3, \quad (2.237a)$$

$$\psi_{2n} = \int_{-1}^1 \left\{ \int_{-1}^1 (1-r)^{-1/2} P_n^{(-1/2,0)}(r) H_{32}(s_3, r) dr \right\} (1-s_3)^{-\beta} (1+s_3)^{-\omega} ds_3, \quad (2.237b)$$

$$\psi_{3n} = \int_{-1}^1 \left\{ \int_{-1}^1 (1-r)^\beta (1+r)^\omega P_n^{(\beta,\omega)}(r) H_{33}(s_3, r) dr \right\} (1-s_3)^{-\beta} (1+s_3)^{-\omega} ds_3, \quad (2.237c)$$

Equation (2.236) provides the profile of the circular stamp. If equation (2.236) is used to eliminate c/R in (2.233c), this equation can be further simplified to

$$\begin{aligned} \sum_{n=0}^N \left(g_{31n}(s_3) - \frac{\sin(\pi\beta)}{\pi} \psi_{1n} \right) A_{1n} + \sum_{n=0}^N \left(g_{32n}(s_3) - \frac{\sin(\pi\beta)}{\pi} \psi_{2n} \right) A_{2n} + \\ + \sum_{n=0}^N \left(g_{33n}(s_3) - \frac{\sin(\pi\beta)}{\pi} \psi_{3n} \right) A_{3n} = -\frac{b-a}{R} P_1^{(-\beta,-\omega)}(s_3), \quad -1 < s_3 < 1. \end{aligned} \quad (2.238)$$

ψ_{1n} , ψ_{2n} and ψ_{3n} involve double integrals and these double integrals increase the computation time compared to the flat and triangular stamp problems. Equations (2.233a, b) and (2.238) are solved using the collocation technique. The number of unknowns is $(3N + 3)$. Roots of the Chebyshev polynomials of the first kind are used as the collocation points as follows:

$$s_{ji} = \cos \left(\frac{\pi(2i-1)}{2(N+1)} \right), \quad j = (1, 2, 3), \quad i = 1, \dots, N+1. \quad (2.239)$$

Equations (2.233) are solved for A_{in} , $(i=1, 2, 3)$. The contact stress $\sigma_{11}(0, x_2)$, stress intensity factors at the crack tip $(d, 0)$, and required contact force $P/\mu_{12}R$ are evaluated by using the results. The stress intensity factors are defined by (2.214). Using equations (2.231), the normalized stress intensity factors and the normal component of the contact stress are expressed as follows:

$$\frac{k_1 \sqrt{R}}{P} = 2^{\alpha_1} \frac{2}{A_{30} \theta_0} \frac{R}{b-a} \sqrt{\frac{d}{R}} \sum_{n=0}^N A_{1n} P_n^{(-1/2,0)}(1), \quad (2.240a)$$

$$\frac{k_2 \sqrt{R}}{P} = 2^{\alpha_1} \frac{2}{A_{30} \theta_0} \frac{R}{b-a} \sqrt{\frac{d}{R}} \sum_{n=0}^N A_{2n} P_n^{(-1/2,0)}(1), \quad (2.240b)$$

$$\frac{\sigma_{11} \left(0, \frac{b-a}{2} s_3 + \frac{b+a}{2} \right)}{P/(b-a)} = -\frac{2}{A_{30} \theta_0} (1-s_3)^\beta (1+s_3)^\omega \sum_{n=0}^N A_{3n} P_n^{(\beta,\omega)}(s_3). \quad (2.240c)$$

CHAPTER 3

NUMERICAL RESULTS

In this section, numerical results obtained for different stamp profiles are presented. The main results in this chapter are the stress intensity factors at the crack tip (k_1, k_2), contact stress ($\sigma_{11}(0, x_2)$) and the required contact force. The effect of the friction coefficient η , material elastic modulus ratios, stamp location and crack length on the stress intensity factors at the crack tip and contact stresses are examined. Computer programs are developed for the implementation of the numerical procedures described in Section 2.2.5 by using Visual Fortran Language.

First some results are given, showing the surface stresses in a homogeneous medium in the absence of a crack and loaded by a sliding flat stamp. It is expected that as the flat stamp moves away from crack plane, the effect of the surface crack on the contact stress distribution will disappear. In such a case, solution valid for a homogeneous half-plane can be recovered. In order to show this effect and to verify the contact stress distributions, the contact problem solutions given in the literature [46] and contact stresses obtained from this study for a large value of a/d are compared. In Appendix D, contact problem solutions for a rigid punch on isotropic and anisotropic elastic half-planes are given. These solutions are developed by Galin [46]. As the material alumina (Al_2O_3) is employed in the numerical calculations. Plasma sprayed alumina coatings are known to possess an orthotropic structure. Sevostianov and Kachanov [49] developed a theoretical model to calculate the elastic and conductive properties of orthotropic plasma-sprayed alumina coatings.

The study by Sevostianov and Kachanov [49] also presents experimental data on the orthotropic elastic properties of alumina. The provided experimental data is originally obtained by Perthasarathi et al. [50] using ultrasound measurements and consists of the stiffness coefficients of the plasma-sprayed alumina coatings. In Dag [51], the experimental data given in [49] is used to calculate the elastic parameters of the orthotropic alumina surface. The material parameters of the alumina are given in Table 3.1. In this table, Figure 3.2 and Figure 3.3 present comparisons of contact stress distributions for isotropic materials with those of Galin [46] for the case of a flat stamp with $(b-a)/d=1.0$, $a/d=6$ for plane strain and plane stress cases, respectively. Contact stress distributions for orthotropic materials with those of Galin [46] for the case of a flat stamp with $(b-a)/d=1.0$, $a/d=6$ for plane strain and plane stress cases are shown in Figure 3.4 and Figure 3.5 respectively. The results are observed to be in excellent agreement. Hence, it can be concluded that the method proposed for contact stress computation leads to numerical results of high accuracy.

Table 3.1: The material parameters of plasma-sprayed alumina

Property	Alumina (Al₂O₃)
E_1	116.36 GPa
E_2	90.43 GPa
μ_{12}	38.21 GPa
ν_{12}	0.28
ν_{13}	0.27
ν_{31}	0.21
ν_{32}	0.14

3.1 Flat Stamp

The geometry of the flat stamp problem is depicted in Figure 2.7. Results pertaining to the flat stamp are provided in Figure 3.6-Figure 3.24. Developed solution method

for the flat stamp is validated by making comparisons to the results available in the literature. Figure 3.6, Figure 3.7 and Figure 3.8 present comparisons of normalized mode I and II stress intensity factors and contact stresses for homogeneous isotropic materials with those of given by Dag [40] ν is taken as 0.25. In this analysis d_{11} , d_{12} and d_{22} given in (2.5c-e) are used as $d_{11}=2.9996$, $d_{12}=1.0008$ and $d_{22}=3.0052$. These values are obtained by using isotropic material properties. As can be seen in these figures the results agree quite well.

Figure 3.9 and Figure 3.10 show the modes I and II stress intensity factors generated for an orthotropic medium by taking $(b-a)/d=0.1$. The results are given for various values of the friction coefficient. In the analysis, the properties of alumina (Al_2O_3) are utilized. As seen in Figure 3.9, for $\eta=0$ mode I stress intensity factors are negative for all values of a/d , which is indicative of crack closure. As the coefficient of friction, hence the tangential force, increases mode I stress intensity factors also increase. In Figure 3.10, for $\eta=0$ mode II stress intensity factors are positive for all values of a/d . If a small element at the crack tip is considered as shown Figure 3.1, the crack bend backwards and it extend in a direction opposite to the applied frictional force.

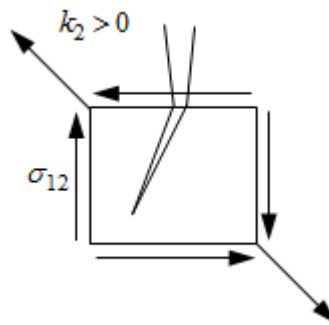


Figure 3.1: Direction of crack extension

As the coefficient of friction increases mode II stress intensity factors are seen to decrease. Contact stresses in plasma-sprayed alumina for $(b-a)/d=0.1$ and $a/d=0.4$ are given in Figure 3.11 for various values of the friction coefficient. For $\eta=0$ singularities are equal at both ends of the contact area but due to the effect of the surface crack, the stress distribution is not exactly symmetric. As the coefficient of friction increases, singularity at the leading end i.e., $-\beta$ decreases and there is higher stress intensification at the trailing end.

Another set of results for the stress intensity factors are given in Figure 3.12 and Figure 3.13 for the relatively larger stamp size of $(b-a)/d=1.0$. The trends are similar to those observed in Figure 3.9 and Figure 3.10. The contact stress distributions for $(b-a)/d=1.0$ are shown in Figure 3.14 for various values of the friction coefficient η .

Figure 3.15 and Figure 3.16 illustrate the effects of elastic modulus ratio E_1/E_2 and a/d on modes I and II stress intensity factors, respectively. Contact stress distributions for various values of elastic modulus ratio E_1/E_2 are given in Figure 3.17. Figure 3.18 and Figure 3.19 show the effect of E_1/E_2 on modes I and II stress intensity factors for. It can be seen that Mode I stress intensity factors increase as E_1/E_2 increases (Figure 3.15 and Figure 3.18). Mode II stress intensity factors drop as E_1/E_2 gets larger (Figure 3.16 and Figure 3.19).

Figure 3.20 and Figure 3.21 present the effects of the elastic modulus ratio E_1/E_3 and a/d on the modes I and II stress intensity factors. Contact stress distributions for various values of E_1/E_3 are given in Figure 3.22. Figure 3.23 and Figure 3.24 show the effects of E_1/E_3 on modes I and II stress intensity factors. The effect of the elastic modulus ratio E_1/E_3 on modes I and II stress intensity factors and contact stress distributions is not that significant (Figure 3.20-Figure 3.24).

3.2 Triangular Stamp

The geometry of the triangular stamp problem is shown in Figure 2.8. In this case, there is a sharp corner at the trailing end $x_2 = a$ hence at this point the contact stress $\sigma_{11}(0, x_2)$ is singular. At point $x_2 = b$ the contact is smooth and $\sigma_{11}(0, x_2)$ is equal to zero. As described in Section 2.2.5.2, in order to avoid an iterative solution method, the problem is solved for a given contact area and corresponding value of the contact force is determined. The results for a triangular stamp sliding on the surface of the half-plane ($a/d > 0$) are given in Figure 3.25-Figure 3.43 and Table 3.2-Table 3.8. Figure 3.25-Figure 3.27 are generated for an isotropic material for which $\nu = 0.25$. Figure 3.25 and Figure 3.26 show the normalized modes I and II stress intensity factors, respectively for various values of the friction coefficient. Table 3.2 tabulates the variation of the normalized force with a/d and Figure 3.27 presents the contact stresses for a stamp whose location is given by $a/d = 0.1$, $b/d = 1.1$. In this analysis d_{11} , d_{12} and d_{22} are set as $d_{11} = 2.9996$, $d_{12} = 1.0008$ and $d_{22} = 3.0052$. These values are obtained by assuming that the material is isotropic. The given results are in excellent agreement with those provided by Dag [40].

The results for orthotropic materials are computed by using the material properties of plasma-sprayed alumina Al_2O_3 given in Table 3.1. Figure 3.28 and Figure 3.29 show the modes I and II stress intensity factors, respectively for an orthotropic material obtained by considering different values of friction coefficient. Table 3.3 shows the variations of the normalized force with a/d . As expected, the required force is larger for larger values of the friction coefficient. It can be seen that for all values of friction coefficient, normalized force quickly approaches a constant value for large values of a/d . The normalized contact force starts decreasing as the stamp gets closer to the crack. Figure 3.30 shows the contact stresses for $a/d = 0.1$, $b/d = 0.2$. In Figure 3.31-Figure 3.33 and Table 3.4, similar results are given for $(b - a)/d = 1.0$.

The effects of the elastic modulus ratio E_1/E_2 on modes I and II stress intensity factors, for various values of the a/d are given in Figure 3.34 and Figure 3.35, respectively. Figure 3.36 shows the effect of E_1/E_2 on the contact stress distribution for $a/d=0.1$, $b/d=1.1$ and $\eta=0.4$. Figure 3.37 and Figure 3.38 show the competing effect of E_1/E_2 on modes I and II stress intensity factors. The effect of E_1/E_2 on normalized contact force is examined in Table 3.5 and Table 3.6. As can be seen, Mode I stress intensity factors increase as E_1/E_2 increases (Figure 3.34 and Figure 3.37). Mode II stress intensity factors drops as E_1/E_2 becomes larger (Figure 3.35 and Figure 3.38).

Figure 3.39 and Figure 3.40 presents the influence of E_1/E_3 on modes I and II stress intensity factors, respectively. Contact stress distributions for various values of E_1/E_3 are given in Figure 3.41. Figure 3.42 and Figure 3.43 show the effect of E_1/E_3 on modes I and II stress intensity factors for various values of the friction coefficient η . The effect of E_1/E_3 on the normalized contact force are examined in Table 3.7 and . It can be seen that the effect of E_1/E_3 on modes I and II stress intensity factors and contact stress distributions is not significant especially when E_1/E_3 is large (Figure 3.39-Figure 3.43).

3.3 Circular Stamp

The geometry of the circular stamp problem is depicted in Figure 2.9. The radius of the circular stamp is denoted by R . There is smooth contact at both ends $x_2 = a$ and $x_2 = b$ hence the contact stress $\sigma_{11}(0, x_2)$ is zero at these points. The centerline of the stamp is at $x_2 = c$. The numerical solution of the problem is described in Section 2.2.5.3. The problem is solved by specifying a and b and corresponding values of the contact force P and c are calculated. Although no iterations are required, the computation time required for the solution of the circular stamp problem is more than that required for flat and triangular stamp problems. The double integrals (see

equations (2.237)) resulting from the consistency condition takes most of the computation time in the circular stamp problem. The results for a circular stamp sliding on the surface of the half-plane ($a/R > 0$) are shown in Figure 3.44-Figure 3.62 and Table 3.9-Table 3.15. Figure 3.44-Figure 3.46 are obtained for an isotropic material with $\nu = 0.25$. Figure 3.44 and Figure 3.45 show normalized modes I and II stress intensity factors, respectively, for various values of the friction coefficient. Table 3.9 presents the variation of the normalized force with a/R and Figure 3.46 depicts the contact stresses for a stamp whose location is given by $a/R=0.1$, $b/R=1.1$, $d/R=1.0$. In this analysis d_{11} , d_{12} and d_{22} are used as $d_{11}=2.9996$, $d_{12}=1.0008$ and $d_{22}=3.0052$. These values are obtained by using isotropic material properties. The results are in excellent agreement with those given by Dag [40].

The results for orthotropic materials are obtained by using the material properties of plasma-sprayed alumina (Al_2O_3) given in Table 3.1. Figure 3.47 and Figure 3.48 show the modes I and II stress intensity factors, respectively for various values of the friction coefficient. Required normalized forces are tabulated in Table 3.10 for different values of the friction coefficient. The variation of the contact force for small values of a/R depends on the size of the contact area between the crack faces. For small values of friction coefficient mode I stress intensity factors are negative and there is a crack closure. If the area of the contacting surfaces of the crack faces is relatively large, an increase in the contact force with the decrease in a/R can be expected and this seems to occur for $\eta=0$ and $\eta=0.2$. From Table 3.10 it can be seen that as a/R decreases required contact force decreases for $\eta=0.4$ and $\eta=0.6$. Hence, the size of the contact area between the crack faces is expected to be smaller for $\eta=0.4$ and $\eta=0.6$. Figure 3.49 shows the distribution of the contact stresses for various values of the friction coefficient with $a/R=0.1$, $b/R=0.2$, $d/R=1.0$. Another set of results for stress intensity factors, contact force and contact stresses are given in Figure 3.50- Figure 3.52 and Table 3.11 for $(b-a)/R=1.0$. As can be seen the trends are similar.

The effect E_1/E_2 on modes I and II stress intensity factors, for various values of the a/R is examined in Figure 3.53 and Figure 3.54, respectively. Figure 3.55 shows the effect of E_1/E_2 on the contact stress distribution for $a/R=0.1$, $b/R=1.1$, $d/R=1.0$ and $\eta=0.4$. Figure 3.56 and Figure 3.57 illustrate the effect of E_1/E_2 on modes I and II stress intensity factors for different values of the friction coefficient η . The E_1/E_2 on the normalized contact force is examined in Table 3.12 and Table 3.13. As can be seen, Mode I stress intensity factor increases as E_1/E_2 gets larger (Figure 3.53 and Figure 3.56). Mode II stress intensity factor decreases as E_1/E_2 increases (Figure 3.54 and Figure 3.57).

Figure 3.58 and Figure 3.59 depict the effect of E_1/E_3 on modes I and II stress intensity factors for various values of the a/R . Contact stress for various values of E_1/E_3 are given in Figure 3.60. Figure 3.61 and Figure 3.62 present the variations of stress intensity factors with respect to E_1/E_3 for different values of the friction coefficient η . The effect of the E_1/E_3 on normalized contact force is examined in Table 3.14 and Table 3.15. It can be seen that the influence of E_1/E_3 on modes I and II stress intensity factors and contact stress distributions is not that significant (Figure 3.58-Figure 3.62).

3.4 Figures

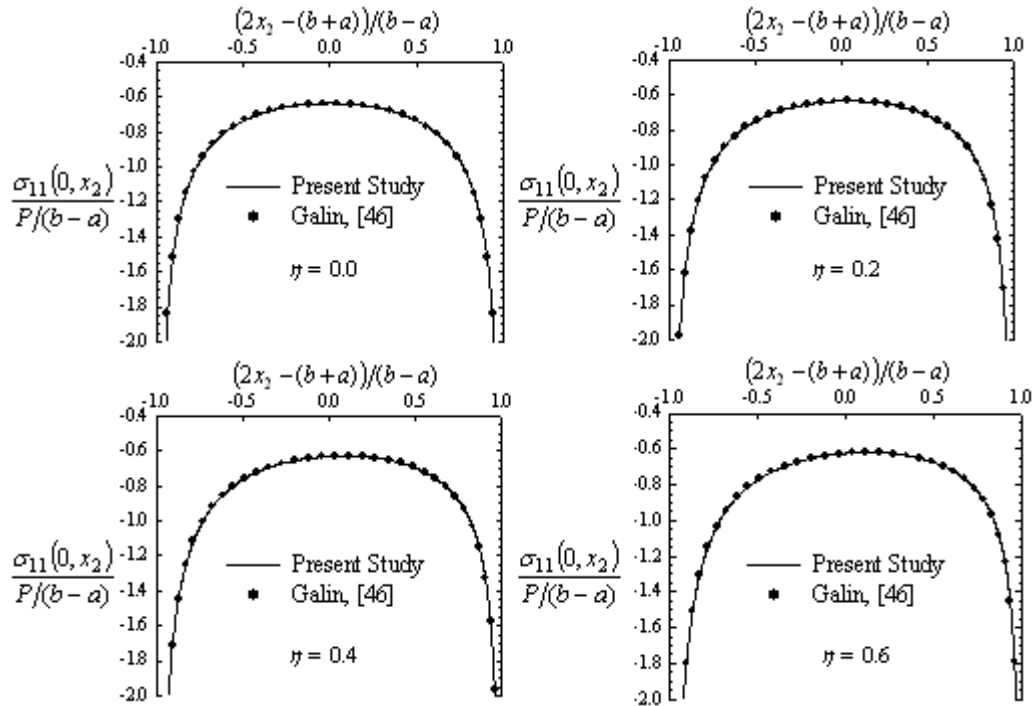


Figure 3.2: Comparisons of contact stress distributions for an isotropic half-plane loaded by a flat stamp, $(b-a)/d=1.0$, $a/d=6$, $d_{11}=2.9996$, $d_{12}=1.0008$, $d_{22}=3.0052$ for plane strain.

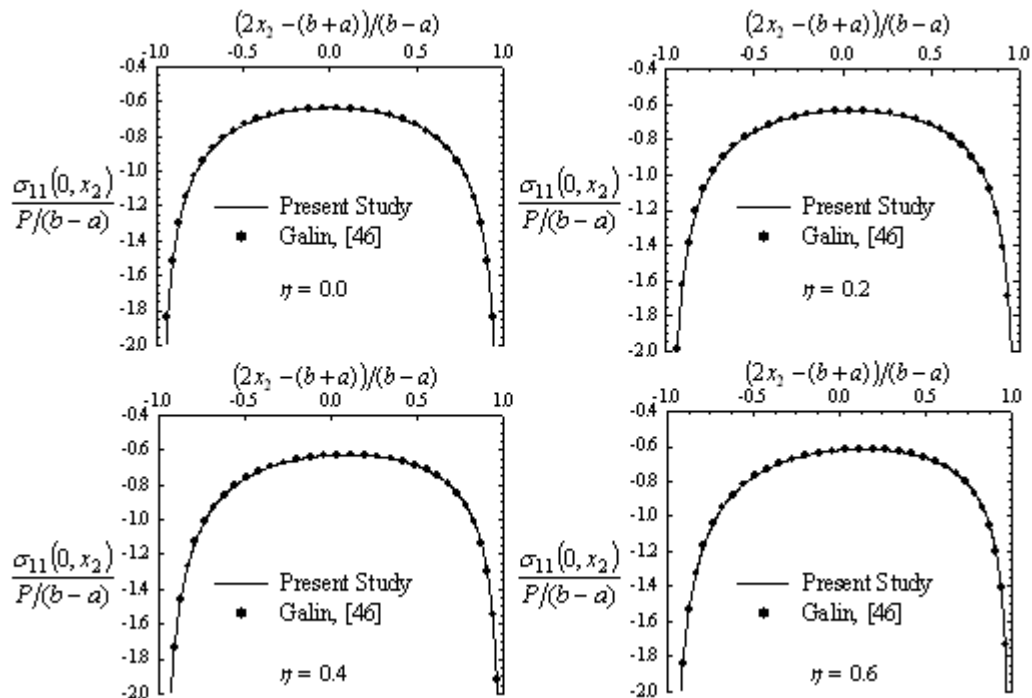


Figure 3.3: Comparisons of contact stress distributions for an isotropic half-plane loaded by a flat stamp, $(b-a)/d=1.0$, $a/d=6$, $d_{11}=2.9996$, $d_{12}=1.0008$, $d_{22}=3.0052$ for plane stress.

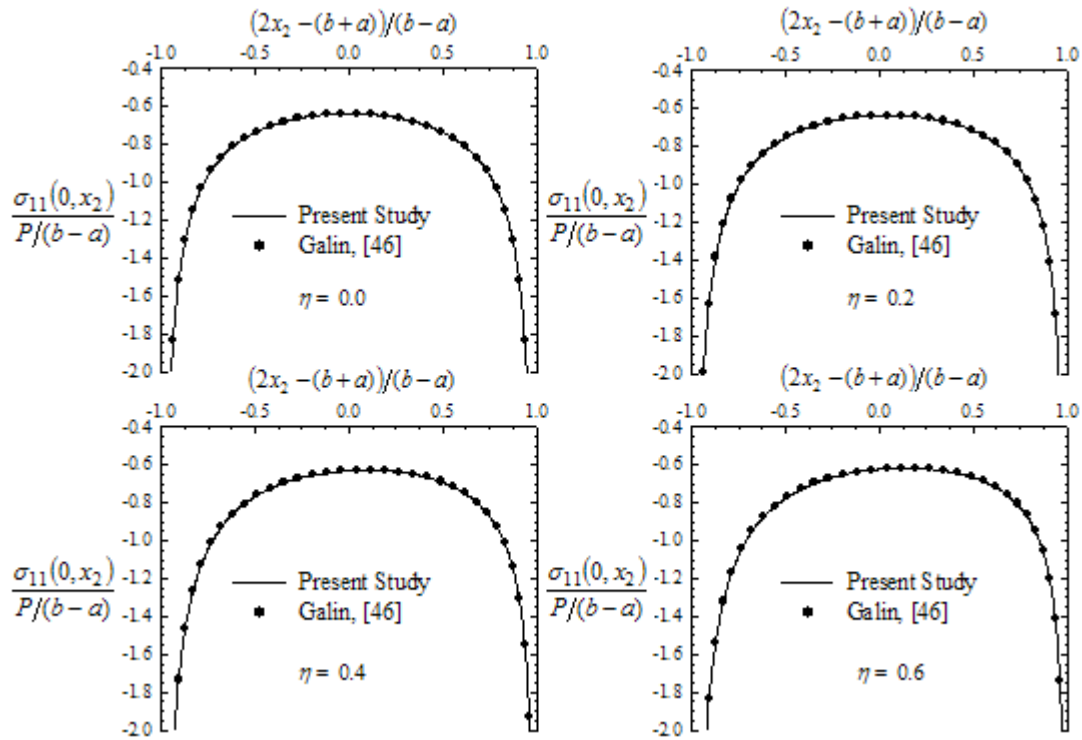


Figure 3.4: Comparisons of contact stress distributions for an orthotropic half-plane loaded by a flat stamp, $(b-a)/d=1.0$, $a/d=6$, $d_{11}=2.9996$, $d_{12}=1.0008$, $d_{22}=3.0052$ for plane strain.

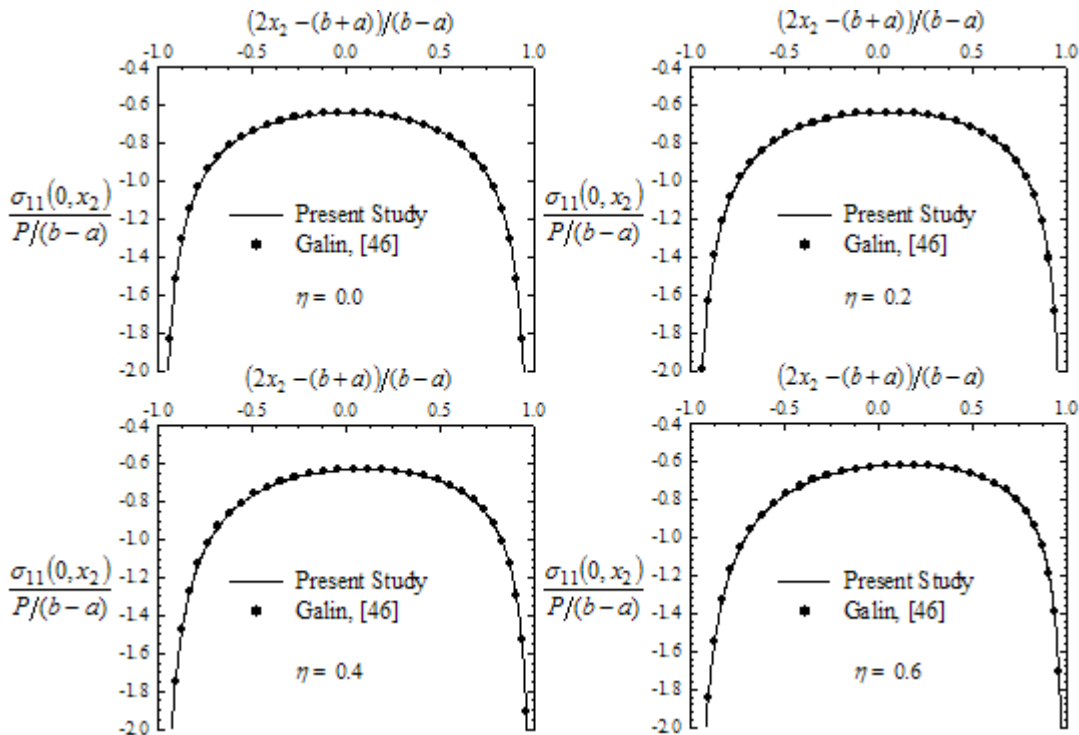


Figure 3.5: Comparison of contact stress distributions for an orthotropic half-plane loaded by a flat stamp, $(b-a)/d=1.0$, $a/d=6$, $d_{11}=2.9996$, $d_{12}=1.0008$, $d_{22}=3.0052$ for plane stress.

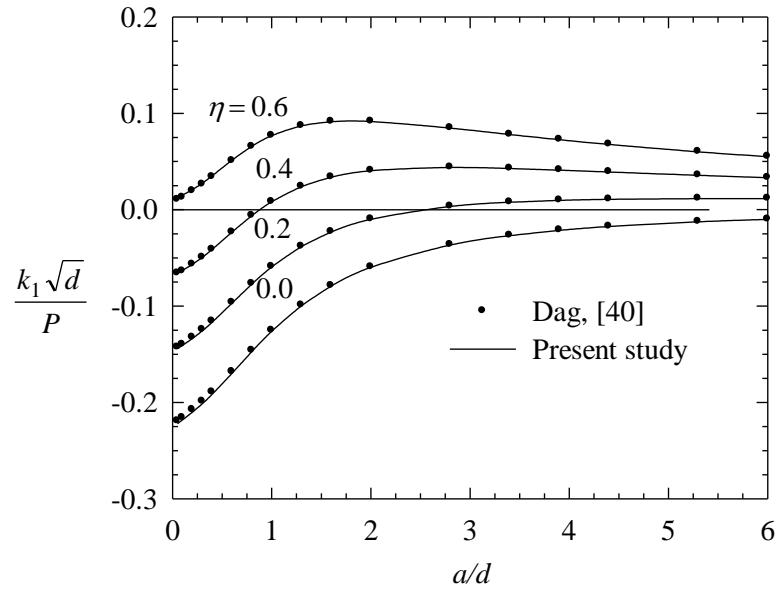


Figure 3.6: Mode I stress intensity factors for an edge crack in an isotropic half-plane loaded by a flat stamp as shown in Figure 2.7, $(b-a)/d=1.0$, $\nu=0.25$, $d_{11}=2.9996$, $d_{12}=1.0008$, $d_{22}=3.0052$.

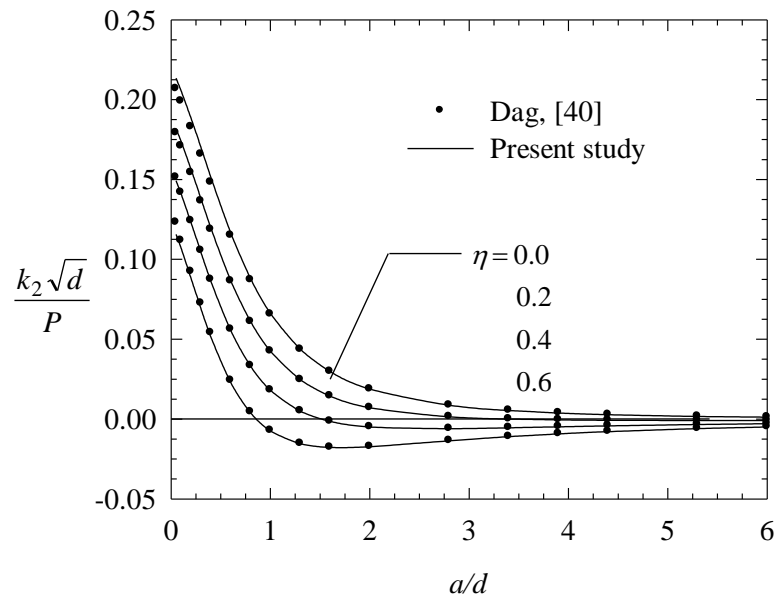


Figure 3.7: Mode II stress intensity factors for an edge crack in an isotropic half-plane loaded by a flat stamp as shown in Figure 2.7, $(b-a)/d=1.0$, $\nu=0.25$, $d_{11}=2.9996$, $d_{12}=1.0008$, $d_{22}=3.0052$.

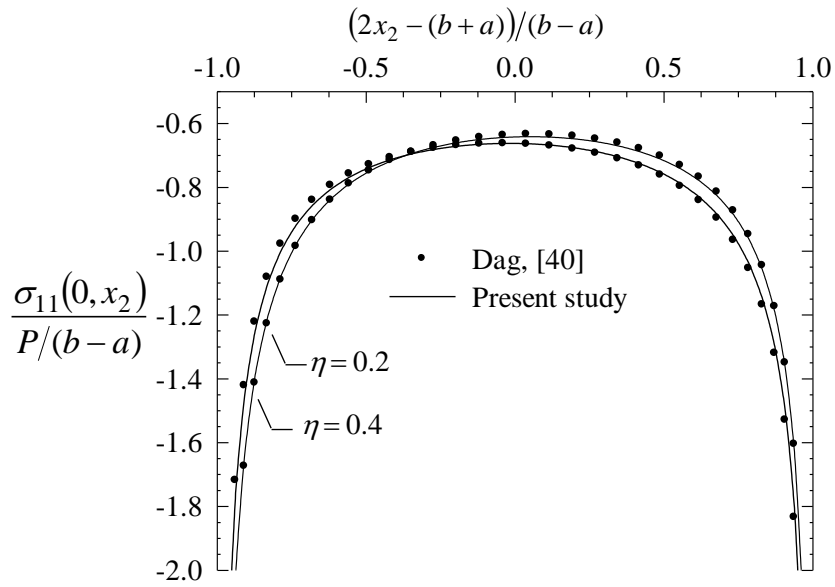


Figure 3.8: Contact stress distributions for an isotropic half-plane with an edge crack and loaded by a flat stamp as shown in Figure 2.7, $(b-a)/d=1.0$, $\nu=0.25$, $a/d=0.4$, $d_{11}=2.9996$, $d_{12}=1.0008$, $d_{22}=3.0052$.

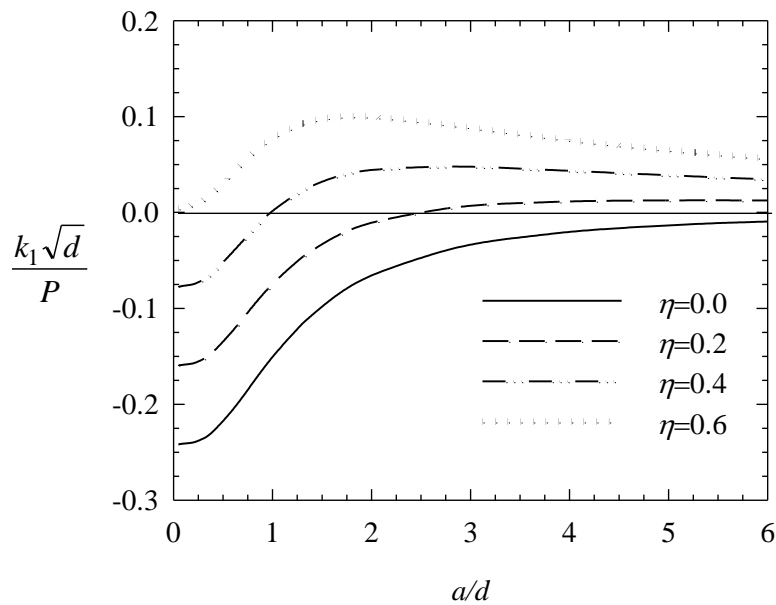


Figure 3.9: Mode I stress intensity factors for an edge crack in an orthotropic half-plane loaded by a flat stamp as shown in Figure 2.7, $(b-a)/d=0.1$.

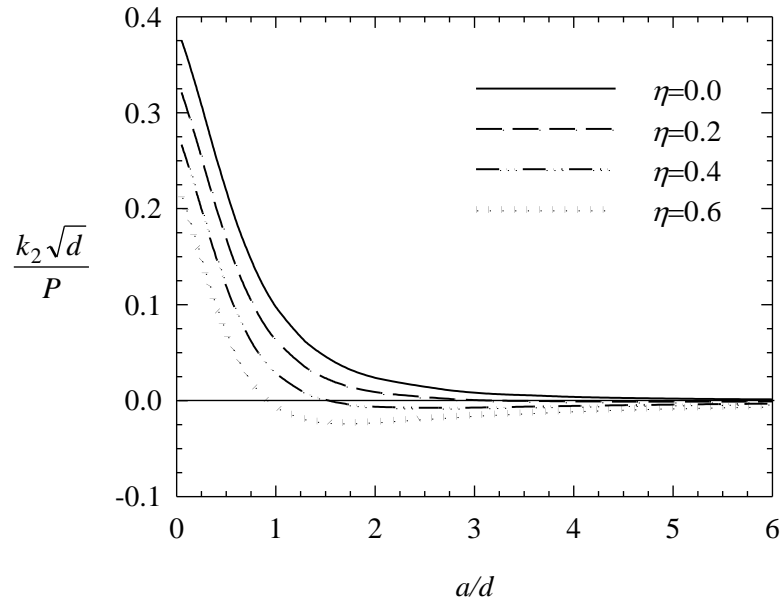


Figure 3.10: Mode II stress intensity factors for an edge crack in an orthotropic half-plane loaded by a flat stamp as shown in Figure 2.7, $(b - a)/d = 0.1$.

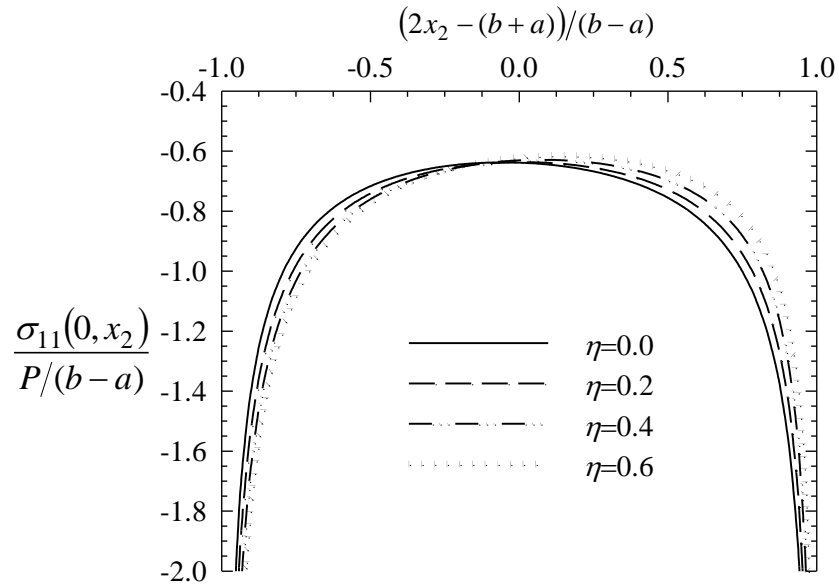


Figure 3.11: Contact stress distributions for an orthotropic half-plane with an edge crack and loaded by a flat stamp as shown in Figure 2.7, $(b - a)/d = 0.1$, $a/d = 0.4$.

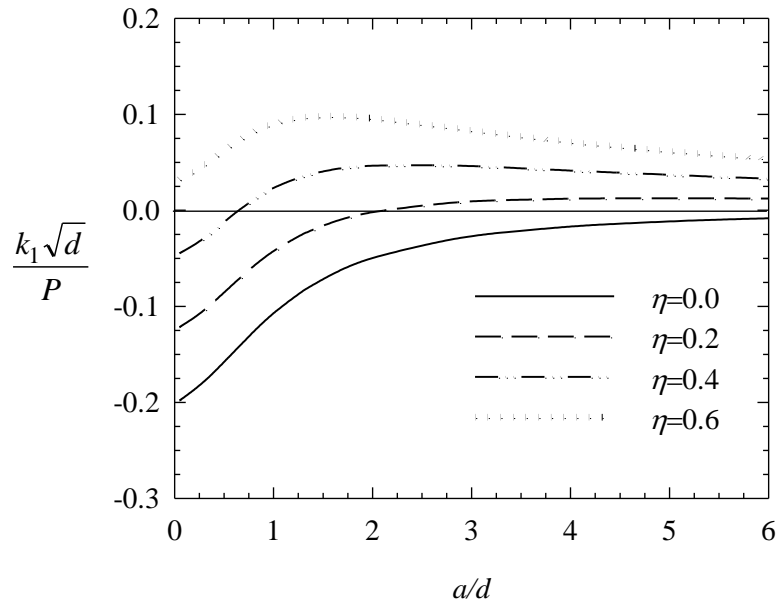


Figure 3.12: Mode I stress intensity factors for an edge crack in an orthotropic half-plane loaded by a flat stamp as shown in Figure 2.7, $(b-a)/d=1.0$.

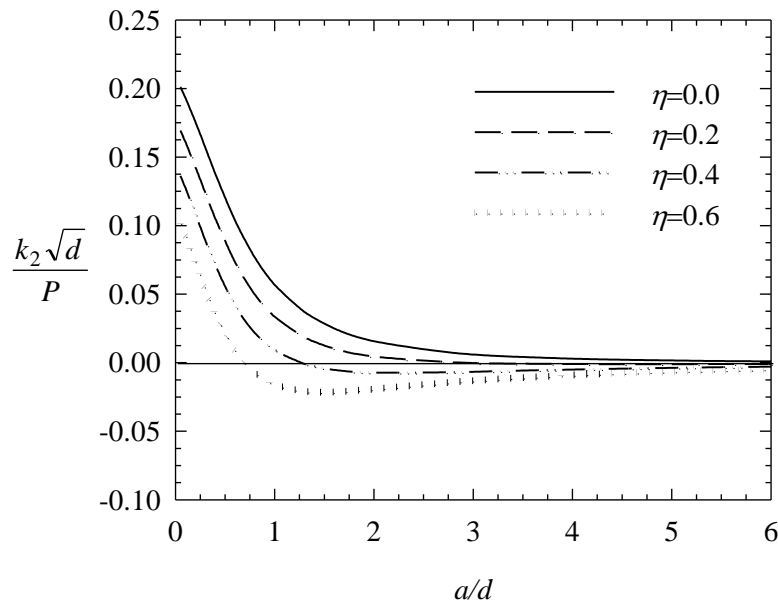


Figure 3.13: Mode II stress intensity factors for an edge crack in an orthotropic half-plane loaded by a flat stamp as shown in Figure 2.7, $(b-a)/d=1.0$.

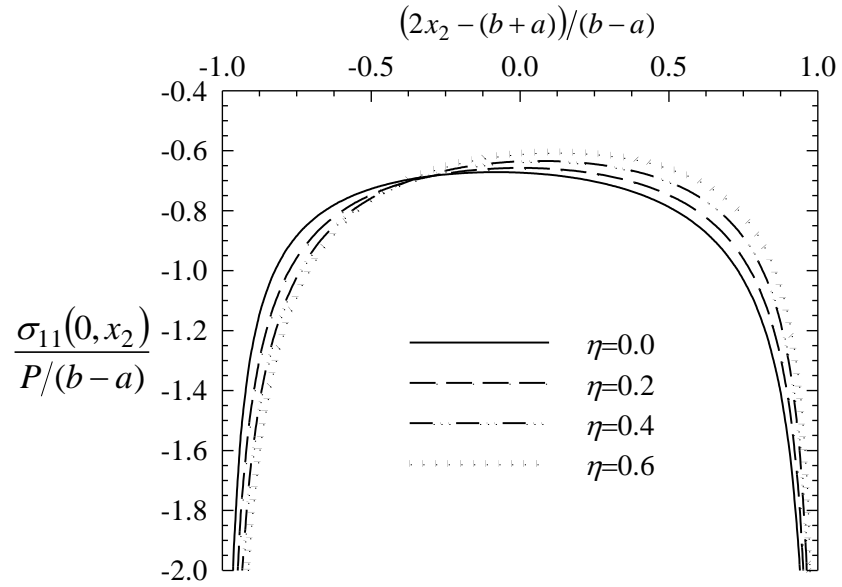


Figure 3.14: Contact stress distributions for an orthotropic half-plane with an edge crack and loaded by a flat stamp as shown in Figure 2.7, $(b-a)/d=1.0$, $a/d=0.4$.

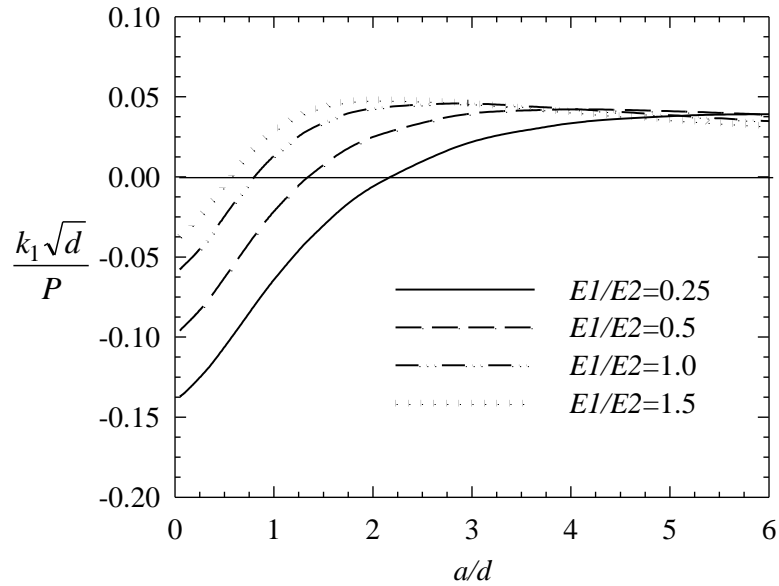


Figure 3.15: Effect of the elastic modulus ratio E_1/E_2 on mode I stress intensity factors for an edge crack in an orthotropic half-plane loaded by a flat stamp as shown in Figure 2.7, $(b-a)/d=1.0$, $\eta=0.4$.

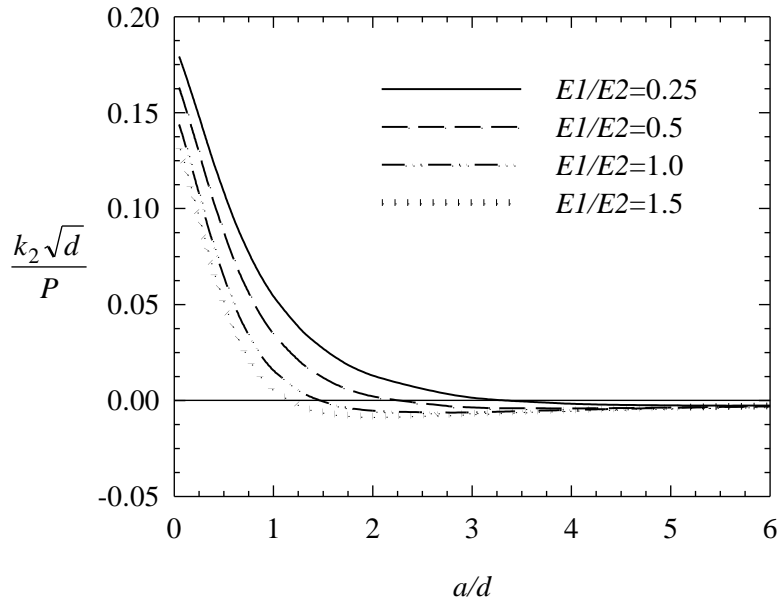


Figure 3.16: Effect of the elastic modulus ratio E_1/E_2 on mode II stress intensity factors for an edge crack in an orthotropic half-plane loaded by a flat stamp as shown in Figure 2.7, $(b-a)/d=1.0$, $\eta=0.4$.

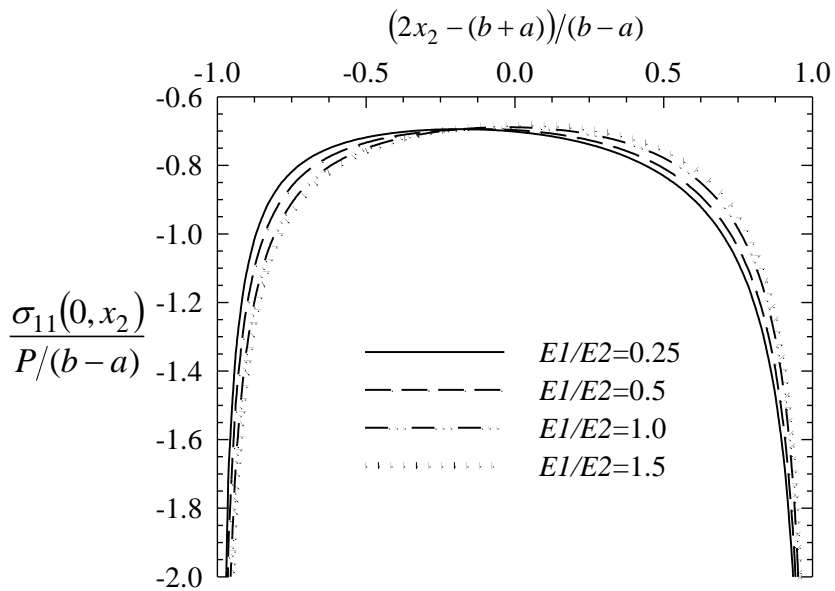


Figure 3.17: Effect of the elastic modulus ratio E_1/E_2 on the contact stress distribution for an edge crack in an orthotropic half-plane loaded by a flat stamp as shown in Figure 2.7, $(b-a)/d=1.0$, $a/d=0.1$, $\eta=0.4$.

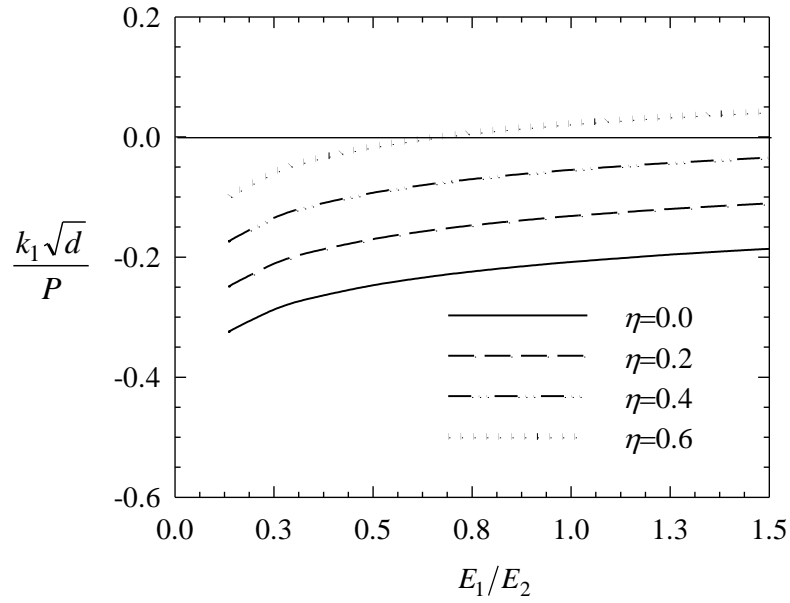


Figure 3.18: Normalized k_1 versus E_1/E_2 and η for an edge crack in an orthotropic half-plane loaded by a flat stamp as shown in Figure 2.7, $(b-a)/d=1.0$, $a/d=0.1$.

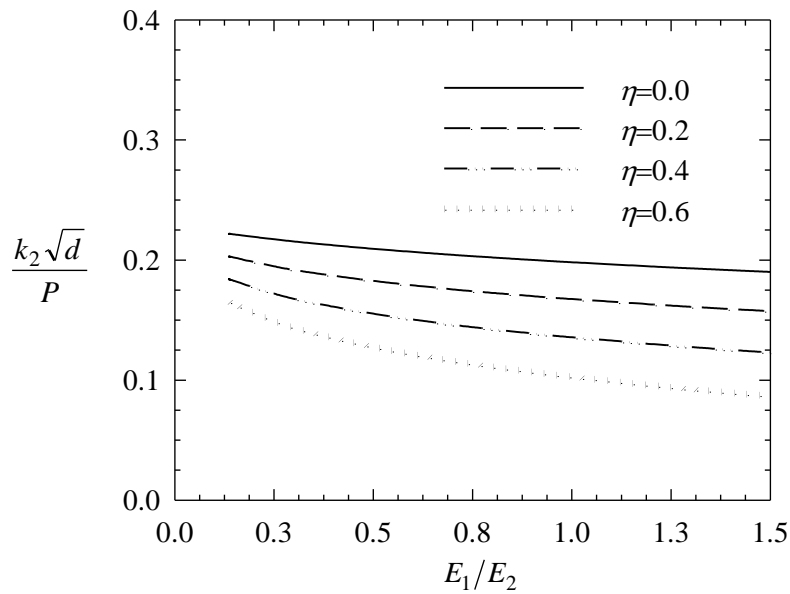


Figure 3.19: Normalized k_2 versus E_1/E_2 and η for an edge crack in an orthotropic half-plane loaded by a flat stamp as shown in Figure 2.7, $(b-a)/d=1.0$, $a/d=0.1$.

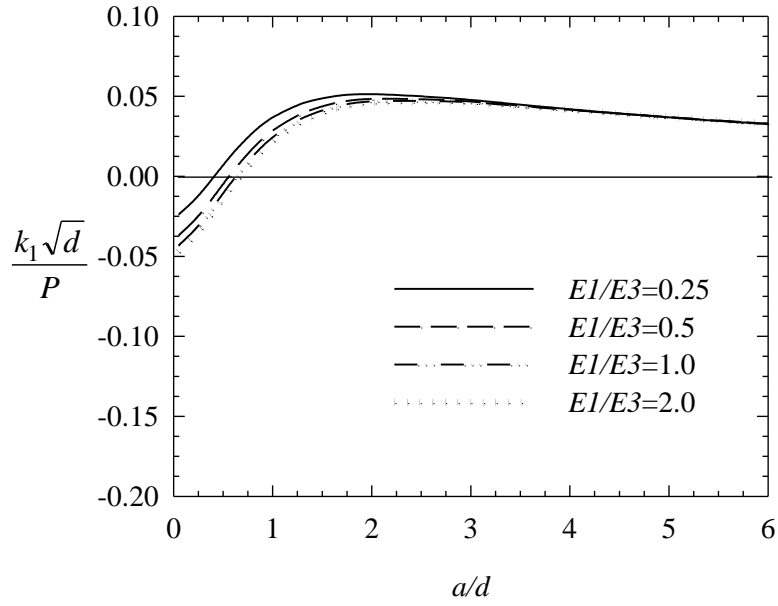


Figure 3.20: Effect of the elastic modulus ratio E_1/E_3 on mode I stress intensity factors for an edge crack in an orthotropic half-plane loaded by a flat stamp as shown in Figure 2.7, $(b-a)/d=1.0$, $\eta=0.4$.

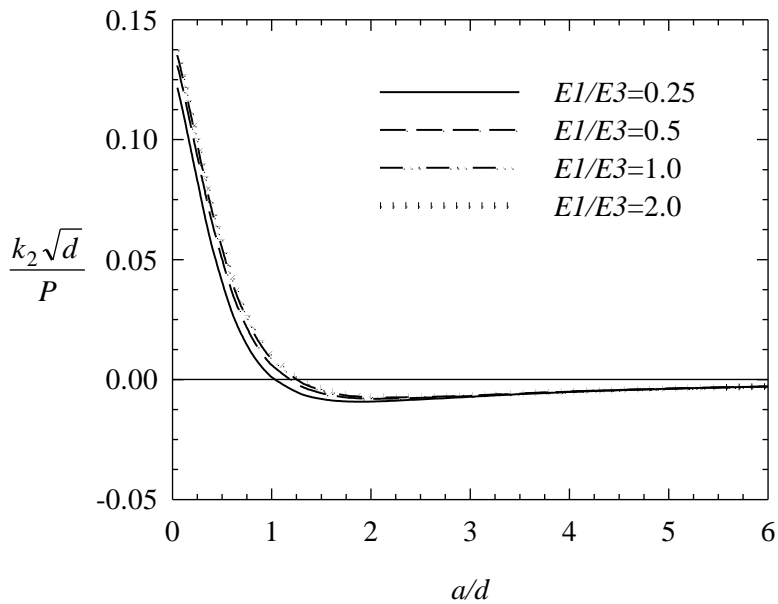


Figure 3.21: Effect of the elastic modulus ratio E_1/E_3 on mode II stress intensity factors for an edge crack in an orthotropic half-plane loaded by a flat stamp as shown in Figure 2.7, $(b-a)/d=1.0$, $\eta=0.4$.

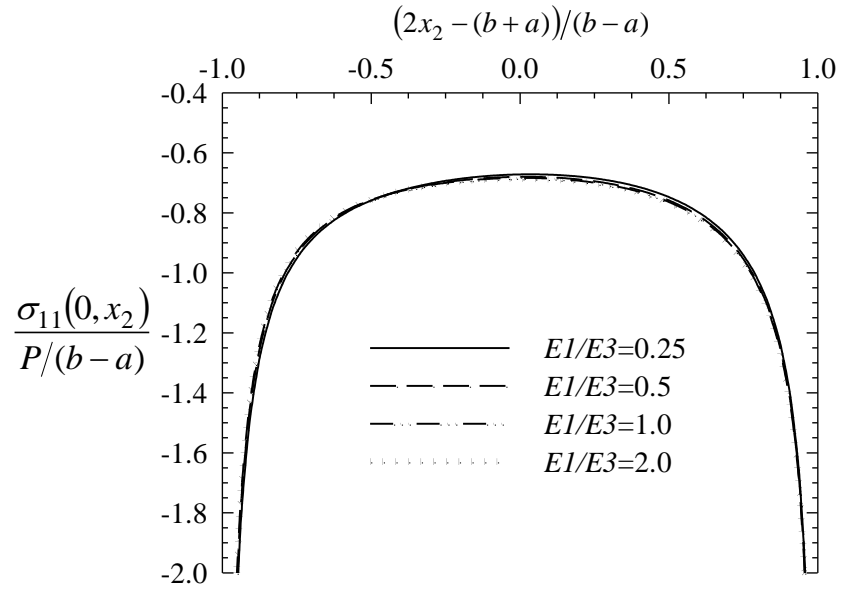


Figure 3.22: Effect of the elastic modulus ratio E_1/E_3 on contact stress distribution for an edge crack in an orthotropic half-plane loaded by a flat stamp as shown in Figure 2.7, $(b-a)/d=1.0$, $a/d=0.1$, $\eta=0.4$.

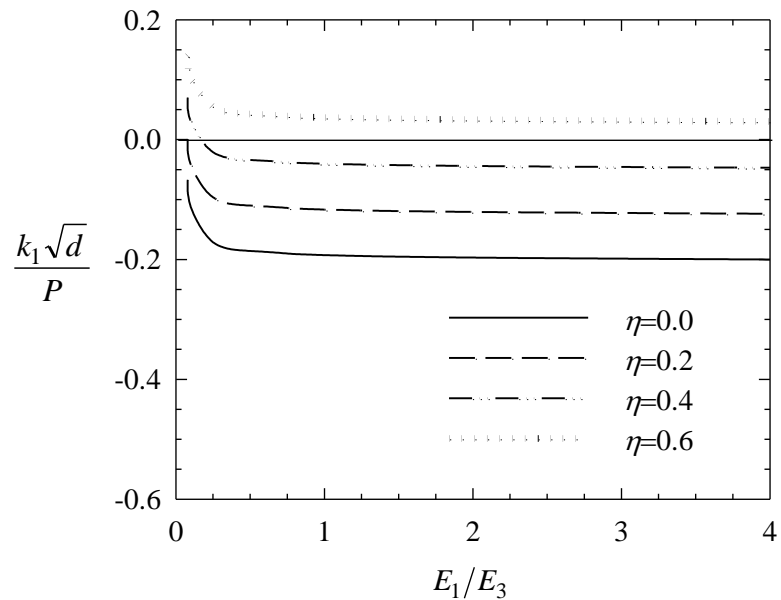


Figure 3.23: Normalized k_1 versus E_1/E_3 and η for an edge crack in an orthotropic half-plane loaded by a flat stamp as shown in Figure 2.7, $(b-a)/d=1.0$, $a/d=0.1$.

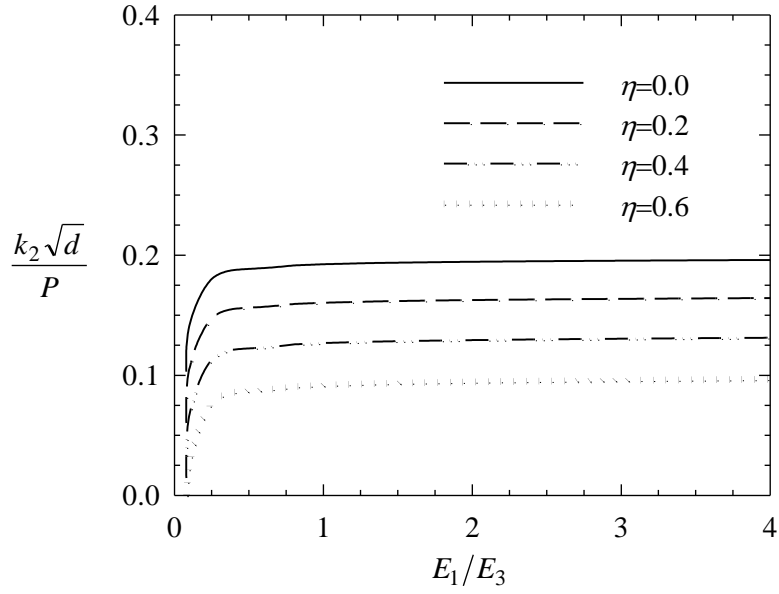


Figure 3.24: Normalized k_2 versus E_1/E_3 and η for an edge crack in an orthotropic half-plane loaded by a flat stamp as shown in Figure 2.7, $(b-a)/d=1.0$, $a/d=0.1$.

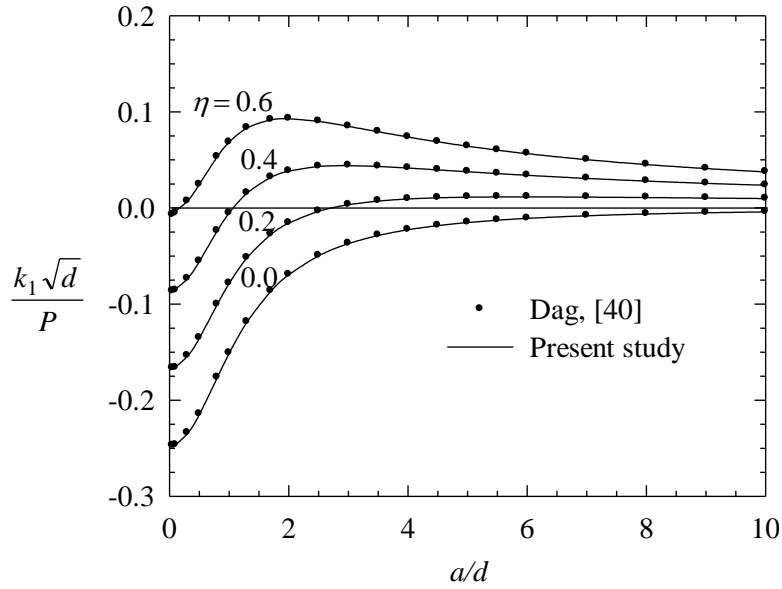


Figure 3.25: Mode I stress intensity factors for an edge crack in an isotropic half-plane loaded by a triangular stamp as shown in Figure 2.8, $(b-a)/d=1.0$, $\nu=0.25$, $d_{11}=2.9996$, $d_{12}=1.0008$, $d_{22}=3.0052$.

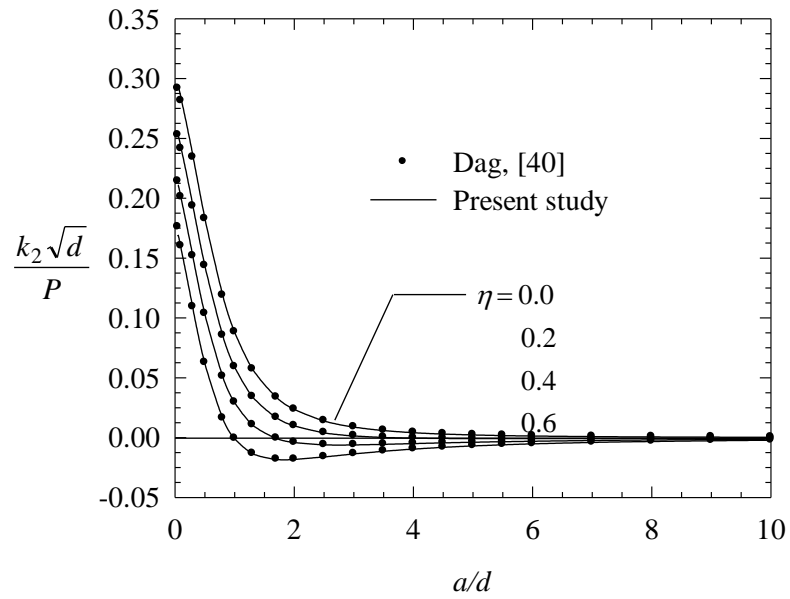


Figure 3.26: Mode II stress intensity factors for an edge crack in an isotropic half-plane loaded by a triangular stamp as shown in Figure 2.8, $(b-a)/d=1.0$, $\nu=0.25$, $d_{11}=2.9996$, $d_{12}=1.0008$, $d_{22}=3.0052$.

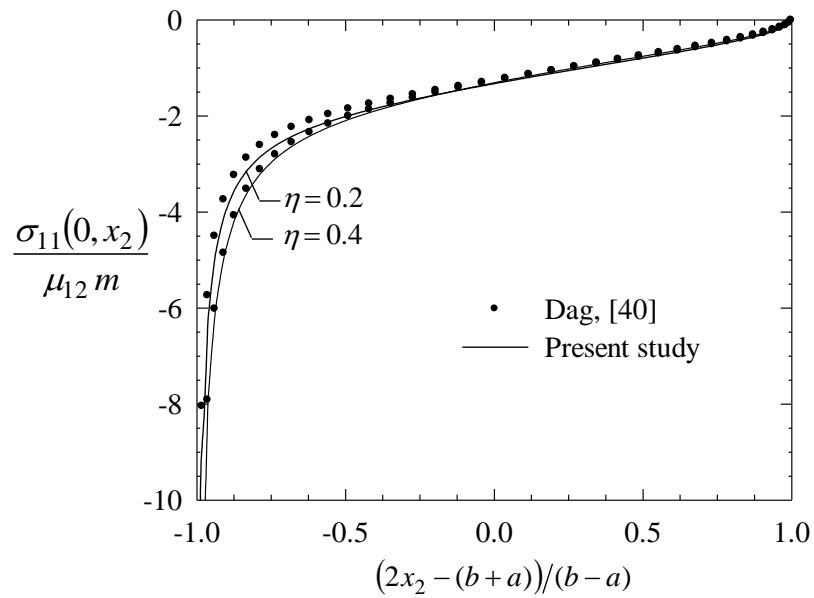


Figure 3.27: Contact stress distributions for an isotropic half-plane with an edge crack and loaded by a triangular stamp as shown in Figure 2.8, $\nu=0.25$, $a/d=0.1$, $b/d=1.1$, $d_{11}=2.9996$, $d_{12}=1.0008$, $d_{22}=3.0052$.

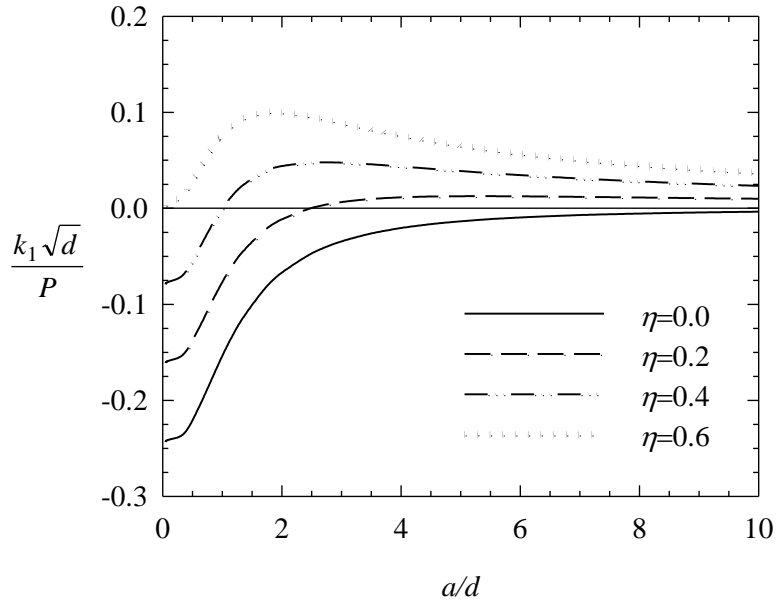


Figure 3.28: Mode I stress intensity factors for an edge crack in an orthotropic half-plane loaded by a triangular stamp as shown in Figure 2.8, $(b - a)/d = 0.1$.

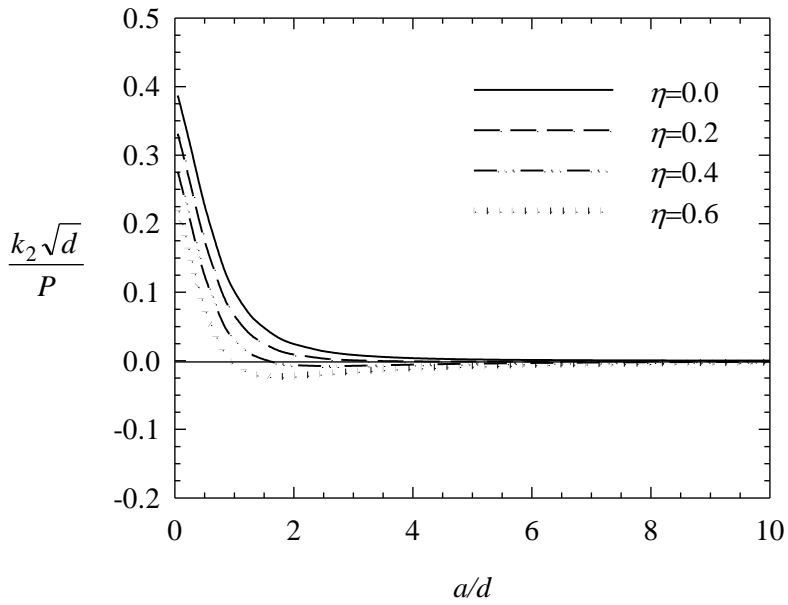


Figure 3.29: Mode II stress intensity factors for an edge crack in an orthotropic half-plane loaded by a triangular stamp as shown in Figure 2.8, $(b - a)/d = 0.1$.

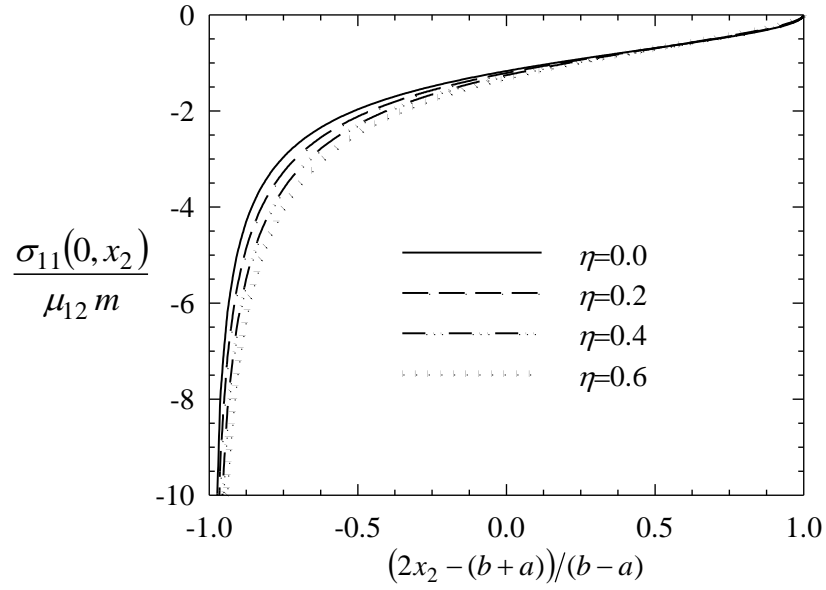


Figure 3.30: Contact stress distributions for an orthotropic half-plane with an edge crack and loaded by a triangular stamp as shown in Figure 2.8, $a/d = 0.1$, $b/d = 0.2$.

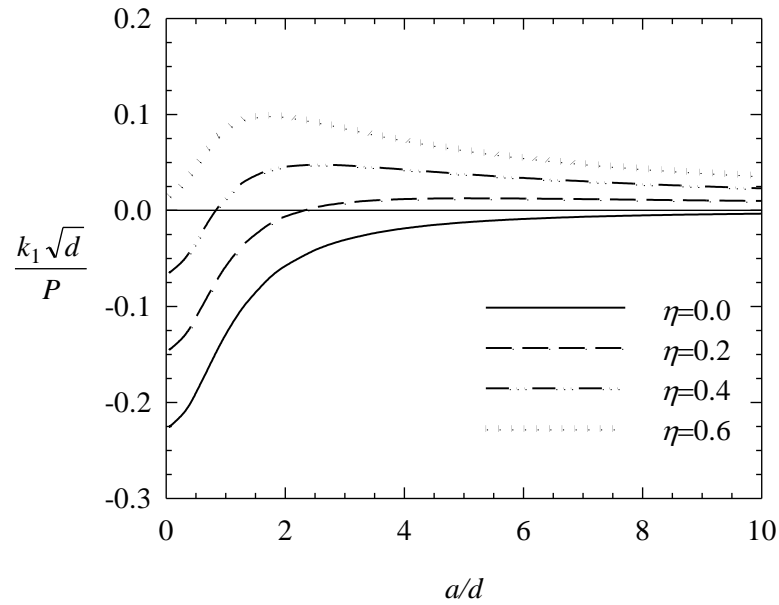


Figure 3.31: Mode I stress intensity factors for an edge crack in an orthotropic half-plane loaded by a triangular stamp as shown in Figure 2.8, $(b-a)/d = 1.0$.

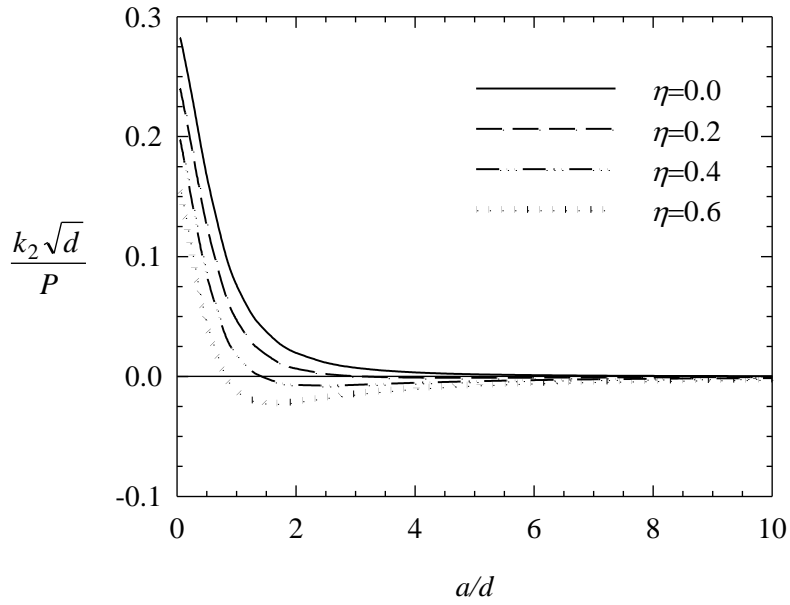


Figure 3.32: Mode II stress intensity factors for an edge crack in an orthotropic half-plane loaded by a triangular stamp as shown in Figure 2.8, $(b - a)/d = 1.0$.

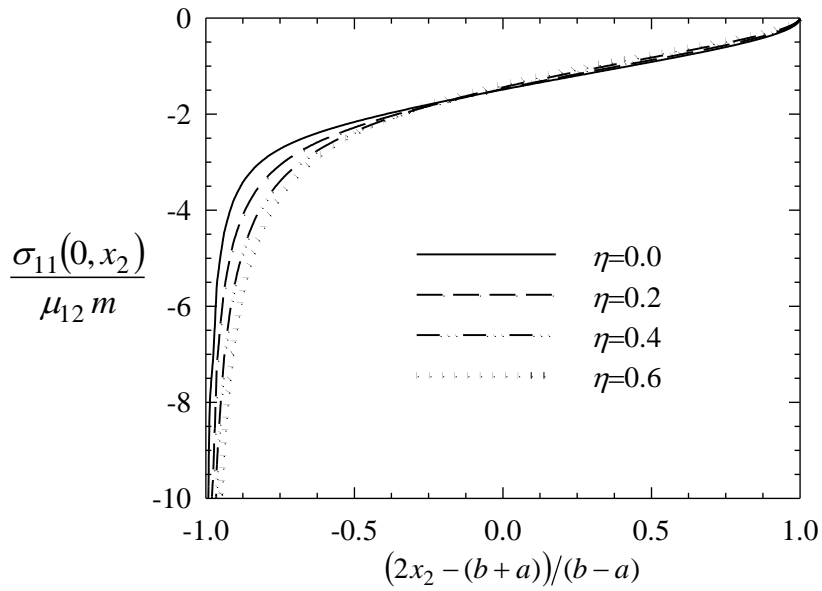


Figure 3.33: Contact stress distribution for an orthotropic half-plane with an edge crack and loaded by a triangular stamp as shown in Figure 2.8, $a/d = 0.1$, $b/d = 1.1$.

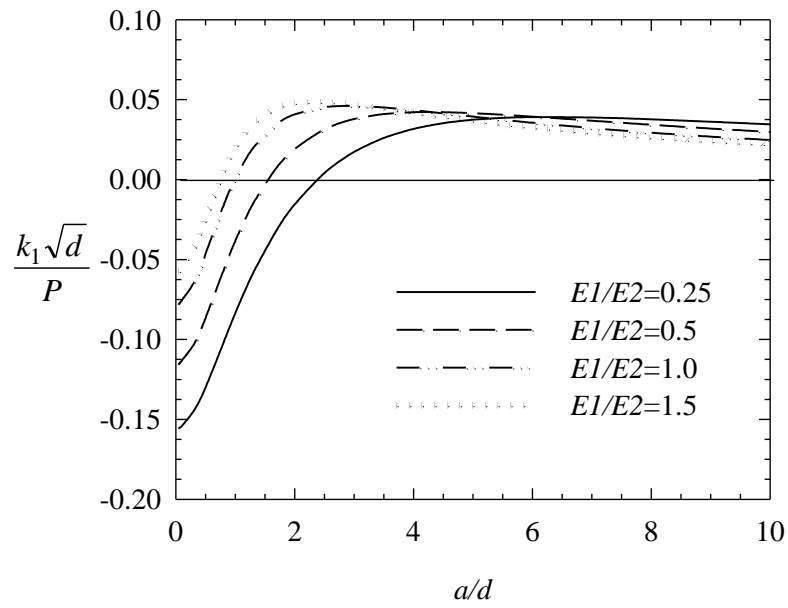


Figure 3.34: Effect of the elastic modulus ratio E_1/E_2 on mode I stress intensity factors for an edge crack in an orthotropic half-plane loaded by a triangular stamp as shown in Figure 2.8, $(b-a)/d=1.0$, $\eta=0.4$.

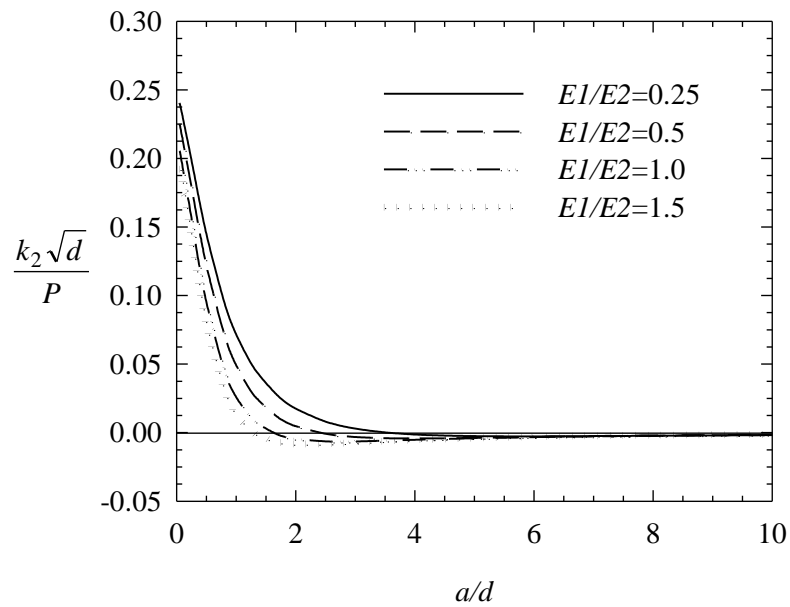


Figure 3.35: Effect of the elastic modulus ratio E_1/E_2 on mode II stress intensity factors for an edge crack in an orthotropic half-plane loaded by a triangular stamp as shown in Figure 2.8, $(b-a)/d=1.0$, $\eta=0.4$.

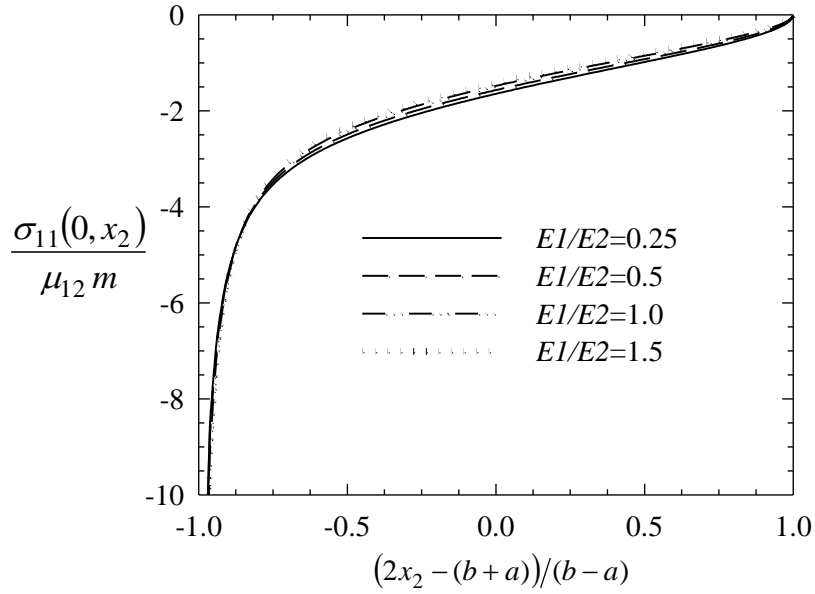


Figure 3.36: Effect of the elastic modulus ratio E_1/E_2 on the contact stress distribution for an edge crack in an orthotropic half-plane loaded by a triangular stamp as shown in Figure 2.8, $a/d=0.1$, $b/d=1.1$, $\eta=0.4$.

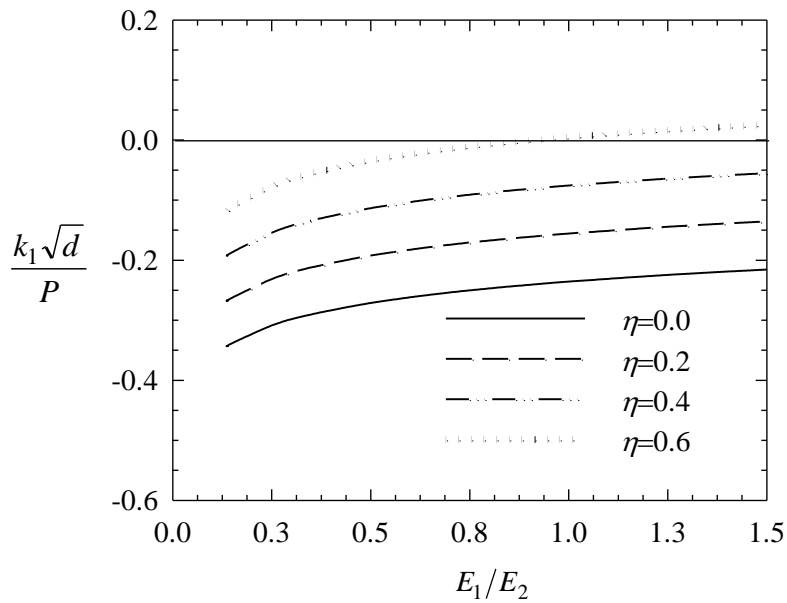


Figure 3.37: Normalized k_1 versus E_1/E_2 and η for an edge crack in an orthotropic half-plane loaded by a triangular stamp as shown in Figure 2.8, $(b-a)/d=1.0$, $a/d=0.1$.

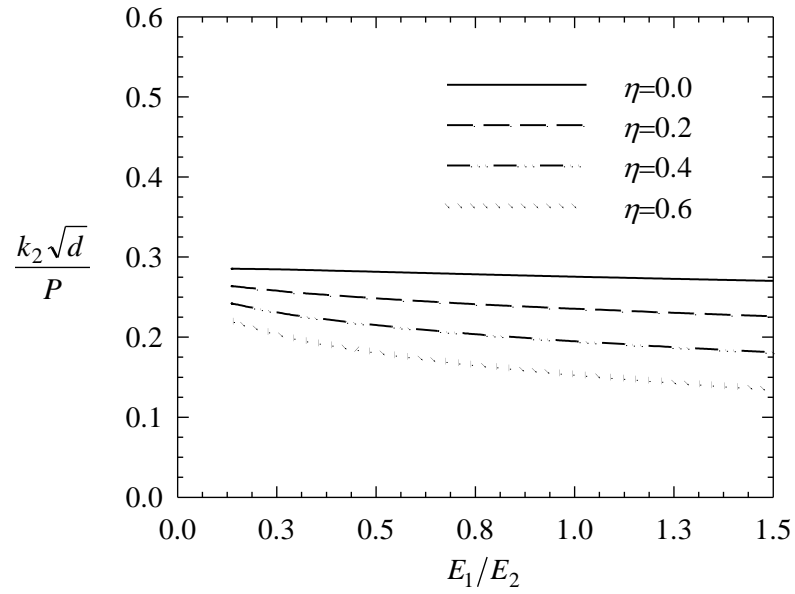


Figure 3.38: Normalized k_2 versus E_1/E_2 and η for an edge crack in an orthotropic half-plane loaded by a triangular stamp as shown in Figure 2.8, $(b-a)/d=1.0$, $a/d=0.1$.

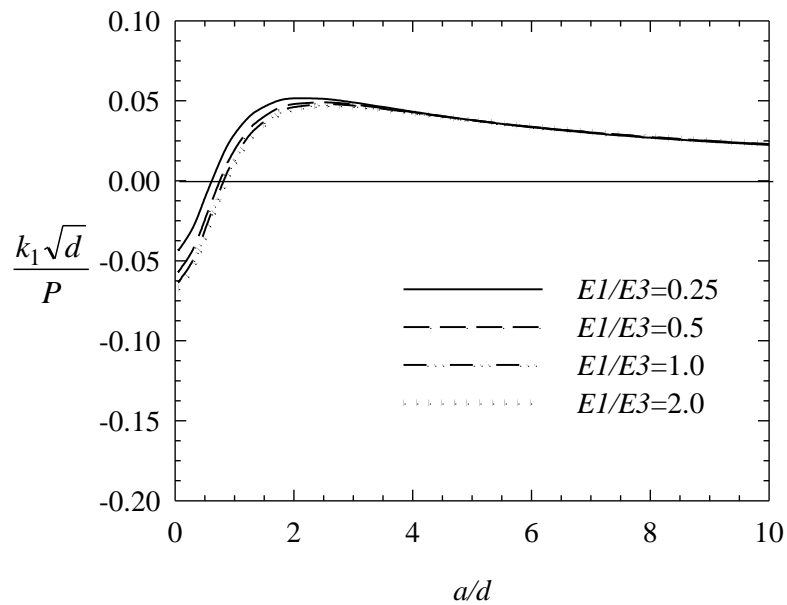


Figure 3.39: Effect of the elastic modulus ratio E_1/E_3 on mode I stress intensity factors for an edge crack in an orthotropic half-plane loaded by a triangular stamp as shown in Figure 2.8, $(b-a)/d=1.0$, $\eta=0.4$.

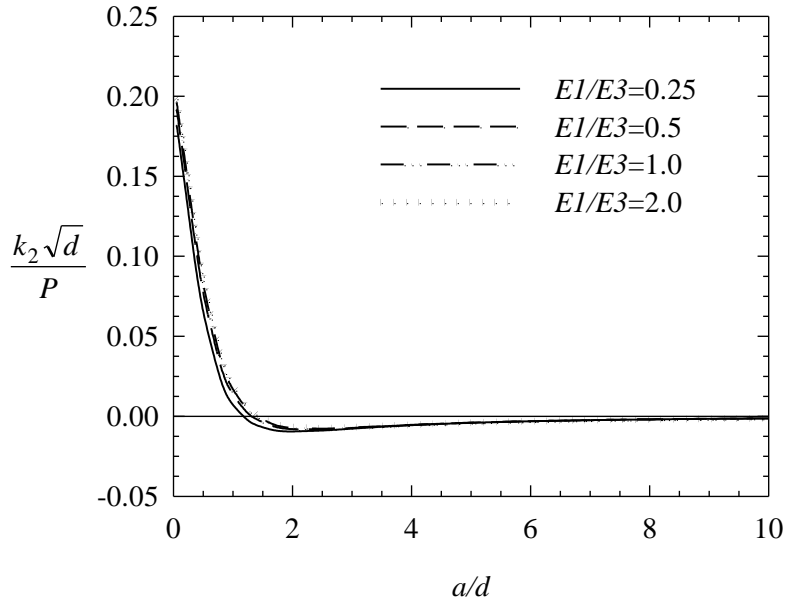


Figure 3.40: Effect of the elastic modulus ratio E_1/E_3 on mode II stress intensity factors for an edge crack in an orthotropic half-plane loaded by a triangular stamp as shown in Figure 2.8, $(b - a)/d = 1.0$, $\eta = 0.4$.

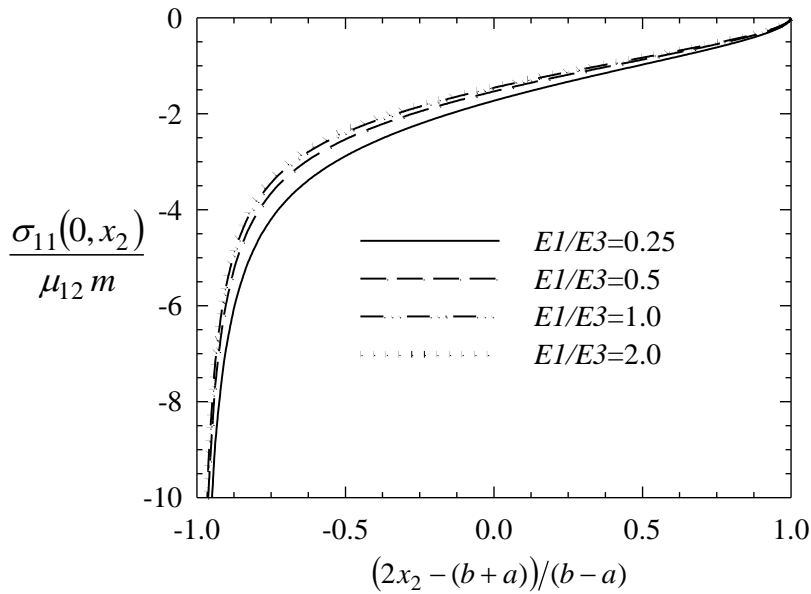


Figure 3.41: Effect of the elastic modulus ratio E_1/E_3 on the contact stress distribution for an edge crack in an orthotropic half-plane loaded by a triangular stamp as shown in Figure 2.8, $a/d = 0.1$, $b/d = 1.1$, $\eta = 0.4$.

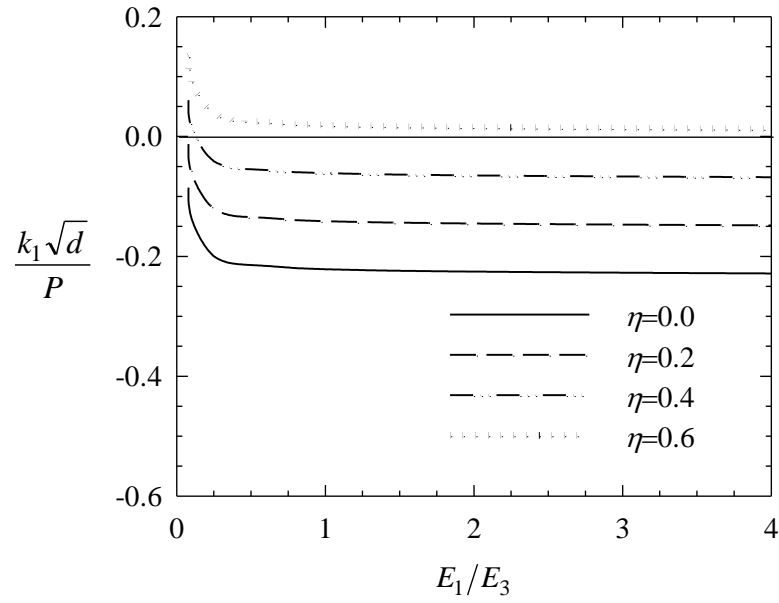


Figure 3.42: Normalized k_1 versus E_1/E_3 and η for an edge crack in an orthotropic half-plane loaded by a triangular stamp as shown in Figure 2.8, $(b-a)/d=1.0$, $a/d=0.1$.

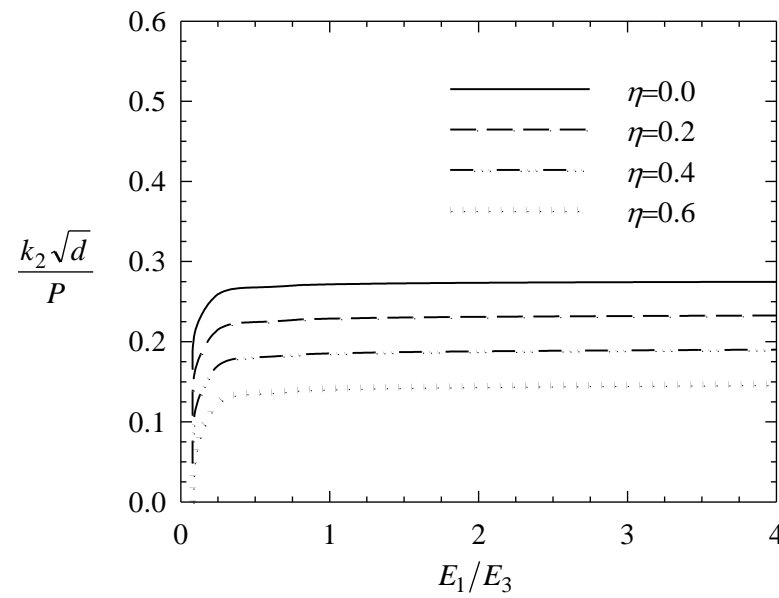


Figure 3.43: Normalized k_2 versus E_1/E_3 and η for an edge crack in an orthotropic half-plane loaded by a triangular stamp as shown in Figure 2.8, $(b-a)/d=1.0$, $a/d=0.1$.

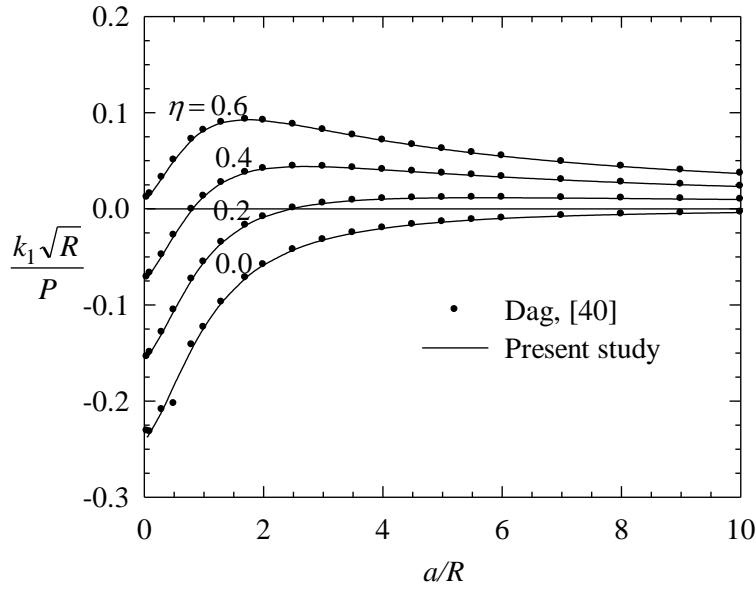


Figure 3.44: Mode I stress intensity factors for an edge crack in an isotropic half-plane loaded by a circular stamp as shown in Figure 2.9, $(b-a)/R=1.0$, $d/R=1.0$, $\nu=0.25$, $d_{11}=2.9996$, $d_{12}=1.0008$, $d_{22}=3.0052$.

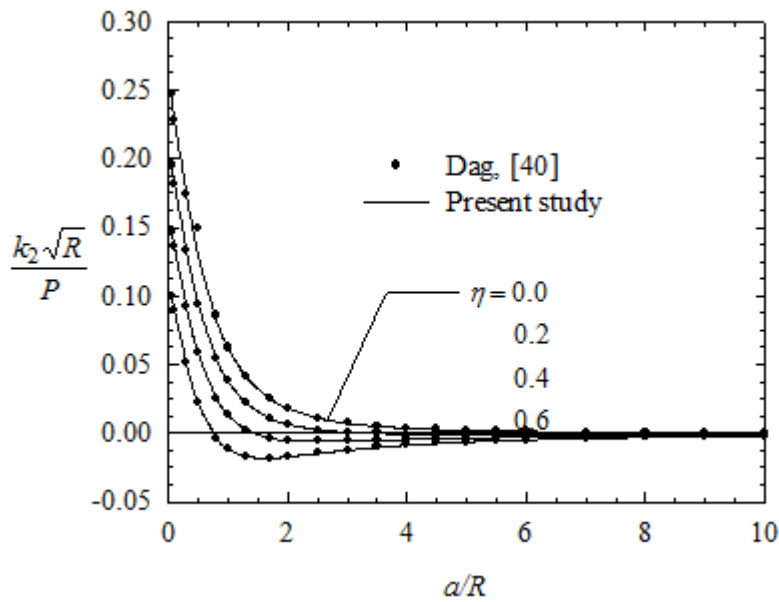


Figure 3.45: Mode II stress intensity factors for an edge crack in an isotropic half-plane loaded by a circular stamp as shown in Figure 2.9, $(b-a)/R=1.0$, $d/R=1.0$, $\nu=0.25$, $d_{11}=2.9996$, $d_{12}=1.0008$, $d_{22}=3.0052$.

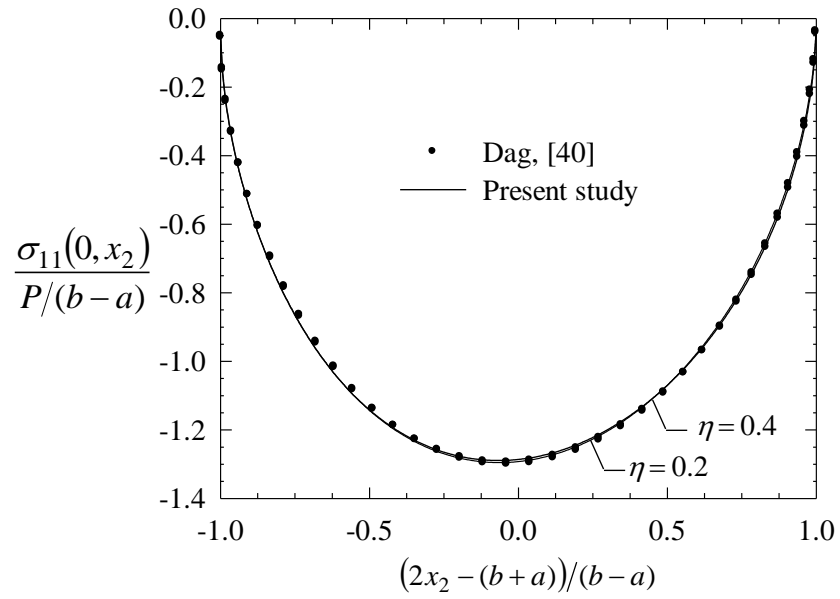


Figure 3.46: Contact stress distribution for an isotropic half-plane with an edge crack and loaded by a circular stamp as shown in Figure 2.9, $a/R=0.1$, $b/R=1.1$, $d/R=1.0$, $\nu=0.25$, $d_{11}=2.9996$, $d_{12}=1.0008$, $d_{22}=3.0052$.

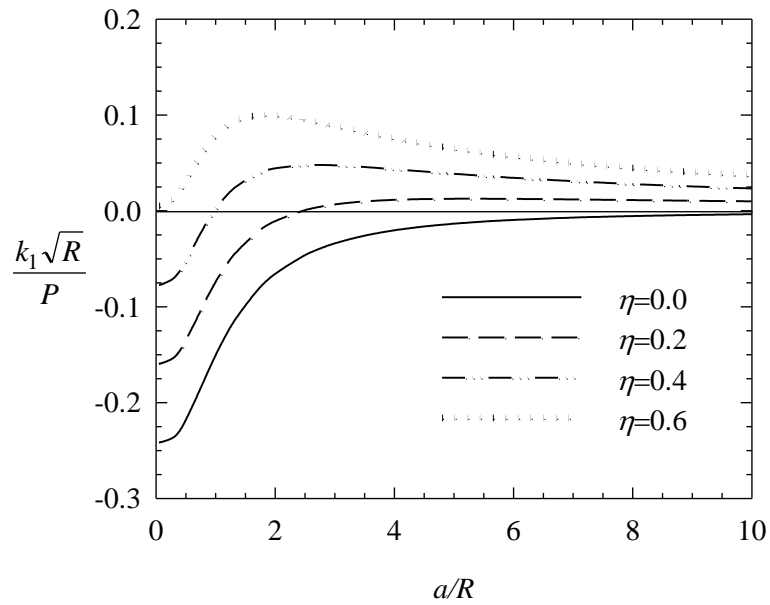


Figure 3.47: Mode I stress intensity factors for an edge crack in an orthotropic half-plane loaded by a circular stamp as shown in Figure 2.9, $(b-a)/R=0.1$, $d/R=1.0$.

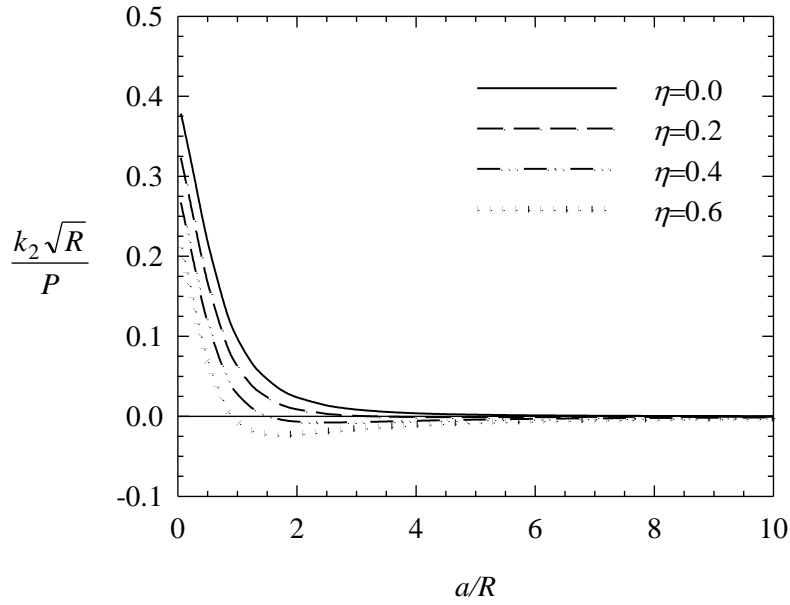


Figure 3.48: Mode II stress intensity factors for an edge crack in an orthotropic half-plane loaded by a circular stamp as shown in Figure 2.9, $(b - a)/R=0.1$, $d/R=1.0$.

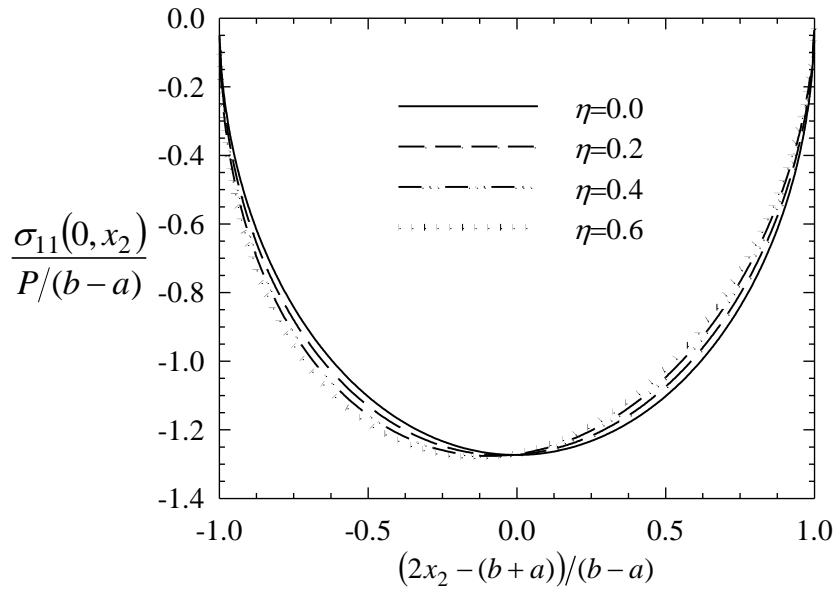


Figure 3.49: Contact stress distributions for an orthotropic half-plane with an edge crack and loaded by a circular stamp as shown in Figure 2.9, $a/R=0.1$, $b/R=0.2$, $d/R=1.0$.

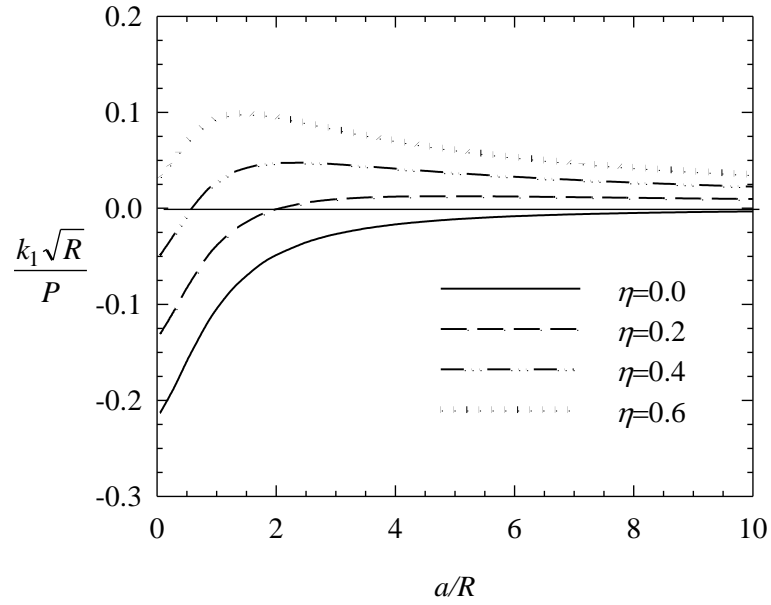


Figure 3.50: Mode I stress intensity factors for an edge crack in an orthotropic half-plane loaded by a circular stamp as shown in Figure 2.9, $(b-a)/R=1.0$, $d/R=1.0$.

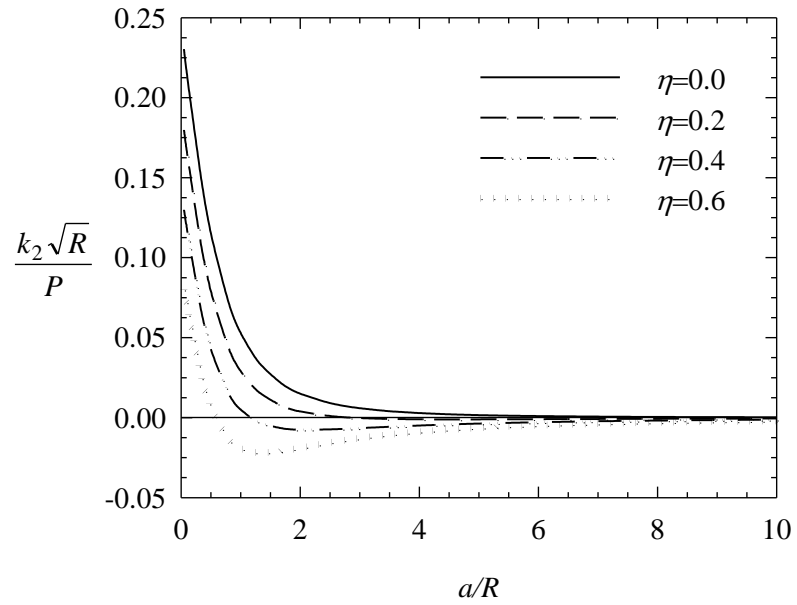


Figure 3.51: Mode II stress intensity factors for an edge crack in an orthotropic half-plane loaded by a circular stamp as shown in Figure 2.9, $(b-a)/R=1.0$, $d/R=1.0$.

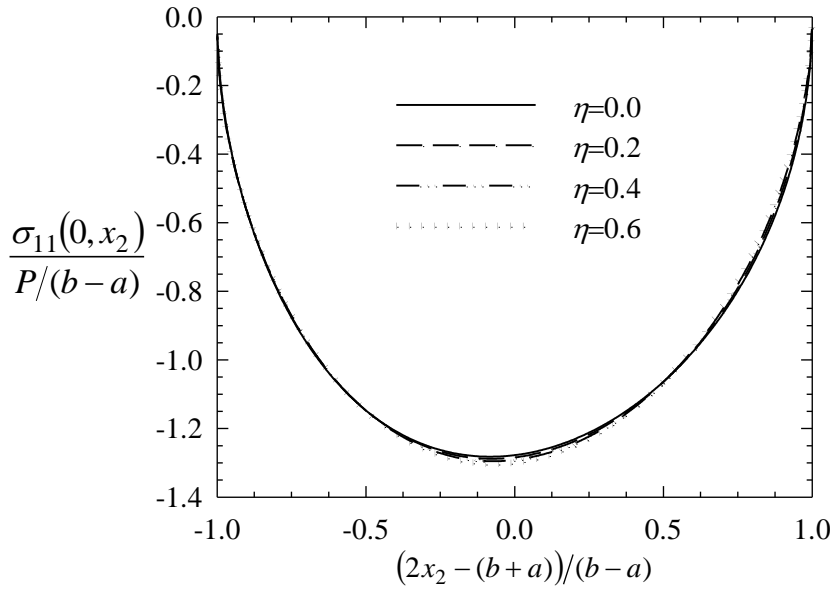


Figure 3.52: Contact stress distributions for an orthotropic half-plane with an edge crack and loaded by a circular stamp as shown in Figure 2.9, $a/R=0.1$, $b/R=1.1$, $d/R=1.0$.

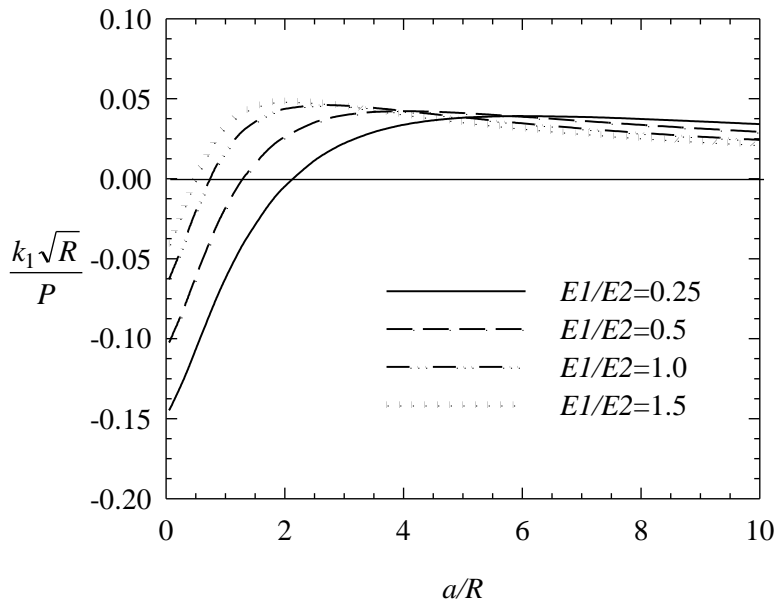


Figure 3.53: Effect of the elastic modulus ratio E_1/E_2 on mode I stress intensity factors for an edge crack in an orthotropic half-plane loaded by a circular stamp as shown in Figure 2.9, $(b-a)/R=1.0$, $d/R=1.0$, $\eta=0.4$.

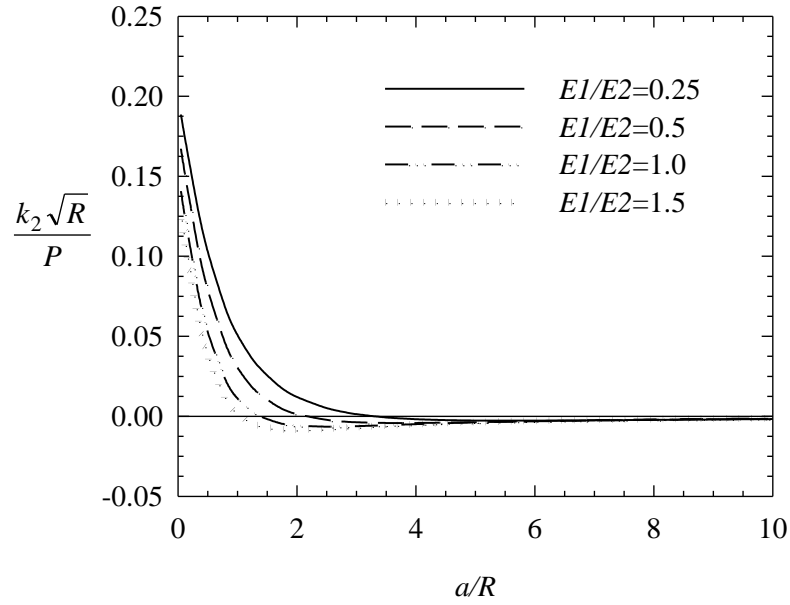


Figure 3.54: Effect of the elastic modulus ratio E_1/E_2 on mode II stress intensity factors for an edge crack in an orthotropic half-plane loaded by a circular stamp as shown in Figure 2.9, $(b-a)/R=1.0$, $d/R=1.0$, $\eta=0.4$.

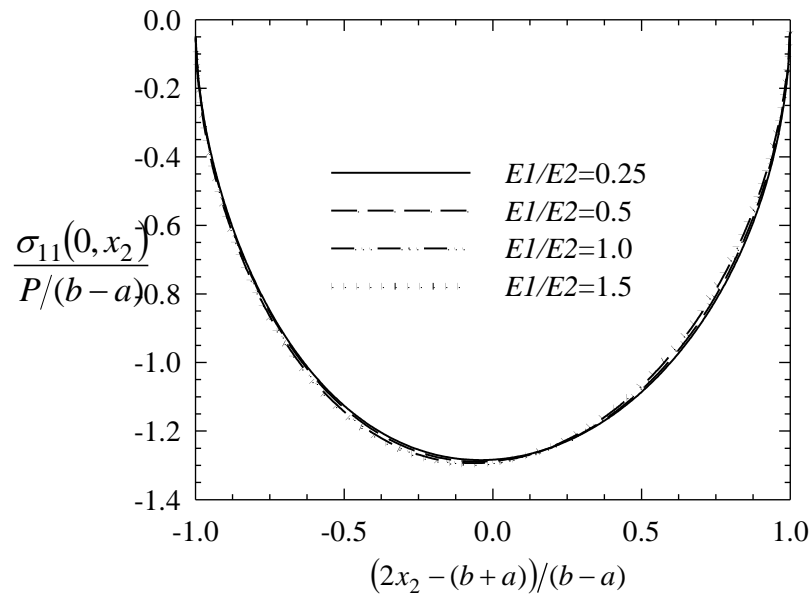


Figure 3.55: Effect of the elastic modulus ratio E_1/E_2 on the contact stress distribution for an edge crack in an orthotropic half-plane loaded by a circular stamp as shown in Figure 2.9, $a/R=0.1$, $b/R=1.1$, $d/R=1.0$, $\eta=0.4$.

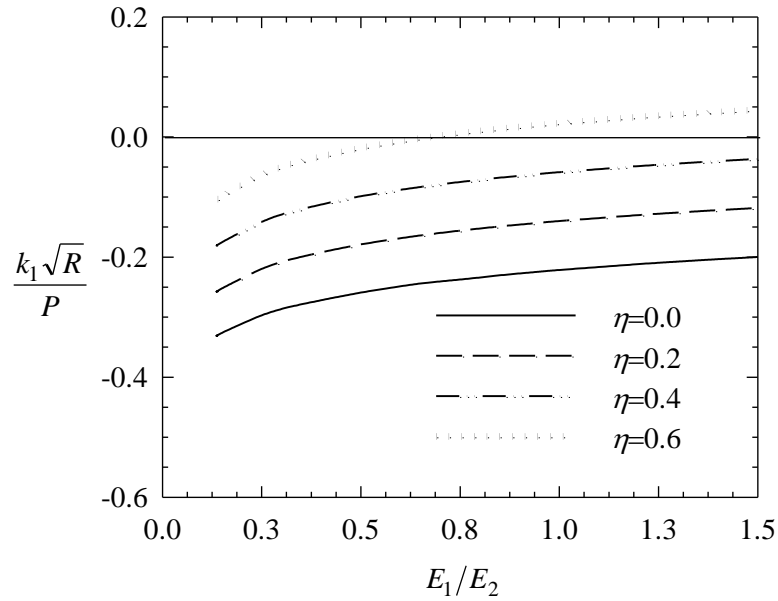


Figure 3.56: Normalized k_1 versus E_1/E_2 and η for an edge crack in an orthotropic half-plane loaded by a circular stamp as shown in Figure 2.9, $(b-a)/R=1.0$, $d/R=1.0$, $a/R=0.1$.

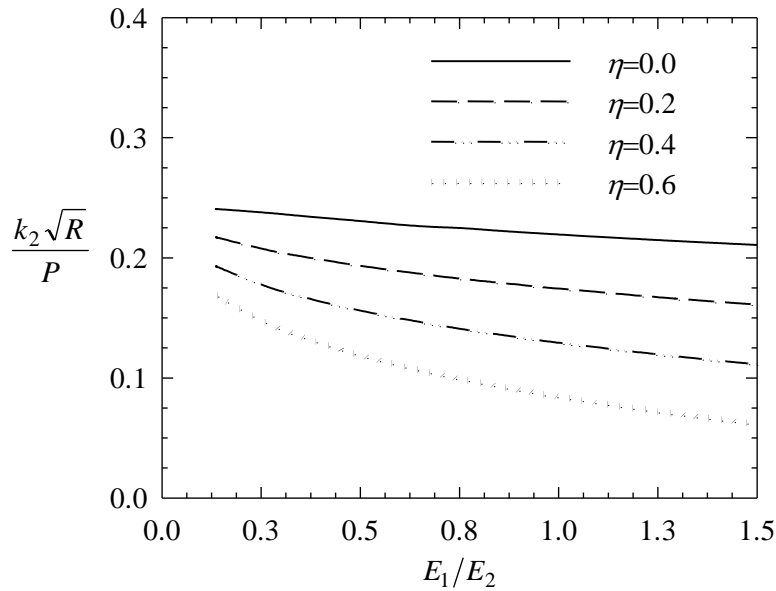


Figure 3.57: Normalized k_2 versus E_1/E_2 and η for an edge crack in an orthotropic half-plane loaded by a circular stamp as shown in Figure 2.9, $(b-a)/R=1.0$, $d/R=1.0$, $a/R=0.1$.

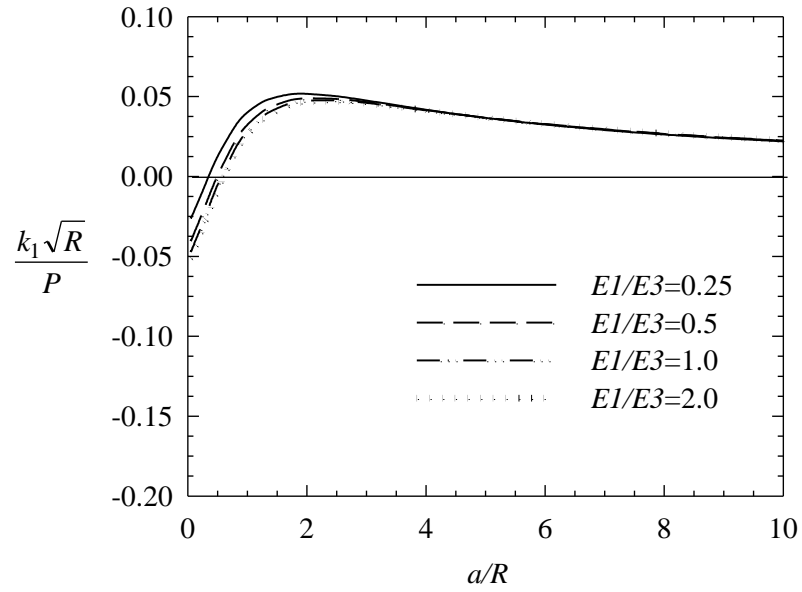


Figure 3.58: Effect of the elastic modulus ratio E_1/E_3 on mode I stress intensity factors for an edge crack in an orthotropic half-plane loaded by a circular stamp as shown in Figure 2.9, $(b-a)/R=1.0$, $d/R=1.0$, $\eta=0.4$.

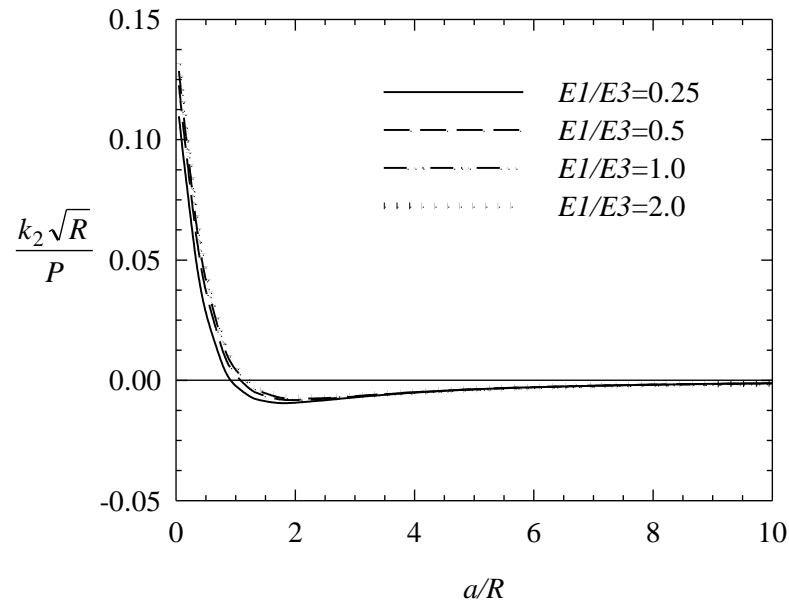


Figure 3.59: Effect of the elastic modulus ratio E_1/E_3 on mode II stress intensity factors for an edge crack in an orthotropic half-plane loaded by a circular stamp as shown in Figure 2.9, $(b-a)/R=1.0$, $d/R=1.0$, $\eta=0.4$.

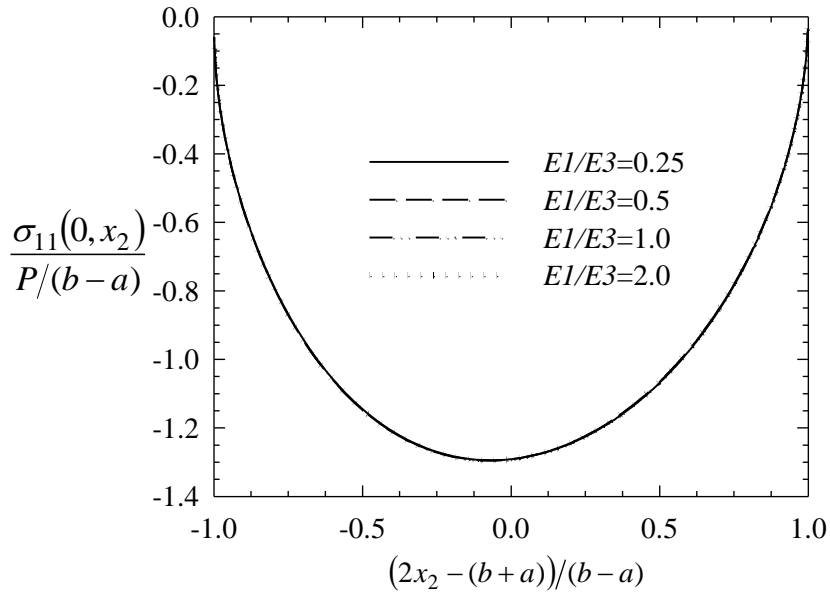


Figure 3.60: Effect of elastic modulus ratio E_1/E_3 on the contact stress distribution for an edge crack in an orthotropic half-plane loaded by a circular stamp as shown in Figure 2.9, $a/R=0.1$, $b/R=1.1$, $d/R=1.0$, $\eta=0.4$.

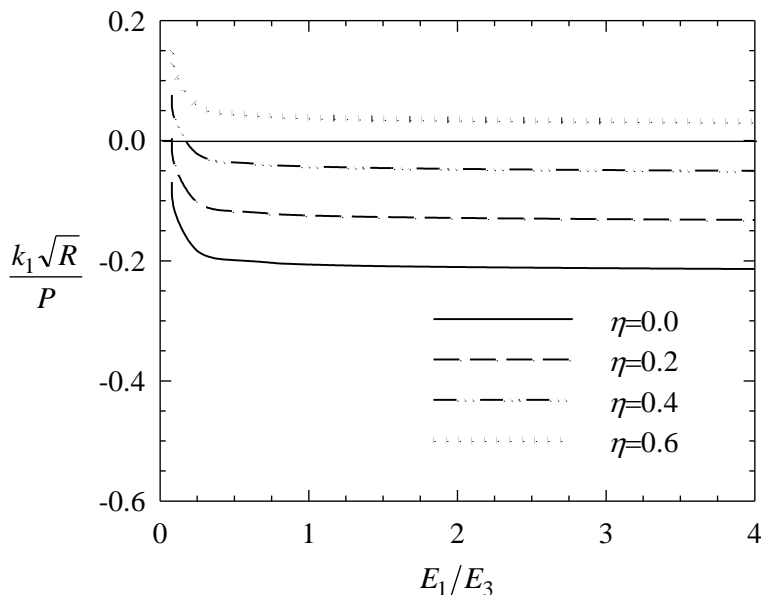


Figure 3.61: Normalized k_1 versus E_1/E_3 and η for an edge crack in an orthotropic half-plane loaded by a circular stamp as shown in Figure 2.9, $(b-a)/R=1.0$, $d/R=1.0$, $a/R=0.1$.

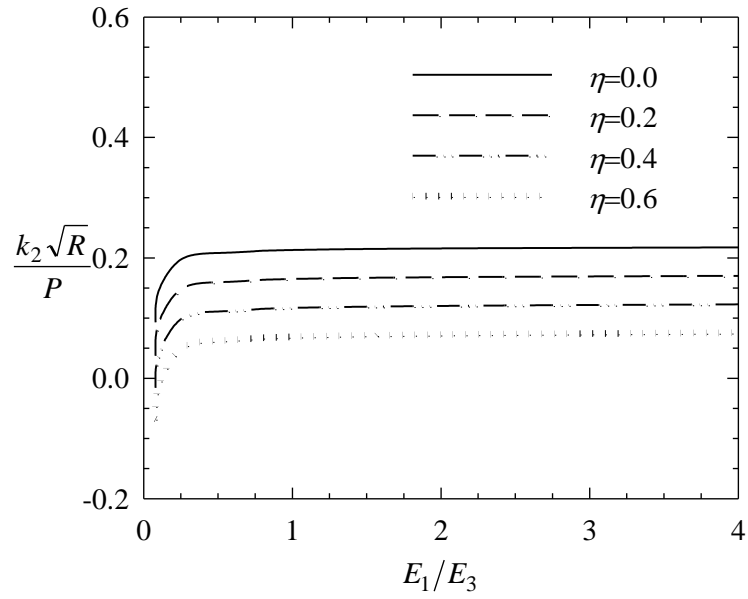


Figure 3.62: Normalized k_2 versus E_1/E_3 and η for an edge crack in an orthotropic half-plane loaded by a circular stamp as shown in Figure 2.9, $(b-a)/R=1.0$, $d/R=1.0$, $a/R=0.1$.

3.5 Tables

Table 3.2: Normalized force values computed for various values of a/d and coefficient of friction η for an isotropic half-plane loaded by a triangular stamp as shown in Figure 2.8, $(b-a)/d=1.0, \nu=0.25, d_{11}=2.9996, d_{12}=1.0008, d_{22}=3.0052$.

a/d	$P/\mu_{12}md$							
	Present Study				Dag, [40]			
	$\eta=0.0$	$\eta=0.2$	$\eta=0.4$	$\eta=0.6$	$\eta=0.0$	$\eta=0.2$	$\eta=0.4$	$\eta=0.6$
0.05	1.4859	1.6329	1.8005	1.9917	1.3367	1.5219	1.7585	2.0212
0.1	1.5644	1.7124	1.8795	2.0683	1.4152	1.6072	1.8515	2.1733
0.3	1.804	1.9424	2.0923	2.2544	1.6791	1.8706	2.1009	2.2640
0.5	1.9445	2.0659	2.1928	2.3246	1.8512	2.0226	2.2083	2.3320
0.8	2.0414	2.1429	2.2454	2.3480	1.9865	2.1266	2.2577	2.3558
1.0	2.0683	2.1623	2.2558	2.3482	2.0302	2.1552	2.2669	2.3560
1.3	2.0859	2.1740	2.2608	2.3455	2.0632	2.1738	2.2776	2.3555
1.7	2.0935	2.1786	2.2623	2.3436	2.0812	2.1816	2.2732	2.3540
2.0	2.0952	2.1798	2.2628	2.3435	2.0869	2.1833	2.2701	2.3530
2.5	2.0958	2.1805	2.2638	2.3447	2.0912	2.1840	2.2766	2.3525
3.0	2.0957	2.1809	2.2647	2.3464	2.0928	2.1839	2.2746	2.3520
3.5	2.0955	2.1812	2.2656	2.3480	2.0936	2.1838	2.2734	2.3517
4.0	2.0953	2.1814	2.2664	2.3494	2.0939	2.1836	2.2726	2.3503
4.5	2.0951	2.1817	2.2670	2.3505	2.0941	2.1835	2.2722	2.3595
5.0	2.0950	2.1818	2.2676	2.3515	2.0942	2.1834	2.2719	2.3589
5.5	2.0949	2.1820	2.2680	2.3523	2.0943	2.1834	2.2717	2.3585
6.0	2.0948	2.1821	2.2684	2.3529	2.0943	2.1833	2.2715	2.3583
7.0	2.0947	2.1824	2.2690	2.3539	2.0944	2.1833	2.2714	2.3580
8.0	2.0947	2.1825	2.2694	2.3547	2.0944	2.1832	2.2713	2.3578
9.0	2.0946	2.1826	2.2697	2.3552	2.0944	2.1832	2.2712	2.3578
10.0	2.0946	2.1827	2.2700	2.3556	2.0944	2.1832	2.2712	2.3577

Table 3.3: Normalized force values computed for various values of a/d and coefficient of friction η for an orthotropic half-plane loaded by a triangular stamp as shown in Figure 2.8, $(b-a)/d=0.1$.

a/d	$P/\mu_{12}md$			
	$\eta=0.0$	$\eta=0.2$	$\eta=0.4$	$\eta=0.6$
0.05	0.1549	0.1738	0.1970	0.2261
0.1	0.1783	0.1965	0.2177	0.2429
0.3	0.2120	0.2267	0.2426	0.2596
0.5	0.2223	0.2353	0.2487	0.2625
0.8	0.2276	0.2392	0.2510	0.2627
1.0	0.2288	0.2401	0.2513	0.2624
1.3	0.2295	0.2405	0.2514	0.2621
1.7	0.2298	0.2406	0.2514	0.2619
2.0	0.2298	0.2406	0.2513	0.2618
2.5	0.2299	0.2407	0.2513	0.2618
3.0	0.2299	0.2407	0.2513	0.2618
3.5	0.2299	0.2407	0.2514	0.2618
4.0	0.2299	0.2407	0.2514	0.2618
4.5	0.2299	0.2407	0.2514	0.2618
5.0	0.2299	0.2407	0.2514	0.2619
5.5	0.2299	0.2407	0.2514	0.2619
6.0	0.2299	0.2407	0.2514	0.2619
7.0	0.2299	0.2407	0.2514	0.2619
8.0	0.2299	0.2407	0.2514	0.2619
9.0	0.2299	0.2407	0.2514	0.2619
10.0	0.2299	0.2407	0.2514	0.2619

Table 3.4: Normalized force values computed for various values of a/d and coefficient of friction η for an orthotropic half-plane loaded by a triangular stamp as shown in Figure 2.8, $(b-a)/d=1.0$.

a/d	P/μ_1md			
	$\eta=0.0$	$\eta=0.2$	$\eta=0.4$	$\eta=0.6$
0.05	1.6820	1.8564	2.0536	2.2758
0.1	1.7685	1.9430	2.1384	2.3563
0.3	2.0245	2.1847	2.3563	2.5390
0.5	2.1651	2.3047	2.4488	2.5962
0.8	2.2550	2.3732	2.4912	2.6077
1.0	2.2784	2.3891	2.4984	2.6049
1.3	2.2930	2.3983	2.5014	2.6011
1.7	2.2988	2.4018	2.5025	2.5997
2.0	2.2999	2.4028	2.5033	2.6004
2.5	2.3001	2.4035	2.5047	2.6027
3.0	2.2999	2.4040	2.5062	2.6052
3.5	2.2996	2.4044	2.5074	2.6074
4.0	2.2993	2.4048	2.5084	2.6093
4.5	2.2991	2.4051	2.5093	2.6108
5.0	2.2990	2.4053	2.5100	2.6120
5.5	2.2989	2.4055	2.5106	2.6130
6.0	2.2988	2.4057	2.5110	2.6138
7.0	2.2987	2.4060	2.5118	2.6150
8.0	2.2987	2.4062	2.5123	2.6159
9.0	2.2986	2.4063	2.5127	2.6166
10.0	2.2986	2.4064	2.5129	2.6171

Table 3.5: Normalized force values computed for various values of a/d and E_1/E_2 for an orthotropic half-plane loaded by a triangular stamp as shown in Figure 2.8, $(b-a)/d=1.0$, $\eta=0.4$.

a/d	$P/\mu_{12}md$			
	$E_1/E_2 = 0.25$	$E_1/E_2 = 0.5$	$E_1/E_2 = 1.0$	$E_1/E_2 = 1.5$
0.05	2.1205	2.0905	2.0640	2.0466
0.1	2.2190	2.1863	2.1523	2.1290
0.3	2.4820	2.4366	2.3812	2.3395
0.5	2.6146	2.5579	2.4829	2.4259
0.8	2.7007	2.6295	2.5337	2.4632
1.0	2.7253	2.6472	2.5434	2.4691
1.3	2.7426	2.6577	2.5478	2.4716
1.7	2.7509	2.6613	2.5489	2.4730
2.0	2.7531	2.6619	2.5493	2.4741
2.5	2.7541	2.6619	2.5501	2.4760
3.0	2.7541	2.6619	2.5511	2.4777
3.5	2.7539	2.6620	2.5520	2.4792
4.0	2.7538	2.6622	2.5527	2.4803
4.5	2.7536	2.6624	2.5534	2.4813
5.0	2.7535	2.6626	2.5540	2.4821
5.5	2.7535	2.6628	2.5545	2.4827
6.0	2.7535	2.6630	2.5549	2.4832
7.0	2.7535	2.6633	2.5555	2.4840
8.0	2.7535	2.6636	2.5560	2.4845
9.0	2.7536	2.6638	2.5563	2.4849
10.0	2.7536	2.6639	2.5566	2.4852

Table 3.6: Normalized force values computed for various values of E_1/E_2 and coefficient of friction η for an orthotropic half-plane loaded by a triangular stamp as shown in Figure 2.8, $(b-a)/d=1.0$, $a/d=0.1$.

E_1/E_2	$P/\mu_{12}md$			
	$\eta=0.0$	$\eta=0.2$	$\eta=0.4$	$\eta=0.6$
0.14	2.0784	2.1596	2.2482	2.3451
0.15	2.0681	2.1524	2.2444	2.3455
0.25	1.9942	2.1008	2.2190	2.3509
0.35	1.9465	2.0676	2.2030	2.3554
0.50	1.8966	2.0329	2.1863	2.3599
0.65	1.8604	2.0078	2.1739	2.3622
0.75	1.8409	1.9941	2.1669	2.3627
0.85	1.8239	1.9823	2.1607	2.3626
0.95	1.8089	1.9717	2.1550	2.3619
1.00	1.8021	1.9669	2.1523	2.3614
1.20	1.7778	1.9496	2.1424	2.3582
1.29	1.7685	1.9430	2.1384	2.3563
1.30	1.7672	1.9421	2.1377	2.3560
1.35	1.7622	1.9385	2.1355	2.3548
1.40	1.7574	1.9350	2.1333	2.3535
1.45	1.7527	1.9317	2.1311	2.3522
1.50	1.7483	1.9284	2.1290	2.3507

Table 3.7: Normalized force values computed for various values of a/d and E_1/E_3 for an orthotropic half-plane loaded by a triangular stamp as shown in Figure 2.8, $(b-a)/d=1.0$, $\eta=0.4$.

a/d	$P/\mu_{12}md$			
	$E_1/E_3 = 0.25$	$E_1/E_3 = 0.5$	$E_1/E_3 = 1.0$	$E_1/E_3 = 2.0$
0.05	2.5235	2.2066	2.0795	2.0225
0.1	2.6205	2.2954	2.1649	2.1065
0.3	2.8523	2.5186	2.3838	2.3237
0.5	2.9368	2.6086	2.4758	2.4169
0.8	2.9685	2.6473	2.5175	2.4604
1.0	2.9722	2.6532	2.5244	2.4679
1.3	2.9731	2.6555	2.5273	2.4710
1.7	2.9736	2.6564	2.5284	2.4722
2.0	2.9744	2.6572	2.5291	2.4730
2.5	2.9761	2.6587	2.5306	2.4744
3.0	2.9778	2.6603	2.5321	2.4758
3.5	2.9792	2.6616	2.5333	2.4770
4.0	2.9804	2.6627	2.5344	2.4780
4.5	2.9814	2.6636	2.5352	2.4788
5.0	2.9822	2.6643	2.5359	2.4795
5.5	2.9829	2.6649	2.5365	2.4801
6.0	2.9834	2.6654	2.5370	2.4806
7.0	2.9842	2.6662	2.5377	2.4813
8.0	2.9848	2.6667	2.5382	2.4818
9.0	2.9852	2.6671	2.5386	2.4821
10.0	2.9856	2.6674	2.5389	2.4824

Table 3.8: Normalized force values computed for various values of E_1/E_3 and coefficient of friction η for an orthotropic half-plane loaded by a triangular stamp as shown in Figure 2.8, $(b-a)/d=1.0$, $a/d=0.1$.

E_1/E_3	$P/\mu_{12}md$			
	$\eta=0.0$	$\eta=0.2$	$\eta=0.4$	$\eta=0.6$
0.08	8.3525	8.9530	9.6690	10.5384
0.10	4.1605	4.5439	4.9803	5.4794
0.25	2.1666	2.3807	2.6205	2.8885
0.50	1.8974	2.0852	2.2954	2.5300
0.80	1.8154	1.9950	2.1959	2.4201
1.00	1.7901	1.9670	2.1649	2.3858
1.29	1.7685	1.9430	2.1384	2.3563
1.50	1.7581	1.9314	2.1254	2.3419
1.80	1.7480	1.9201	2.1127	2.3277
2.00	1.7431	1.9145	2.1065	2.3208
2.20	1.7392	1.9101	2.1014	2.3151
2.40	1.7360	1.9065	2.0973	2.3104
2.80	1.7312	1.9009	2.0909	2.3031
3.00	1.7294	1.8988	2.0884	2.3003
3.20	1.7279	1.8969	2.0862	2.2978
3.40	1.7266	1.8953	2.0844	2.2956
4.00	1.7238	1.8918	2.0800	2.2904

Table 3.9: Normalized force values computed for various values of a/R and coefficient of friction η for an isotropic half-plane loaded by a circular stamp as shown in Figure 2.9, $(b-a)/R=1.0$, $d/R=1.0$, $\nu=0.25$, $d_{11}=2.9996$, $d_{12}=1.0008$, $d_{22}=3.0052$..

a/R	$P/\mu_{12}R$							
	Present Study				Dag, [40]			
	$\eta=0.0$	$\eta=0.2$	$\eta=0.4$	$\eta=0.6$	$\eta=0.0$	$\eta=0.2$	$\eta=0.4$	$\eta=0.6$
0.05	0.6877	0.5946	0.5094	0.4525	0.7164	0.5855	0.5074	0.4487
0.1	0.6424	0.5801	0.5147	0.4648	0.6523	0.5743	0.5127	0.4628
0.3	0.5758	0.5481	0.5164	0.4901	0.5817	0.5478	0.5164	0.4872
0.5	0.5473	0.5343	0.5179	0.5011	0.5436	0.5347	0.5159	0.4968
0.8	0.5322	0.5262	0.5183	0.5097	0.5361	0.5264	0.5163	0.5049
1.0	0.5281	0.5243	0.5188	0.5116	0.5301	0.5243	0.5170	0.5082
1.3	0.5254	0.5232	0.5192	0.5135	0.5264	0.5231	0.5180	0.5113
1.7	0.5242	0.5228	0.5196	0.5146	0.5247	0.5226	0.5188	0.5133
2.0	0.5239	0.5227	0.5197	0.5150	0.5241	0.5226	0.5192	0.5141
2.5	0.5237	0.5227	0.5199	0.5153	0.5238	0.5226	0.5195	0.5148
3.0	0.5237	0.5227	0.5199	0.5154	0.5237	0.5226	0.5197	0.5150
3.5	0.5236	0.5227	0.5199	0.5154	0.5236	0.5226	0.5198	0.5152
4.0	0.5236	0.5227	0.5199	0.5154	0.5236	0.5226	0.5198	0.5152
4.5	0.5236	0.5227	0.5199	0.5154	0.5236	0.5226	0.5198	0.5153
5.0	0.5236	0.5227	0.5199	0.5154	0.5236	0.5227	0.5199	0.5153
5.5	0.5236	0.5227	0.5199	0.5154	0.5236	0.5227	0.5199	0.5153
6.0	0.5236	0.5227	0.5199	0.5154	0.5236	0.5227	0.5199	0.5153
7.0	0.5236	0.5227	0.5199	0.5154	0.5236	0.5227	0.5199	0.5153
8.0	0.5236	0.5227	0.5199	0.5154	0.5236	0.5227	0.5199	0.5153
9.0	0.5236	0.5227	0.5199	0.5154	0.5236	0.5227	0.5199	0.5153
10.0	0.5236	0.5227	0.5199	0.5154	0.5236	0.5227	0.5199	0.5153

Table 3.10: Normalized force values computed for various values of a/R and coefficient of friction η for an orthotropic half-plane loaded by a circular stamp as shown in Figure 2.9, $(b-a)/R=0.1$, $d/R=1.0$.

a/R	$P/\mu_{12}R$			
	$\eta=0.0$	$\eta=0.2$	$\eta=0.4$	$\eta=0.6$
0.05	0.0061	0.0059	0.0056	0.0055
0.1	0.0059	0.0058	0.0057	0.0056
0.3	0.0058	0.0057	0.0057	0.0056
0.5	0.0058	0.0057	0.0057	0.0056
0.8	0.0057	0.0057	0.0057	0.0056
1.0	0.0057	0.0057	0.0057	0.0056
1.3	0.0057	0.0057	0.0057	0.0056
1.7	0.0057	0.0057	0.0057	0.0056
2.0	0.0057	0.0057	0.0057	0.0056
2.5	0.0057	0.0057	0.0057	0.0056
3.0	0.0057	0.0057	0.0057	0.0056
3.5	0.0057	0.0057	0.0057	0.0056
4.0	0.0057	0.0057	0.0057	0.0056
4.5	0.0057	0.0057	0.0057	0.0056
5.0	0.0057	0.0057	0.0057	0.0056
5.5	0.0057	0.0057	0.0057	0.0056
6.0	0.0057	0.0057	0.0057	0.0056
7.0	0.0057	0.0057	0.0057	0.0056
8.0	0.0057	0.0057	0.0057	0.0056
9.0	0.0057	0.0057	0.0057	0.0056
10.0	0.0057	0.0057	0.0057	0.0056

Table 3.11: Normalized force values computed for various values of a/R and coefficient of friction η for an orthotropic half-plane loaded by a circular stamp as shown in Figure 2.9, $(b-a)/R=1.0$, $d/R=1.0$.

a/R	$P/\mu_{12}R$			
	$\eta=0.0$	$\eta=0.2$	$\eta=0.4$	$\eta=0.6$
0.05	0.7544	0.6455	0.5667	0.5062
0.1	0.7034	0.6307	0.5711	0.5213
0.3	0.6279	0.5970	0.5691	0.5419
0.5	0.5977	0.5832	0.5671	0.5499
0.8	0.5825	0.5760	0.5673	0.5566
1.0	0.5786	0.5745	0.5679	0.5592
1.3	0.5762	0.5736	0.5687	0.5614
1.7	0.5751	0.5734	0.5692	0.5627
2.0	0.5749	0.5734	0.5694	0.5631
2.5	0.5747	0.5734	0.5695	0.5634
3.0	0.5746	0.5734	0.5696	0.5635
3.5	0.5746	0.5734	0.5696	0.5635
4.0	0.5746	0.5734	0.5696	0.5635
4.5	0.5746	0.5734	0.5696	0.5635
5.0	0.5746	0.5734	0.5696	0.5635
5.5	0.5746	0.5734	0.5696	0.5635
6.0	0.5746	0.5734	0.5696	0.5635
7.0	0.5746	0.5734	0.5696	0.5635
8.0	0.5746	0.5734	0.5696	0.5634
9.0	0.5746	0.5734	0.5696	0.5634
10.0	0.5746	0.5734	0.5696	0.5634

Table 3.12: Normalized force values computed for various values of a/R and E_1/E_2 for an orthotropic half-plane loaded by a circular stamp as shown in Figure 2.9, $(b-a)/R=1.0$, $d/R=1.0$, $\eta=0.4$.

a/R	$P/\mu_{12}R$			
	$E_1/E_2 = 0.25$	$E_1/E_2 = 0.5$	$E_1/E_2 = 1.0$	$E_1/E_2 = 1.5$
0.05	0.7284	0.6623	0.5928	0.5506
0.1	0.7212	0.6611	0.5960	0.5557
0.3	0.6955	0.6465	0.5909	0.5555
0.5	0.6835	0.6387	0.5873	0.5545
0.8	0.6769	0.6349	0.5864	0.5554
1.0	0.6754	0.6342	0.5866	0.5562
1.3	0.6745	0.6340	0.5872	0.5570
1.7	0.6742	0.6342	0.5876	0.5576
2.0	0.6742	0.6343	0.5878	0.5578
2.5	0.6742	0.6344	0.5880	0.5579
3.0	0.6743	0.6345	0.5881	0.5580
3.5	0.6743	0.6345	0.5881	0.5580
4.0	0.6744	0.6345	0.5881	0.5580
4.5	0.6744	0.6346	0.5881	0.5580
5.0	0.6744	0.6346	0.5881	0.5580
5.5	0.6744	0.6346	0.5881	0.5579
6.0	0.6744	0.6346	0.5881	0.5579
7.0	0.6744	0.6346	0.5881	0.5579
8.0	0.6744	0.6346	0.5881	0.5579
9.0	0.6744	0.6346	0.5881	0.5579
10.0	0.6744	0.6346	0.5881	0.5579

Table 3.13: Normalized force values computed for various values of E_1/E_2 and coefficient of friction η for an orthotropic half-plane loaded by a circular stamp as shown in Figure 2.9, $(b-a)/R=1.0$, $d/R=1.0$, $a/R=0.1$.

E_1/E_2	$P/\mu_{12}R$			
	$\eta=0.0$	$\eta=0.2$	$\eta=0.4$	$\eta=0.6$
0.14	0.8620	0.8130	0.7681	0.7286
0.15	0.8579	0.8080	0.7626	0.7227
0.25	0.8277	0.7702	0.7212	0.6788
0.35	0.8054	0.7439	0.6926	0.6487
0.50	0.7790	0.7147	0.6611	0.6156
0.65	0.7564	0.6923	0.6370	0.5903
0.75	0.7492	0.6798	0.6236	0.5762
0.85	0.7383	0.6686	0.6117	0.5637
0.95	0.7290	0.6586	0.6009	0.5525
1.00	0.7247	0.6540	0.5960	0.5473
1.20	0.7094	0.6372	0.5780	0.5285
1.29	0.7034	0.6307	0.5711	0.5213
1.30	0.7026	0.6297	0.5701	0.5202
1.35	0.6993	0.6262	0.5663	0.5163
1.40	0.6962	0.6227	0.5626	0.5125
1.45	0.6932	0.6194	0.5591	0.5088
1.50	0.6903	0.6162	0.5557	0.5052

Table 3.14: Normalized force values computed for various values of a/d and E_1/E_3 for an orthotropic half-plane loaded by a circular stamp as shown in Figure 2.9, $(b-a)/R=1.0$, $d/R=1.0$, $\eta=0.4$.

a/R	$P/\mu_{12}R$			
	$E_1/E_3 = 0.25$	$E_1/E_3 = 0.5$	$E_1/E_3 = 1.0$	$E_1/E_3 = 2.0$
0.05	0.6612	0.5973	0.5717	0.5612
0.1	0.6689	0.6028	0.5763	0.5653
0.3	0.6717	0.6023	0.5746	0.5630
0.5	0.6723	0.6011	0.5727	0.5608
0.8	0.6746	0.6020	0.5730	0.5608
1.0	0.6758	0.6028	0.5737	0.5613
1.3	0.6770	0.6037	0.5745	0.5620
1.7	0.6777	0.6043	0.5750	0.5626
2.0	0.6780	0.6045	0.5752	0.5627
2.5	0.6782	0.6047	0.5754	0.5629
3.0	0.6782	0.6047	0.5754	0.5629
3.5	0.6782	0.6047	0.5754	0.5630
4.0	0.6782	0.6047	0.5754	0.5630
4.5	0.6782	0.6047	0.5754	0.5629
5.0	0.6782	0.6047	0.5754	0.5629
5.5	0.6782	0.6047	0.5754	0.5629
6.0	0.6782	0.6047	0.5754	0.5629
7.0	0.6782	0.6047	0.5754	0.5629
8.0	0.6782	0.6047	0.5754	0.5629
9.0	0.6782	0.6047	0.5754	0.5629
10.0	0.6782	0.6047	0.5754	0.5629

Table 3.15: Normalized force values computed for various values of E_1/E_3 and coefficient of friction η for an orthotropic half-plane loaded by a circular stamp as shown in Figure 2.9, $(b-a)/R=1.0$, $d/R=1.0$, $a/R=0.1$.

E_1/E_3	$P/\mu_{12}R$			
	$\eta=0.0$	$\eta=0.2$	$\eta=0.4$	$\eta=0.6$
0.08	2.5499	2.2406	2.0143	1.8388
0.10	1.4273	1.2546	1.1254	1.0239
0.25	0.8321	0.7416	0.6689	0.6092
0.50	0.7454	0.6667	0.6028	0.5497
0.80	0.7187	0.6437	0.5825	0.5315
1.00	0.7104	0.6366	0.5763	0.5259
1.29	0.7034	0.6307	0.5711	0.5213
1.50	0.7001	0.6279	0.5686	0.5191
1.80	0.6969	0.6252	0.5664	0.5172
2.00	0.6954	0.6240	0.5653	0.5163
2.20	0.6942	0.6230	0.5645	0.5156
2.40	0.6933	0.6222	0.5639	0.5151
2.80	0.6920	0.6212	0.5631	0.5144
3.00	0.6915	0.6208	0.5628	0.5142
3.20	0.6911	0.6206	0.5626	0.5141
3.40	0.6908	0.6204	0.5625	0.5140
4.00	0.6902	0.6201	0.5624	0.5141

CHAPTER 4

CONCLUSIONS AND FUTURE WORK

4.1 Conclusions

In this study, a method is developed to examine the problem of surface cracking in orthotropic materials due to sliding contact by a rigid stamp. Calculated results consist of the effect of the friction coefficient η , stamp location, crack length and material properties on the stress intensity factors at the crack tip and contact stresses.

In Chapter 2, the basic method to solve coupled crack and contact problem is developed for different stamp profiles. The coupled crack/contact problem is formulated by using the equations of elasticity and reduced to a system of singular integral equations. The solution procedure of the problem can be visualized in Figure 2.2. In Section 2.2.1, the contact problem for an orthotropic medium under a rigid stamp is examined first by reducing the governing equations to a system of ordinary differential equations by using Fourier transformation. In Section 2.2.2, it is observed that, in the orthotropic half-plane problem having a symmetry with respect to $x_2 = 0$ (see Figure 2.4) in geometry and material property distribution, the mode I (or the opening mode) and mode II (or the sliding mode) problems are uncoupled. Thus, the mode I and mode II problems are formulated separately. The stress and displacement fields are obtained in terms of the unknown functions in Section 2.2.3. In order to determine the singular behavior of the unknown functions, the singular terms in the kernels of the integral equations are extracted by performing asymptotic

analyses for a stamp sliding on the surface ($a > 0$). It can be concluded that in the coupled crack/contact problems for an orthotropic medium stress singularities ω and β (see equations (2.203) and (2.204)) depend on the friction coefficient η (through e_{10} given in Appendix A by equation (A.11e)) and the Poisson's ratio (through e_{10} and e_{20} given in Appendix A by equations equation (A.11e-f)). In order to solve the integral equations, methods are developed for stamps of flat, triangular and circular profiles. Jacobi polynomials are used to reduce the singular integral equations to systems of linear algebraic equations. The unknown functions f_1 , f_2 and f_3 are expanded into series of Jacobi polynomials. Then, the unknown constants of expansions are determined by using the collocation method.

Numerical results of the problem are presented in Chapter 3. The results are given for stamps of flat, triangular and circular profiles. For the large values of crack-to-stamp distance, it is seen that the effect of the surface crack on the contact stress distribution is negligible. Also, contact stress distributions are verified by making comparisons to the results given in the literature [46] for large values of a/d (see Figure 3.2, Figure 3.3, Figure 3.4 and Figure 3.5).

The accuracy of the results is tested by comparing the results obtained for homogeneous isotropic materials for all stamp profiles with those of given by Dag [40]. In this study, elastic modulus ratios are taken as $E_1/E_2 = 0.998$ and $E_1/E_3 = 1.002$ for isotropic materials. The reason is that, when these ratios are taken as exactly 1, there could be differences between compared results, due to the numerical errors. By using the values of 0.998 and 1.002 instead of 1 for E_1/E_2 and E_1/E_3 , respectively, better convergences are obtained and the results are found to be in very good agreement with those of Dag [40] (see Figure 3.6, Figure 3.7, Figure 3.8, Figure 3.25, Figure 3.26, Table 3.2, Figure 3.27, Figure 3.44, Figure 3.45, Table 3.9 and Figure 3.46). Thus, developed solution methods for stamps of flat, triangular and circular profiles sliding on the surface of the half-plane are validated.

In order to obtain the results for orthotropic materials, the material alumina (Al_2O_3) is employed in the numerical calculations. Plasma sprayed alumina coatings are known to possess an orthotropic structure. The material constants are given in Table 3.1. The basic trends obtained for flat, triangular and circular stamps can be summarized as follows:

When no tangential force is transferred by the contact (i.e., coefficient of friction $\eta = 0$),

- Mode I stress intensity factors are negative regardless of the location of the stamp (see Figure 3.9, Figure 3.12, Figure 3.28, Figure 3.31, Figure 3.47 and Figure 3.50). This would lead to crack closure.
- Mode II stress intensity factors are positive regardless of the location of the stamp (see Figure 3.10, Figure 3.13, Figure 3.29, Figure 3.32, Figure 3.48 and Figure 3.51) which means, the crack bends backwards and it extends in a direction opposite to the applied frictional force (see Figure 3.1).
- For flat stamp, singularities are equal at both ends of the contact area but due to the effect of the surface crack, the stress distribution is not exactly symmetric (see Figure 3.11 and Figure 3.14).

When the tangential force increases,

- Mode I stress intensity factors increase (see Figure 3.9, Figure 3.12, Figure 3.28, Figure 3.31, Figure 3.47 and Figure 3.50). Since, as the coefficient of friction increases, state of the normal stress at the crack tip changes from compression to tension.
- Mode II stress intensity factors decrease (see Figure 3.10, Figure 3.13, Figure 3.29, Figure 3.32, Figure 3.48 and Figure 3.51). Since, as the coefficient of

friction increases, sign of the shear stress at the crack tip changes from positive to negative.

- For flat stamp, singularity at the leading end decreases and there is higher stress intensification at the trailing end (see Figure 3.11 and Figure 3.14).

For $\eta=0.4$ and $\eta=0.6$, the mode I stress intensity factors are positive regardless of the location of the stamp and the crack is open (see Figure 3.9, Figure 3.12, Figure 3.28, Figure 3.31, Figure 3.47 and Figure 3.50).

In Chapter 3, results related to the required contact force for triangular and circular stamps are also given. The triangular and circular stamp problems are defined as incomplete contact mechanics problems where the size of the contact region is a function of the applied force. The required force approaches a constant value for large values of crack-to-stamp distance. Depending on the values of friction coefficient and stamp profile, the contact forces increase or decrease, as the stamp gets closer to the crack.

The effect of elastic modulus ratio E_1/E_2 is also investigated in Chapter 3. It is seen that as E_1/E_2 increases,

- Mode I stress intensity factors get larger (see Figure 3.15, Figure 3.18, Figure 3.34, Figure 3.37, Figure 3.53 and Figure 3.56),
- Mode II stress intensity factors decrease (see Figure 3.16, Figure 3.19, Figure 3.35, Figure 3.38, Figure 3.54 and Figure 3.57).

The effect of the elastic modulus ratio E_1/E_3 is also investigated in Chapter 3. It is found that the effect of E_1/E_3 on modes I and II stress intensity factors and contact stress distributions is not that significant (Figure 3.20-Figure 3.24, Figure 3.39-Figure 3.43 and Figure 3.58-Figure 3.62).

4.2 Future Work

In Section 2.2, we classified the orthotropic materials. This classification is related to the roots of the characteristic equation. If there are four real roots, the material is classified as type I. Otherwise; it is classified as type II. In this study, type I materials are studied. Such an undertaking can also be performed for type II materials.

In order to determine the effect of nonhomogeneity, numerical methods can be developed for a problem involving a nonhomogeneous orthotropic medium such as a graded orthotropic half-plane. In the literature, there are numerous studies regarding the FGMs. In practice, the nature of processing techniques of some FGMs may lead to loss of isotropy. Using the averaged constants of plane orthotropic elasticity, which are first introduced by Krenk [52], the fracture and contact problems can be formulated in coupled form.

In Section 2.2.4, the solution of the singular integral equations is obtained through function-theoretic method as described by Dag [40] and Erdogan [43] by assuming that $a > 0$. By using this method, singularity analysis can also be performed for $a = 0$ case. Also, as an alternative means of verification, the singularity analysis can be carried out by considering another method such as Williams' method [53]. This singularity analysis and verification study can be considered as parts of a future study.

REFERENCES

- [1] Dag, S., and Erdogan, F., 2002, "A surface Crack in a Graded Medium Loaded by a Sliding Rigid Stamp", *Engineering Fracture Mechanics*, Vol. 69, pp. 1729-1751.
- [2] Dag, S. and Erdoğan, F., 2002, "A Surface Crack in a Graded Medium Under General Loading Conditions", *Transactions of the ASME Journal of Applied Mechanics*, Vol. 69, pp. 580-588.
- [3] Delale, F and Erdogan F., 1977, "The Problem of Internal and Edge Cracks in an Orthotropic Strip", *Journal of Applied Mechanics Transactions of the ASME*, Vol. 44, pp. 237-242.
- [4] Guo, L.-C., Wu, L.-Z., Zeng, T. and Ma, L., 2004, "Mode I Crack Problem for a Functionally Graded Orthotropic Strip", *European Journal of Mechanics A/Solids*, Vol. 23, pp. 219-234.
- [5] Ozturk, M. and Erdogan F., 1997, "Mode I Crack Problem in an Inhomogeneous Orthotropic Medium", *International Journal of Engineering Science*, Vol. 35, pp. 869-883.
- [6] Ozturk, M. and Erdogan F., 1998, "The Mixed Mode Crack Problem in an Inhomogeneous Orthotropic Medium" *International Journal of Fracture*, Vol. 98, pp. 243-261.

- [7] Gupta, G.D. Erdogan F., 1974, "The Problem Edge Cracks in an Infinite Strip", *Journal of Applied Mechanics Transactions of the ASME*, Vol. 41, pp. 1001-1006.
- [8] Mahajan, R., Erdogan F. and Chou, Y.T.,1993, "The Crack Problem for an Orthotropic Half-plane Stiffened by Elastic Films", *International Journal of Engineering Science*, Vol.31, pp. 403-424.
- [9] Hasebe, N., Okumura, M. and Nakamura, T., 1989, "Frictional Punch and Crack in Plane Elasticity", *ASCE Journal of Engineering Mechanics*, Vol. 115, pp. 1137-1149.
- [10] Okumura, M., Hasebe, N. and Nakamura, T., 1990, " Crack Due to Wedge Shaped Punch with Friction", *ASCE Journal of Engineering Mechanics*, Vol. 119, pp.2173-2185.
- [11] Hasebe, N. and Quian, J., 1997, "Circular Rigid Punch with One Smooth and Another Sharp Ends on a Half-Plane with Edge Crack", *ASME Journal of Applied Mechanics*, Vol. 64, pp. 73-79.
- [12] Hasebe, N. and Quian, J., 1998, "Edge Crack Due to Rigid Punch in Incomplete Contact", *Mechanics of Materials*, Vol. 28, pp. 271-279.
- [13] De, J. and Patra, B., 1989, "Edge Crack in Orthotropic Elastic Half-Plane", *Journal of Applied Mathematics*, Vol.20, pp. 923-930.
- [14] Konda, N. and Erdogan, F., 1994, "Mixed Mode Crack Problem in a Nonhomogeneous Elastic Medium", *Engineering Fracture Mechanics*, Vol. 47, pp. 533-545.

- [15] Cinar, A. and Erdogan, F., 1982, "The Crack and Wedging Problem for an Orthotropic Strip", *International Journal of Fracture*, Vol. 23, pp. 83-102.
- [16] Loboda, V.V., 1996, "The Problem of Orthotropic Semi-Infinite Strip with a Crack Along the Fixed End", *Engineering Fracture Mechanics*, Vol. 55, pp. 7-17
- [17] Kim, J.-H. and Paulino, G.H., 2003, "The Interaction Integral for Fracture of Orthotropic Functionally Graded Materials : Evaluation of Stress Intensity Factors", *International Journal of Solids and Structures*, Vol 40, pp. 3967-4001.
- [18] Dag, S., Yildirim, B., Erdogan. F., 2004, "Interface Crack Problems in Graded Orthotropic Media: Analytical and Computational Approaches", *International Journal of Fracture*, Vol. 130, pp. 471-496.
- [19] Kim, J.-H. and Paulino, G.H., 2002, "Mixed Mode Fracture of Orthotropic Functionally Graded Materials Using Finite Elements and The Modified Crack Closure Method", *Engineering Fracture Mechanics*, Vol. 69, pp. 1557-1586.
- [20] Guler, M.A., and Erdogan, F., 2004, "Contact Mechanics of Graded Coatings", *International Journal of Solids and Structures*, Vol. 41, pp. 3865-3889.
- [21] Shah, K.R. and Wang, T.F., 1997, "Fracturing at Contact Surfaces Subjected to Normal and Tangential Loads", *International Journal of Rock Mechanics and Mining Sciences* Vol. 34, pp. 727-739.
- [22] Giannakopoulos, A.E. and Pallot, P., 2000, "Two-Dimensional Contact Analysis of Elastic Graded Materials", *Journal of the Mechanics and Physics of Solids*, Vol. 48, pp. 1597-1631.

- [23] Barber, J.R., 1990, "Contact Problems for The Thin Elastic Layer", *International Journal of Mechanical Science*, Vol. 32, pp. 129-132.
- [24] Barber, J.R., and Billings, D.A., 1990, "An Approximate Solution for The Contact Area and Elastic Compliance of a Smooth Punch of Arbitrary Shape", *International Journal of Mechanical Science*, Vol. 32, pp. 991-997.
- [25] Prasad, A., Dao, M., and Suresh, S., 2009, "Steady-State Frictional Sliding Contact on Surfaces of Plastically Graded Materials", *Acta Materialia*, Vol.57, pp. 511-524.
- [26] Ke, L.-L., and Wang, Y.-S., 2007, "Two-Dimensional Sliding Frictional Contact of Functionally Graded Materials", *European Journal of Mechanics*, Vol. 26, pp. 171-188.
- [27] Ke, L.-L., and Wang, Y.-S., 2006, "Two-Dimensional Contact Mechanics of Functionally Graded Materials with Arbitrary Spatial Variations of Material Properties", *International Journal of Solids and Structures*, Vol. 43, pp. 5779-5798.
- [28] Malzbender, J. and de With, G., 2000, "Modeling of the Fracture of a Coating under Sliding Indentation", *Wear*, Vol. 239, pp.21-26.
- [29] Oliveira, S.A.G. and Bower, A.F., 1996, "An Analysis of Fracture and Delamination in Thin Coatings Subjected to Contact Loading", *Wear*, Vol. 198, pp. 15-32.
- [30] Stephen, R.S., 2005, "Contact Deformation and Stress in Orthotropic Plates", *Composites Part A: Applied Science and Manufacturing*, Vol. 36, pp. 1421-1429.

- [31] Stephen, R.S., 2004, "Hertzian Contact of Orthotropic Materials", *International Journal of Solids and Structures*, Vol. 41, pp. 1945-1959.
- [32] Mahajan, P., 1998, "Contact Behavior of an Orthotropic Laminated Beam Indented by a Rigid Cylinder", *Composites Science and Technology*, Vol. 58, pp. 505-513.
- [33] Erbas, B., Yusufoglu, E. and Kaplunov, J., 2011, "A Plane Contact Problem for an Orthotropic Strip", *Journal of Engineering Mathematics*, Vol. 70, pp. 399-409.
- [34] De, J. and Patra, B., 1994, "Dynamic Punch Problems in an Orthotropic Elastic Half-Plane", *Journal of Applied Mathematics*, Vol. 25, pp. 767-776.
- [35] Chen, Y.Z., Lin, X.Y. and Wang, Z.X., 2011, "Singular Integral Equation Method for Contact Problem for Rigidly Connected Punches on Elastic Half-Plane", *Applied Mathematics and Computation*, Vol. 217, pp. 5680-5694.
- [36] Lin, R. L., 2011, "Punch Problem for Planar Anisotropic Elastic Half-Plane", *Journal of Mechanics*, Vol. 27, pp. 215-226.
- [37] Hwu, C. B. and Fan, C. W., 1998, "Sliding Punches with or without Friction along the Surface of an Anisotropic Elastic Half-Plane", *Quarterly Journal of Mechanics and Applied Mathematics*, Vol. 51, pp. 159-177
- [38] Lawn, B., 1995, *Fracture of Brittle Solids*, Cambridge University Press, Cambridge, UK.
- [39] Isaac, M.D., Ori, I., 1994, *Engineering Mechanics of Composite Materials*, Oxford University Press, NY, USA.

- [40] Dag, S., 2001, "Crack and Contact Problems in Graded Materials", Ph.D. Dissertation, Department of Mechanical Engineering and Mechanics, Lehigh University, Bethlehem, Pennsylvania, USA.
- [41] Hildebrand, Francis Begnaud, 1976, *Advanced Calculus For Applications*, Englewood Cliffs, N.J., Prentice-Hall.
- [42] Fds Kreyszig, Erwin, 2006, *Advanced Engineering Mathematics*, John Willey & Sons, Inc.
- [43] Erdogan, F., 1978, "Mixed Boundary-Value Problems in Mechanics", *Mechanics Today*, Vol. 4, Nemat-Nasser, S., ed., Pergamon Press, Elmsford, New York, pp. 1-84.
- [44] Erdogan F., Gupta, G.D. and Cook, T.S., 1973, "Numerical Solution of Singular Integral Equations", *Recent Developments in Fracture Mechanics: Theory and Methods of Solving Crack Problems*, Sih, G.C., ed., Noordhoff International Publishing, Leyden, pp.368-425.
- [45] Tricomi, F.G., 1951, "On the Finite Hilbert Transformation", *The Quarterly Journal of Mathematics Oxford Series*, Vol.2, pp. 199-211.
- [46] Galin, L. A., 1953, *Contact Problems in the Classical Theory of Elasticity*.
- [47] Gladwell, G. M. L., 2008, *Contact Problems the Legacy of L. A. Galin*, Springer.
- [48] Kachanov, M., Shafiro, B., Tsukrov, I., 2003, *Handbook of Elasticity Solutions*, Kluwer Academic Publishers.

- [49] Sevostianov, I., Kachanov, M., 2001, "Plasma-Sprayed Ceramic Coatings: Anisotropic Elastic and Conductive Properties in Relation to The Microstructure; Cross-Property Correlations", *Material Science and Engineering*, Vol.297, pp.235-243.
- [50] Parthasarathi, S., Tittmann, BR., Sampath, K., Onesto, EJ., 1995, "Ultrasonic Characterization of Elastic Anisotropy in Plasma Sprayed Alumina Coatings", *Journal of Thermal Spray Technology*, Vol.4, pp. 367-373.
- [51] Dag, S., 2006, "Thermal Fracture Analysis of Orthotropic Functionally Graded Materials Using an Equivalent Domain Integral Approach", *Engineering Fracture Mechanics*, Vol.73, pp. 2802-2828.
- [52] Krenk, S., 1979 "On the Elastic Constants of Plane Orthotropic Elasticity", *Journal of Composite Materials*, Vol. 13, pp. 108-116.
- [53] Recho, N., 2012, *Fracture Mechanics and Crack Growth*, Wiley.

APPENDIX A

ASYMPTOTIC EXPANSION COEFFICIENTS

$$a_{210} = - \frac{E \left(C_{12} F^2 d_{12}^2 + C_{12} d_{11} d_{12} + C_{11} F^2 d_{12} + C_{12} d_{11} + E^2 C_{22} F^2 d_{12} \right) + C_{22} E^2 d_{11} - C_{22} F^2 d_{11} d_{12} - C_{22} d_{11}^2}{d_{11} (E^2 - F^2) (1 + d_{12})}, \quad (\text{A.1a})$$

$$a_{220} = \frac{F (E^2 d_{12} + d_{11}) (C_{12} + C_{12} d_{12} - C_{22} d_{11} + C_{22} F^2)}{d_{11} (E^2 - F^2) (1 + d_{12})}, \quad (\text{A.1b})$$

$$a_{20} = a_{210} + a_{220} = \frac{\begin{pmatrix} -E^2 C_{22} F^2 d_{12} - C_{22} E^2 d_{11} + E C_{12} F d_{12} + E C_{12} F d_{12}^2 \\ -E C_{22} F d_{11} d_{12} - E C_{22} F d_{11} - C_{12} d_{11} - C_{22} d_{11}^2 - C_{12} d_{11} d_{12} \\ -C_{22} F^2 d_{11} \end{pmatrix}}{d_{11} (E + F) (1 + d_{12})}, \quad (\text{A.1c})$$

$$b_{110} = \frac{\left(d_{11} + E^2 d_{12} \right) \begin{pmatrix} C_{12} A^2 + C_{12} A^2 d_{12} \\ + C_{22} - C_{22} d_{11} A^2 \end{pmatrix} \begin{pmatrix} B^3 F C_{11} d_{11} d_{12} - B^3 F C_{12} d_{11}^2 \\ + B^3 F C_{11} d_{11} + B^3 F^3 d_{11} C_{12} \\ + B F C_{11} d_{12}^2 - B F d_{12} C_{12} d_{11} \\ + B F C_{11} d_{12} + B F^3 d_{12} C_{12} \\ + C_{11} B^2 d_{11} + C_{11} B^2 d_{12} F^2 \\ + C_{11} B^2 d_{11} d_{12} + C_{11} B^2 d_{12}^2 F^2 \\ + C_{12} d_{11} + d_{12} F^2 C_{12} - C_{12} d_{11}^2 B^2 \\ - C_{12} d_{11} B^2 d_{12} F^2 \end{pmatrix}}{2\pi d_{11} F (E^2 - F^2) (1 + d_{12}) \begin{pmatrix} -C_{11} A^2 B^3 d_{11} d_{12} + C_{12} B d_{11} A^2 d_{12} \\ + C_{11} B^2 A^3 d_{11} d_{12} - C_{12} A d_{11} B^2 d_{12} \\ - C_{11} A^2 B d_{12} - C_{11} A^2 B^3 d_{11} - C_{11} A^2 B d_{12}^2 \\ + C_{12} B^3 d_{11}^2 A^2 + C_{11} B^2 A d_{12} + C_{11} B^2 A^3 d_{11} \\ + C_{11} B^2 A d_{12}^2 - C_{12} A^3 d_{11}^2 B^2 - C_{12} B^3 d_{11} \\ - C_{12} B d_{12} + C_{12} A^3 d_{11} + C_{12} A d_{12} \end{pmatrix}}, \quad (\text{A.2a})$$

$$b_{120} = \frac{\left(d_{11} + F^2 d_{12} \right) \begin{pmatrix} C_{12} A^2 + C_{12} A^2 d_{12} \\ + C_{22} - C_{22} d_{11} A^2 \end{pmatrix} \begin{pmatrix} B^3 E C_{11} d_{11} d_{12} - B^3 E C_{12} d_{11}^2 \\ + B^3 E C_{11} d_{11} + B^3 E^3 d_{11} C_{12} \\ + B E C_{11} d_{12}^2 - B E d_{12} C_{12} d_{11} \\ + B E C_{11} d_{12} + B E^3 d_{12} C_{12} \\ + C_{11} B^2 d_{11} + C_{11} B^2 d_{12} E^2 \\ + C_{11} B^2 d_{11} d_{12} + C_{11} B^2 d_{12}^2 E^2 \\ + C_{12} d_{11} + d_{12} E^2 C_{12} - C_{12} d_{11}^2 B^2 \\ - C_{12} d_{11} B^2 d_{12} E^2 \end{pmatrix}}{2\pi d_{11} E (E^2 - F^2) (1 + d_{12}) \begin{pmatrix} -C_{11} A^2 B^3 d_{11} d_{12} + C_{12} B d_{11} A^2 d_{12} \\ + C_{11} B^2 A^3 d_{11} d_{12} - C_{12} A d_{11} B^2 d_{12} \\ - C_{11} A^2 B d_{12} - C_{11} A^2 B^3 d_{11} - C_{11} A^2 B d_{12}^2 \\ + C_{12} B^3 d_{11}^2 A^2 + C_{11} B^2 A d_{12} + C_{11} B^2 A^3 d_{11} \\ + C_{11} B^2 A d_{12}^2 - C_{12} A^3 d_{11}^2 B^2 - C_{12} B^3 d_{11} \\ - C_{12} B d_{12} + C_{12} A^3 d_{11} + C_{12} A d_{12} \end{pmatrix}}, \quad (\text{A.2b})$$

$$b_{210} = \frac{\left(d_{11} + E^2 d_{12} \right) \begin{pmatrix} C_{12} B^2 + C_{12} B^2 d_{12} \\ + C_{22} - C_{22} d_{11} B^2 \end{pmatrix} \begin{pmatrix} A^3 F C_{11} d_{11} d_{12} - A^3 F C_{12} d_{11}^2 \\ + A^3 F C_{11} d_{11} + A^3 F^3 d_{11} C_{12} \\ + A F C_{11} d_{12}^2 - A F d_{12} C_{12} d_{11} \\ + A F C_{11} d_{12} + A F^3 d_{12} C_{12} \\ + C_{11} A^2 d_{11} + C_{11} A^2 d_{12} F^2 \\ + C_{11} A^2 d_{11} d_{12} + C_{11} A^2 d_{12}^2 F^2 \\ + C_{12} d_{11} + d_{12} F^2 C_{12} - C_{12} d_{11}^2 A^2 \\ - C_{12} d_{11} A^2 d_{12} F^2 \end{pmatrix}}{2\pi d_{11} F (E^2 - F^2) (1 + d_{12}) \begin{pmatrix} -C_{11} A^2 B^3 d_{11} d_{12} + C_{12} B d_{11} A^2 d_{12} \\ + C_{11} B^2 A^3 d_{11} d_{12} - C_{12} A d_{11} B^2 d_{12} \\ - C_{11} A^2 B d_{12} - C_{11} A^2 B^3 d_{11} - C_{11} A^2 B d_{12}^2 \\ + C_{12} B^3 d_{11}^2 A^2 + C_{11} B^2 A d_{12} + C_{11} B^2 A^3 d_{11} \\ + C_{11} B^2 A d_{12}^2 - C_{12} A^3 d_{11}^2 B^2 - C_{12} B^3 d_{11} \\ - C_{12} B d_{12} + C_{12} A^3 d_{11} + C_{12} A d_{12} \end{pmatrix}}, \quad (\text{A.2c})$$

$$b_{210} = \frac{\left(d_{11} + F^2 d_{12} \right) \begin{pmatrix} C_{12} B^2 + C_{12} B^2 d_{12} \\ + C_{22} - C_{22} d_{11} B^2 \end{pmatrix} \begin{pmatrix} A^3 E C_{11} d_{11} d_{12} - A^3 E C_{12} d_{11}^2 \\ + A^3 E C_{11} d_{11} + A^3 E^3 d_{11} C_{12} \\ + A E C_{11} d_{12}^2 - A E d_{12} C_{12} d_{11} \\ + A E C_{11} d_{12} + A E^3 d_{12} C_{12} \\ + C_{11} A^2 d_{11} + C_{11} A^2 d_{12} E^2 \\ + C_{11} A^2 d_{11} d_{12} + C_{11} A^2 d_{12}^2 E^2 \\ + C_{12} d_{11} + d_{12} E^2 C_{12} - C_{12} d_{11}^2 A^2 \\ - C_{12} d_{11} A^2 d_{12} E^2 \end{pmatrix}}{2\pi d_{11} E (E^2 - F^2) (1 + d_{12}) \begin{pmatrix} -C_{11} A^2 B^3 d_{11} d_{12} + C_{12} B d_{11} A^2 d_{12} \\ + C_{11} B^2 A^3 d_{11} d_{12} - C_{12} A d_{11} B^2 d_{12} \\ - C_{11} A^2 B d_{12} - C_{11} A^2 B^3 d_{11} - C_{11} A^2 B d_{12}^2 \\ + C_{12} B^3 d_{11}^2 A^2 + C_{11} B^2 A d_{12} + C_{11} B^2 A^3 d_{11} \\ + C_{11} B^2 A d_{12}^2 - C_{12} A^3 d_{11}^2 B^2 - C_{12} B^3 d_{11} \\ - C_{12} B d_{12} + C_{12} A^3 d_{11} + C_{12} A d_{12} \end{pmatrix}}, \quad (\text{A.2d})$$

$$g_{110} = \frac{-2(d_{12} + B^2 d_{11})B(C_{12}A^2 + C_{12}A^2 d_{12} + C_{22} - C_{22}d_{11}A^2)}{\left(\begin{array}{l} C_{12}Bd_{11}A^2 d_{12} - C_{12}Ad_{11}B^2 d_{12} - C_{11}A^2 B d_{12} - C_{11}A^2 B d_{12}^2 \\ - C_{11}A^2 B^3 d_{11}d_{12} + C_{11}B^2 A d_{12} + C_{11}B^2 A d_{12}^2 + C_{11}B^2 A^3 d_{11}d_{12} \\ - C_{11}A^2 B^3 d_{11} - C_{12}B^3 d_{11} + C_{12}B^3 d_{11}^2 A^2 + C_{11}B^2 A^3 d_{11} + C_{12}A^3 d_{11} \\ - C_{12}A^3 d_{11}^2 B^2 - C_{12}B d_{12} + C_{12}A d_{12} \end{array} \right)}, \quad (\text{A.3a})$$

$$g_{120} = \frac{2(d_{12} + A^2 d_{11})A(C_{12}B^2 + C_{12}B^2 d_{12} + C_{22} - C_{22}d_{11}B^2)}{\left(\begin{array}{l} C_{12}Bd_{11}A^2 d_{12} - C_{12}Ad_{11}B^2 d_{12} - C_{11}A^2 B d_{12} - C_{11}A^2 B d_{12}^2 \\ - C_{11}A^2 B^3 d_{11}d_{12} + C_{11}B^2 A d_{12} + C_{11}B^2 A d_{12}^2 + C_{11}B^2 A^3 d_{11}d_{12} \\ - C_{11}A^2 B^3 d_{11} - C_{12}B^3 d_{11} + C_{12}B^3 d_{11}^2 A^2 + C_{11}B^2 A^3 d_{11} + C_{12}A^3 d_{11} \\ - C_{12}A^3 d_{11}^2 B^2 - C_{12}B d_{12} + C_{12}A d_{12} \end{array} \right)}, \quad (\text{A.3b})$$

$$g_{210} = \frac{-4\eta \left(\begin{array}{l} -C_{12}B^2 d_{11} + C_{11}B^2 d_{12} \\ + C_{12} + C_{11}B^2 \end{array} \right) \left(\begin{array}{l} C_{12}A^2 + C_{12}A^2 d_{12} \\ + C_{22} - C_{22}d_{11}A^2 \end{array} \right)}{C_{66} \left(\begin{array}{l} C_{12}Bd_{11}A^2 d_{12} - C_{12}Ad_{11}B^2 d_{12} - C_{11}A^2 B d_{12} - C_{11}A^2 B d_{12}^2 \\ - C_{11}A^2 B^3 d_{11}d_{12} + C_{11}B^2 A d_{12} + C_{11}B^2 A d_{12}^2 + C_{11}B^2 A^3 d_{11}d_{12} \\ - C_{11}A^2 B^3 d_{11} - C_{12}B^3 d_{11} + C_{12}B^3 d_{11}^2 A^2 + C_{11}B^2 A^3 d_{11} \\ + C_{12}A^3 d_{11} - C_{12}A^3 d_{11}^2 B^2 - C_{12}B d_{12} + C_{12}A d_{12} \end{array} \right)}, \quad (\text{A.3c})$$

$$g_{220} = \frac{4\eta \left(\begin{array}{l} -C_{12}A^2 d_{11} + C_{11}A^2 d_{12} \\ + C_{12} + C_{11}A^2 \end{array} \right) \left(\begin{array}{l} C_{12}B^2 + C_{12}B^2 d_{12} \\ + C_{22} - C_{22}d_{11}B^2 \end{array} \right)}{C_{66} \left(\begin{array}{l} C_{12}Bd_{11}A^2 d_{12} - C_{12}Ad_{11}B^2 d_{12} - C_{11}A^2 B d_{12} - C_{11}A^2 B d_{12}^2 \\ - C_{11}A^2 B^3 d_{11}d_{12} + C_{11}B^2 A d_{12} + C_{11}B^2 A d_{12}^2 + C_{11}B^2 A^3 d_{11}d_{12} \\ - C_{11}A^2 B^3 d_{11} - C_{12}B^3 d_{11} + C_{12}B^3 d_{11}^2 A^2 + C_{11}B^2 A^3 d_{11} \\ + C_{12}A^3 d_{11} - C_{12}A^3 d_{11}^2 B^2 - C_{12}B d_{12} + C_{12}A d_{12} \end{array} \right)}, \quad (\text{A.3d})$$

$$g_{20} = g_{210} + g_{220} = \frac{4\eta \begin{pmatrix} -AC_{12}^2 d_{12} + AC_{11}C_{12} + AC_{11}d_{12}C_{12} - AC_{12}^2 \\ -BC_{12}^2 d_{12} + BC_{11}C_{12} + BC_{11}d_{12}C_{12} - BC_{12}^2 \end{pmatrix}}{C_{66} \begin{pmatrix} A^2 C_{11} B^2 d_{11} d_{12} + A^2 C_{11} B^2 d_{11} + C_{12} A^2 d_{11} \\ -A^2 C_{12} d_{11}^2 B^2 - AC_{11} B d_{12} - AC_{11} B d_{12}^2 + AC_{12} B d_{11} d_{12} \\ + ABC_{12} d_{11} + C_{12} d_{12} + C_{12} B^2 d_{11} \end{pmatrix}}, \quad (\text{A.3e})$$

$$m_{210} = \frac{(E^2 d_{12} + d_{11})(C_{12} + C_{12} d_{12} - C_{22} d_{11} + F^2 C_{22})}{C_{22} E (E^2 - F^2) (1 + d_{12})}, \quad (\text{A.4a})$$

$$m_{220} = -\frac{(F^2 d_{12} + d_{11})(C_{12} + C_{12} d_{12} - C_{22} d_{11} + E^2 C_{22})}{C_{22} F (E^2 - F^2) (1 + d_{12})}, \quad (\text{A.4b})$$

$$m_{20} = m_{210} + m_{220} = \frac{\begin{pmatrix} -F^2 C_{22} E^2 d_{12} - E^2 C_{22} d_{11} + EFC_{12} d_{12}^2 - EFC_{22} d_{11} d_{12} \\ + EFC_{12} d_{12} - EFC_{22} d_{11} + C_{22} d_{11}^2 - C_{12} d_{11} - C_{12} d_{12} d_{11} \\ - F^2 C_{22} d_{11} \end{pmatrix}}{C_{22} EF (E + F) (1 + d_{12})}, \quad (\text{A.4c})$$

$$n_{110} = \frac{(d_{11}A^2 + d_{12})A \begin{pmatrix} C_{12} + E^2C_{22} \\ + C_{12}d_{12} - C_{22}d_{11} \end{pmatrix} \begin{pmatrix} B^3F^3d_{11}C_{12} - B^3FC_{12}d_{11}^2 \\ + B^3FC_{11}d_{11}d_{12} + B^3FC_{11}d_{11} \\ + BF^3d_{12}C_{12} - BFd_{12}C_{12}d_{11} \\ + BFC_{11}d_{12}^2 + BFC_{11}d_{12} \\ + C_{11}B^2d_{12}F^2 + C_{11}B^2d_{11} \\ + C_{11}B^2d_{12}^2F^2 + C_{11}B^2d_{11}d_{12} \\ - C_{12}d_{11}B^2d_{12}F^2 - C_{12}d_{11}^2B^2 \\ + d_{12}F^2C_{12} + C_{12}d_{11} \end{pmatrix}}{2\pi C_{22}F^2(E^2 - F^2)(1 + d_{12}) \begin{pmatrix} -C_{11}A^2B^3d_{11} - C_{11}A^2Bd_{12} - C_{11}A^2Bd_{12}^2 \\ + C_{12}B^3d_{11}^2A^2 + C_{11}B^2A^3d_{11} + C_{11}B^2Ad_{12} \\ + C_{11}B^2Ad_{12}^2 - C_{12}A^3d_{11}^2B^2 + C_{12}Ad_{12} \\ - C_{11}A^2B^3d_{11}d_{12} + C_{12}Bd_{11}A^2d_{12} \\ + C_{11}B^2A^3d_{11}d_{12} - C_{12}Ad_{11}B^2d_{12} \\ - C_{12}B^3d_{11} - C_{12}Bd_{12} + C_{12}A^3d_{11} \end{pmatrix}} \quad (\text{A.5a})$$

$$n_{120} = \frac{(d_{11}A^2 + d_{12})A \begin{pmatrix} C_{12} + F^2C_{22} \\ + C_{12}d_{12} - C_{22}d_{11} \end{pmatrix} \begin{pmatrix} B^3E^3d_{11}C_{12} - B^3EC_{12}d_{11}^2 \\ + B^3EC_{11}d_{11}d_{12} + B^3EC_{11}d_{11} \\ + BE^3d_{12}C_{12} - BEd_{12}C_{12}d_{11} \\ + BEC_{11}d_{12}^2 + BEC_{11}d_{12} \\ + C_{11}B^2d_{12}E^2 + C_{11}B^2d_{11} \\ + C_{11}B^2d_{12}^2E^2 + C_{11}B^2d_{11}d_{12} \\ - C_{12}d_{11}B^2d_{12}E^2 - C_{12}d_{11}^2B^2 \\ + d_{12}E^2C_{12} + C_{12}d_{11} \end{pmatrix}}{2\pi C_{22}E^2(E^2 - F^2)(1 + d_{12}) \begin{pmatrix} -C_{11}A^2B^3d_{11} - C_{11}A^2Bd_{12} - C_{11}A^2Bd_{12}^2 \\ + C_{12}B^3d_{11}^2A^2 + C_{11}B^2A^3d_{11} + C_{11}B^2Ad_{12} \\ + C_{11}B^2Ad_{12}^2 - C_{12}A^3d_{11}^2B^2 + C_{12}Ad_{12} \\ - C_{11}A^2B^3d_{11}d_{12} + C_{12}Bd_{11}A^2d_{12} \\ + C_{11}B^2A^3d_{11}d_{12} - C_{12}Ad_{11}B^2d_{12} \\ - C_{12}B^3d_{11} - C_{12}Bd_{12} + C_{12}A^3d_{11} \end{pmatrix}}, \quad (\text{A.5b})$$

$$\begin{aligned}
& \left(d_{11}B^2 + d_{12} \right) B \begin{pmatrix} C_{12} + E^2C_{22} \\ + C_{12}d_{12} - C_{22}d_{11} \end{pmatrix} \begin{pmatrix} A^3F^3d_{11}C_{12} - A^3FC_{12}d_{11}^2 \\ + A^3FC_{11}d_{11}d_{12} + A^3FC_{11}d_{11} \\ + AF^3d_{12}C_{12} - AFd_{12}C_{12}d_{11} \\ + AFC_{11}d_{12}^2 + AFC_{11}d_{12} \\ + C_{11}A^2d_{12}F^2 + C_{11}A^2d_{11} \\ + C_{11}A^2d_{12}^2F^2 + C_{11}A^2d_{11}d_{12} \\ - C_{12}d_{11}A^2d_{12}F^2 - C_{12}d_{11}^2A^2 \\ + d_{12}F^2C_{12} + C_{12}d_{11} \end{pmatrix} \\
n_{210} = & \frac{\left(d_{11}B^2 + d_{12} \right) B \begin{pmatrix} C_{12} + E^2C_{22} \\ + C_{12}d_{12} - C_{22}d_{11} \end{pmatrix} \begin{pmatrix} A^3F^3d_{11}C_{12} - A^3FC_{12}d_{11}^2 \\ + A^3FC_{11}d_{11}d_{12} + A^3FC_{11}d_{11} \\ + AF^3d_{12}C_{12} - AFd_{12}C_{12}d_{11} \\ + AFC_{11}d_{12}^2 + AFC_{11}d_{12} \\ + C_{11}A^2d_{12}F^2 + C_{11}A^2d_{11} \\ + C_{11}A^2d_{12}^2F^2 + C_{11}A^2d_{11}d_{12} \\ - C_{12}d_{11}A^2d_{12}F^2 - C_{12}d_{11}^2A^2 \\ + d_{12}F^2C_{12} + C_{12}d_{11} \end{pmatrix}}{2\pi C_{22}F^2(E^2 - F^2)(1 + d_{12}) \begin{pmatrix} -C_{11}A^2B^3d_{11} - C_{11}A^2Bd_{12} - C_{11}A^2Bd_{12}^2 \\ + C_{12}B^3d_{11}^2A^2 + C_{11}B^2A^3d_{11} + C_{11}B^2Ad_{12} \\ + C_{11}B^2Ad_{12}^2 - C_{12}A^3d_{11}^2B^2 + C_{12}Ad_{12} \\ - C_{11}A^2B^3d_{11}d_{12} + C_{12}Bd_{11}A^2d_{12} \\ + C_{11}B^2A^3d_{11}d_{12} - C_{12}Ad_{11}B^2d_{12} \\ - C_{12}B^3d_{11} - C_{12}Bd_{12} + C_{12}A^3d_{11} \end{pmatrix}}, \tag{A.5c}
\end{aligned}$$

$$\begin{aligned}
f_{110} = & \frac{4\eta A(d_{12} + A^2d_{11})(-C_{12}B^2d_{11} + C_{11}B^2d_{12} + C_{12} + C_{11}B^2)}{C_{66} \begin{pmatrix} -C_{11}A^2Bd_{12} - C_{11}A^2Bd_{12}^2 - C_{11}A^2B^3d_{11}d_{12} \\ + C_{11}B^2Ad_{12} + C_{11}B^2Ad_{12}^2 + C_{11}B^2A^3d_{11}d_{12} \\ - C_{11}A^2B^3d_{11} - C_{12}B^3d_{11} + C_{12}B^3d_{11}^2A^2 \\ + C_{11}B^2A^3d_{11} + C_{12}A^3d_{11} - C_{12}A^3d_{11}^2B^2 \\ + C_{12}Bd_{11}A^2d_{12} - C_{12}Ad_{11}B^2d_{12} - C_{12}Bd_{12} \\ + C_{12}Ad_{12} \end{pmatrix}}, \tag{A.6a}
\end{aligned}$$

$$f_{120} = -\frac{4\eta B(d_{12} + B^2 d_{11})(-C_{12}A^2 d_{11} + C_{11}A^2 d_{12} + C_{12} + C_{11}A^2)}{C_{66} \begin{pmatrix} -C_{11}A^2 B d_{12} - C_{11}A^2 B d_{12}^2 - C_{11}A^2 B^3 d_{11} d_{12} \\ + C_{11}B^2 A d_{12} + C_{11}B^2 A d_{12}^2 + C_{11}B^2 A^3 d_{11} d_{12} \\ - C_{11}A^2 B^3 d_{11} - C_{12}B^3 d_{11} + C_{12}B^3 d_{11}^2 A^2 \\ + C_{11}B^2 A^3 d_{11} + C_{12}A^3 d_{11} - C_{12}A^3 d_{11}^2 B^2 \\ + C_{12}B d_{11} A^2 d_{12} - C_{12}A d_{11} B^2 d_{12} - C_{12}B d_{12} \\ + C_{12}A d_{12} \end{pmatrix}}, \quad (\text{A.6b})$$

$$f_{120} = -\frac{2AB(d_{12} + A^2 d_{11})(d_{12} + B^2 d_{11})}{\begin{pmatrix} -C_{11}A^2 B d_{12} - C_{11}A^2 B d_{12}^2 - C_{11}A^2 B^3 d_{11} d_{12} \\ + C_{11}B^2 A d_{12} + C_{11}B^2 A d_{12}^2 + C_{11}B^2 A^3 d_{11} d_{12} \\ - C_{11}A^2 B^3 d_{11} - C_{12}B^3 d_{11} + C_{12}B^3 d_{11}^2 A^2 \\ + C_{11}B^2 A^3 d_{11} + C_{12}A^3 d_{11} - C_{12}A^3 d_{11}^2 B^2 \\ + C_{12}B d_{11} A^2 d_{12} - C_{12}A d_{11} B^2 d_{12} - C_{12}B d_{12} \\ + C_{12}A d_{12} \end{pmatrix}}, \quad (\text{A.6c})$$

$$f_{220} = \frac{2AB(d_{12} + A^2 d_{11})(d_{12} + B^2 d_{11})}{\begin{pmatrix} -C_{11}A^2 B d_{12} - C_{11}A^2 B d_{12}^2 - C_{11}A^2 B^3 d_{11} d_{12} \\ + C_{11}B^2 A d_{12} + C_{11}B^2 A d_{12}^2 + C_{11}B^2 A^3 d_{11} d_{12} \\ - C_{11}A^2 B^3 d_{11} - C_{12}B^3 d_{11} + C_{12}B^3 d_{11}^2 A^2 \\ + C_{11}B^2 A^3 d_{11} + C_{12}A^3 d_{11} - C_{12}A^3 d_{11}^2 B^2 \\ + C_{12}B d_{11} A^2 d_{12} - C_{12}A d_{11} B^2 d_{12} - C_{12}B d_{12} \\ + C_{12}A d_{12} \end{pmatrix}}, \quad (\text{A.6d})$$

$$f_{20} = f_{210} + f_{220} = 0, \quad (\text{A.6e})$$

$$h_{110} = -\frac{E^2(F^2 d_{12} + d_{11})}{(E^2 - F^2)d_{11}}, \quad (\text{A.7a})$$

$$h_{120} = \frac{F^2(E^2 d_{12} + d_{11})}{(E^2 - F^2)d_{11}}, \quad (\text{A.7b})$$

$$l_{110} = -\frac{(d_{11} + E^2 d_{12}) A \left(\begin{array}{l} B^3 F C_{11} d_{11} d_{12} - B^3 F C_{12} d_{11}^2 \\ + B^3 F C_{11} d_{11} + B^3 F^3 d_{11} C_{12} \\ + B F C_{11} d_{12}^2 - B F d_{12} C_{12} d_{11} \\ + B F C_{11} d_{12} + B F^3 d_{12} C_{12} \\ + C_{11} B^2 d_{11} + C_{11} B^2 d_{12} F^2 \\ + C_{11} B^2 d_{11} d_{12} + C_{11} B^2 d_{12}^2 F^2 \\ + C_{12} d_{11} + d_{12} F^2 C_{12} - C_{12} d_{11}^2 B^2 \\ - C_{12} d_{11} B^2 d_{12} F^2 \end{array} \right)}{2\pi d_{11} F (E^2 - F^2) \left(\begin{array}{l} -C_{11} A^2 B^3 d_{11} d_{12} + C_{12} B d_{11} A^2 d_{12} \\ + C_{11} B^2 A^3 d_{11} d_{12} - C_{12} A d_{11} B^2 d_{12} \\ - C_{11} A^2 B d_{12} - C_{11} A^2 B^3 d_{11} - C_{11} A^2 B d_{12}^2 \\ + C_{12} B^3 d_{11}^2 A^2 + C_{11} B^2 A d_{12} + C_{11} B^2 A^3 d_{11} \\ + C_{11} B^2 A d_{12}^2 - C_{12} A^3 d_{11}^2 B^2 - C_{12} B^3 d_{11} \\ - C_{12} B d_{12} + C_{12} A^3 d_{11} + C_{12} A d_{12} \end{array} \right)}, \quad (\text{A.8a})$$

$$\begin{aligned}
& \left(d_{11} + F^2 d_{12} \right) A \begin{pmatrix} B^3 E C_{11} d_{11} d_{12} - B^3 E C_{12} d_{11}^2 \\ + B^3 E C_{11} d_{11} + B^3 E^3 d_{11} C_{12} \\ + B E C_{11} d_{12}^2 - B E d_{12} C_{12} d_{11} \\ + B E C_{11} d_{12} + B E^3 d_{12} C_{12} \\ + C_{11} B^2 d_{11} + C_{11} B^2 d_{12} E^2 \\ + C_{11} B^2 d_{11} d_{12} + C_{11} B^2 d_{12}^2 E^2 \\ + C_{12} d_{11} + d_{12} E^2 C_{12} - C_{12} d_{11}^2 B^2 \\ - C_{12} d_{11} B^2 d_{12} E^2 \end{pmatrix} \\
l_{120} = & \frac{\left(d_{11} + F^2 d_{12} \right) A \begin{pmatrix} B^3 E C_{11} d_{11} d_{12} - B^3 E C_{12} d_{11}^2 \\ + B^3 E C_{11} d_{11} + B^3 E^3 d_{11} C_{12} \\ + B E C_{11} d_{12}^2 - B E d_{12} C_{12} d_{11} \\ + B E C_{11} d_{12} + B E^3 d_{12} C_{12} \\ + C_{11} B^2 d_{11} + C_{11} B^2 d_{12} E^2 \\ + C_{11} B^2 d_{11} d_{12} + C_{11} B^2 d_{12}^2 E^2 \\ + C_{12} d_{11} + d_{12} E^2 C_{12} - C_{12} d_{11}^2 B^2 \\ - C_{12} d_{11} B^2 d_{12} E^2 \end{pmatrix}}{2\pi d_{11} E (E^2 - F^2) \begin{pmatrix} -C_{11} A^2 B^3 d_{11} d_{12} + C_{12} B d_{11} A^2 d_{12} \\ + C_{11} B^2 A^3 d_{11} d_{12} - C_{12} A d_{11} B^2 d_{12} \\ - C_{11} A^2 B d_{12} - C_{11} A^2 B^3 d_{11} - C_{11} A^2 B d_{12}^2 \\ + C_{12} B^3 d_{11}^2 A^2 + C_{11} B^2 A d_{12} + C_{11} B^2 A^3 d_{11} \\ + C_{11} B^2 A d_{12}^2 - C_{12} A^3 d_{11}^2 B^2 - C_{12} B^3 d_{11} \\ - C_{12} B d_{12} + C_{12} A^3 d_{11} + C_{12} A d_{12} \end{pmatrix}}, \tag{A.8b}
\end{aligned}$$

$$\begin{aligned}
& \left(d_{11} + E^2 d_{12} \right) B \begin{pmatrix} A^3 F C_{11} d_{11} d_{12} - A^3 F C_{12} d_{11}^2 \\ + A^3 F C_{11} d_{11} + A^3 F^3 d_{11} C_{12} \\ + A F C_{11} d_{12}^2 - A F d_{12} C_{12} d_{11} \\ + A F C_{11} d_{12} + A F^3 d_{12} C_{12} \\ + C_{11} A^2 d_{11} + C_{11} A^2 d_{12} F^2 \\ + C_{11} A^2 d_{11} d_{12} + C_{11} A^2 d_{12}^2 F^2 \\ + C_{12} d_{11} + d_{12} F^2 C_{12} - C_{12} d_{11}^2 A^2 \\ - C_{12} d_{11} A^2 d_{12} F^2 \end{pmatrix} \\
l_{210} = & \frac{\left(d_{11} + E^2 d_{12} \right) B \begin{pmatrix} A^3 F C_{11} d_{11} d_{12} - A^3 F C_{12} d_{11}^2 \\ + A^3 F C_{11} d_{11} + A^3 F^3 d_{11} C_{12} \\ + A F C_{11} d_{12}^2 - A F d_{12} C_{12} d_{11} \\ + A F C_{11} d_{12} + A F^3 d_{12} C_{12} \\ + C_{11} A^2 d_{11} + C_{11} A^2 d_{12} F^2 \\ + C_{11} A^2 d_{11} d_{12} + C_{11} A^2 d_{12}^2 F^2 \\ + C_{12} d_{11} + d_{12} F^2 C_{12} - C_{12} d_{11}^2 A^2 \\ - C_{12} d_{11} A^2 d_{12} F^2 \end{pmatrix}}{2\pi d_{11} F (E^2 - F^2) \begin{pmatrix} -C_{11} A^2 B^3 d_{11} d_{12} + C_{12} B d_{11} A^2 d_{12} \\ + C_{11} B^2 A^3 d_{11} d_{12} - C_{12} A d_{11} B^2 d_{12} \\ - C_{11} A^2 B d_{12} - C_{11} A^2 B^3 d_{11} - C_{11} A^2 B d_{12}^2 \\ + C_{12} B^3 d_{11}^2 A^2 + C_{11} B^2 A d_{12} + C_{11} B^2 A^3 d_{11} \\ + C_{11} B^2 A d_{12}^2 - C_{12} A^3 d_{11}^2 B^2 - C_{12} B^3 d_{11} \\ - C_{12} B d_{12} + C_{12} A^3 d_{11} + C_{12} A d_{12} \end{pmatrix}}, \tag{A.8c}
\end{aligned}$$

$$l_{220} = \frac{(d_{11} + F^2 d_{12}) B \begin{pmatrix} A^3 E C_{11} d_{11} d_{12} - A^3 E C_{12} d_{11}^2 \\ + A^3 E C_{11} d_{11} + A^3 E^3 d_{11} C_{12} \\ + A E C_{11} d_{12}^2 - A E d_{12} C_{12} d_{11} \\ + A E C_{11} d_{12} + A E^3 d_{12} C_{12} \\ + C_{11} A^2 d_{11} + C_{11} A^2 d_{12} E^2 \\ + C_{11} A^2 d_{11} d_{12} + C_{11} A^2 d_{12}^2 E^2 \\ + C_{12} d_{11} + d_{12} E^2 C_{12} - C_{12} d_{11}^2 A^2 \\ - C_{12} d_{11} A^2 d_{12} E^2 \end{pmatrix}}{2\pi d_{11} E (E^2 - F^2) \begin{pmatrix} -C_{11} A^2 B^3 d_{11} d_{12} + C_{12} B d_{11} A^2 d_{12} \\ + C_{11} B^2 A^3 d_{11} d_{12} - C_{12} A d_{11} B^2 d_{12} \\ - C_{11} A^2 B d_{12} - C_{11} A^2 B^3 d_{11} - C_{11} A^2 B d_{12}^2 \\ + C_{12} B^3 d_{11}^2 A^2 + C_{11} B^2 A d_{12} + C_{11} B^2 A^3 d_{11} \\ + C_{11} B^2 A d_{12}^2 - C_{12} A^3 d_{11}^2 B^2 - C_{12} B^3 d_{11} \\ - C_{12} B d_{12} + C_{12} A^3 d_{11} + C_{12} A d_{12} \end{pmatrix}}, \quad (\text{A.8d})$$

$$l_{10} = l_{110} + l_{210} = \frac{(d_{11} + E^2 d_{12}) \begin{pmatrix} A^2 B F C_{11} d_{11} d_{12} + A^2 B F C_{11} d_{11} \\ + A^2 B F^3 d_{11} C_{12} - A^2 B F C_{12} d_{11}^2 \\ - A B C_{12} d_{11} d_{12} F^2 + A B C_{11} d_{11} \\ + A B C_{11} d_{12} F^2 + A B C_{11} d_{11} d_{12} \\ - A B C_{12} d_{11}^2 + A B C_{11} d_{12}^2 F^2 \\ + A B^2 d_{12} F C_{11} d_{11} + A B^2 F C_{11} d_{11} \\ + A B^2 F^3 d_{11} C_{12} - A B^2 F d_{11}^2 C_{12} \\ - C_{12} d_{11} - d_{12} F^2 C_{12} \end{pmatrix}}{2\pi d_{11} F (E^2 - F^2) \begin{pmatrix} A^2 C_{11} B^2 d_{11} d_{12} + A^2 C_{11} B^2 d_{11} \\ + C_{12} A^2 d_{11} - A^2 C_{12} d_{11}^2 B^2 \\ + A C_{12} B d_{11} d_{12} - A C_{11} B d_{12} \\ - A C_{11} B d_{12}^2 + A B C_{12} d_{11} + C_{12} d_{12} \\ + C_{12} d_{11} B^2 \end{pmatrix}}, \quad (\text{A.8e})$$

$$\begin{aligned}
l_{20} = l_{120} + l_{220} = & - \frac{(d_{11} + F^2 d_{12}) \left(\begin{aligned} & A^2 BEC_{11} d_{11} d_{12} + A^2 BEC_{11} d_{11} \\ & + A^2 BE^3 d_{11} C_{12} - A^2 BEC_{12} d_{11}^2 \\ & - ABC_{12} d_{11} d_{12} E^2 + ABC_{11} d_{11} \\ & + ABC_{11} d_{12} E^2 + ABC_{11} d_{11} d_{12} \\ & - ABC_{12} d_{11}^2 + ABC_{11} d_{12}^2 E^2 \\ & + AB^2 d_{12} EC_{11} d_{11} + AB^2 EC_{11} d_{11} \\ & + AB^2 E^3 d_{11} C_{12} - AB^2 E d_{11}^2 C_{12} \\ & - C_{12} d_{11} - d_{12} E^2 C_{12} \end{aligned} \right)}{2\pi d_{11} E (E^2 - F^2) \left(\begin{aligned} & A^2 C_{11} B^2 d_{11} d_{12} + A^2 C_{11} B^2 d_{11} \\ & + C_{12} A^2 d_{11} - A^2 C_{12} d_{11}^2 B^2 \\ & + AC_{12} B d_{11} d_{12} - AC_{11} B d_{12} \\ & - AC_{11} B d_{12}^2 + ABC_{12} d_{11} + C_{12} d_{12} \\ & + C_{12} d_{11} B^2 \end{aligned} \right)}, \tag{A.8f}
\end{aligned}$$

$$\begin{aligned}
& \left(\begin{aligned}
& AEd_{11}C_{11}B^2d_{12}F^2 + AEd_{11}C_{11}B^2d_{12}^2F^2 \\
& - AEC_{12}d_{11}^2B^2d_{12}F^2 + AFE^2d_{12}C_{11}B^2d_{11} \\
& + AFE^2d_{12}^2C_{11}B^2d_{11} - AFE^2d_{12}C_{12}d_{11}^2B^2 \\
& - BEC_{12}d_{11}^2A^2d_{12}F^2 + BEd_{11}C_{11}A^2d_{12}^2F^2 \\
& + BEd_{11}C_{11}A^2d_{12}F^2 - BFE^2d_{12}C_{12}d_{11}^2A^2 \\
& + BFE^2d_{12}^2C_{11}A^2d_{11} + BFE^2d_{12}C_{11}A^2d_{11} \\
& - d_{11}d_{12}F^2C_{12} - E^2d_{12}C_{12}d_{11} - E^2d_{12}^2F^2C_{12} \\
& - ABC_{12}d_{11}^3 + ABC_{11}d_{11}^2 - C_{12}d_{11}^2 - ABE^2d_{12}C_{12}d_{11}^2 \\
& + ABE^2d_{12}^2C_{11}d_{11} + ABE^2d_{12}C_{11}d_{11} - ABC_{12}d_{11}^2d_{12}F^2 \\
& + ABd_{11}C_{11}d_{12}^2F^2 + ABd_{11}C_{11}d_{12}F^2 - E^2ABd_{12}^2C_{12}d_{11}F^2 \\
& + ABC_{11}d_{11}^2d_{12} + E^2ABd_{12}^3C_{11}F^2 + E^2ABd_{12}^2C_{11}F^2 \\
& - E^2AB^2Fd_{11}^2C_{12} - E^2A^2BFd_{11}^2C_{12} - E^2AB^2F^2d_{11}^2C_{12} \\
& - EA^2BF^2d_{11}^2C_{12}
\end{aligned} \right) \tag{A.8g} \\
l_0 = l_{10} + l_{20} = & \frac{\left(\begin{aligned}
& A^2C_{11}B^2d_{11}d_{12} + A^2C_{11}B^2d_{11} \\
& + C_{12}A^2d_{11} - A^2C_{12}d_{11}^2B^2 \\
& + AC_{12}Bd_{11}d_{12} - AC_{11}Bd_{12} \\
& - AC_{11}Bd_{12}^2 + ABC_{12}d_{11} + C_{12}d_{12} \\
& + C_{12}d_{11}B^2
\end{aligned} \right)}{2\pi d_{11}EF(E+F)},
\end{aligned}$$

$$r_{210} = \frac{E(C_{12} + C_{12}d_{12} - C_{22}d_{11} + F^2C_{22})}{(E^2 - F^2)C_{22}}, \tag{A.9a}$$

$$r_{220} = -\frac{F(C_{12} + C_{12}d_{12} - C_{22}d_{11} + E^2C_{22})}{(E^2 - F^2)C_{22}}, \tag{A.9b}$$

$$r_{20} = r_{210} + r_{220} = \frac{-FC_{22}E + C_{12} + C_{12}d_{12} - C_{22}d_{11}}{(E+F)C_{22}}, \tag{A.9c}$$

$$s_{110} = \frac{(C_{12} + E^2 C_{22} + C_{12} d_{12} - C_{22} d_{11}) A \begin{pmatrix} B^3 F^3 d_{11} C_{12} - B^3 F C_{12} d_{11}^2 \\ + B^3 F C_{11} d_{11} d_{12} + B^3 F C_{11} d_{11} \\ + B F^3 d_{12} C_{12} - B F d_{12} C_{12} d_{11} \\ + B F C_{11} d_{12}^2 + B F C_{11} d_{12} \\ + C_{11} B^2 d_{12} F^2 + C_{11} B^2 d_{11} \\ + C_{11} B^2 d_{12}^2 F^2 + C_{11} B^2 d_{11} d_{12} \\ - C_{12} d_{11} B^2 d_{12} F^2 - C_{12} d_{11}^2 B^2 \\ + d_{12} F^2 C_{12} + C_{12} d_{11} \end{pmatrix}}{2\pi C_{22} F^2 (E^2 - F^2) \begin{pmatrix} -C_{11} A^2 B^3 d_{11} - C_{11} A^2 B d_{12} - C_{11} A^2 B d_{12}^2 \\ + C_{12} B^3 d_{11}^2 A^2 + C_{11} B^2 A^3 d_{11} + C_{11} B^2 A d_{12} \\ + C_{11} B^2 A d_{12}^2 - C_{12} A^3 d_{11}^2 B^2 + C_{12} A d_{12} \\ - C_{11} A^2 B^3 d_{11} d_{12} + C_{12} B d_{11} A^2 d_{12} \\ + C_{11} B^2 A^3 d_{11} d_{12} - C_{12} A d_{11} B^2 d_{12} \\ - C_{12} B^3 d_{11} - C_{12} B d_{12} + C_{12} A^3 d_{11} \end{pmatrix}}, \quad (\text{A.10a})$$

$$s_{120} = \frac{(C_{12} + F^2 C_{22} + C_{12} d_{12} - C_{22} d_{11}) A \begin{pmatrix} B^3 E^3 d_{11} C_{12} - B^3 E C_{12} d_{11}^2 \\ + B^3 E C_{11} d_{11} d_{12} + B^3 E C_{11} d_{11} \\ + B E^3 d_{12} C_{12} - B E d_{12} C_{12} d_{11} \\ + B E C_{11} d_{12}^2 + B E C_{11} d_{12} \\ + C_{11} B^2 d_{12} E^2 + C_{11} B^2 d_{11} \\ + C_{11} B^2 d_{12}^2 E^2 + C_{11} B^2 d_{11} d_{12} \\ - C_{12} d_{11} B^2 d_{12} E^2 - C_{12} d_{11}^2 B^2 \\ + d_{12} E^2 C_{12} + C_{12} d_{11} \end{pmatrix}}{2\pi C_{22} E^2 (E^2 - F^2) \begin{pmatrix} -C_{11} A^2 B^3 d_{11} - C_{11} A^2 B d_{12} - C_{11} A^2 B d_{12}^2 \\ + C_{12} B^3 d_{11}^2 A^2 + C_{11} B^2 A^3 d_{11} + C_{11} B^2 A d_{12} \\ + C_{11} B^2 A d_{12}^2 - C_{12} A^3 d_{11}^2 B^2 + C_{12} A d_{12} \\ - C_{11} A^2 B^3 d_{11} d_{12} + C_{12} B d_{11} A^2 d_{12} \\ + C_{11} B^2 A^3 d_{11} d_{12} - C_{12} A d_{11} B^2 d_{12} \\ - C_{12} B^3 d_{11} - C_{12} B d_{12} + C_{12} A^3 d_{11} \end{pmatrix}}, \quad (\text{A.10b})$$

$$s_{210} = \frac{\left(C_{12} + E^2 C_{22} + C_{12} d_{12} - C_{22} d_{11} \right) \mathbf{B} \begin{pmatrix} A^3 F^3 d_{11} C_{12} - A^3 F C_{12} d_{11}^2 \\ + A^3 F C_{11} d_{11} d_{12} + A^3 F C_{11} d_{11} \\ + A F^3 d_{12} C_{12} - A F d_{12} C_{12} d_{11} \\ + A F C_{11} d_{12}^2 + A F C_{11} d_{12} \\ + C_{11} A^2 d_{12} F^2 + C_{11} A^2 d_{11} \\ + C_{11} A^2 d_{12}^2 F^2 + C_{11} A^2 d_{11} d_{12} \\ - C_{12} d_{11} A^2 d_{12} F^2 - C_{12} d_{11}^2 A^2 \\ + d_{12} F^2 C_{12} + C_{12} d_{11} \end{pmatrix}}{2\pi C_{22} F^2 (E^2 - F^2) \begin{pmatrix} -C_{11} A^2 B^3 d_{11} - C_{11} A^2 B d_{12} - C_{11} A^2 B d_{12}^2 \\ + C_{12} B^3 d_{11}^2 A^2 + C_{11} B^2 A^3 d_{11} + C_{11} B^2 A d_{12} \\ + C_{11} B^2 A d_{12}^2 - C_{12} A^3 d_{11}^2 B^2 + C_{12} A d_{12} \\ - C_{11} A^2 B^3 d_{11} d_{12} + C_{12} B d_{11} A^2 d_{12} \\ + C_{11} B^2 A^3 d_{11} d_{12} - C_{12} A d_{11} B^2 d_{12} \\ - C_{12} B^3 d_{11} - C_{12} B d_{12} + C_{12} A^3 d_{11} \end{pmatrix}}, \quad (\text{A.10c})$$

$$s_{220} = \frac{\left(C_{12} + F^2 C_{22} + C_{12} d_{12} - C_{22} d_{11} \right) \mathbf{B} \begin{pmatrix} A^3 E^3 d_{11} C_{12} - A^3 E C_{12} d_{11}^2 \\ + A^3 E C_{11} d_{11} d_{12} + A^3 E C_{11} d_{11} \\ + A E^3 d_{12} C_{12} - A E d_{12} C_{12} d_{11} \\ + A E C_{11} d_{12}^2 + A E C_{11} d_{12} \\ + C_{11} A^2 d_{12} E^2 + C_{11} A^2 d_{11} \\ + C_{11} A^2 d_{12}^2 E^2 + C_{11} A^2 d_{11} d_{12} \\ - C_{12} d_{11} A^2 d_{12} E^2 - C_{12} d_{11}^2 A^2 \\ + d_{12} E^2 C_{12} + C_{12} d_{11} \end{pmatrix}}{2\pi C_{22} E^2 (E^2 - F^2) \begin{pmatrix} -C_{11} A^2 B^3 d_{11} - C_{11} A^2 B d_{12} - C_{11} A^2 B d_{12}^2 \\ + C_{12} B^3 d_{11}^2 A^2 + C_{11} B^2 A^3 d_{11} \\ + C_{11} B^2 A d_{12} + C_{11} B^2 A d_{12}^2 - C_{12} A^3 d_{11}^2 B^2 \\ + C_{12} A d_{12} - C_{11} A^2 B^3 d_{11} d_{12} \\ + C_{12} B d_{11} A^2 d_{12} + C_{11} B^2 A^3 d_{11} d_{12} \\ - C_{12} A d_{11} B^2 d_{12} - C_{12} B^3 d_{11} - C_{12} B d_{12} \\ + C_{12} A^3 d_{11} \end{pmatrix}}, \quad (\text{A.10d})$$

$$s_{10} = s_{110} + s_{210} = \frac{\begin{pmatrix} C_{12} + E^2 C_{22} \\ + C_{12} d_{12} - C_{22} d_{11} \end{pmatrix} \begin{pmatrix} -A^2 B F C_{12} d_{11}^2 + A^2 B F C_{11} d_{11} \\ + A^2 B F^3 d_{11} C_{12} + A^2 B F C_{11} d_{11} d_{12} \\ + A B C_{11} d_{11} d_{12} - A B C_{12} d_{11} F^2 d_{12} \\ + A B C_{11} d_{11} - A B C_{12} d_{11}^2 \\ + A B C_{11} d_{12}^2 F^2 + A B C_{11} F^2 d_{12} \\ - A B^2 F C_{12} d_{11}^2 + A B^2 F C_{11} d_{11} \\ + A B^2 F^3 d_{11} C_{12} + A B^2 F C_{11} d_{11} d_{12} \\ - d_{12} C_{12} F^2 - C_{12} d_{11} \end{pmatrix}}{2\pi C_{22} F^2 (E^2 - F^2) \begin{pmatrix} C_{11} A^2 B^2 d_{11} + C_{11} A^2 B^2 d_{11} d_{12} \\ - C_{12} B^2 d_{11}^2 A^2 + C_{12} A^2 d_{11} \\ - C_{11} A B d_{12} + C_{12} B d_{11} A d_{12} \\ - C_{11} A B d_{12}^2 + A B C_{12} d_{11} \\ + C_{12} d_{12} + C_{12} d_{11} B^2 \end{pmatrix}}, \quad (\text{A.10e})$$

$$s_{20} = s_{120} + s_{220} = \frac{\begin{pmatrix} C_{12} + F^2 C_{22} \\ + C_{12} d_{12} - C_{22} d_{11} \end{pmatrix} \begin{pmatrix} -A^2 B E C_{12} d_{11}^2 + A^2 B E C_{11} d_{11} \\ + A^2 B E^3 d_{11} C_{12} + A^2 B E C_{11} d_{11} d_{12} \\ + A B C_{11} d_{11} d_{12} - A B C_{12} d_{11} E^2 d_{12} \\ + A B C_{11} d_{11} - A B C_{12} d_{11}^2 \\ + A B C_{11} d_{12}^2 E^2 + A B C_{11} E^2 d_{12} \\ - A B^2 E C_{12} d_{11}^2 + A B^2 E C_{11} d_{11} \\ + A B^2 E^3 d_{11} C_{12} + A B^2 E C_{11} d_{11} d_{12} \\ - d_{12} C_{12} E^2 - C_{12} d_{11} \end{pmatrix}}{2\pi C_{22} E^2 (E^2 - F^2) \begin{pmatrix} C_{11} A^2 B^2 d_{11} + C_{11} A^2 B^2 d_{11} d_{12} \\ - C_{12} B^2 d_{11}^2 A^2 + C_{12} A^2 d_{11} \\ - C_{11} A B d_{12} + C_{12} B d_{11} A d_{12} \\ - C_{11} A B d_{12}^2 + A B C_{12} d_{11} \\ + C_{12} d_{12} + C_{12} d_{11} B^2 \end{pmatrix}}, \quad (\text{A.10f})$$

$$e_{110} = \frac{4\eta A(1+d_{12})(-C_{12}B^2d_{11} + C_{11}B^2d_{12} + C_{12} + C_{11}B^2)}{C_{66} \begin{pmatrix} -C_{11}A^2Bd_{12} - C_{11}A^2Bd_{12}^2 - C_{11}A^2B^3d_{11}d_{12} \\ + C_{11}B^2Ad_{12} + C_{11}B^2Ad_{12}^2 + C_{11}B^2A^3d_{11}d_{12} \\ - C_{11}A^2B^3d_{11} - C_{12}B^3d_{11} + C_{12}B^3d_{11}^2A^2 \\ + C_{11}B^2A^3d_{11} + C_{12}A^3d_{11} - C_{12}A^3d_{11}^2B^2 \\ + C_{12}Bd_{11}A^2d_{12} - C_{12}Ad_{11}B^2d_{12} - C_{12}Bd_{12} \\ + C_{12}Ad_{12} \end{pmatrix}}, \quad (\text{A.11a})$$

$$e_{120} = -\frac{4\eta B(1+d_{12})(-C_{12}A^2d_{11} + C_{11}A^2d_{12} + C_{12} + C_{11}A^2)}{C_{66} \begin{pmatrix} -C_{11}A^2Bd_{12} - C_{11}A^2Bd_{12}^2 - C_{11}A^2B^3d_{11}d_{12} \\ + C_{11}B^2Ad_{12} + C_{11}B^2Ad_{12}^2 + C_{11}B^2A^3d_{11}d_{12} \\ - C_{11}A^2B^3d_{11} - C_{12}B^3d_{11} + C_{12}B^3d_{11}^2A^2 \\ + C_{11}B^2A^3d_{11} + C_{12}A^3d_{11} - C_{12}A^3d_{11}^2B^2 \\ + C_{12}Bd_{11}A^2d_{12} - C_{12}Ad_{11}B^2d_{12} - C_{12}Bd_{12} \\ + C_{12}Ad_{12} \end{pmatrix}}, \quad (\text{A.11b})$$

$$e_{210} = -\frac{2AB(d_{12} + B^2d_{11})(1+d_{12})}{\begin{pmatrix} -C_{11}A^2Bd_{12} - C_{11}A^2Bd_{12}^2 - C_{11}A^2B^3d_{11}d_{12} \\ + C_{11}B^2Ad_{12} + C_{11}B^2Ad_{12}^2 + C_{11}B^2A^3d_{11}d_{12} \\ - C_{11}A^2B^3d_{11} - C_{12}B^3d_{11} + C_{12}B^3d_{11}^2A^2 \\ + C_{11}B^2A^3d_{11} + C_{12}A^3d_{11} - C_{12}A^3d_{11}^2B^2 \\ + C_{12}Bd_{11}A^2d_{12} - C_{12}Ad_{11}B^2d_{12} - C_{12}Bd_{12} \\ + C_{12}Ad_{12} \end{pmatrix}}, \quad (\text{A.11c})$$

$$e_{220} = \frac{2AB(d_{12} + A^2 d_{11})(1 + d_{12})}{\left(\begin{array}{l} -C_{11}A^2 B d_{12} - C_{11}A^2 B d_{12}^2 - C_{11}A^2 B^3 d_{11} d_{12} \\ + C_{11}B^2 A d_{12} + C_{11}B^2 A d_{12}^2 + C_{11}B^2 A^3 d_{11} d_{12} \\ - C_{11}A^2 B^3 d_{11} - C_{12}B^3 d_{11} + C_{12}B^3 d_{11}^2 A^2 \\ + C_{11}B^2 A^3 d_{11} + C_{12}A^3 d_{11} - C_{12}A^3 d_{11}^2 B^2 \\ + C_{12}B d_{11} A^2 d_{12} - C_{12}A d_{11} B^2 d_{12} - C_{12}B d_{12} \\ + C_{12}A d_{12} \end{array} \right)}, \quad (\text{A.11d})$$

$$e_{10} = e_{110} + e_{120} = -\frac{4\eta(AC_{11}B + AC_{11}Bd_{12} - AC_{12}Bd_{11} - C_{12})(1 + d_{12})}{C_{66} \left(\begin{array}{l} A^2 C_{11}B^2 d_{11} d_{12} - A^2 C_{12} d_{11}^2 B^2 + A^2 C_{11}B^2 d_{11} \\ + C_{12}A^2 d_{11} - AC_{11}Bd_{12} - AC_{11}Bd_{12}^2 \\ + AC_{12}B d_{11} d_{12} + AC_{12}B d_{11} + C_{12}d_{12} + C_{12}B^2 d_{11} \end{array} \right)}, \quad (\text{A.11e})$$

$$e_{20} = e_{210} + e_{220} = \frac{2(A + B)d_{11}(1 + d_{12})AB}{\left(\begin{array}{l} A^2 C_{11}B^2 d_{11} d_{12} - A^2 C_{12} d_{11}^2 B^2 + A^2 C_{11}B^2 d_{11} \\ + C_{12}A^2 d_{11} - AC_{11}Bd_{12} - AC_{11}Bd_{12}^2 + AC_{12}B d_{11} d_{12} \\ + AC_{12}B d_{11} + C_{12}d_{12} + C_{12}B^2 d_{11} \end{array} \right)}. \quad (\text{A.11f})$$

APPENDIX B

CLOSED FORM EXPRESSIONS FOR CAUCHY PRINCIPAL VALUE INTEGRALS

Following result, which is given by Tricomi [45], is used in the evaluation of the Cauchy principal value integrals,

$$\frac{1}{\pi} \int_{-1}^1 (1-t)^\alpha (1+t)^\beta P_n^{(\alpha, \beta)}(t) \frac{dt}{t-x} = \cot(\pi\alpha) (1-x)^\alpha (1+x)^\beta P_n^{(\alpha, \beta)}(x) - \frac{2^{(\alpha+\beta)} \Gamma(\alpha) \Gamma(n+\beta+1)}{\pi \Gamma(n+\alpha+\beta+1)} F\left(n+1; -n-\alpha-\beta; 1-\alpha; \frac{1-x}{2}\right), \quad (\text{B.1})$$

where $\alpha > -1$, $\beta > -1$, $\alpha \neq 0, 1, 2, \dots$ Γ is the gamma function, and $F()$ is the hypergeometric function. If $(\alpha + \beta)$ is equal to -1 , 0 or 1 , (B.1) can be further simplified as follows,

$$\frac{1}{\pi} \int_{-1}^1 (1-t)^\alpha (1+t)^\beta P_n^{(\alpha, \beta)}(t) \frac{dt}{t-x} = \cot(\pi\alpha) (1-x)^\alpha (1+x)^\beta P_n^{(\alpha, \beta)}(x) - \frac{2^{-\chi}}{\sin(\pi\alpha)} P_{n-\chi}^{(\alpha, \beta)}(x), \quad (\text{B.2})$$

where, $\chi = -(\alpha + \beta)$.

APPENDIX C

FUNCTIONS USED IN THE NUMERICAL SOLUTION OF THE INTEGRAL EQUATIONS

The transformed forms of the kernels used in equations (2.209a-c), are given as,

$$H_{11}(s_1, r) = \frac{d}{2} (H_{11s}(s_1, r) + H_{11f}(s_1, r)), \quad (\text{C.1a})$$

$$H_{13}(s_1, r) = \frac{b-a}{2} (H_{13s}(s_1, r) + H_{13f}(s_1, r)), \quad (\text{C.1b})$$

$$H_{22}(s_2, r) = \frac{d}{2} (H_{22s}(s_2, r) + H_{22f}(s_2, r)), \quad (\text{C.1c})$$

$$H_{23}(s_2, r) = \frac{b-a}{2} (H_{23s}(s_2, r) + H_{23f}(s_2, r)), \quad (\text{C.1d})$$

$$H_{31}(s_3, r) = \frac{d}{2} (H_{31s}(s_3, r) + H_{31f}(s_3, r)), \quad (\text{C.1e})$$

$$H_{32}(s_3, r) = \frac{d}{2} (H_{32s}(s_3, r) + H_{32f}(s_3, r)), \quad (\text{C.1f})$$

$$H_{33}(s_3, r) = \frac{b-a}{2} H_{33f}(s_3, r), \quad (\text{C.1g})$$

where,

$$H_{ijs}(s_i, r) = h_{ijs}(x, t), \quad (\text{C.2a})$$

$$H_{ijf}(s_i, r) = h_{ijf}(x, t), \quad (\text{C.2b})$$

$$x = \begin{cases} \frac{d}{2}s_i + \frac{d}{2}, & i=1, 2 \\ \frac{b-a}{2}s_i + \frac{b+a}{2}, & i=3 \end{cases} \quad (\text{C.3a})$$

$$t = \begin{cases} \frac{d}{2}r + \frac{d}{2}, & j=1, 2 \\ \frac{b-a}{2}r + \frac{b+a}{2}, & j=3 \end{cases} \quad (\text{C.3b})$$

The terms used in equations (2.212) are given in the following form,

$$m_{11n}(s_1) = \frac{a_{20}}{2} \frac{2^{\alpha_1-1/2} \Gamma(-1/2) \Gamma(n + \alpha_1 + 1)}{\pi \Gamma(n + 1/2 + \alpha_1)} \times F\left(n + 1; -n + 1/2 - \alpha_1; 3/2; \frac{1-s_1}{2}\right) + \int_{-1}^1 (1-r)^{-1/2} (1+r)^{\alpha_1} P_n^{(-1/2, \alpha_1)}(r) H_{11}(s_1, r) dr, \quad (\text{C.4a})$$

$$m_{13n}(s_1) = \int_{-1}^1 (1-r)^\beta (1+r)^{\alpha_2} P_n^{(\beta, \alpha_2)}(r) H_{13}(s_1, r) dr, \quad (\text{C.4b})$$

$$m_{22n}(s_2) = \frac{m_{20}}{2} \frac{2^{\alpha_1-1/2} \Gamma(-1/2) \Gamma(n + \alpha_1 + 1)}{\pi \Gamma(n + 1/2 + \alpha_1)} \times F\left(n + 1; -n + 1/2 - \alpha_1; 3/2; \frac{1-s_2}{2}\right) + \int_{-1}^1 (1-r)^{-1/2} (1+r)^{\alpha_1} P_n^{(-1/2, \alpha_1)}(r) H_{22}(s_2, r) dr, \quad (\text{C.4c})$$

$$m_{23n}(s_2) = \int_{-1}^1 (1-r)^\beta (1+r)^{\alpha_2} P_n^{(\beta, \alpha_2)}(r) H_{23}(s_2, r) dr, \quad (\text{C.4d})$$

$$m_{31n}(s_3) = \int_{-1}^1 (1-r)^{-1/2} (1+r)^{\alpha_1} P_n^{(-1/2, \alpha_1)}(r) H_{31}(s_3, r) dr, \quad (\text{C.4e})$$

$$m_{32n}(s_3) = \int_{-1}^1 (1-r)^{-1/2} (1+r)^{\alpha_1} P_n^{(-1/2, \alpha_1)}(r) H_{32}(s_3, r) dr, \quad (\text{C.4f})$$

$$m_{33n}(s_3) = \frac{e_{20}}{2} \frac{2^{\beta+\alpha_2} \Gamma(\beta) \Gamma(n+\alpha_2+1)}{\pi \Gamma(n+\beta+\alpha_2+1)} \times F\left(n+1; -n-\beta-\alpha_2; 1-\beta; \frac{1-s_3}{2}\right) \\ + \int_{-1}^1 (1-r)^\beta (1+r)^{\alpha_2} P_n^{(\beta, \alpha_2)}(r) H_{33}(s_3, r) dr, \quad (\text{C.4g})$$

where a_{20} , m_{20} and e_{20} are given in Appendix A by equations (A.1c), (A.4c) and (A.11f), respectively.

Note that if $\alpha_2 + \beta = -1, 0$, or 1 (C.4g) reduces to

$$m_{33n}(s_3) = \frac{e_{20}}{2} \frac{2^{\beta+\alpha_2}}{\sin(\pi\beta)} P_{n+(\alpha_2+\beta)}^{(-\beta, -\alpha_2)}(s_3) + \int_{-1}^1 (1-r)^\beta (1+r)^{\alpha_2} P_n^{(\beta, \alpha_2)}(r) H_{33}(s_3, r) dr. \quad (\text{C.5a})$$

In this case, if $\alpha_2 + \beta = -1$ and $n=0$;

$$m_{330}(s_3) = \int_{-1}^1 (1-r)^\beta (1+r)^{\alpha_2} H_{33}(s_3, r) dr. \quad (\text{C.5b})$$

The terms used (2.233) in are given as follows:

$$g_{11n}(s_1) = \frac{a_{20}}{2} \frac{2^{-1/2} \Gamma(-1/2) \Gamma(n+1)}{\pi \Gamma(n+1/2)} \times F\left(n+1; -n+1/2; 3/2; \frac{1-s_1}{2}\right) + \int_{-1}^1 (1-r)^{-1/2} P_n^{(-1/2,0)}(r) H_{11}(s_1, r) dr, \quad (\text{C.6a})$$

$$g_{13n}(s_1) = \int_{-1}^1 (1-r)^\beta (1+r)^\omega P_n^{(\beta,\omega)}(r) H_{13}(s_1, r) dr, \quad (\text{C.6b})$$

$$g_{22n}(s_2) = \frac{m_{20}}{2} \frac{2^{-1/2} \Gamma(-1/2) \Gamma(n+1)}{\pi \Gamma(n+1/2)} \times F\left(n+1; -n+1/2; 3/2; \frac{1-s_2}{2}\right) + \int_{-1}^1 (1-r)^{-1/2} P_n^{(-1/2,0)}(r) H_{22}(s_2, r) dr, \quad (\text{C.6c})$$

$$g_{23n}(s_2) = \int_{-1}^1 (1-r)^\beta (1+r)^\omega P_n^{(\beta,\omega)}(r) H_{23}(s_2, r) dr, \quad (\text{C.6d})$$

$$g_{31n}(s_3) = \int_{-1}^1 (1-r)^{-1/2} P_n^{(-1/2,0)}(r) H_{31}(s_3, r) dr, \quad (\text{C.6e})$$

$$g_{32n}(s_3) = \int_{-1}^1 (1-r)^{-1/2} P_n^{(-1/2,0)}(r) H_{32}(s_3, r) dr, \quad (\text{C.6f})$$

$$g_{33n}(s_3) = \frac{e_{20}}{2} \frac{2}{\sin(\pi\beta)} P_{n+1}^{(-\beta,-\omega)}(s_3) + \int_{-1}^1 (1-r)^\beta (1+r)^\omega P_n^{(\beta,\omega)}(r) H_{33}(s_3, r) dr. \quad (\text{C.6g})$$

APPENDIX D

CLOSED FORM CONTACT MECHANICS SOLUTIONS INVOLVING ISOTROPIC AND ANISOTROPIC HALF-PLANES

The sliding contact problem involving a rigid flat punch and an isotropic half-plane; and that pertaining to a rigid punch and anisotropic half-plane are solved by Galin [46]. Also in [36], [47] and [48] to solve the contact problem, Galin's [46] approach is utilized. We provide below Galin's results.

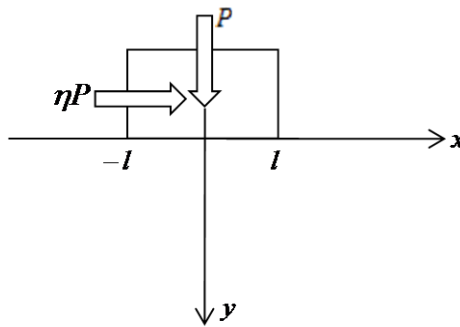


Figure D. 1: Geometry of the contact problem

The entire interval $-l < x < l$ of the boundary of the half-plane is in contact with the flat punch and the normal pressure distribution $p(x)$ under the punch is given in the following form:

For isotropic half-plane frictionless contact:

$$p(x) = \frac{P}{\pi \sqrt{l^2 - x^2}}, \quad -l < x < l. \quad (\text{D.1})$$

For anisotropic half-plane frictionless contact:

$$p(x) = P \frac{\cos \pi \alpha}{\pi} \frac{1}{(l+x)^{\alpha+1/2} (l-x)^{\alpha+1/2}}, \quad -l < x < l, \quad (\text{D.2a})$$

$$\alpha = \frac{1}{\pi} \arctan \theta, \quad (\text{D.2b})$$

$$\theta = \frac{S_{26} - \frac{S_{22}}{2} \left(\frac{1}{m_1} + \frac{1}{\bar{m}_1} + \frac{1}{m_2} + \frac{1}{\bar{m}_2} \right)}{2i \left(\frac{1}{m_1} - \frac{1}{\bar{m}_1} + \frac{1}{m_2} - \frac{1}{\bar{m}_2} \right)}, \quad (\text{D.2c})$$

where m_1 , m_2 and their complex conjugates \bar{m}_1 , \bar{m}_2 are roots of the following characteristic equation:

$$S_{11}m^4 - 2S_{16}m^3 + (2S_{12} + S_{66})m^2 - 2S_{26}m + S_{22} = 0, \quad (\text{D.3})$$

In which S_{11} , S_{12} , S_{22} , S_{16} , S_{26} and S_{66} are compliance coefficients. In the case when the half-plane is orthotropic and one of the axes of orthotropy is parallel to the boundary, $S_{16} = S_{26} = 0$. The equation above is then biquadratic and its roots m_1 and m_2 are purely imaginary.

For isotropic half-plane frictional contact:

$$p(x) = P \frac{\cos \pi \alpha}{\pi} \frac{1}{(l+x)^{\alpha+1/2} (l-x)^{\alpha+1/2}}, \quad -l < x < l, \quad (\text{D.4a})$$

$$\alpha = \frac{1}{\pi} \arctan \theta, \quad (\text{D.4b})$$

$$\theta = \eta \frac{(\kappa - 1)}{(\kappa + 1)}, \quad (\text{D.4c})$$

where η is the coefficient of friction, $\kappa = 3 - 4\nu$ for plane strain, $\kappa = (3 - \nu)/(1 + \nu)$ for generalized plane stress and ν is the Poissons's ratio.

For anisotropic half-plane frictional contact:

$$p(x) = P \frac{\cos \pi \alpha}{\pi} \frac{1}{(l+x)^{\alpha+1/2} (l-x)^{\alpha+1/2}}, \quad -l < x < l, \quad (\text{D.5a})$$

$$\alpha = \frac{1}{\pi} \arctan \theta, \quad (\text{D.5b})$$

$$\theta = \frac{-\frac{S_{22}}{2} \left(\frac{1}{m_1} + \frac{1}{\bar{m}_1} + \frac{1}{m_2} + \frac{1}{\bar{m}_2} \right) + S_{26} - \eta \left[\frac{S_{22}}{2} \left(\frac{1}{m_1 m_2} + \frac{1}{\bar{m}_1 \bar{m}_2} \right) + S_{12} \right]}{\frac{S_{22}}{2i} \left(\frac{1}{m_1} - \frac{1}{\bar{m}_1} + \frac{1}{m_2} - \frac{1}{\bar{m}_2} \right) - \eta \frac{S_{22}}{2i} \left(\frac{1}{m_1 m_2} - \frac{1}{\bar{m}_1 \bar{m}_2} \right)}. \quad (\text{D.5c})$$

For an orthotropic half-plane the equation (D.5c) becomes

$$\theta = \frac{\eta [S_{22} + S_{12} \nu_1 \nu_2]}{-S_{22} (\nu_1 + \nu_2)}. \quad (\text{D.5d})$$

Since, the coordinate axes in this study do not match up with the coordinate axes of contact problem given in [46], the results given above are not used directly for comparison. The results given by Galin [46] are rearranged according to the coordinate axes used in this study (Figure D. 2). In order to get the solutions, in the procedure described in [36] are followed.

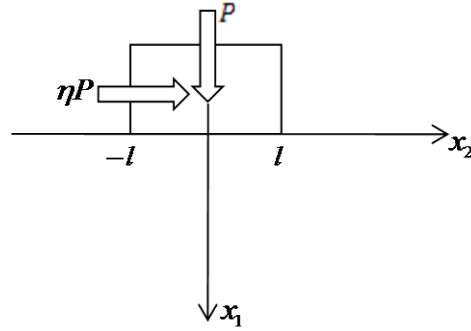


Figure D. 2: Geometry of the contact problem and principal axes x_1 , x_2 .

For a two-dimensional plane problem, stresses in the body can be expressed in terms of the Airy stress function $\Phi(x_1, x_2)$ as follows:

$$\sigma_{11} = \frac{\partial^2 \Phi}{\partial x_2^2}, \quad (\text{D.6a})$$

$$\sigma_{22} = \frac{\partial^2 \Phi}{\partial x_1^2}, \quad (\text{D.6b})$$

$$\sigma_{12} = -\frac{\partial^2 \Phi}{\partial x_1 \partial x_2}. \quad (\text{D.6c})$$

Substituting (D.6) into the compatibility equation, the governing equation is expressed in terms of $\Phi(x_1, x_2)$. In absence of body forces, the governing equation is obtained as follows:

$$S_{11} \frac{\partial^4 \Phi}{\partial x_2^4} - 2S_{16} \frac{\partial^4 \Phi}{\partial x_1 x_2^3} + (2S_{12} + S_{66}) \frac{\partial^4 \Phi}{\partial x_1^2 x_2^2} - 2S_{26} \frac{\partial^4 \Phi}{\partial x_1^3 x_2} + S_{22} \frac{\partial^4 \Phi}{\partial x_1^4} = 0, \quad (\text{D.7})$$

where S_{11} , S_{12} , S_{22} , S_{16} , S_{26} and S_{66} are compliance coefficients. Considering Fourier transformation in x_2 , Airy stress function can be expressed as,

$$\phi(x_1, x_2) = \frac{1}{2\pi} \int_{-\infty}^{\infty} \Phi(x_1, \omega) \exp(i\omega x_2) d\omega. \quad (\text{D.8})$$

Substituting (D.8) in (D.7) following ordinary differential equations are obtained,

$$S_{11}\omega^4 - 2S_{16}i\omega^3 \frac{d\Phi}{dx_1} - (2S_{12} + S_{66})\omega^2 \frac{d^2\Phi}{dx_1^2} - 2S_{26}i\omega \frac{d^3\Phi}{dx_1^3} + S_{22} \frac{d^4\Phi}{dx_1^4} = 0. \quad (\text{D.9})$$

Assuming a solution of the form $\exp(mx_1)$ for Φ , characteristic equation of the problem is determined as,

$$S_{22}m^4 - 2S_{26}m^3 + (2S_{12} + S_{66})m^2 - 2S_{16}m + S_{11} = 0. \quad (\text{D.10})$$

After applying the steps described in [36], normal pressure distribution $p(x_2)$ under the punch is obtained in the following form,

For isotropic half-plane frictionless contact:

$$p(x_2) = \frac{P}{\pi \sqrt{l^2 - x_2^2}}, \quad -l < x_2 < l. \quad (\text{D.11})$$

For anisotropic half-plane frictionless contact:

$$p(x_2) = P \frac{\cos \pi \alpha}{\pi} \frac{1}{(l + x_2)^{\alpha+1/2} (l - x_2)^{\alpha+1/2}}, \quad -l < x_2 < l, \quad (\text{D.12a})$$

$$\alpha = \frac{1}{\pi} \arctan \theta, \quad (\text{D.12b})$$

$$\theta = - \frac{S_{16} - \frac{S_{11}}{2} \left(\frac{1}{m_1} + \frac{1}{\bar{m}_1} + \frac{1}{m_2} + \frac{1}{\bar{m}_2} \right)}{\frac{S_{11}}{2i} \left(\frac{1}{m_1} - \frac{1}{\bar{m}_1} + \frac{1}{m_2} - \frac{1}{\bar{m}_2} \right)}. \quad (\text{D.12c})$$

For isotropic half-plane frictional contact:

$$p(x_2) = P \frac{\cos \pi \alpha}{\pi} \frac{1}{(l+x_2)^{\alpha+1/2} (l-x_2)^{\alpha+1/2}}, \quad -l < x_2 < l, \quad (\text{D.13a})$$

$$\alpha = \frac{1}{\pi} \arctan \theta, \quad (\text{D.13b})$$

$$\theta = \eta \frac{(\kappa-1)}{(\kappa+1)}. \quad (\text{D.13c})$$

For anisotropic half-plane frictional contact:

$$p(x_2) = P \frac{\cos \pi \alpha}{\pi} \frac{1}{(l+x_2)^{\alpha+1/2} (l-x_2)^{\alpha+1/2}}, \quad -l < x_2 < l, \quad (\text{D.14a})$$

$$\alpha = \frac{1}{\pi} \arctan \theta, \quad (\text{D.14b})$$

$$\theta = - \frac{-\frac{S_{11}}{2} \left(\frac{1}{m_1} + \frac{1}{\bar{m}_1} + \frac{1}{m_2} + \frac{1}{\bar{m}_2} \right) + S_{16} - \eta \left[\frac{S_{11}}{2} \left(\frac{1}{m_1 m_2} + \frac{1}{\bar{m}_1 \bar{m}_2} \right) - S_{12} \right]}{\frac{S_{11}}{2i} \left(\frac{1}{m_1} - \frac{1}{\bar{m}_1} + \frac{1}{m_2} - \frac{1}{\bar{m}_2} \right) - \eta \frac{S_{11}}{2i} \left(\frac{1}{m_1 m_2} - \frac{1}{\bar{m}_1 \bar{m}_2} \right)}, \quad (\text{D.14c})$$

where m_1 , m_2 , \bar{m}_1 , \bar{m}_2 are roots of the characteristic equation given by (D.10). For an orthotropic half-plane, equation (D.14c) becomes,

$$\theta = \frac{\eta [S_{11} + S_{12} \nu_1 \nu_2]}{S_{11} (\nu_1 + \nu_2)}. \quad (\text{D.14d})$$

CURRICULUM VITAE

PERSONAL INFORMATION

Surname, Name: Duygu, Sarıkaya
Nationality: Turkish (TC)
Date and Place of Birth: 03 August 1979, Ankara
Marital Status: Single
Phone: +90 312 811 18 00
email: duysarikaya@tai.com.tr

EDUCATION

Degree	Institution	Year of Graduation
MS	METU Mechanical Engineering	2005
BS	Gazi University Mechanical Engineering	2002
High School	Ankara High School, Ankara	1996

WORK EXPERIENCE

Year	Place	Enrollment
2008-Present	Turkish Aerospace Industries (TAI)	Specialty Engineering Leader
2005-2008	ROKETSAN A.Ş.	System Engineer

FOREIGN LANGUAGES

English

PUBLICATIONS

1. Sarıkaya, D., Dag, S., and Yildirim, B., 2007, "Mixed-Mode Fracture Analysis of Orthotropic Functionally Graded Materials Under Mechanical and Thermal Loads", *International Journal of Solids and Structures*", Vol. 44, pp. 7816-7840.